Developmental Regulation of Mitochondrial Function in Ovine Fetal Skeletal Muscle

Katie Louisa Davies

Jesus College

University of Cambridge

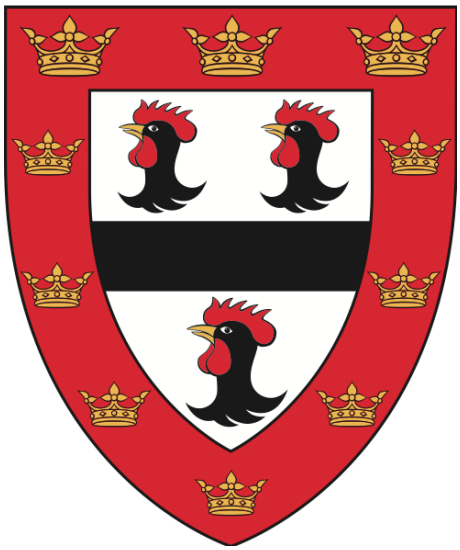

This dissertation is submitted for the degree of Doctor of Philosophy

January 2018

Abstract

Skeletal muscle is a highly metabolically active tissue, both in the adult and the fetus. Mitochondria are essential in providing energy in the form of ATP from the oxidative metabolism of carbohydrates, fats and amino acids. Mitochondrial function is influenced by the abundance and activity of the complexes comprising the electron transfer system (ETS) and the balance between mitochondrial fusion and fission. Any factors which affect the development of skeletal muscle, and mitochondria in particular, may have an impact not only on neonatal health but also on the metabolic health of the adult offspring. However, the normal developmental profile of skeletal muscle mitochondrial function as the fetus prepares for the increased metabolic challenges associated with extrauterine life, is not well characterised. The hormones, cortisol and triiodothyronine (T_3) are known to be crucial in the maturation of several physiological processes during late gestation. Further, their role in regulating adult metabolism is well-documented. However, whether they play a role in regulating fetal mitochondrial function is unknown. Using fetal sheep, the aims of this project were twofold: 1) to determine any changes in skeletal muscle mitochondrial function which occur over the last third of gestation and in the first two days of neonatal life and 2) to determine any regulatory roles of cortisol and T_3 in these developmental changes.

Mixed fibre-type skeletal muscle was collected from fetuses at 3 time points over late gestation and from newborn lambs. In addition, skeletal muscle samples were taken from fetuses which had been thyroidectomised (TX) and fetuses infused with either T_3 or cortisol. Respirometry, enzyme assays, qRT-PCR and western blotting were carried out on the skeletal muscle samples in order to assess mitochondrial parameters.

Mitochondrial activity, as measured by carbohydrate- and fat- stimulated ADP-coupled oxygen uptake, increased with age in a thyroid hormone dependent manner, rising predominantly postnatally. Mitochondrial density, abundance of ETS complexes I-IV and ATP-synthase and expression of the adenine nucleotide transferase 1 and mitofusin 2 were all positively influenced by age, with the natural prepartum rise being prevented in the thyroidectomised fetuses. However, T_3 infusion alone was insufficient to raise any of these factors prematurely. Cortisol infusion resulted in an increase in some aspects of mitochondrial oxidative capacity in a muscle-specific manner.

Overall, the data presented shows that there are developmental changes in skeletal muscle mitochondria during the perinatal period. They also suggest that these changes are regulated by both cortisol and thyroid hormones in preparation for birth, although neither hormone alone was sufficient to induce all the functional changes.

Declaration

This dissertation is the result of my own work and includes nothing which is the outcome of work done in collaboration except as declared in the Preface and specified in the text.

It is not substantially the same as any that I have submitted, or, is being concurrently submitted for a degree or diploma or other qualification at the University of Cambridge or any other University or similar institution except as declared in the Preface and specified in the text. I further state that no substantial part of my dissertation has already been submitted, or, is being currently submitted for any such degree, diploma or other qualification at the University of Cambridge or any other University or similar institution except as declared in the Preface and specified in the text.

It does not exceed the prescribed word limit for the relevant Degree Committee.

Acknowledgements

Firstly, and most importantly, I need to thank my supervisor, Abby Fowden, whose constant support on a personal and academic level throughout this PhD has made this process possible. I could not have asked for a more understanding mentor, whose wealth of knowledge and enthusiasm for this field of research has been truly inspiring throughout my PhD. Abby was also involved with all the animal work, undertaking the surgeries, without which this project could not have happened. At a personal level, without Abby's help and constant positivity, I would not have had the experience that I did; I would never have found the confidence to present my work and from working with Abby I have gained a wealth of practical and scientific knowledge and understanding. I know that Abby is hugely respected as a colleague and mentor for so many people and I could not be more thankful for having had the fortune to work so closely with her.

Andrew Murray was my PhD advisor, and again I have been so fortunate for having the support from such a friendly, enthusiastic and knowledgeable second supervisor. I am indebted to Andrew and the members of the Murray Lab for their help and guidance with the mitochondrial protocols, troubleshooting and of course for their company during the long experimental days!

Throughout my time in the lab I have had the pleasure to work with more people than I can mention who have helped me, encouraged me when times got tough and made the lab a fun place to come to work every day. Firstly Owen Vaughan who has taught me most of what I know in the lab and whose patience and dedication helped me enormously as I started out on my PhD. Emily Camm and Alison Forhead worked alongside Abby and I to carry out the animal work and their input was invaluable. Tereza Cindrova-Davies and Billy Yung were always so willing to help with their knowledge of experimental procedures. A huge thank you must also go to my Part II student, Emily Atkinson, who worked very hard to produce much of the work presented in this thesis on the semitendinosus. She was a joy to work with throughout her 2 terms in the lab.

I am hugely thankful to the animal technicians at the Barcroft Centre, Scott Gentle, Sharon Pickering, Craig Forest and Anne Chapman, who carried out all animal care up until surgery and helped monitor the ewes wellbeing post-surgery, as well as regulating the sheep breeding and carrying out the ultrasound scans.

As well as everyone listed above, I have been lucky enough to be provided with constant support from friends and family. My parents have unlimited faith in me and have managed to keep me motivated when I needed it the most, particularly during the writing up period. Day to day in PDN, I have always been grateful for the company of Sarah Burgess, Ross Lindsay and Nadia Capatina to name a few, who have been there when the science worked and the times it didn't! Finally, a big thank you needs to go to Sam Braidley, who has stuck by me through a tough 3 years. He has always been at the end of the phone when I needed encouragement or just a chat, has picked me up whenever I've been down and has been very understanding of the time commitment required for the PhD.

I am enormously grateful for the funding from the Wellcome Trust which has allowed this project to go ahead.

Contents

Abbreviations

ACTH	Adrenocorticotropin hormone
ADP	Adenosine diphosphate
AMP	Adenine monophosphate
AMPK	AMP-activated protein kinase
ANOVA	Analysis of variance
ANT	Adenine nucleotide translocase
ATP	Adenosine triphosphate
BCA	Bicinchoninic Acid
BF	Biceps femoris
BIOPS	Biopsy preservation medium
BSA	Bovine serum albumin
CI-IV	ETS complexes I-IV
CV	ATP-synthase
cDNA	Complementary DNA
CoA	Coenzyme A
CRH	Corticotropin releasing hormone
CRL	Crown-rump length
CS	Citrate synthase
D1/2/3	Deiodinase type 1/2/3
dGA	Days of gestational age
DNA	Deoxyribose nucleic acid
DTNB	5,5'-Dithio-bis(2-nitrobenzoic acid)
EDTA	Ethylenediaminetetraacetic acid
EGTA	Ethylene glycol tetraacetic acid
ETS	Electron transfer system
FA	Fatty acid
FAD	Flavin adenine dinucleotide (oxidised form)
$FADH_2$	Flavin adenine dinucleotide (reduced form)

GC	Glucocorticoid
GLUT	Glucose transporter
GR	Glucocorticoid receptor
GRE	Glucocorticoid responsive element
HIF	Hypoxia-inducible factor
HOAD	β-hydroxyacyl-CoA dehydrogenase
HPA	Hypothalamic-pituitary-adrenal
HPT	Hypothalamic-pituitary-thyroid
H_2O_2	Hydrogen peroxide
IGF	Insulin-like growth factor
IMF	Intermyofibrillar
IMM	Inner mitochondrial membrane
IMS	Intermembrane space
IUGR	Intrauterine growth restriction
MCU	Mitochondrial calcium uniporter
MEF	Mouse embryonic fibroblast
MICU	Mitochondrial calcium uptake protein
NAD+	Nicotinamide adenine dinucleotide (oxidised form)
NADH	Nicotinamide adenine dinucleotide (reduced form)
NRF	Nuclear respiratory factor
OMM	Outer mitochondrial membrane
Oxphos	Oxidative phosphorylation
PC	Palmitoylcarnitine
pCO_2	Partial pressure of carbon dioxide
PGC1α	PPARγ coactivator 1 alpha
P_i	Inorganic phosphate
PMF	Proton motive force
pO_2	Partial pressure of oxygen
PPAR	Peroxisome proliferator-activated receptor

Py	Pyruvate
qRT-PCR	Quantitative real time polymerase chain reaction
Redox	Reduction and oxidation
RCR	Respiratory control ratio
RIA	Radioimmunoassay
RNA	Ribose nucleic acid
ROS	Reactive oxygen species
rT_3	Reverse T_3
SD	Standard deviation
SDF	Superficial digital flexor
SEM	Standard error of the mean
SOD	Superoxide dismutase
SS	Subsarcolemmal
ST	Semitendinosus
TBS	Tris-buffered saline
TCA	Tricarboxylic acid
TH	Thyroid hormone
THR	Thyroid hormone receptor
TRE	Thyroid response element
TRH	Thyrotropin releasing hormone
TSH	Thyroid-stimulating hormone
TX	Thyroidectomised
T_2	Diiodo-thyronine
T_3	Triiodothyronine
T_4	Thyroxine
UCP	Uncoupling protein

1 General Introduction

Metabolic syndrome is increasing in incidence in the adult population in both developed and developing countries (Kaur, 2014). It is characterised by conditions including obesity, glucose intolerance, insulin resistance, dyslipidaemia, type 2 diabetes and cardiac dysfunction, all of which reduce the quality of life and shorten lifespan (Alberti et al., 2005). Worldwide, 20-25% of the adult population has metabolic syndrome, a figure which rises to 35% in the USA and to 50% in American citizens over the age of 60 years (Kaur, 2014, Aguilar et al., 2015). Of increasing concern is the fact that diagnoses of metabolic syndrome are occurring at younger and younger ages (Reinehr, 2013, Cook et al., 2003). Amongst the overweight and obese adolescent population, the incidence of metabolic syndrome is estimated to be between 30-50% with 40% of all adolescents and nearly 90% of obese adolescents having at least one of the risk factors (Weiss et al., 2004, Cook et al., 2003). In developed countries, the rising prevalence and predisposition to metabolic syndrome closely tracks with more sedentary lifestyles and increasing consumption of diets high in fats and sugar (Hu, 2011). However, in developing countries like India where there is rapid urbanisation of the population within a single generation, prevalence of metabolic syndrome and its risk factors is already at 40% of the population with the incidence rising rapidly even in the poorest states (Ramachandran, 2005, Ramachandran et al., 2003). This suggests a disparity between the environments experienced by an individual during early life and adulthood may also play a role in determining the subsequent risk of developing metabolic dysfunction.

1.1 Developmental programming of metabolic dysfunction

The 'developmental origins of health and disease' theory was first put forward by David Barker after noting a geographical correlation between areas with high infant mortality and high incidence of adult cardiovascular disease (Barker and Osmond, 1986). Since then, several human epidemiological studies have shown associations between low birth weight and a predisposition not only to impaired cardiovascular function but also to metabolic dysfunction in adult populations of different ethnicity (Barker et al., 1989, Barker et al., 2002, Hales et al., 1991, Chaudhari et al., 2017). The hypothesis is that exposure to suboptimal conditions *in utero* can affect fetal growth and development which, through poorly understood mechanisms, programmes a predisposition to symptoms of the metabolic syndrome, including

obesity, insulin resistance and hypertension (McMillen and Robinson, 2005, Roseboom et al., 2006).

Numerous studies on experimental animals have also shown that a low birthweight is associated with long term adverse effect on offspring metabolic health (Bertram and Hanson, 2001). Intrauterine growth restriction (IUGR) induced by maternal undernutrition, placental insufficiency and glucocorticoid overexposure have all been shown to cause glucose intolerance, insulin resistance and pancreatic β cell dysfunction in the adult offspring (Petrik et al., 1999, Nyirenda et al., 1998, Ozanne et al., 2003, Ozanne et al., 2005, Nyirenda et al., 2009, Owens et al., 2007). These changes in metabolic phenotype are multifactorial in origin and involve functional and morphological alterations from the gene to the system level (Bertram and Hanson, 2001). For instance, there can be changes in the number and type of cells within a tissue or organ and at the cellular level, there are alterations in the abundance of enzymes, hormone receptors, ion channels and transporters as well as in the expression and activity of key signalling pathways (Bertram and Hanson, 2001). All these alterations will affect the tissue functional capacity and ability to maintain homeostasis in response to environmental challenges. In addition, there is increasing evidence that mitochondria have a role in the developmental programming of metabolism through their central roles in cellular energetics and oxidative stress (Lee et al., 2005).

1.2 Mitochondria

Mitochondria are vital components of eukaryotic cells, thought to originate from α-Proteobacterium (Yang et al., 1985, Gray, 2012). They contain their own genome of 37 genes, 13 of which encode proteins expressed via mitochondrial-specific transcriptional and translational mechanisms (Taanman, 1999). The majority of mitochondrial proteins, however, are encoded by nuclear DNA, translated in the cytoplasm and translocated to their required location in the mitochondria (Neupert, 1997). Their basic structure, as first viewed by transverse electron microscopy in the 1950s, consists of a highly folded inner membrane (IMM) surrounding the inner matrix, and an outer membrane (OMM) separated from the IMM by the intermembrane space (IMS; Figure 1.1; Palade, 1953).

Mitochondria have a number of functions essential for life. Their best-known role is in the production of energy, in the form of adenonsine triphosphate (ATP), for cell metabolism. They

are also important in cell signalling as they are a site of production of reactive oxygen species (ROS) and contribute to intracellular calcium regulation. In addition, they play a role in cell death and, in some cells, are the site of steroid hormone synthesis (Brand and Nicholls, 2011, Miller, 2013). Abnormalities in mitochondrial function can be fatal and are associated with several diseases including neurodegenerative disorders, cardiomyopathy and metabolic dysfunction (Duchen, 2004).

The pathways of ATP and ROS generation, the primary focus of this thesis, are outlined in Figure 1.1. Briefly, carbohydrate and fatty acid metabolism result in the production of reducing equivalents (NADH and $FADH_2$) from glycolysis, the link reaction (catalysed by pyruvate dehydrogenase), the tricarboxylic acid (TCA) cycle and β-oxidation. In turn, these donate electrons to protein complexes of the mitochondrial electron transfer system (ETS) situated in the IMM. The ETS harnesses the energy from a series of reduction and oxidation (redox) reactions to pump protons into the IMS. The resulting proton-motive force drives ATP synthase, which phosphorylates adenosine diphosphate (ADP) to form ATP (Nunnari and Suomalainen, 2012). Oxygen acts as the final electron acceptor at complex IV and the rate of oxygen uptake is proportional to the electron flux through the ETS and the proton current (Brand and Nicholls, 2011). The overall process is known as oxidative phosphorylation (oxphos). ROS are generated by electron leak onto oxygen at complexes I and III, particularly if there is an altered oxygen supply or a high proton gradient (Murphy, 2009). More details of these processes are given in the sections below.

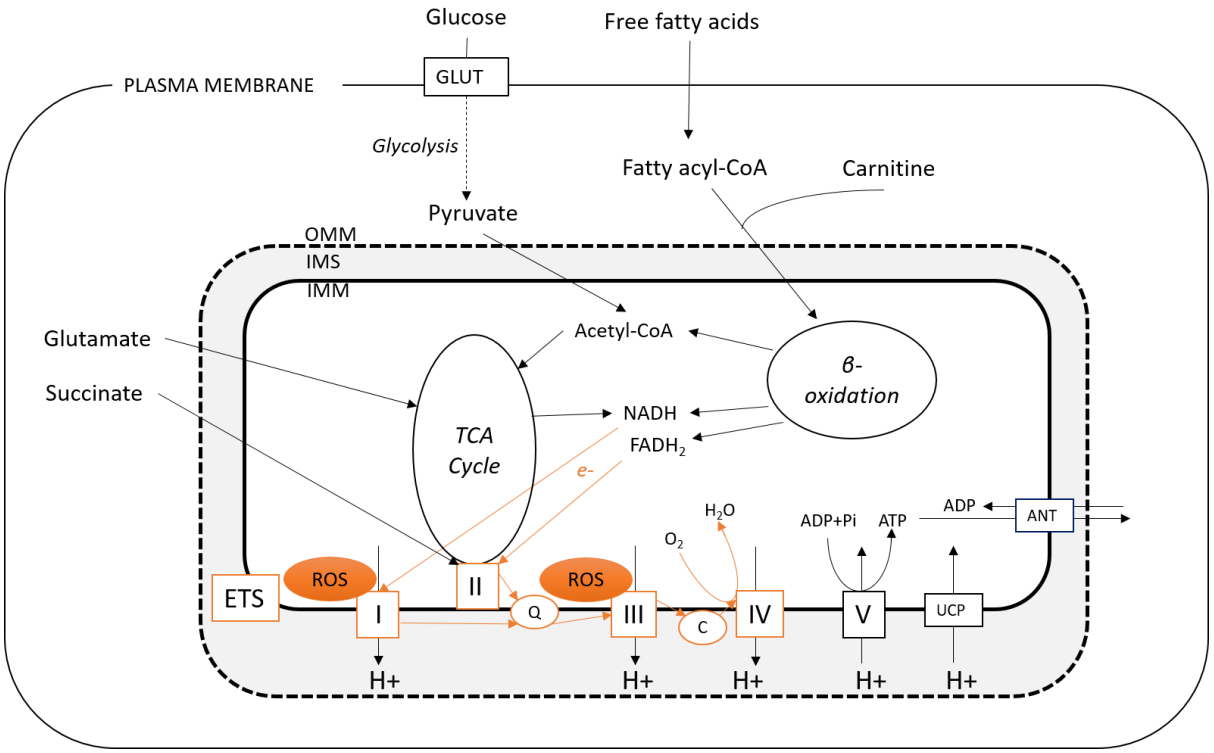

Figure 1.1 A simplified diagram of mitochondrial metabolism (modified from Murray, 2012). OMM, outer mitochondrial membrane; IMS, intermembrane space; IMM, inner mitochondrial membrane; NADH, reduced nicotinamide adenine dinucleotide; $FADH_2$, reduced flavin adenine dinucleotide; TCA, tricarboxylic acid; ETS I-IV, electron transfer system complexes I-IV; V, ATP-synthase; Q, ubiquinone; c, cytochrome c; ROS, reactive oxygen species; ANT, adenine nucleotide translocase. Electron (e^-) transfer through the electron transfer system is shown in orange.

1.2.1 ATP production

1.2.1.1 Substrate uptake and utilisation

Mitochondria are able to metabolise carbohydrates, fatty acids, ketone bodies and amino acids for energy production (Figure 1.1), although the vast majority of energy production comes from carbohydrates and lipids in the fed-state (Hoppeler, 1999). These substrates are obtained either from the blood supply or from endogenous reserves when there is a rise in energy demands or a fall in the circulating substrate concentrations. Intracellular stores of glycogen (carbohydrate) and lipid droplets are present in skeletal muscle, observed in close proximity to the mitochondria (Hoppeler, 1999, Philp et al., 2012).

As the primary source of ATP, the mitochondria play a key role in the metabolic response to changes in the cellular environment such as altered energy demands, substrate supply and oxygen availability. Fatty acid oxidation produces more ATP per gram than carbohydrate (Hall et al., 2012), however, produces less ATP for the same amount of oxygen consumed (Spriet, 2014). Therefore, carbohydrate oxidation occurs preferentially in several tissues, although fatty acid oxidation is essential in skeletal muscle at rest and during endurance exercise to preserve glycogen stores, and for use when the glycogen stores are depleted (Hood et al., 2006, Kimber et al., 2003, Spriet, 2014).

Substrate availability is also important to mitochondrial function and significant interaction has been observed between the carbohydrate and lipid oxidation pathways, allowing for metabolic flexibility both at the whole body level (Randle et al., 1963, McGarry et al., 1977, Lossow and Chaikoff, 1955) and at the mitochondrial level (Jorgensen et al., 2017). The 'glucose/fatty acid cycle' has been used to describe the inhibitory effect of carbohydrates on fatty acid oxidation while upregulating glucose oxidation, and vice versa (Dimitriadis et al., 2011).

Glycolysis and glucose oxidation

Glucose is transported into the cell via facilitated diffusion through glucose transporters (GLUTs) in an insulin-dependent or independent manner (via GLUT4 and GLUT1 respectively in skeletal muscle; Ebeling et al., 1998, Gaster et al., 2000). Glycolysis takes place in the cytosol, whereby one glucose molecule undergoes a series of 10 enzyme-catalysed reactions resulting in its conversion to 2 molecules of pyruvate, with a net production of 2 ATP through substrate-level phosphorylation and 2 reduced nicotinamide adenine dinucleotide (NADH; Li et al., 2015). In anaerobic conditions, glycolysis is the primary source of ATP. In order to maintain glycolysis, the resulting NADH must be re-oxidised to NAD^+, which occurs through the reduction of pyruvate to lactate. Under aerobic conditions glycolysis and lactate production still occur (Almeida et al., 2010), however, the glucose molecule can be completely oxidised in the mitochondria producing approximately 30 ATP per glucose molecule. Thus, when oxygen is available, the pyruvate produced by glycolysis is preferentially transported into the mitochondria for oxidative phosphorylation (Figure 1.1).

Pyruvate must be transported into the mitochondrial matrix. This occurs first via passive diffusion through non-selective channels in the OMM (Schell and Rutter, 2013, Huizing et al., 1996) followed by more restricted transport through the IMM mitochondrial pyruvate carrier utilising the proton gradient (Bricker et al., 2012, Halestrap and Denton, 1974, Halestrap, 1978). In the matrix, the pyruvate dehydrogenase complex catalyses the conversion of pyruvate to the 2-carbon moiety acetyl-coenzyme A (acetyl-CoA) which can enter the TCA cycle (Schell and Rutter, 2013).

Fatty acid oxidation

Fatty acid oxidation via the β-oxidation pathway is a source of energy in numerous tissues although it is of particular importance in adult cardiac and skeletal muscle (Bartlett and Eaton, 2004). Fatty acids (FAs) enter the cell rapidly by simple or facilitated diffusion using FA transport proteins (Su and Abumrad, 2009, Simard et al., 2008). In the cytosol the FA is conjugated to Coenzyme A to form a fatty acyl-CoA. When conjugated instead with a carnitine molecule, forming acyl-carnitine, the FA can be transported into the mitochondria (Figure 1.2) (Sharma and Black, 2009). This reaction is catalysed by carnitine palmitoyltransferase I (CPTI), with the reverse reaction to re-form the acyl-CoA catalysed by carnitine palmitoyltransferase II (CPTII) in the mitochondrial matrix (Figure 1.2).

The acyl-CoA then undergoes β-oxidation as shown in Figure 1.2. Each cycle of the β-oxidation pathway removes a 2-carbon moiety from the FA chain, producing acetyl-CoA which can enter the TCA cycle, and a shorter FA chain which can undergo further cycles of β-oxidation (Bartlett and Eaton, 2004). Additional products of the β-oxidation pathway are the reducing equivalents NADH and flavin adenine dinucleotide ($FADH_2$) which donate electrons to complexes I and II of the ETS respectively (section 1.2.1.3).

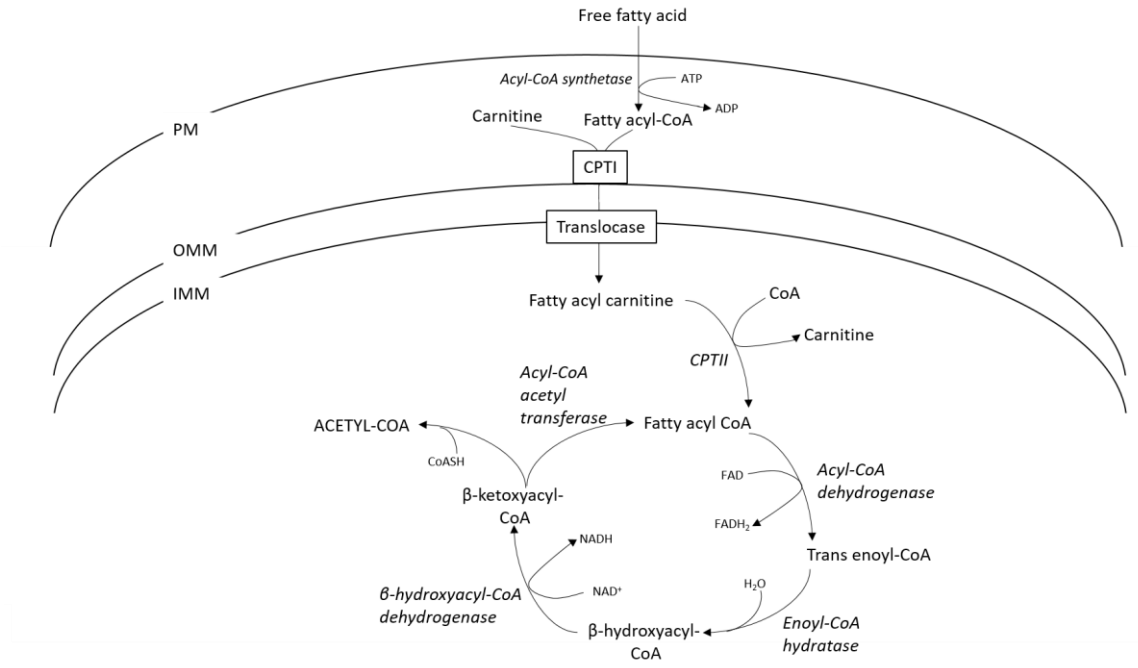

Figure 1.2 Fatty acid uptake and ß-oxidation. PM, plasma membrane; OMM, outer mitochondrial membrane; IMM, inner mitochondrial membrane; CPTI and II, carnitine palmitoyltransferase I and II; CoA, Coenzyme A; NAD^+/NADH, oxidised/reduced form of nicotinamide adenine dinucleotide; FAD/$FADH_2$, oxidised/reduced form of flavin adenine dinucleotide. (Sharma and Black, 2009, Bartlett and Eaton, 2004)

Protein

Amino acids, obtained from the diet or by protein catabolism, cross the cell membrane using amino acid transporters (Hyde et al., 2003). In the liver and skeletal muscle, amino acids can be deaminated and, for certain amino acids, the product can be converted to pyruvate or acetyl-CoA which can feed into the TCA cycle (Chang and Goldberg, 1978). Alternatively, some amino acids, such as glutamate, can be converted into TCA cycle intermediates which can therefore directly enter the cycle (Figure 1.1; Chang and Goldberg, 1978).

1.2.1.2 The tricarboxylic acid cycle

The TCA cycle was first elucidated by Hans Krebs in 1937 (Krebs and Johnson, 1937). Briefly, citrate synthase catalyses the entry of acetyl-CoA into the cycle with its reaction with the 4-carbon oxaloacetate to form the 6-carbon molecule citrate. Substrate oxidation and decarboxylation through the 7-step pathway outlined in Figure 1.3 regenerates oxaloacetate and produces 3 NADH and 1 $FADH_2$ for each acetyl-CoA molecule that enters the cycle. NADH and $FADH_2$ produced from the TCA cycle provide the majority of the reducing potential required for ATP synthesis via oxidative phosphorylation.

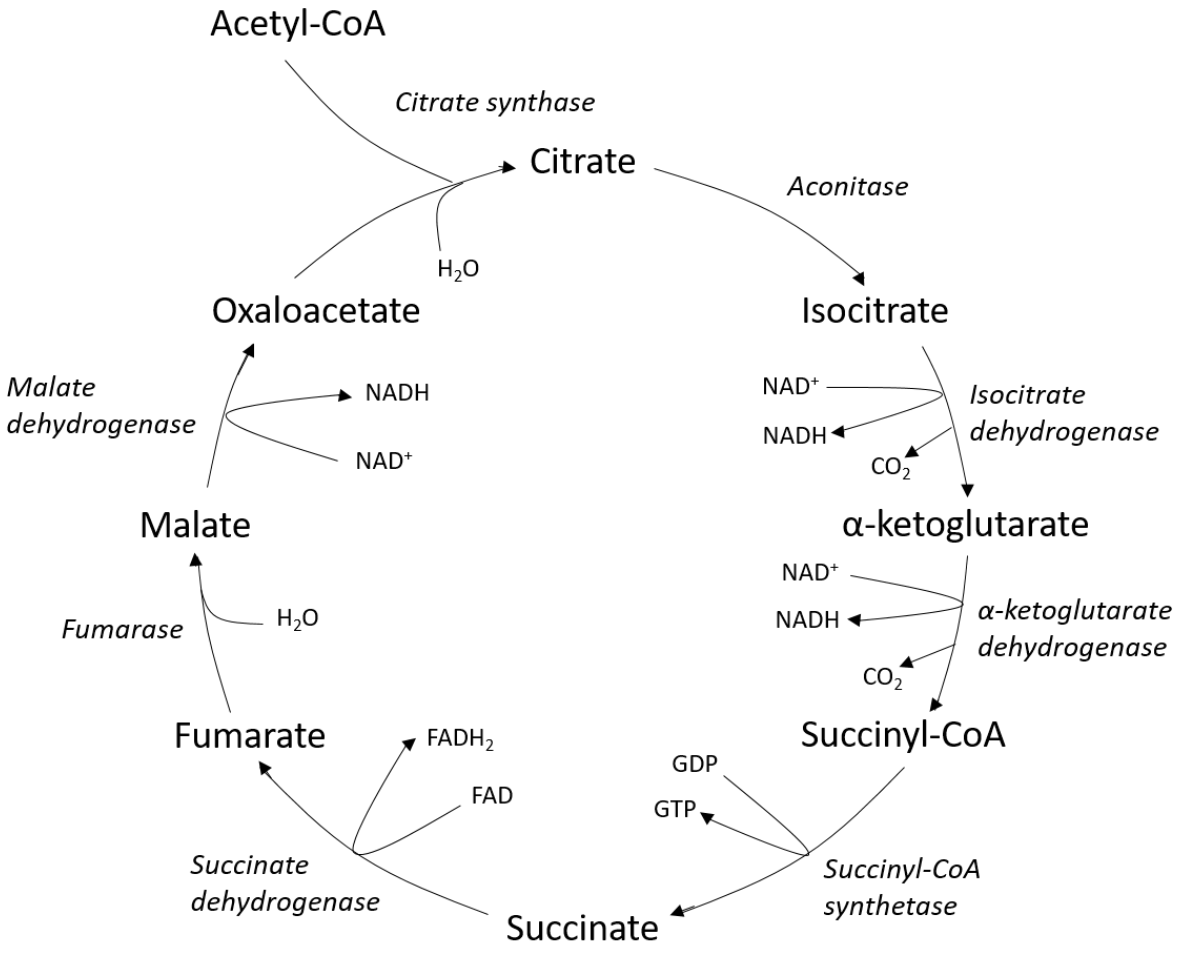

Figure 1.3 The tricarboxylic acid cycle. NAD^+/NADH, oxidised/reduced form of nicotinamide adenine dinucleotide; FAD/$FADH_2$, oxidised/reduced form of flavin adenine dinucleotide. (Cardaci and Ciriolo, 2012)

1.2.1.3 Oxidative phosphorylation

In 1961, Peter Mitchell described the theory of chemiosmotic coupling, the concept describing the coupling of substrate oxidation to ATP synthesis by a proton gradient generated across a membrane by the energy released from electron transfer (Mitchell, 1961). In the mitochondria, the highly invaginated IMM acts as the energy-transducing membrane as it is the site of ETS complexes I-IV and ATP-synthase (Figure 1.1).

Complex I (NADH dehydrogenase; CI) and complex II (succinate dehydrogenase; CII) accept electrons from NADH and $FADH_2$ respectively and at both complexes this potential is used to reduce ubiquinone to ubiquinol through the addition of 2 protons and 2 electrons (Sazanov, 2015, Murray, 2012). The drop in redox potential at CI is sufficient to pump protons from the matrix into the IMS. Ubiquinol migrates through the IMM to be oxidised at complex III (cytochrome bc_1 complex; CIII) and the protons are released into the IMS contributing to the proton gradient (Huttemann et al., 2007). One electron is used to reduce a separate ubiquinone, therefore, greatly increasing the efficiency of the process while the second electron is passed onto complex IV (cytochrome c oxidase; CIV) via cytochrome c (Sazanov, 2015). Cytochrome c is loosely bound to the IMS side of the IMM (Kuznetsov et al., 2008). At CIV, oxygen acts as the final electron acceptor and is reduced to water. CIV also pumps protons into the IMS and is the enzyme controlling the rate of flux through the ETS and thus the respiratory rate (Huttemann et al., 2008). The complexes may be physically separated from one another in the IMM although recent evidence is emerging of the existence of 'supercomplexes'. The most common of these, the respirasome, is thought to comprise of complex I, a dimer of complex III and complex IV and has been identified in ovine cardiac mitochondria (Letts et al., 2016).

The protons pumped into the IMS build up a concentration difference across the relatively impermeable IMM. The result is that the IMS becomes positively charged and acidic relative to the matrix. The proton gradient across the membrane, made up of a chemical (pH) gradient and electrical potential difference, provides a free energy driving force of ~200mV, the proton motive force (PMF; Mitchell and Moyle, 1969). The PMF is used to drive a secondary proton pump, ATP-synthase, to synthesise ATP from ADP and inorganic phosphate (P_i). Energy from the PMF is required for the rotation of the protein motor and each full rotation results in the release of 3 ATP from the catalytic binding sites (Noji et al., 1997). ATP is transported out of

the mitochondria in exchange for ADP by the adenine nucleotide translocase (ANT) located in the IMM (Figure 1.1).

1.2.2 Reactive oxygen species production

Reactive oxygen species (ROS) play a role in physiological signalling but in excess are implicated in oxidative damage and the pathogenesis of numerous diseases. The predominant contribution to mitochondrial ROS is from electron leakage onto oxygen at complex I and complex III to form the superoxide free radical, $\dot{O}_2^-$ (St-Pierre et al., 2002). Although a high proportion, up to 90%, of total ROS production is often assumed to be of mitochondrial origin, evidence for this is limited and it is a point of current controversy (Aledo, 2014, Brown and Borutaite, 2012). Additionally, cell culture studies estimate that 1-2% of oxygen consumed is converted to the superoxide anion rather than water, although whether this is true *in vivo* remains unclear (Kudin et al., 2004).

The production of ROS is a normal component of cell signalling, for example they are believed to be involved in mediating the response to hypoxia (Mansfield et al., 2005). However, when excessive ROS generation occurs, ROS cause damage to cellular proteins, nucleic acids and lipids, as well as having an inhibitory effect on mitochondrial energy production (Aledo, 2014). The risk of excessive ROS production increases at higher metabolic rates, as there is an increased risk of electron slippage from the ETS. Therefore mechanisms that increase respiratory rate (section 1.2.6) may also increase ROS production (Peng and Jou, 2010). Additionally, a very high PMF is associated with increased ROS production as is a high NADH concentration and abnormally high or low oxygen levels, or fluctuations in oxygen, seen in hypoxia-reperfusion as occurs, for instance, during labour and delivery (Lambert and Brand, 2004, Boveris and Chance, 1973, Mansfield et al., 2005).

In order to prevent excessive oxidative damage, ROS detoxifying enzymes are expressed. The superoxide anion is converted to hydrogen peroxide (H_2O_2) by superoxide dismutase (SOD) enzymes (Figure 1.4; Loschen et al., 1974). There are 3 different forms of SOD, of which one, MnSOD (SOD2), is mitochondria-specific (Weisiger and Fridovich, 1973, Fukai and Ushio-Fukai, 2011). Catalase is required to breakdown the H_2O_2 (Figure 1.4) to prevent its conversion in the cytosol to the very reactive hydroxyl radical, $\dot{O}H$ (Aledo, 2014, Fukai and Ushio-Fukai, 2011).

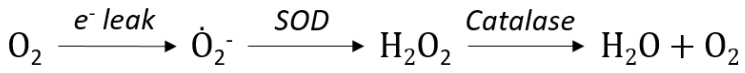

Figure 1.4 Reactive oxygen species formation and detoxification. SOD, superoxide dismutase. (Jaimes et al., 2001)

Additional protective mechanisms against oxidative damage may include a decrease in specific ETS complex abundance and an increase in uncoupling protein abundance (discussed in section 1.2.3.1), which have been reported in mitochondria of hypoxic muscle (Levett et al., 2012). Additionally, the existence of ETS supercomplexes have been suggested to reduce ROS production at CIII at the expense of lowering the maximal capacity of this complex due to conformational limitations of electron transfer (Letts et al., 2016).

1.2.3 Regulators

The ability of the mitochondria to carry out oxphos is highly reliant on the maintenance of the proton gradient. However, leak of protons across the membrane has been reported to account for about half of the resting oxygen consumption of skeletal muscle (Brand et al., 1994). While reducing the efficiency of ATP production, proton leak is important for physiological processes including protection against excessive ROS production. The mechanism by which 'proton leak' occurs is very poorly understood and whether the lipid composition of the IMM plays a role in regulating proton leak is under debate (Brookes et al., 1997, Chen and Li, 2001, Pehowich, 1999). Uncoupling proteins (UCPs) are present in the IMM and provide one route by which the proton gradient might be dissipated, while transport of substances into and out of the mitochondria (for example ATP export via the adenine nucleotide translocase) often harnesses the proton gradient and, therefore, provides an alternative route for proton re-entry (Halestrap, 1978, Enerback et al., 1997).

1.2.3.1 Uncoupling Proteins

There are 3 major uncoupling proteins: UCP1, 2 and 3. UCP1 was the first to be identified and is present predominantly in brown adipose tissue (BAT) where it has an essential role in non-shivering thermogenesis by dissipating the proton gradient as heat (Heaton et al., 1978, Enerback et al., 1997). It may also have a role in regulating energy balance (Oliver et al., 2007, Kontani et al., 2005, Rippe et al., 2000). However, mice lacking UCP1 do not become obese (Enerback et al., 1997), which suggests UCP2 and UCP3 may 'rescue' the metabolic phenotype and they show a 59% and 57% homology to UCP1 respectively (Fleury et al., 1997, Vidal-Puig et al., 1997). UCP3 and to a lesser extent UCP2 are expressed in skeletal muscle (Ricquier and Bouillaud, 2000). Indeed UCP3 is specific to skeletal-muscle in humans (Vidal-Puig et al., 1997, Ricquier and Bouillaud, 2000) and has been shown to contribute significantly to proton leak (Gong et al., 2000). Although the major roles of UCP2 and UCP3 in skeletal muscle are yet to be determined, they both appear to have metabolic effects (Schrauwen and Hesselink, 2002). The uncoupling effect of UCP2 has been associated with regulating energy balance and metabolic rate (Nordfors et al., 1998, Barbe et al., 2001) and may play a tissue-wide role in minimising oxidative stress through preventing excessive ROS production (Arsenijevic et al., 2000). UCP3, on the other hand, may play a role in thermogenesis alongside influencing metabolic efficiency and may be particularly important in regulating lipid metabolism (Russell et al., 2003, Schrauwen et al., 2001, Clapham et al., 2000, Simonyan et al., 2001).

1.2.3.2 Adenine nucleotide translocase

The predominant role of ANT is to catalyse the exchange of ATP and ADP in a 1:1 ratio across the IMM, a process driven by the PMF (Pfaff et al., 1965, Pfaff and Klingenberg, 1968). The essential role of ANT in oxidative metabolism necessitates a very high abundance of ANT within the mitochondria. Three isoforms have been identified in the human, ANT1, 2 and 3 and, of these, ANT1 is the predominant form expressed in skeletal and cardiac muscle (Stepien et al., 1992). Mouse *Ant1* knockout and overexpression studies indicate that half to two-thirds of the basal proton conductance of the IMM is due to the presence of ANT (Brand et al., 2005). Altered expression of UCPs and ANTs provide a mechanism by which oxphos efficiency and metabolic rate can be regulated. Changing mitochondrial abundance and network dynamics are two other such mechanisms and these are discussed below.

1.2.4 Mitochondrial biogenesis

Increasing the density of mitochondria, by organelle growth and division, occurs when energy supply is insufficient to meet the cellular demands (Hood et al., 2011, Nunnari and Suomalainen, 2012). The process of mitochondrial biogenesis requires the coordination of several processes including regulation of both the mitochondrial and nuclear genomes, lipid and protein synthesis for the assembly of the ETS complexes, import of metabolic enzymes and membrane expansion (Hood et al., 2006). Several messengers have been shown to influence biogenesis, including thyroid hormones, calcium and adenine monophosphate (AMP)-activated protein kinase (AMPK), and the biogenic response is thought to often involve one key transcriptional regulator, peroxisome proliferator-activated receptor gamma (PPARγ) coactivator 1 alpha (PGC1α; Irrcher et al., 2003, Ojuka et al., 2003, Jäger et al., 2007). PGC1α is capable of driving mitochondrial biogenesis through its interaction with a range of transcription factors (Scarpulla et al., 2012, Lehman et al., 2000). Some of the best-characterised mitochondrial biogenesis activators regulated by PGC1α are the transcription factors nuclear respiratory factor (NRF) 1 and 2. NRFs upregulate the expression of several nuclear-encoded components of the ETS complexes and proteins involved in mitochondrial DNA biogenesis (Marin-Garcia, 2010).

1.2.5 Mitochondrial fusion and fission

For over a century, mitochondria have been known to be highly dynamic organelles, constantly changing location within the cell and altering their conformation, in part through fusion and fragmentation (Lewis and Lewis, 1914). Since then, the importance and mechanism of the fusion and fission events have been the subject of numerous studies. Fission and fusion allow mitochondria to share solutes, metabolites, membranes and electrochemical gradients (Schrepfer and Scorrano, 2016). Maintaining a dynamic network is thought to be important in balancing energy supply and demand, with increased fusion observed when demand for ATP is high (Schrepfer and Scorrano, 2016). Network plasticity is also vital for mitochondrial quality control and mediating organelle and cellular degradation in response to damage (Jin and Youle, 2012).

The complex mechanisms of fusion and fission are yet to be fully elucidated, however 4 key dynamin-like GTPases have been identified as integral to maintaining the mitochondrial network plasticity: mitofusins (MFN 1 and 2) and optic atrophy protein 1 (OPA1) are important

in driving mitochondrial fusion of the OMM and IMM respectively and dynamin-related protein 1 (DRP1) is involved in fission (Cipolat et al., 2004, Schrepfer and Scorrano, 2016). All 4 are important during development as inhibiting their expression results in embryonic lethality in mice (Chen et al., 2003, Ishihara et al., 2009, Davies et al., 2007).

Fusion

MFN1 and 2 are located on the OMM and are thought to increase the number of mitochondrial contact events resulting in fusion through predominantly homotypic interactions of their cytosolic coiled coil domains (Rojo et al., 2002, Cipolat et al., 2004, Ishihara et al., 2004). Mouse embryonic fibroblasts (MEFs) derived from *Mfn*-knockout embryos have a fragmented mitochondrial network with reduced motility and fewer fusion events (Chen et al., 2003), whereas *Mfn* overexpression results in increased mitochondrial clustering (Rojo et al., 2002). MFN1 and MFN2 show 70% sequence homology and overexpression of MFN1 can rescue mitochondrial morphology defects in MFN2-deficient cells and vice versa (Chen et al., 2003). However, there is evidence that MFN1 and MFN2 carry out distinct functions in regulating fusion.

The morphology of the mitochondria differ between the *Mfn1*- and *Mfn2*-knockout MEFs; the mitochondria are all very small in the *Mfn1*-knockout, whereas in the *Mfn2*-knockout, the mitochondria are of varying sizes but are all spherical (Chen et al., 2003). MFN1 tethering efficiency and GTPase activity were shown to be significantly greater than MFN2, which again suggests that while both are required for fusion, they perhaps are important at distinct stages of the process (Ishihara et al., 2004). In skeletal muscle specifically, while MFN1 and MFN2 are both expressed in human and mouse muscle cell lines (Rojo et al., 2002), only MFN1 was associated with fusion events in the rat (Eisner et al., 2014).

OPA1 is located on the IMM and, like the mitofusins, regulates mitochondrial fusion through GTPase activity and interaction of the coiled coil domain (Cipolat et al., 2004). Further, OPA1 has been shown to be important for mitochondrial fusion in skeletal muscle (Eisner et al., 2014, Cipolat et al., 2004). OPA1 stability and function are dependent on the mitochondrial membrane potential which is hypothesised to be an important check-point in place to prevent the fusion of a damaged or dysfunctional mitochondrion into the healthy network (Song et al., 2007).

Fission

Mitochondrial fission is associated with a decreased energy demand but also with apoptosis. Experiments inhibiting DRP1 function reveal an excessive fission defect with closed networks of elongated mitochondria, which have collapsed around the nucleus (Pitts et al., 1999, Gandre-Babbe and van der Bliek, 2008). The overall mechanism of fission is thought to involve the recruitment of DRP1 and other proteins involved in forming a 'scission complex' which form a ring to constrict the mitochondrion and divide the organelle. The GTPase activity of DRP1 is thought to drive the final constriction events, but ultimately the mechanism and role of individual proteins remain unclear (Gandre-Babbe and van der Bliek, 2008).

1.2.6 Responding to the environment

The rate of respiration must be appropriate for both the cellular energy demand and the substrate availability. Coordinating this balance is mediated through cellular messengers conveying the current metabolic environment, as well as by endocrine messengers allowing an appropriate response at the organ and organism level. The interactions between substrate levels and metabolic response has already been discussed (Section 1.2.1.1). Additional mechanisms are numerous and interlinked, but some of the key regulatory pathways in skeletal muscle are summarised below.

Monitoring cellular energy demand

AMPK monitors cellular AMP:ATP levels to convey the energy status of the cell. Skeletal muscle undergoes high energy turnover for example during exercise, and this results in a greater increase in AMP than the concomitant decrease in ATP (Jäger et al., 2007). When AMP levels are high, AMP molecules bind to AMPK, resulting in an increased likelihood of phosphorylation to the active form, pAMPK (Long and Zierath, 2006). Activated AMPK then regulates downstream pathways in order to upregulate metabolism and provide the ATP required by increasing mitochondrial biogenesis and upregulating TCA cycle enzymes and components of the ETS (Winder et al., 2000, Bergeron et al., 2001). In addition, increased AMPK during times of energy deprivation and during exercise is believed to be linked to a

switch to fatty acid oxidation, which spares glucose for use by the brain (Jeoung et al., 2006, Winder and Hardie, 1996).

Monitoring whole body energy demand

Numerous hormones, including insulin, glucocorticoids (GCs), catecholamines and thyroid hormones (THs), are involved in regulating a whole body metabolic response. Insulin, secreted in response to high circulating glucose levels, is important in regulating substrate preference and driving carbohydrate metabolism. This is achieved predominantly by upregulating GLUT4 delivery to the sarcolemmal membrane thereby increasing glucose uptake, the rate limiting step in glucose metabolism (Holman and Cushman, 1994, Leto and Saltiel, 2012). Additionally, high insulin and glucose availability have been shown to limit fatty acid oxidaiton (Wagenmakers, 1996), and have a general stimulatory effect on mitochondrial protein expression (Boirie et al., 2001, Stump et al., 2003).

The predominant metabolic effect of GCs and catecholamines is to increase the availability of glucose during times of stress (Newton, 2000, Barth et al., 2007). Although the regulatory role of both GCs and cathecholamines on mitochondrial function has not been widely investigated, there are some studies reporting that GCs (Weber et al., 2002, Scheller et al., 2000, Morgan et al., 2016) and catecholamines (Shukla et al., 2000) upregulate mitochondrial oxidative metabolism.

The best studied endocrine regulators of mitochondrial activity are the THs which are important metabolic regulators, and associations between TH levels, body weight and energy expenditure in adults are clear (Mullur et al., 2014). Human and animal studies investigating the effects of THs on specific mitochondrial protein expression and activity have suggested several mechanisms by which THs increase metabolic rate. First, THs have been associated with an increase in expression and activity of components of the TCA cycle and ETS (Winder, 1979, Clement et al., 2002). Secondly, THs increase metabolic rate through decreased oxphos efficiency, both by altered IMM leak and increased UCP and ANT expression (Dummler et al., 1996, Barbe et al., 2001, Pehowich, 1999). Additionally, THs are involved in promoting lipid metabolism via the inhibition of the pyruvate dehydrogenase complex and activation of AMPK signalling (Lombardi et al., 2009, Irrcher et al., 2008, Clement et al., 2002).

1.2.7 Mitochondrial dysfunction and metabolic syndrome

As central coordinators of energy balance with substrate uptake and utilisation, mitochondrial damage and dysfunction have been linked to the metabolic syndrome (Duchen, 2004). A reduction in mitochondrial density, due to decreased mitochondrial number and size, a more fragmented mitochondrial network and structural abnormalities have been reported in tissues from patients with obesity and insulin resistance (Kelley et al., 2002, Bach et al., 2003, Hernandez-Alvarez et al., 2010). Whether the reduction in oxidative capacity seen in type 2 diabetes, both at basal level and in response to exercise, is simply down to the reduced mitochondrial content in muscle is unclear (Boushel et al., 2007, Antoun et al., 2015, Ritov et al., 2005, Burns et al., 2007). As well as morphological abnormalities, a reduction in ETS activity, ATP-synthase content and maximal mitochondrial respiration rates have been reported in muscles of diabetic patients (Hernandez-Alvarez et al., 2010, Antoun et al., 2015, Ritov et al., 2005).

Whether mitochondrial dysfunction is a cause or consequence of insulin resistance is a topic of debate (Muoio and Neufer, 2012). A reduction in mitochondrial density specifically in the subsarcolemmal region of muscle fibres may contribute to insulin resistance by affecting substrate delivery and signal transduction (Ritov et al., 2005). Additionally, altered lipid metabolism and increased ROS production in obesity may down-regulate the insulin signalling pathway (Muoio and Neufer, 2012). Metabolic syndrome is associated with aging, which itself is associated with mitochondrial defects including reduced enzyme activity, lower respiratory capacity and increased ROS production (Sun et al., 2016). Mitochondria, therefore, are of interest in understanding any underlying predisposition to symptoms of the metabolic syndrome. As discussed in Section 1.1, fetal growth restriction has been associated with predisposition to symptoms of metabolic syndrome. In addition, as summarised in Table 1.1, numerous animal studies have demonstrated a link between prenatal insult and mitochondrial dysfunction of the postnatal offspring. However, whether these changes occur predominantly *in utero* and continue until adulthood or arise postnatally as a result of other programmed metabolic changes and/or when additional stress is placed on the system, is not well understood.

Prenatal insults are likely to have tissue-specific effects as when fetal growth is compromised, blood is preferentially shunted towards more vital organs such as the brain and heart, leaving

other tissues including skeletal muscle more vulnerable to insult (Brown, 2014). Skeletal muscle is a highly metabolically active tissue and, hence, any impairment in its energetic potential is likely to result in a predisposition to metabolic syndrome (Brown, 2014, Hoppeler, 1999). However, in order to further investigate the role of mitochondria in intrauterine programming of metabolism and to determine the mechanistic pathways involved, a better understanding of the normal developmental profile of mitochondria is required, as currently very little is known of the ontogeny of mitochondrial function during intrauterine development.

Table 1.1 Intrauterine programming of mitochondrial dysfunction in postnatal offspring

Challenge *in utero*	**Species**	**Tissue**	**Mitochondrial Dysfunction**	**Reference**
Maternal high fat diet	Rat	Skeletal muscle (soleus)	↓CI and CIII (g,a), ↓NRF1 (g)	(Pileggi et al., 2016)
	Rat	Skeletal muscle (soleus)	↓CI-IV and ATP-synthase (p)	(Latouche et al., 2014)
	Rat	Heart	↑mtDNA	(Mdaki et al., 2016)
	Rat	Liver	↓mtDNA, ↓PGC1α (g)	(Burgueno et al., 2013)
	Rat	Kidney	↓mtDNA	(Taylor et al., 2005)
Maternal obesity	Rat	Skeletal muscle (gastrocnemius)	↓MFN1 (g), ↓PGC1α (g)	(Borengasser et al., 2014)
	Rat	Liver	↓MFN2 (g)	(Borengasser et al., 2014)
Maternal low protein diet	Rat	Skeletal muscle (vastus lateralis)	↓CS (a), ↑CI-IV (a normalised to CS), ↑SOD1, SOD2, catalase (p)	(Tarry-Adkins et al., 2016)
	Rat	Skeletal muscle (quadriceps)	↓mtDNA	(Park et al., 2004)
	Rat	Liver	↓mtDNA	(Park et al., 2003)
	Mouse	Skeletal muscle (gastrocnemius)	↑CIV (p,g,a normalised to CS), ↓density	(Jousse et al., 2014)
	Mouse	Adipose tissue	↑PGC1α, NRF1, UCP2 (g), ↑density	(Jousse et al., 2014)
Undernutrition	Mouse	Skeletal muscle (various)	↓respiratory capacity, ↓density	(Beauchamp et al., 2015a)
	Mouse	Heart	↓respiratory capacity	(Beauchamp et al., 2015b)
Maternal diabetes	Rat	Heart	↓respiratory capacity, ↓mtDNA	(Mdaki et al., 2016)
Maternal hypoxia	Guinea pig	Heart	↓CIV (p,g,a), ↓PGC1α (g)	(Al-Hasan et al., 2014)
Uteroplacental insufficiency	Rat	Skeletal muscle (unspecified)	↓carbohydrate oxidation and ATP production	(Selak et al., 2003)
	Rat	Skeletal muscle (unspecified)	↓CI, ANT1, ATP-synthase (g)	(Lane et al., 1998)
	Pig	Skeletal muscle (unspecified)	↓CS (g), ↓CIV (g), ↓biogenesis	(Liu et al., 2012)

CI-IV, ETS complexes I-IV; NRF1, nuclear respiratory factor 1; mtDNA, mitochondrial DNA; MFN1/2, mitofusin 1/2; PGC1α, Peroxisome proliferator-activated receptor γ coactivator 1α; SOD1/2, superoxide dismutase 1/2; UCP2, uncoupling protein 2; ANT1, adenine nucleotide translocase 1; CS, citrate synthase; (p) protein abundance; (g) gene expression; (a) activity.

1.3 Fetal development and maturation

Over late gestation, physiological systems of the fetus need to undergo maturational processes to prepare for postnatal life. In particular, organs including the lungs, gastro-intestinal tract and kidneys must be able to immediately take over the role of the placenta in supplying metabolic substrates and oxygen and in removing waste products (Fowden et al., 1998). In babies born preterm, immaturity of these organ systems and of the brain and immune system dramatically increase the risk of acute neonatal illness and mortality which highlights the importance of prepartum tissue maturation in ensuring a smooth transition to extrauterine life (Behrman and Butler, 2007). Several of the key maturational processes essential for neonatal viability are known to be driven by fetal hormones, in particular by GCs (Fowden et al., 1998).

1.3.1 Endocrine regulation

1.3.1.1 Glucocorticoids

In the adult, GCs are generally released in response to physiological or mental stress and carry out roles including immunosuppression and the regulation of several metabolic processes to increase the glucose availability (Newton, 2000). Glucocorticoids are also secreted in response to stressful conditions in the fetus (Giussani et al., 2011, Roelfsema et al., 2005). However, they have additional roles *in utero* as they act both as the normal maturational signal towards term and as programming signals in determining the physiological phenotype of the offspring in relation to the prevailing environmental conditions *in utero* (Fowden et al., 1998, Kapoor et al., 2006).

Cortisol is the predominant GC circulating in both humans and sheep (Challis et al., 2001). It is synthesised in the zona fasciculata of the adrenal cortex and secreted in response to adrenocorticotropin hormone (ACTH) released from the pituitary gland under the control of hypothalamic corticotropin releasing hormone (CRH, Figure 1.5; Newton, 2000). The hypothalamic-pituitary-adrenal (HPA) axis is controlled, in part, by negative feedback of cortisol which inhibits production of CRH and ACTH (Figure 1.5). This results in cortisol concentrations being maintained within a narrow range around a set point, at least in adult animals (Akana et al., 1985).

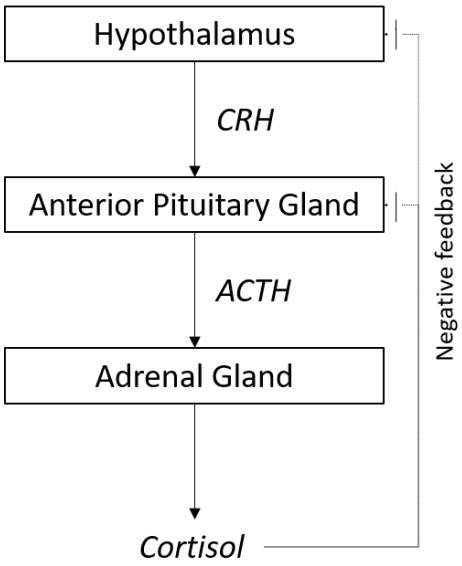

Figure 1.5 A simplified diagram of the hypothalamic-pituitary-adrenal axis. CRH, corticotropin releasing hormone; ACTH, adrenocorticotropic hormone (Newton, 2000).

The fetal HPA axis is functional from early on in gestation although fetal cortisol concentrations are lower than maternal values for most of pregnancy (Wintour et al., 1975). However, in every species studied to date, there is a surge in the circulating concentration of cortisol in the fetus just before term, which often exceeds maternal values (Fowden et al., 1998). The mechanism for the prepartum rise in cortisol appears to involve species-specific positive and negative influences on the HPA axis acting through central and peripheral mechanisms (Wood and Keller-Wood, 2016). In fetal sheep, the concentrations of CRH and ACTH rise towards term and the adrenal glands become progressively more responsive to ACTH over late gestation with increases in ACTH receptor abundance and activity of the enzymes involved in cortisol synthesis (Saoud and Wood, 1996, Castro et al., 1992, Jacobs et al., 1994, Fraser et al., 2001). In the last few days before term, the sensitivity to the negative feedback of cortisol on ACTH production seen earlier in gestation (Wood and Rudolph, 1983) is also reduced significantly (Wood, 1988). This may be achieved by downregulation of the glucocorticoid receptor (GR) or reducing bioavailability of cortisol in the pituitary gland (Challis et al., 2001). Thus, the prepartum increase in fetal cortisol concentrations is a normal developmental event unrelated to stress of the fetus.

As lipophilic steroid hormones, GCs can bidirectionally cross the placenta, and therefore a proportion of the circulating fetal GC pool is maternal in origin before term, with the amount

varying by species and gestational age (Migeon et al., 1957, Hennessy et al., 1982). Despite the protection offered by the activity of placental 11β-hydroxysteroid dehydrogenase-2 which converts cortisol to its inactive metabolite, cortisone (Stewart et al., 1995, Wyrwoll et al., 2009), high maternal GC concentrations can lead to fetal GC overexposure and alter HPA activity with detrimental impacts on offspring development both in the short- and long-term (Seckl, 2004, Wood and Rudolph, 1984). Similarly, adverse intrauterine conditions which raise fetal GC concentrations independently of the mother in late gestation affect fetal development with potential consequences long after birth.

In the fetus, the role of cortisol is predominantly to initiate the switch from cell proliferation to terminal differentiation (Fowden et al., 1998). As such, fetuses exposed to high levels of cortisol before term, due to stress during pregnancy, are more likely to be born small for gestational age (Jensen et al., 2002). In addition, in some species such as sheep, the cortisol surge also drives parturition (Liggins, 1969). Cortisol can act directly, but also many of the cortisol-driven maturational changes are mediated by other hormones, whose bioavailiabilty or receptor expression is regulated by cortisol. Examples include insulin-like growth factors, leptin and triiodothyronine (T_3; Figure 1.6; Fowden et al., 1998).

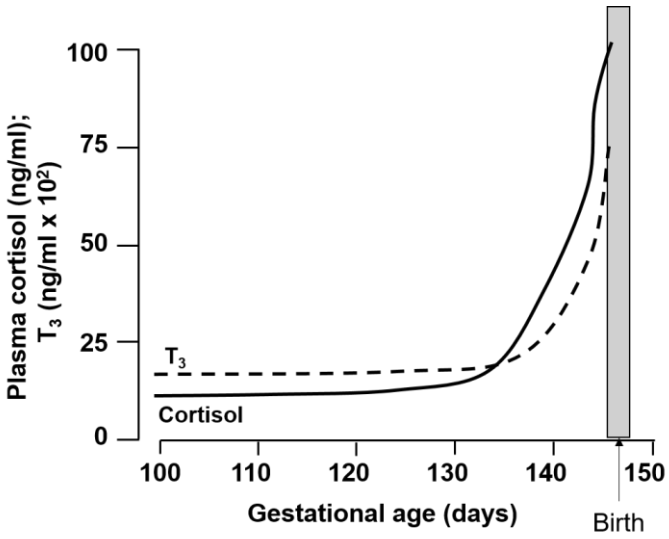

Figure 1.6 The profile of plasma cortisol and tri-iodothyronine (T_3) in the ovine fetus over late gestation (Polk, 1995)

1.3.1.2 Thyroid hormones

Thyroid hormones act on almost every cell in the body and carry out numerous roles in a regulated cell-specific and time-dependent manner (Brent, 2012). As discussed in Section 1.2.6, THs play an important role in upregulating metabolic rate in adult organisms (Mullur et al., 2014). Additionally, in adult tissues, including skeletal muscle, THs are involved in normal cell proliferation, homeostasis and repair (Milanesi et al., 2016, Wu and Koenig, 2000) and can alter the contractile properties of skeletal muscle (Larsson et al., 1994, Salvatore et al., 2014). They also have an important role in the development of fetal tissues including skeletal muscle (Forhead and Fowden, 2014).

Thyroid hormones are produced from the thyroid gland under control of the hypothalamic-pituitary-thyroid axis (HPT; Figure 1.7). The predominant secretory product of the thyroid gland in sheep and humans is thyroxine (T_4), a relatively biologically inactive molecule in adults (Gereben et al., 2008). TH transporter proteins are required for the uptake of THs into cells, the best characterised of these being the TH-specific transporter, monocarboxylate transporter 8 (MCT8; Visser et al., 2011). Within peripheral tissues, further metabolism of the THs by deiodinase enzymes alter the local TH bioavailability (Figure 1.7). Deiodination of T_4, by type 1 deiodinase (D1) in liver is believed to supply the majority of the circulating T_3, the most active form of TH (Gereben et al., 2008). D2, present in tissues including skeletal muscle, increases the local bioavailability of T_3 (Figure 1.7) via the same mechanism as D1 (Gereben et al., 2008). Type 3 deiodinase (D3) is also expressed in skeletal muscle and inactivates THs through the conversion of T_3 to di-iodothyronine (T_2) and T_4 to reverse T_3 (rT_3; Figure 1.7) which cannot bind to the thyroid hormone receptor (THR; Gereben et al., 2008). In the human fetus, T_4, T_3 and thyroid-stimulating hormone (TSH) are produced early in pregnancy and continue to rise during gestation (Thorpe-Beeston et al., 1991a). The timings of TH system development in the sheep is similar to the human (Forhead and Fowden, 2014).

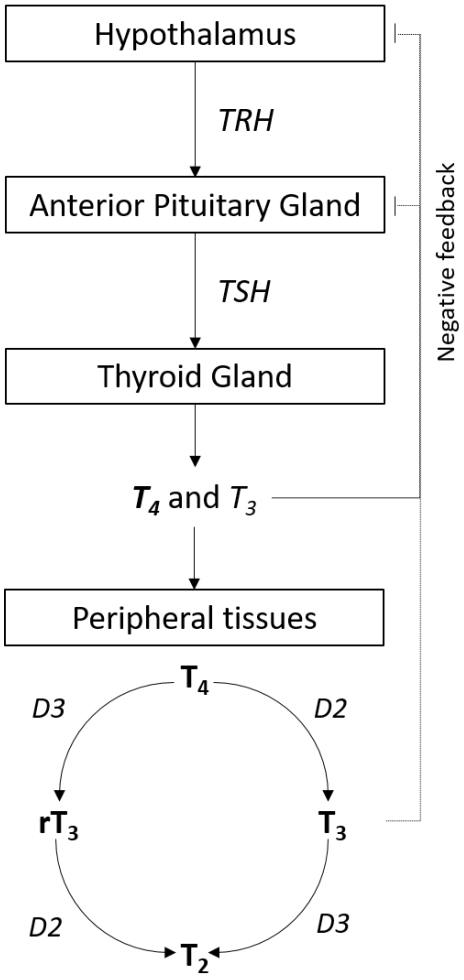

Figure 1.7 A simplified diagram of the hypothalamic-pituitary-adrenal axis. TRH, thyrotropin releasing hormone; TSH, thyroid-stimulating hormone, T_4, thyroxine; T_3, tri-iodothyronine; rT_3, reverse T_3; D2 and D3, deiodinases (Forhead and Fowden, 2014).

A further mechanism of regulating TH activity is sulfation of THs by sulfotransferases, which prevents T_3 binding to the TH receptor (THR) and increases the likelihood of T_4 conversion to rT_3 (Visser, 1994). Sulfatases can convert the sulfated hormones back to their biologically active forms, and this may be an important source of tissue T_3 during fetal development (Santini et al., 1992). Overall, the response to THs is highly complex, dependent not only on the activity of the HPT axis maintaining the circulating TH pool, but also on the cell-specific, environmentally and temporally regulated expression of deiodinases, sulfotransferases, sulfatases and transcriptional regulatory elements (Wu and Koenig, 2000, Silva and Larsen, 1985, Visser, 1994). As in adult tissues, bioavailability of TH in the fetus is under the control of deiodination and sulfation (Hurd et al., 1993, Wu et al., 1993, Polk et al., 1988).

As shown in Figure 1.7, the HPT axis is subject to negative regulation in order to tightly control the circulating TH levels, in a similar manner to the regulation of the HPA axis. Ligand bound THR suppresses the expression of TSH and thyrotropin releasing hormone (TRH). Conversely, the THR without ligand is thought to upregulate the expression of TSH and TRH (Wu and Koenig, 2000). In the fetus, this negative feedback mechanism is evident from early in gestation (Polk et al., 1991, Greenberg et al., 1970). The importance of maintaining the optimal level of circulating THs *in utero* is shown as both under- and over-exposure to THs result in altered development (Hernandez et al., 2006, Erenberg et al., 1974). Additionally, fetal T_3 concentrations are low in cases of IUGR (Thorpe-Beeston et al., 1991b). However, there is a surge of T_3 towards term (Figure 1.6) which has led to the hypothesis that the set point is higher in the fetus than in the adult (Ballabio et al., 1989). This rise in T_3 in fetal sheep is driven, at least in part, by cortisol upregulating hepatic and renal D1 and downregulating renal and placental D3 activity which, during most of gestation, converts the majority of T_4 to biologically inactive rT_3 (Forhead et al., 2006). After birth, the rise in T_3 continues, stimulated upon exposure to the cold and responsible for initiating thermogenic mechanisms (Clarke et al., 1997).

In some species including humans, maternal TH can cross the placenta and contribute to the fetal TH pool (Chan et al., 2009), despite the placental expression of D3 (Forhead and Fowden, 2014). In these species, maternal THs are likely to be important in development, particularly before the fetal HPT axis becomes active, and can also compensate for fetal hypothyroidism, minimising any detrimental effects of fetal TH deficiency on development (Chan et al., 2009). However, in some species, including sheep, THs cannot cross the placenta (Forhead et al., 2009), which makes the fetus dependent on its own thyroid gland and, hence, a useful experimental model for studying the effects of hypothyroidism *in utero*.

THs are important to development throughout gestation, influencing metabolism, growth and differentiation (Erenberg et al., 1974, Fowden and Silver, 1995). THs are particularly crucial to the development of the central nervous system (Chan et al., 2009), but they are also involved in maturation of tissues including the liver, lungs and heart, often acting in cooperation with cortisol (Mai et al., 2004, Erenberg et al., 1974, Forhead and Fowden, 2014). THs have also been shown to play an important role in development of fetal skeletal muscle (Lee et al., 2014) which is discussed in more detail below (Section 1.3.2).

Hormone molecular signalling pathways

The action of cortisol is mediated through its binding to cytosolic receptors which then rapidly translocate into the nucleus (Guertin et al., 1983). The predominant regulatory mechanism of GCs is in up- or down- regulation of transcription of its target genes (Guertin et al., 1983, Groner et al., 1983). The hormone-receptor complex binds with the GC responsive element upstream of the target gene and interactions with chromatin and other nuclear regulatory proteins ensure an appropriate cell- and environment-specific response (Rousseau, 1984, Oakley et al., 1996). Further GC-mediated cellular response mechanisms are thought to be via regulating mRNA stability and altering expression at the level of translation (Newton et al., 1998, Lee et al., 1988, Han et al., 1990, Meyuhas et al., 1987).

Thyroid hormones can exert effects in the cell directly at the plasma membrane or in the cytoplasm but, like GCs, the predominant mechanism involves T_3 binding to the nuclear THR to give genomic effects (Anyetei-Anum et al., 2018). THRs are encoded by 2 genes to generate THRα and THRβ isoforms, of which THRα is the predominant form expressed in pre- and postnatal skeletal muscle (White et al., 2001). Like the GR, the THR is a ligand-activated transcription factor which mediates a cellular response through the activation or repression of target gene expression (Wu and Koenig, 2000). Conversely, unliganded THR suppresses the normal T_3 signalling, for example through their binding corepressors at a positively-regulated TH locus (Wulf et al., 2008). Upon binding T_3, THRs bind to the DNA either as homodimers or as a heterodimer with a retinoid X receptor, and also bind cofactors to mediate the suitable cellular response to the hormone (Wulf et al., 2008). This direct binding and transcriptional regulation accounts for the more rapid TH response which is apparent within 6 hours, followed by an indirect response mediated by intermediate regulators after a 48 hour lag period (Weitzel et al., 2001).

As discussed in Section 1.2.6, the association between thyroid hormones (TH) and mitochondrial biogenesis has been well documented. In this example, the rapid response of TH signalling is thought to be due to TH-mediated transcriptional regulation of target genes such as the transcriptional coactivator, PGC1α (Weitzel et al., 2001). Specifically, upon T_3 binding to the nuclear THR, the complex binds to a thyroid response element (TRE) in the promoter region, 4 kilobases upstream of the transcriptional start site of PGC1α (Wulf et al., 2008). Expression is upregulated, at least in part, due to an increase in histone acetylation and corresponding opening of the chromatin structure (Wulf et al., 2008). Some of the early

response genes, including PGC1α, have been hypothesised to be responsible for regulating the second wave of TH-induced gene expression, involving genes with, as yet, no identified TRE such as NRF1 and 2 (Weitzel and Iwen, 2011, Wulf et al., 2008). Overall, several factors are involved in mediating TH-driven mitochondrial biogenesis, but PGC1α is thought to be a crucial element in this pathway and its regulation is relatively well understood. Whether this is true in fetal skeletal muscle, however, is unclear.

1.3.2 Skeletal muscle development

The majority of skeletal muscle fibres are formed during mid-gestation, with myoblast proliferation replaced by terminal differentiation of the fibres during late gestation (Brown, 2014). Thus the number of fibres is generally set *in utero*, with late gestation and postnatal muscle growth involving predominantly hypertrophy and not hyperplasia (White et al., 2010). Therefore, conditions during intrauterine development can have consequences on muscle structure and functional capacity, as well as whole body metabolism long after birth (Brown, 2014).

Late gestation is important in skeletal muscle structural and functional development (Javen et al., 1996). Both cortisol and THs are reported to be involved in the maturation of skeletal muscle over this period. Both these hormones are required for the downregulation of insulin-like growth factor-I (IGF-I) expression in skeletal muscle, thereby playing an indirect role in the transition from proliferation to differentiation (Forhead et al., 2002). T_3 in particular is also believed to have a direct role in the terminal differentiation of fibres through upregulating myogenesis genes, as shown *in vitro* (Carnac et al., 1992). Ovine fetuses thyroidectomised (TX) during the second half of gestation show multiple differences in skeletal muscle development compared with sham-operated controls. Muscles of TX fetuses have reduced protein and DNA content, slower contraction and relaxation times and a reduced contractile force (Erenberg et al., 1974, Finkelstein et al., 1991).

Muscle fibres are subdivided into 2 main classifications: type I fibres which are slow twitch fibres carrying out predominantly oxidative metabolism, and type II fibres which are fast twitch. The latter are further classified as type IIa, oxidative/glycolytic, and type IIx, glycolytic, fibres. The fibre types can be identified by their expression of different myosin heavy chain (MHC) isoforms: MHC-I, MHC-IIa and MHC-IIx (Yates et al., 2016). The fibre types demonstrate

distinct characteristics, for example type I fibres contain a higher abundance of mitochondria and have a higher rate of insulin-stimulated glucose uptake than type II fibres which contain more glycogen (Goodyear et al., 1991, Fernandez et al., 1995).

Muscles generally consist of a heterogeneous mixture of fibre types, with the ratio dependent on the muscle function and the frequency of neuronal stimulation, as well as TH exposure (Gambke et al., 1983). The different fibre phenotypes are expressed *in utero* but remain plastic into adulthood when an increase in the ratio of type I:type II fibres is seen in response to impaired TH signalling and exercise (Green et al., 1984b, Yu et al., 2000) whereas a decrease in the type I:type II ratio is associated with insulin resistance (Stuart et al., 2013). In precocial species, including sheep, development of both slow and fast twitch fibres must occur prior to birth to enable immediate neonatal muscle function (Finkelstein et al., 1991). The fibre type ratio is sensitive to prenatal insult; ovine hyperthermia, associated with fetal growth restriction, hypoxia and hypoglycaemia, has been shown to lower the proportion of oxidative fibres (Yates et al., 2016). THs appear to be important in regulating fibre type with hypothyroidism during ovine fetal development resulting in a shift towards an increased proportion of type II fibres compared with euthyroid controls (Finkelstein et al., 1991). Both IUGR and reduced fetal TH exposure impair the structural and functional development of fetal skeletal muscle as well as the oxidative capacity of the tissue.

1.3.2.1 Skeletal muscle chosen for this study

For the current study 3 muscles were used: biceps femoris (BF), semitendinosus (ST) and superficial digital flexor (SDF). The BF and ST are commonly studied muscles in the fetus (Yates et al., 2016, Jellyman et al., 2012, Forhead et al., 2009) whereas the SDF has not been the focus of much research, particularly in the sheep. All 3 are hind limb muscles of mixed fibre type. However, they carry out distinct roles, have different maximal power outputs and elasticity parameters and, therefore, may show different maturational profiles towards term (Wilson and Lichtwark, 2011). The BF and ST are both hamstring muscles, used for extending the hip and flexing the stifle during locomotion (Frandson et al., 2013). They are located adjacent to one another and have a similar fibre type ratio (Yates et al., 2016). They do, however, differ in their innervation, blood supply and developmental profile of myogenic markers (Yates et al., 2016, Woodley and Mercer, 2005, Rab et al., 1997, Deveaux et al., 2003). The SDF is located at the back of the calf and forms part of the muscle group involved in

preventing ankle extension while walking (McGuigan and Wilson, 2003). The role of the SDF, as a muscle-tendon unit, is in increasing the efficiency of locomotion, displaying substantial elastic energy recovery, while the larger, proximal muscles including the BF and ST are required for increasing workload when running (McGuigan and Wilson, 2003, McGuigan et al., 2009). Thus, the BF and ST can generate more mechanical power through fibre shorting, whereas the SDF generates force through predominantly isometric contraction (Biewener, 1998). In addition, the structure of the SDF is quite different to the BF and ST; the SDF contains accessory ligaments throughout the muscle joined with short, multipennate, fibres in contrast to the parallel fibre arrangement of the fusiform BF and ST (McGuigan and Wilson, 2003, Butcher et al., 2010).

Studying these muscles with their differing structure and function should give an insight into whether there are muscle specific differences in the development and regulation of mitochondrial function over late gestation.

1.3.3 Fetal metabolism

The transition to extrauterine life is associated with a significant metabolic challenge. Firstly, the energy demands are rapidly upregulated as organs need to take on new roles; skeletal muscle must be able to support locomotion and thermogenesis for the first time. The increased energy requirement for the new postnatal activities is predominantly provided by the mitochondrial supply of ATP via oxphos, and as such, the oxygen consumption of certain tissues including liver and brain increases rapidly at birth (Klein et al., 1983). Furthermore, in tissues like adipose tissue increased mitochondrial activity occurs for non-shivering thermogenesis, by which energy is released as heat by uncoupling the mitochondrial proton gradient from ATP production (Simonyan et al., 2001). However, this is not the only challenge during the perinatal period; there is an increased risk of excessive ROS production and the associated oxidative damage due to fluctuating partial pressure of oxygen (pO_2) associated with the uterine contractions of labour, followed by the rise in pO_2 after birth with the onset of pulmonary gas exchange (Rogers et al., 1998, Minai et al., 2008). However, relatively little is known about how fetal mitochondria prepare for the challenges of birth and neonatal life.

1.3.3.1 Substrate availability

Metabolic development in terms of substrate delivery, production and storage is relatively well understood (Jones and Rolph, 1985). Fetal metabolism relies predominantly on carbohydrates, with the majority of fetal glucose obtained from the maternal circulation (Hay et al., 1981, Morriss et al., 1973). At birth, however, the neonate must be able to access a supply of metabolic substrates before the onset of enteral nutrition (Fowden et al., 1998). During late gestation, there is a cortisol-driven increase in glycogen deposition in tissues including the liver and skeletal muscle, alongside a rise in the activity of glycogenolytic enzymes (Barnes et al., 1978, Jones and Rolph, 1985, Fowden et al., 1991). The fetal expression of hepatic and renal gluconeogenic enzymes has also been reported to increase towards term in a cortisol-dependent manner (Fowden et al., 1993), with gluconeogenesis responsible for around 75% of the glucose requirements of the neonatal ruminant (Nafikov and Beitz, 2007). At birth, therefore, skeletal muscle can draw initially on its own glycogen stores as well as obtaining glucose from the circulation. This is reflected in the skeletal muscle and liver glycogen stores being rapidly diminished within hours of birth (Mellor and Cockburn, 1986).

In addition to glucose, adult skeletal muscle metabolises lipids. Fatty acids are able cross the placenta from maternal to the fetal circulation in some species (Hull, 1975). However, in sheep, the role of lipids in fetal metabolism, in particular lipids of maternal origin, is thought to be minimal (James et al., 1971). Fetal skeletal muscle does, however, have the capacity for lipid oxidation and therefore may metabolise FAs when glucose levels are low, in line with the metabolic flexibility seen in adult tissues, as discussed in Section 1.2.1.1 (James et al., 1971, Morriss et al., 1973, Beatty and Bocek, 1970). The fetus has been shown to be capable of lipogenesis and, as with glycogen, lipid deposition occurs during fetal maturation predominantly in adipose tissue and liver, but also in skeletal muscle (Hull, 1975, Christie et al., 1985, Beatty and Bocek, 1970). At birth, lipid mobilisation due to neural stimulation of adipocytes and the loss of prostaglandin inhibition (Mostyn et al., 2003) results in a rapid increase in the circulating FA concentration (Vanduyne et al., 1965) and lipids become an important source of fuel postnatally (Mellor and Cockburn, 1986). Fatty acids, both from mobilisation of stores laid down during fetal life, and from intake of the high-fat content colostrum, help to preserve the carbohydrate stores of the neonate (Mellor and Cockburn, 1986).

1.3.3.2 Mitochondrial development

Relatively few studies have investigated mitochondria during development. Those which have, have used a number of species and different tissues and the changes in mitochondrial density, structure and function are summarised in Table 1.2. Some of the developmental changes in fetal mitochondria may be regulated by maturational hormones. THs are important for regulating whole body fetal oxygen consumption (Fowden and Silver, 1995, Lorijn et al., 1980), likely to be largely due to the TH acting on skeletal muscle (Forhead and Fowden, 2014). THs are also important for the upregulation of mitochondrial protein content and oxphos capacity in fetal porcine muscle, with a TH-dependent increase in ANT possibly playing a role in regulating metabolic rate (Herpin et al., 1996). Both cortisol and T_3 have been implicated in the increased UCP expression in adipose tissue (Mostyn et al., 2003, Gnanalingham et al., 2005a, Gnanalingham et al., 2005b, Schermer et al., 1996). However, few studies have looked at skeletal muscle mitochondrial function during the perinatal period, and little is known about its endocrine regulatory mechanisms.

Table 1.2 Mitochondrial changes during development

Species	**Tissue**	**Developmental period studied (proportion of gestation or incubation period)**	**Mitochondrial change during development**	**Reference**
Human	Heart	~0.2 to ~0.35	↑CS (a), ↑CIV and ATP synthase (a,p), ↑mtDNA	(Marin-Garcia et al., 2000)
Chick	Heart Skeletal muscle (hind limb)	0.4 to 1.0 0.5 to 1.0	↑ CII and CIV (a) ↑CII and CIV (a)	(Greenfield and Boell, 1968)
Sheep	Perirenal adipose tissue	0.55 to 0.65	↑density	(Gemmell and Alexander, 1978)
Rat	Brain	0.65 to 1hour postnatal	↑RCR	(Nakai et al., 2000)
Human	Skeletal muscle (quadriceps)	Neonates: born preterm to full-term; 0.65 to 1.0	↑respiratory capacity, ↑CS (a)	(Sperl et al., 1992)
Rat	Liver	0.7 to 10 days postnatal	↑CII and III (a)	(Jakovcic et al., 1971)
Sheep	Perirenal adipose tissue	0.9 to 1.0	↑UCP1 (p)	(Mostyn et al., 2003)
Rabbit	Heart	0.9 to 4 days postnatal	↑density, ↑cristae density	(Smith and Page, 1977)

CS, citrate synthase; CI-IV, ETS complexes I-IV; mtDNA, mitochondrial DNA; UCP1, uncoupling protein 1; (p) protein abundance; (a) activity.

1.4 Aims and Hypotheses

The first hypothesis of this thesis has two inter-related parts: (i) that there would be an increase in mitochondrial number and oxidative capacity in fetal skeletal muscle towards term in preparation for the increased energy demands immediately after birth and (ii) because this would increase the potential for excessive ROS production and oxidative damage during labour and delivery, there would be a simultaneous upregulation of mitochondrial mechanisms to protect against this risk. The second hypothesis was that cortisol and thyroid hormones would play an important role in regulating mitochondrial development in preparation for extrauterine life given their known roles in prepartum maturation of other physiological systems.

The specific aims of this project were two-fold:

1) To determine whether any changes occur in skeletal muscle mitochondrial number and function over the last third of gestation and in the first two days of neonatal life and
2) To determine whether the maturational hormones, cortisol and T_3 play a regulatory role in any of these ontogenic changes.

2 General Methods

2.1 Animals

All animal procedures were regulated under the UK Animals (Scientific Procedures) Act 1986 Amendment Regulations 2012 following ethical review by the University of Cambridge Animal Welfare and Ethical Review Body (AWERB). This thesis presents data from a total of 35 pregnant Welsh Mountain ewes of known gestational age (23 bearing twins and 12 bearing single fetuses) and 6 newborn twin lambs (1 from each of 6 ewes).

2.1.1 Breeding

The non-pregnant ewes were purchased from farms in Wales and were bred to Welsh Mountain rams on site in the research facility at the University of Cambridge. Welsh Mountain sheep are seasonal breeders, which naturally have a short breeding season of 3-4 months and an oestrus cycle of 14-19 days. In order to manipulate the breeding cycle and allow for time-dated pregnancy and breeding throughout the year, intra-vaginal progesterone sponges were used. Sponges were inserted for 12-14 days and at the end of this period pregnant mares' serum gonadotropin (PMSG; 8 IU/kg Folligon; Intervet UK Ltd, Cambridge, UK) was injected for those outside the natural breeding season. The drop in progesterone alongside high gonadotropin triggers oestrus to occur outside the normal period.

Gestational age was calculated from the first day on which the ewe had a raddle-ink mark. Ultrasound scans were carried out after 60, 80 and 100 days in order to confirm pregnancy and determine how many fetuses the ewe was carrying.

2.1.2 Housing and Husbandry

All pregnant ewes were group housed. Ewes were preferentially kept outside in the pasture or, during winter, were kept in a barn. Ewes kept indoors had free access to hay and water. The well-being of the ewes was routinely checked.

2.2 Surgery

Twenty-nine of the pregnant ewes underwent surgery to manipulate the fetal endocrine environment. The surgeries and post-surgery protocols are summarised in Table 2.1.

Table 2.1 Summary of animal experimental procedures used throughout the thesis.

Experimental Procedure	**Twin or Single**	**Gestational Age at Surgery**	**Age at Tissue Collection**	**Number of Ewes**	**Number of Fetuses/Newborns (male:female)**	**Chapter**
Unoperated Fetus	Twin	N/A	102-105dGA	6	6 (2:4)	3
Unoperated Newborn	Twin	N/A	1-2 days	6	6 (3:3)	3
Anaesthetised (sham procedure)	Single	130dGA	130dGA	1	1 (1:0)	5,6
Fetal TX or sham operation	Twin	102-105dGA	125-129dGA	6	6 TX (3:3) 6 sham (3:3)	3,4,6
Fetal TX or sham operation	Twin	102-105dGA	140-145dGA	6	6 TX (2:4) 6 sham (2:4)	3,4
Saline infusion or T_3 infusion	Twin	116-119dGA	127-130dGA	5	4 saline infused (4:0) 5 T_3 infused (3:2)	4,6
Saline infusion	Single	118-119dGA	128-131dGA	5	5 (3:2)	5,6
Cortisol infusion	Single	118-119dGA	128-131dGA	6	6 (3:3)	5

dGA: days of gestational age; TX: thyroidectomised

2.2.1 Preparation for Surgery

2.2.1.1 Sterilisation of surgical equipment

Catheters which were to be inserted into the fetal vein and artery were made from 1mm bore PVC tubing (Altec, St Austell, UK) cut to 1.2m in length. A 15cm piece of 0.86mm diameter PVC tubing (Microtube Extrusions, New South Wales, Australia) was inserted at one end of the catheter to a depth of 0.5cm and secured in place with cyclohexanone (Technicon, Dublin, Ireland). The seal was tested to ensure the join was secure and there were no air leaks. Catheters which were to be inserted into the maternal femoral artery were made from 1mm bore PTFE (Altec). These were cut to 1.2m and a 30cm mark drawn onto the catheter. All catheters were double bagged and gas-sterilised using ethylene oxide for 48 hours and then kept in room air for a minimum of 24 hours before use.

Surgical drapes, gowns and towels were packaged into metal drums to be steam-sterilised using an autoclave. Surgical instruments, sutures, swabs and diathermy tip were packed, wrapped in a drape and also steam-sterilised. Pins, blunt needles and trays, all required for the daily blood sampling of catheterised animals were steam-sterilised in self-seal sterilisation pouches.

2.2.1.2 Animal preparation

Ewes had an additional ultrasound scan immediately prior to surgery to confirm the number of fetuses and that there were no obvious complications. Ewes were brought into the holding pens at least 24 hours before the day of surgery in order to acclimatise them to where they would be held post-surgery. Here the ewes were in an individual pen with at least one other sheep in the same room. The ewes had free access to hay and water, until food (but not water) was withheld 18-24 hours before surgery in order to reduce the risk of regurgitation during surgery.

2.2.2 Surgical Procedures

On the day of surgery, after scanning, the ewes were brought into the pre-operative preparation room and their neck shorn in order to expose the position of the jugular vein. The shorn area was cleaned with ethanol and anaesthesia was induced by an intravenous bolus injection of Alfaxalone (1.5-2mg/kg Alfaxan; Jurox). The ewe was immediately transferred onto the preparation table in the supine dorsal position and, using a laryngoscope, intubated with an endotracheal tube (8.0mm ID, 10.9mm OD; 30mm cuff diameter Portex® Tracheal Tube; Smiths Medical International Ltd., Kent, UK). Anaesthesia was maintained by 1.5-2% isofluorane in oxygen (Isoflo; Zoetis, London, UK). The abdomen, from the bottom of the rib cage until the top of the hind limbs was shaved and, if the ewe was to be catheterised, the right flank was also shaved. Pre-surgery analgesia was given to the ewe as a subcutaneous injection (55mg carprofen; Rimadyl; Zoetis).

The ewe was then transferred into the surgery room and onto the operating table where the 4 limbs were secured to the table with adjustable ropes. From this point, the anaesthesia was maintained by 1.5-2% isofluorane in 5:1 oxygen:nitrous oxide mixture using positive pressure ventilation in an automatic set-up (Manley Pulmovent Model MPP; Ohmeda, GE Healthcare, Amersham, UK). The tidal volume was set at approximately 10ml/kg and pressure was 20cmH_2O. Waste gases were scavenged. Throughout the maintenance of anaesthetic the ewe was closely monitored and records taken of the heartrate, pO_2, pCO_2 and breathing rate at approximately 10 minute intervals. The oxygen flow rate or the percentage isofluorane could be adjusted accordingly.

All shaved areas were washed using swabs by wiping from the midline where the incision would be made and working outwards in order to cover the whole area. Initially, HibiScrub Surgical Scrub (4% w/v chlorhexidine gluconate diluted 1:10 in 80% ethanol; Mölnlycke Health Care Ltd., Lancashire, UK) was applied. Secondly, iodine solution (7.5% w/v povidone-iodine; Animalcare Ltd, York, UK) was applied and any excess removed before 100% ethanol was applied and the area thoroughly dried. From this point aseptic techniques were followed.

An incision (~15cm) was made through the abdominal skin to the side of the mammary vein, and any bleeding controlled using monopolar diathermy (Solstar Diathermy; G.U. manufacturing Co. Ltd., London, UK). The underlying fascia and peritoneum were cut to expose the uterus.

2.2.2.1 Thyroidectomy

Before making an incision into the uterus, each fetus was manipulated in order to make a small incision (~5cm) by the fetal head using the diathermy, avoiding any major vessels and placentomes. All membranes were cut and the head and neck were brought through the incision and clamps put in place to minimise amniotic fluid loss. A 1-2cm incision was made in the fetal neck and blunt dissection used to locate the thyroid glands which were then removed by cauterisation. The incision was sewn up using continuous stitching and the fetus placed back into the uterus. All membranes were brought together and tightly tied to prevent fluid loss and the uterus was sewn up by continuous infolding of the uterine wall. Intra-amnion antibiotics were given (560mg benzylpenicillin; Crystapen, Genus Pharmaceuticals, Newbury, Berkshire, UK). The whole procedure was then repeated on the second fetus, although after making the incision on its neck the thyroid glands were exposed but left intact.

The uterus was replaced and the peritoneum sewn up using interrupted stitches and the skin sewn using continuous stitching to allow the skin to heal (Polypropylene non-resorbable suture; Ethicon, Livingstone, UK). Ewes received intramuscular antibiotics of 15mg/kg Depocillin (Intervet UK Ltd) and 20mg/kg Terramycin (Zoetis). In some cases, where the ewes coughed post-surgery, this was supplemented with a third antibiotic: 2mg/kg Draxxin (Tulathromycin; Zoetis) given intramuscularly on the day of surgery and 3 days following surgery. A tubular bandage was put around the abdomen of the ewe for additional support (Tubigrip; Mölnlycke Health Care Ltd).

2.2.2.2 Catheterisation

After exposure of the uterus, each fetus was manipulated in order to make a small incision (5cm) by the fetal hindlimbs by diathermy. All membranes were cut and the hindlimbs were brought through the incision and clamps put in place to minimise amniotic fluid loss. An incision was made using the diathermy into the inner thigh between the knee and the femoral triangle. Blunt dissection was used to locate branches of the femoral artery and vein. Two pieces of ligature were wrapped around each vessel using an aneurysm needle and a clamp was placed onto the artery. A sterilised catheter was filled with saline (0.9%; Aqupharm; Animalcare Ltd) containing heparin (100units/ml; Wockhardt UK Ltd, Wrexham, UK) and the end cut to length (~10cm) diagonally to a point. A small horizontal cut was made into the artery using spring scissors and the catheter was inserted, the clamp removed and the

catheter end fed into the vessel towards the abdomen. The catheter was tied into place and the patency of the catheter tested by drawing blood into the catheter before flushing in 5ml heparin-saline, clamping under pressure and placing a sterilised pin into the end of the catheter. This was repeated with the fetal femoral vein. Antibiotics were given to the fetus (560mg benzylpenicillin); half were given via the venous catheter and half via the intra-amniotic route. The incision was closed around the protruding catheters which were subsequently secured to the fetal skin to minimise pull on the catheter due to fetal movements. The amnion and uterus were sewn up as described previously (Section 2.2.2.1) around the catheters. When applicable, the process was repeated on the second fetus, using catheters of different colours to differentiate between each fetus and the vein or artery. The catheters were exteriorised at the dorsal flank of the ewe, the uterus returned and the peritoneum and skin sutured as described in section 2.2.2.1.

An incision was made into the maternal femoral triangle and blunt dissection used to locate a branch of the superficial femoral artery. As with the fetal artery, a ligature was put in place around the vessel and a clamp put in place to cut the blood supply. A sterilised PTFE catheter was filled with heparin-saline and inserted 30cm through a small incision made into the vessel wall. The catheter was secured and 5ml heparin-saline was flushed through the catheter, clamped under pressure and pinned. The catheter was threaded subcutaneously to be exteriorised through the same point in the dorsal flank of the ewe as the fetal catheters and the incision at the leg was sutured using polypropylene non-resorbable suture (Ethicon) as for the abdominal skin. The ewe was turned onto her side and a PVC-coated, zip-opening bag sewn to the skin in which the exteriorised catheters were contained. Ewes received intramuscular antibiotics and a tubular bandage was used for support as described previously (Section 2.2.2.1).

2.2.3 Post-surgery care

The ewes were taken off anaesthetics and supplied with oxygen until they took breaths unaided. At this point the endotracheal tube was removed and they were transferred into a cot for recovery. They were closely monitored until they were standing and eating and were able to be transferred to the individual holding pen. Here they were given hay, water and concentrates (100g twice a day; Sheep Nuts #6; H&C Beart Ltd, King's Lynn, UK). On the 2 days

following surgery ewes were given a further dose of 15mg/kg Depocillin and their wellbeing was regularly checked. Pens were swept daily and cleaned thoroughly on a twice-weekly basis.

One week following surgery ewes carrying thyroidectomised fetuses had their tubigrip bandage removed and one week later the abdominal skin sutures were taken out. Pregnancy continued until 125-129d (n=6 ewes) or 140-145d (n=6 ewes). Those in the latter group were able to be group housed indoors following the removal of their sutures.

All ewes which had undergone catheterisation were kept in the individual holding pens until they were euthanised in order to maintain sterility.

2.2.3.1 Blood Sampling

All catheters were flushed daily with 5ml heparin-saline and a 0.4ml blood sample was taken from the fetal and maternal arteries in order to monitor the fetal and maternal well-being. As soon as possible after the sample was taken, blood glucose and lactate levels were measured using a YSI 2300 Stat Plus glucose and lactate analyser (YSI Incorporated, Ohio, USA) and blood pH, haemoglobin, pO_2, percentage oxygen saturation, pCO_2 and HCO_3 levels were measured using an ABL90 Flex Analyzer (Radiometer, Crawley, UK). In addition, throughout the infusion period (section 2.2.3.2) 4ml blood was taken from the fetal artery into heparin coated tubes. Samples were centrifuged at 5000rpm at 4°C for 5 minutes and the plasma stored at -20°C for future hormone analysis.

2.2.3.2 Infusion

Following a recovery period of at least 5 days after surgery a larger PVC-coated, zip-opening bag was secured to the tubigrip bandage over the position of the catheter-containing bag on the side of the ewe. The fetal vein catheters were connected to a syringe held in a pump set to infuse 3ml over a 24 hour period, with this set-up held in the larger bag. With the catheterised twin, one of each pair was randomly assigned to receive a continuous infusion of T_3 (8-12µg/kg/day; Sigma-Aldrich, Gillingham, Dorset, UK) while the other twin received a continuous saline infusion (0.9%NaCl, 3ml/day) into the femoral vein. The fetuses were infused for a 5-day period until they were 127-130d (Table 2.1). Singleton fetuses were randomly assigned to receive a continuous infusion of cortisol (2-3mg/kg/day Solu-Cortef

(Hydrocortisone as the sodium succinate); Pharmacia, Kent, UK) or a continuous saline infusion (0.9%NaCl, 3ml/day) into the femoral vein. The fetuses were infused for a 5-day period until they were 128-131d (Table 2.1).

2.2.4 Tissue and plasma collection

2.2.4.1 Fetuses

Before euthanasia of uncatheterised animals, a 10ml blood sample was taken from the maternal jugular vein, divided into heparin and EDTA coated tubes which were kept on ice. The ewes were euthanised by an intravenous overdose of anaesthetic (200mg/kg sodium pentobarbitone; Pentoject, Animalcare Ltd,). Immediately the breathing and the heartbeat had stopped, the abdomen and uterus were opened in order to expose the fetus(es). A 10ml blood sample was taken from the umbilical artery of each fetus which was divided into heparin and EDTA coated tubes and kept on ice. All blood samples were centrifuged at 5000rpm at 4°C for 5 minutes and the plasma stored at -20°C for future hormone analysis. Fetuses were euthanised by an injection of a lethal dose of sodium pentobarbitone into the umbilical vein (200mg/kg). The umbilical cord was tied and cut to deliver the fetus. With twins, it was randomised as to which twin (TX/sham or T_3/saline infused) was delivered first.

Immediately following fetal euthanasia, the fetus was weighed and biometric measurements taken including the crown-rump length (CRL) and limb lengths. Samples of the 3 skeletal muscle types, biceps femoris, semitendinosus and superficial digital flexor were immediately dissected and weighed. A portion from the centre of each muscle (Kohn and Myburgh, 2007) was collected into preservation medium (section 2.3.2). A second portion of the muscle, also from the central region was fix-frozen by being immersed in phosphate buffered saline (PBS; Oxoid Limited, Basingstoke, UK) in order to remove blood from the section, before transferring to isopentane, which had been pre-cooled using dry ice, for 20 seconds. The fix-frozen tissue was then stored at -80°C until required and the remaining tissue was snap-frozen in liquid nitrogen and stored at -80°C. Other tissues including the brain, heart, liver, lung, gastro-intestinal tract, kidneys, adrenal glands and gonads were also collected, weighed and fixed and frozen for separate studies beyond the scope of this thesis. All frozen samples were kept at -80°C.

2.2.4.2 Newborn Lambs

One lamb from a pair of 1-2 day old twins, where the ewe had not undergone any form of surgery, was selected randomly for tissue collection. A 10ml blood sample was collected from the jugular vein for hormone analysis. The lambs were euthanised by an intravenous overdose of anaesthetic (200mg/kg sodium pentobarbitone). Biometric measurements were taken, and tissues dissected, weighed and collected as for the fetuses.

2.3 Experimental Procedures

2.3.1 Plasma Hormone concentrations

Fetal and neonatal plasma hormone concentrations were measured in previously unthawed aliquots of heparinised plasma using immunoassays and samples were run in duplicate. Cortisol values were measured using a commercial enzyme-linked immunoassay for human serum and plasma (IBL International, Hamburg, Germany), previously validated for use with sheep plasma (Vaughan et al., 2016). Two control samples (68.7±1.5ng/ml and 214.3±4.5ng/ml) were run in duplicate across the 5 plates. From the results of the control samples the calculated inter-assay variation was 4.80% and the intra-assay variation was 2.65%. The limit of detection of the assay was 5.2ng/ml as determined by the value of 2 standard deviations subtracted from the zero standard value averaged across the 5 plates. The cross reactivity of the assay, as stated by the manufacturer, was 1.4% for corticosterone, 7% for 11-desoxy-cortisol, 0.4% for 17α-OH-progesterone and 0.9% for desoxycorticosterone which have been previously detected in fetal sheep plasma (Thomas et al., 1976, Jensen et al., 1988, Magyar et al., 1981).

Fetal total T_3 and T_4 were measured using radioimmunoassays (RIA; MP Biomedical; Santa Ana, USA) previously validated for use with sheep plasma (Lanham et al., 2011). For the total T_3 RIA kit, interassay variation was 7.59% and intra-assay variation was 2.28%. The limit of detection of the assay was 0.1ng/ml. The cross reactivity of the assay, as stated by the assay manufacturer, was 0.18% for T_4 and 0.44% for T_2. For the T_4 total mAb RIA kit, interassay variation was 4.57% and intra-assay variation was 3.04%. The limit of detection of the assay was 11.3ng/ml. The cross reactivity of the assay, as stated by the assay manufacturer, was 1% for T_3.

2.3.2 Biochemical Composition

2.3.2.1 Water content

100-200mg samples of frozen tissue were cut, weighed, allowed to defrost at room temperature and freeze-dried for 24 hours (Edwards Modulyo Freeze-Dryer System; Edwards Limited, Crawley, UK). Samples were reweighed and the percentage water content of the tissue was calculated.

2.3.2.2 Protein Content

Frozen skeletal muscle samples (55mg ± 10%) were cut on dry ice and placed in tubes for homogenisation (FastPrep Lysing Matrix A; MP Biomedical) with 300µl lysis buffer (20mM Trizma-hydrochloride (pH7.5), 150mM NaCl, 1mM Na_2EDTA, 1mM EGTA, 1% Triton, 2.5mM sodium pyrophosphate, 1mM β-glycerophosphate, 1mM sodium orthovanadate and containing cOmplete mini protease cocktail inhibitor (Sigma)). The samples were ribolysed at 6000rpm for 2x30 seconds with 5 minutes on ice in between. 200µl more lysis buffer was added, tubes were ribolysed for a further 30 seconds at 6000rpm and kept on ice for 20 minutes in order to dissociate the proteins. Tubes were centrifuged at 10,000rpm for 10 minutes at 4°C, the supernatant collected and centrifuged at 14,000rpm for 15 minutes at 4°C. The supernatant was collected and kept on ice.

The protein concentration of the samples was determined using a Bicinchoninic Acid (BCA) assay (Sigma). Bovine serum albumin (BSA; 1mg/ml; Sigma) was diluted to produce a standard curve on each 96-well assay plate. All samples from groups to be directly compared were run in duplicate on the same plate. Protein content is expressed as mg protein per gram tissue (wet weight) and as mg protein/mg dry weight.

2.3.2.3 Glycogen content

Samples of frozen tissue (~100mg) were powdered, weighed and homogenised in 500µl ice cold distilled water. 100µl homogenate was incubated in acetate buffer (pH4.5) at 55°C in a water bath for 10 minutes before amyloglucosidase (70 units/reaction) was added and incubated at 55°C for a further 10 minutes. Reaction mixtures were also set up for each sample omitting the amyloglucosidase. The reaction was halted upon addition of 500µl of 0.3M zinc sulphate and 0.3M barium hydroxide solutions (Sigma). The supernatant was collected after

contents were centrifuged for 10 minutes at 3000rpm. The glucose concentrations of the supernatants were measured using a YSI 2300 Stat Plus glucose and lactate analyser (YSI Incorporated) and the tissue glycogen content (mg) per gram of tissue wet weight and per mg dry weight was calculated.

2.3.2.4 Lipid Content

The lipid content of the BF muscle was determined using the Folch method (Folch et al., 1957). Frozen tissue chunks (~100mg) were cut into small pieces, weighed and ribolysed in 1ml Folch mixture (2:1 chloroform:methanol) for 6x30 seconds at 6000rpm in FastPrep tubes containing Lysing Matrix C (MP Biomedical). 200µl of water was added and the samples shaken for 1.5 hours. Tubes were centrifuged at 15000rpm for 10 minutes and 400µl was collected from the lipid phase into pre-weighed soda glass specimen tubes. The contents were dried at 37°C in a heat block overnight and the remaining lipid weighed after 24 hours. The lipid content is expressed as mg lipid/g tissue and mg lipid/mg dry tissue weight.

2.3.3 Respirometry

Respirometry was carried out as described previously for skeletal muscle samples (Pesta and Gnaiger, 2012, Kuznetsov et al., 2008). Immediately after euthanasia, a small section of all 3 muscles were collected into ice cold biopsy preservation medium (BIOPS; pH7.1 solution containing 10mM Ca-EGTA buffer, 0.1µM free Ca^{2+}, 1mM free Mg^{2+}, 20mM imidazole, 20mM taurine, 50mM K-MES, 0.5mM ditriothreitol (DTT), 6.56mM $MgCl_2$, 5.77mM ATP and 15mM phosphocreatine). Samples were kept in BIOPS medium on ice for dissection of the sample into 2-3mg pieces. Connective tissue was removed and the individual fibres teased apart by blunt dissection. Fibre plasma membranes were permeabilised in saponin solution (100µg/ml BIOPS; Sigma-Aldrich), gently rocking for 20 minutes at 4°C. Permeabilised samples were transferred into MiR05 (pH7.1 solution containing 20mM HEPES, 0.46mM EGTA, 2.1mM free Mg^{2+}, 90mM K^+, 10mM P_i, 20mM taurine, 110mM sucrose, 60mM lactobionate and 1g/l BSA) for 2 x 5 minute washes on ice to remove excess saponin and wash out intracellular metabolites.

Four Clark-type electrodes (Strathkelvin Instruments, Glasgow, UK) were used for the respirometry. Chambers were maintained at 37°C by water jackets connected to a water bath

and pump. 500µl MiR05 was added to each chamber, allowed to warm to 37°C and computer-calibrated to air-saturated respiratory medium following stirring (210.3µM oxygen) prior to each experiment. One permeabilised muscle sample was added to each chamber, which was then sealed ensuring all air bubbles were removed. After a baseline period, substrates were introduced into the chambers according to 3 different protocols as outlined in Figure 2.1 (Gnaiger, 2012).

Protocol 1) Malate (2mM; Sigma) and pyruvate (Py; 5mM; Sigma) were added followed by ADP (10mM; Sigma). Py, the product of glycolysis as the first stage in carbohydrate metabolism, is transported into the mitochondrion and converted to Acetyl-CoA which enters the TCA cycle (Figure 1.1). Thus, protocol 1 measured oxphos via complex 1, limited by flux via the TCA cycle (Gnaiger, 2012).

Protocol 2) Malate (2mM) and palmitoyl-carnitine (PC; 40µM; Sigma) were added before ADP (10mM). PC is transported into the mitochondrion and processed before entering the β-oxidation pathway (Figure 1.2). Oxygen consumption following this protocol is believed to be limited by the β-oxidation capacity (Gnaiger, 2012). Py was added subsequently, and the proportion of the maximal oxygen consumption accounted for by PC-supported oxygen consumption could be determined.

Protocol 3) Malate (2mM) and glutamate (10mM; Sigma) were added followed by ADP (10mM) and succinate (10mM; Sigma), a well-established protocol to measure the maximal total electron flux through complexes I and II of the ETS (Pesta and Gnaiger, 2012). Rotenone (0.5µM; Sigma), an inhibitor of complex I activity, was added and the chamber was reoxygenated after the addition of rotenone by lifting the seal for ~1 minute. Oxygen consumption was not significantly affected upon the addition of rotenone, and there were no differences between treatment groups which may be due to insufficient time of rotenone exposure for its uptake and inhibitory effect. Therefore, the results following rotenone addition have not been presented.

The rate of oxygen uptake was calculated after the addition of the tissue and each substrate. Results were excluded if the rate of oxygen uptake over the baseline period, before substrates were added, exceeded 0.001µmol oxygen/minute as this would indicate insufficient permeabilisation of the cell membrane. A measure of the leak state respiration was taken after the addition of substrate and before ADP. State 3 oxygen consumption was measured

when the rate of oxygen consumption stabilised following ADP addition. The respiratory control ratio (RCR) was then calculated as the ratio of respiration rate after the addition of ADP to the respiration rate before ADP. All RCR values for Py- and glut-supported respiration were within the limits of previously reported data, indicating good coupling between oxidation and phosphorylation and mitochondrial inner membrane integrity (Kuznetsov et al., 2008). All 3 protocols ended with the addition of cytochrome c (10µM; Sigma) in order to check the integrity of the outer mitochondrial membrane and results were excluded if there was an increase in oxygen consumption of 15% or more upon cytochrome c addition (Kuznetsov et al., 2008). The entry points of all the substrates are shown on sample traces in Figure 1.1.

Muscle samples were removed at the end of the protocol and the chambers were thoroughly washed with water and 70% ethanol to remove all traces of substrates before beginning a new experiment. After protocol 3, 100% ethanol was used for 45 minutes in order to remove all traces of rotenone. The samples were dried at 80°C for 48 hours and weighed in order to normalise the results to the tissue dry weight. Results are given as ADP-coupled oxygen uptake/mg dry weight.

Protocol 1: Carbohydrate oxidative metabolism

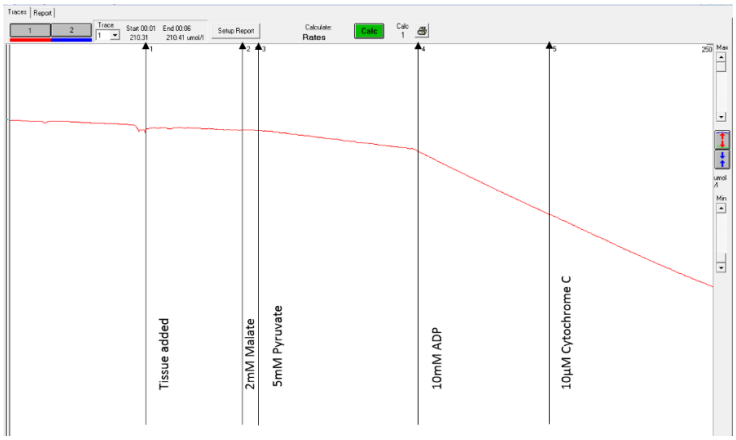

Protocol 2: Fatty acid and carbohydrate oxidative metabolism

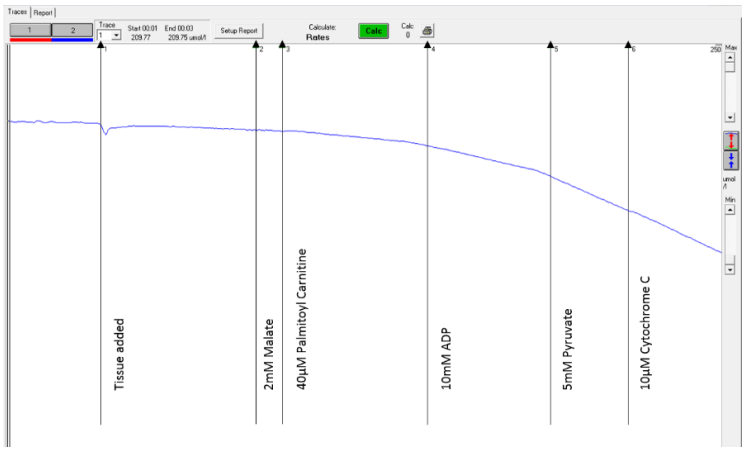

Protocol 3: Total oxphos; metabolism through complexes I and II of the ETS

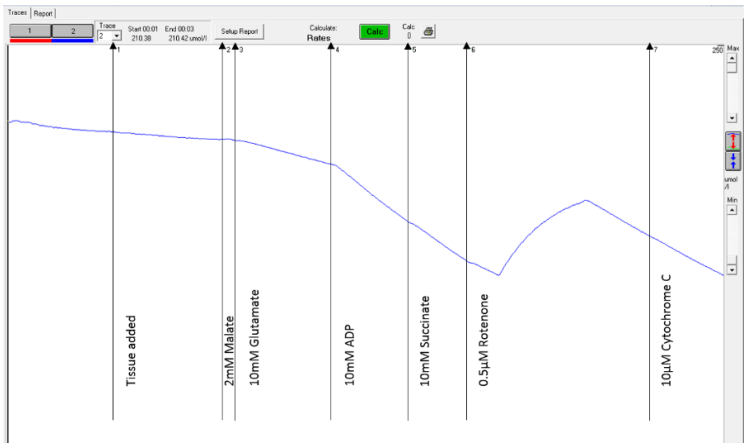

Figure 2.1 Respirometry experimental protocols and example traces

2.3.4 Mitochondrial Enzyme Activity

2.3.4.1 Sample Preparation

Frozen muscle samples from the middle depth region of muscle (Kohn and Myburgh, 2007) were powdered and manually homogenised in 300µl buffer (pH 7.2; containing 20mM HEPES, 1mM EDTA, 50mM sodium fluoride, 10mM sodium dichloroacetate and 0.1% triton). Samples were centrifuged for 30 seconds at 4000rpm at 4°C and the supernatant collected. The protein content of the supernatant was measured in duplicate using a Bicinchoninic Acid (BCA) assay using BSA to produce a standard curve on each 96-well assay plate.

2.3.4.2 Citrate Synthase Assay

As a putative marker of mitochondrial density (Larsen et al., 2012), citrate synthase (CS) activity was measured spectrophotometrically as described previously (Murray et al., 2008) using an Evolution 220 UV-visible spectrophotometer (ThermoScientific). Homogenised skeletal muscle protein (30µg) was added to the assay buffer (pH8, 20mM Tris-base) containing 0.1mM 5,5'-Dithio-bis(2-nitrobenzoic acid) (DTNB; Sigma). Oxaloacetate (1mM; Sigma) was added and the mixture warmed for 3 minutes to 37°C. Citrate synthase catalyses the reaction between acetyl-CoA and oxaloacetate (Equation 2.1), and the product, CoA-SH, reacts with DTNB to produce the absorbing product, TNB (Equation 2.2). The absorbance at 412nm was measured at 5 second intervals for a baseline reading of 3 minutes before acetyl-CoA (0.3mM; Sigma) was added and the absorbance measured over 9 minutes. The maximal rate of change over a 3 minute period was used to determine the CS activity and every sample was run in duplicate. The activity is expressed per mg protein.

$$Acetyl - CoA + Oxaloacetate + H_2O \rightarrow Citrate + CoA - SH$$

Equation 2.1 Reaction catalysed by citrate synthase

$$CoA - SH + DTNB \rightarrow TNB + CoA - S - S - TNB$$

Equation 2.2 Reaction coupled to citrate synthase activity

An initial optimisation was performed in order to determine the protein quantity to use for each reaction. Reaction saturation was confirmed through doubling the concentrations of both oxaloacetate and acetyl-CoA with no increase in CS activity. Further, readings were taken for an additional 15 minutes for samples of all groups to confirm no increase in maximal rate of change, with and without the addition of more oxaloacetate and acetyl-CoA. Citrate synthase (0.04 units; Sigma) replaced sample protein as a positive control.

2.3.4.3 HOAD assay

The activity of β-hydroxyacyl-CoA dehydrogenase (HOAD), part of the β-oxidation pathway, was measured spectrophotometrically in the BF as described previously (McClelland et al., 2005) using an Evolution 220 UV-visible spectrophotometer (ThermoScientific). 20µg homogenised skeletal muscle protein was added to the assay buffer (pH7.4 containing 50mM imidazole and 0.1% triton X-100). NADH (0.15mM; Sigma) was added and the mixture warmed for 6 minutes to 37°C. The absorbance at 340nm was measured at 5 second intervals for a baseline reading of 3 minutes before acetoacetyl-CoA (0.1mM; Sigma) was added and the absorbance measured over a further 3 minutes. HOAD catalyses the conversion of acetoacetyl-CoA to β-hydroxyacyl-CoA while NADH is oxidised to NAD^+ (Equation 2.3; Stern, 1957). NADH absorbs 340nm wavelength light and thus the rate of change of 340nm absorbance over this 3 minute period was used to determine the HOAD activity. Every sample was run in duplicate and results are expressed per mg protein.

$$Acetoacetyl - CoA + NADH \leftrightarrow NAD^+ + \beta - hydroxyacyl - CoA$$

Equation 2.3 Reaction catalysed by β-hydroxyacyl-CoA dehydrogenase

An initial optimisation was performed in order to determine the protein quantity to use for each reaction. Reaction saturation was confirmed through doubling the concentrations of both NADH and acetoacetyl-CoA and there being no increase in HOAD activity. Further readings were taken for an additional 6 minutes for samples of all groups to confirm no increase in maximal rate of change.

2.3.5 Protein expression by Western Blotting

2.3.5.1 Sample preparation

Protein was extracted as described in section 2.3.2.1. The samples were diluted to give a final concentration of 2.5µg/µl in a 0.2M Tris-HCl solution (pH6.8) containing 8% sodium dodecyl sulphate (SDS), 6% DTT, 40% glycerol and bromophenol blue. Samples were heated to 80°C for 5 minutes, before being aliquoted and stored at -20°C until use.

2.3.5.2 SDS-PAGE

Acrylamide gels were prepared the day prior to the samples being run and kept at 4°C overnight. The separating gel (pH8.5, containing 0.01% SDS and 10-14% acrylamide, the percentage determined according to the molecular weight and relative abundance of the protein of interest; Table 2.2) was pipetted into the chamber created between glass plates. Isobutanol was layered over the gel to ensure the gel set evenly and it was left to set for at least 30 minutes. The isobutanol was removed and any remaining was washed away and the plates blotted dry. The stacking gel (pH6.8 containing 4% acrylamide and 0.1% SDS) was prepared, pipetted onto the separating gel, a 15- or 21-well plastic comb inserted and left to set for at least 30 minutes.

The combs were removed and the wells thoroughly washed with milliQ water. Gels were placed in the gel tank which was filled with electrophoresis buffer (2.5mM Tris-base, 25mM glycine and 0.01% SDS). Table 2.2 gives the specific conditions when blotting for the specific target proteins. In general, the 1xSDS sample solutions were heated before 10µl or 20µl was loaded into the wells. Either a 14-well (20µl; 50µg protein) or a 21-well (10µl; 25µg protein) set up was used in order to compare all samples from relevant treatment groups on one gel and avoid comparing across gels. A pre-stained protein ladder was run alongside the samples for comparison of the protein band molecular weights (Thermo Scientific; 26616). Additionally, a well with half the protein content was run on every gel. The samples were run on ice for 30 minutes at 60V followed by 2.5-3.5 hours at 110V.

Proteins were transferred to a nitrocellulose membrane (VWR, Lutterworth, UK) using a semi-dry transfer cell (Bio-Rad Laboratories, Hemel Hempstead, UK). Filter paper, membrane and gel were soaked in transfer buffer (8mM tris-base, 39mM glycine, 0.037% SDS in 4:1 H_2O:methanol), formed into stacks and run at 0.8mA/cm^2 of membrane and 5V for 1.5 hours.

The membranes were stained using Ponceau-S (Sigma) in order to normalise protein loading. Membranes were blocked using 5% milk protein in tris-buffered saline containing 0.1% Tween-20 (TBS-T) for 1 hour at room temperature followed by incubation with the primary antibody (Table 2.2) diluted in a solution of TBS-T containing 0.02% sodium azide overnight at 4°C followed by one hour at room temperature.

Table 2.2 Western Blotting Antibody Specifications.

Target Protein(s)	Sample denaturation	Percentage Acrylamide Gel	Primary Antibody	Primary Antibody Dilution in TBS-T	Secondary Antibody	Secondary Antibody Dilution in TBS-T
ETS complexes I-IV and ATP-synthase	40°C for 5 minutes	14%	Oxphos antibody cocktail (Life Technologies; 458099)	1:250	HRP-linked sheep anti-mouse IgG (GE Healthcare; NIF825)	1:5000
ANT1	70°C for 5 minutes	12%	Abcam (Cambridge, UK; ab102032)	1:1000 in 5% milk	HRP-linked donkey anti-rabbit IgG (GE Healthcare; NA934V)	1:5000 in 2.5% milk
p-AMPKα (T172)	70°C for 5 minutes	10%	Cell Signalling Technology #2535 (CST; New England Biolabs, Hitchin, UK)	1:1000	HRP-linked donkey anti-rabbit IgG (GE Healthcare; NA934V)	1:5000 in 2.5% milk
AMPKα	70°C for 5 minutes	12%	CST #2532	1:1000	HRP-linked donkey anti-rabbit IgG (GE Healthcare; NA934V)	1:5000 in 2.5% milk

TBS-T, tris-buffered saline containing 0.1% Tween-20; ETS, electron transfer system; ANT1, adenine nucleotide translocase 1; (p)AMPKα, (phopshorylated) adenine monophosphate-activated protein kinase α.

Excess primary antibody was removed in 2x20 minutes washes in TBS-T. Membranes were incubated with the secondary antibody (Table 2.2) for 1 hour at room temperature, before excess was removed in a further 2x20 minutes washes in TBS-T. Enhanced chemiluminescence (ECL) detection reagent (GE Healthcare) was used to visualise the protein bands on Hyperfilm ECL (GE Healthcare).

The ponceau-S staining and the protein band intensities were quantified using ImageJ software (http://rsb.info.nih.gov/ij/). Ponceau-S staining was analysed in order to determine the variance of protein loading and the band intensity of the lane with half the loaded protein was used in order to ensure the antibody signal was not saturated and was kept in the linear range. Values of protein abundance were expressed normalised to Ponceau-S staining.

2.3.5.3 Primary Antibody Information

None of the antibodies used had been previously tested for use on sheep tissue. The specific targets and homology to the sheep protein (as determined using Protein Blast) are outlined in Table 2.3. The 5 targets of the oxphos antibody cocktail were selected as they are labile when the complex is disassembled and are of different molecular weights such that they are easily resolved by gel electrophoresis.

Table 2.3 Western blotting antibodies: target protein information

Target	**Subunit against which the antibody was raised**	**Homology to sheep protein**	**Molecular weight (kDa)**
Oxphos antibody cocktail: Complex I	NADH Dehydrogenase β complex 8 (cow whole protein)	98%	19
Oxphos antibody cocktail: Complex II	Succinate dehydrogenase Fe-S subunit (cow)	87%	30
Oxphos antibody cocktail: Complex III	Ubiquinol-cytochrome C reductase core 3 (cow)	98%	48
Oxphos antibody cocktail: Complex IV	Cytochrome c oxidase (human; temperature sensitive)	96%	57 (band at 40)
Oxphos antibody cocktail: ATP-synthase	ATP synthase F1 α subunit (cow)	99%	53
ANT1	Synthetic peptide based on human ANT1 amino acids 35-84	100%	33
p-AMPKα (T172)	Synthetic peptide based on the human sequence	98%	62
AMPKα	Synthetic peptide based on the human sequence	98%	62

TBS-T, tris-buffered saline containing 0.1% Tween-20; ETS, electron transfer system; ANT1, adenine nucleotide translocase 1; (p)AMPKα, (phosphorylated) adenine monophosphate-activated protein kinase α.

2.3.6 Gene Expression

2.3.6.1 RNA Extraction

The work area used for RNA extraction was cleaned with 70% ethanol and RNAseZAP (ThermoScientific) prior to use. Frozen skeletal muscle samples were powdered using a pestle and mortar on dry ice. In batches of up to 10 samples, the powdered tissue was added to 1ml Trizol (ThermoScientific) and vortexed frequently over a 5 minute period. After 5 minutes, 200µl chloroform was added and the mixture was vortexed for 2x15 seconds, 1 minute apart. Tubes were centrifuged at 14000rpm for 10 minutes and 200µl of the upper aqueous phase was collected for RNA extraction using RNeasy Plus Mini Kit (Qiagen, Manchester, UK). 700µl buffer RLT Plus (containing 1% β-mercaptoethanol) and 500µl ethanol were added and the solution was passed through RNeasy GenElute Columns in order to bind the RNA to the silica membrane. The RNA was washed according to the protocol contained with the Qiagen RNeasy Plus Kit. To the column were added buffer RW1 (to remove biomolecules including proteins, carbohydrates and fatty acids while leaving RNA molecules longer than 200bp bound to the membrane) and buffer RPE (to remove any salt traces). Columns were centrifuged at 10000rpm for 15 seconds and the flow-through discarded. The membrane was dried to remove all traces of ethanol and the RNA was eluted in 30µl of RNAse-free water. The concentration of the eluted RNA was measured using a Nanodrop ND-1000 spectrophotometer and the RNA purity was assessed by the 260/280nm ratio being close to 2.0. RNA was diluted to 50ng/µl in RNAse-free water.

2.3.6.2 cDNA Synthesis

Reverse transcription (RT) was performed to synthesise complementary DNA (cDNA; High Capacity cDNA Reverse Transcription Kit; Applied Biosystems, California, USA). An equal volume of RT mastermix (containing RT buffer, dNTP mix, random primers and reverse transcriptase) and RNA were combined, briefly centrifuged and RT was run according to the recommended protocol: 25°C for 10 minutes, 37°C for 2 hours, 85°C for 5 minutes and then held at 4°C for up to an hour before dilution (GenePro Thermal Cycler; Alpha Laboratories, Eastleigh, Hampshire, UK). Control samples were also generated in reactions omitting the reverse transcriptase. Control and sample cDNA were diluted 10-fold and single-use aliquots stored at -20°C until use. Samples of cDNA were pooled, diluted 5-fold and stored in single-use aliquots at -20°C to produce a standard curve.

2.3.6.3 qRT-PCR

Quantitative real-time polymerase chain reaction (qRT-PCR) was performed in triplicate on a 7500 Fast Real-Time PCR System (Applied Biosystems) using a SYBR Mastermix (MESA BLUE qPCR Mastermix Plus for SYBR Assay; Eurogentec, Seraing, Belgium), a reaction mix containing Meteor*Taq* HotStart DNA polymerase and an inert blue dye for the detection of double stranded DNA. The primer pairs for housekeeping genes and target genes are listed in Table 2.4. Primer sequences were used that had been previously published as referenced in Table 2.4, or were designed using Primer Blast (Ye et al., 2012). Ensembl (Release 89; Aken et al., 2016) was used in order to ensure all primer pairs spanned an intron, and Primer Blast was used to make appropriate modifications to any primer pairs originally designed for species other than sheep. All primers were produced by Sigma. Primers were reconstituted to 100µM, diluted 10-fold and stored at -20°C in aliquots. In each reaction well, 6µl SYBR Mastermix, 0.25µl forward and reverse primers, 2.5µl DNAse-free water and 3µl cDNA sample were added. Following the recommended protocol for the SYBR, an initial denaturation step (5 minutes at 95°C) was followed by 40 amplification cycles (15 seconds at 95°C and 1 minute at 60°C). Finally, a melting curve was run in order to ensure there was a single PCR product, with no non-specific amplicons or primer-dimers. This was also verified using a negative control containing water in replacement for the cDNA, and the control sample (produced with no reverse transcriptase) was run for each primer pair to ensure no amplification of any genomic DNA remaining in the mixture. The PCR products from every primer pair were run on a 1.5% agarose gel containing ethidium bromide to ensure a single product that was of the correct size.

Data were analysed using the $2^{-\Delta\Delta Ct}$ method (Schmittgen and Livak, 2008). Gene expression was expressed relative to the geometric mean of 2 housekeepers: *18S* and *S15* ribosomal RNA, and set relative to 1 experimental sample. This sample was chosen as the closest to the average in the 104dGA age group for the ontogeny study (Chapter 3) or the average in the relevant ~129dGA control groups for the TX and infusion studies (Chapters 4 and 5). The data from this sample were excluded from the calculations of the mean and SEM. An exception to this was the analysis of gene expression in the ontogeny study (Chapter 3) where only *S15* was used as a housekeeping gene because *18S* expression was significantly higher in the 104dGA group than the other 3 ages studied in the SDF, as analysed using the standard curve method and shown in Figure 2.2.

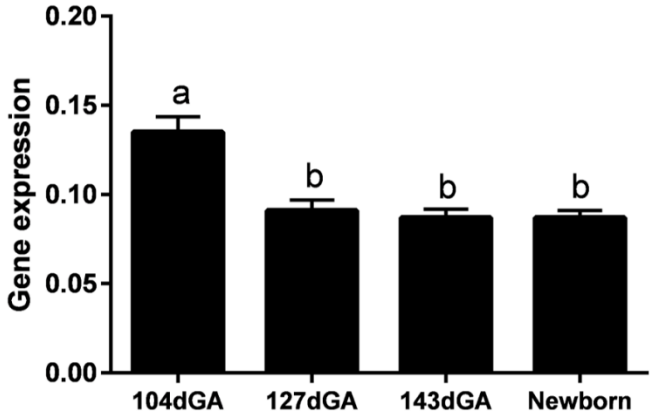

Figure 2.2 18S gene expression in the superficial digital flexor. N=6 per group. Different letters are significantly different to each other (P<0.05 by Tukey's post hoc test following one-way ANOVA).

Table 2.4 Forward and reverse primer sequences used for SYBR qRT-PCR.

Target Gene and Protein	Primer Sequences	Product Length (bp)	Reference
RPS15 S15	F: ATCATTCTGCCCGAGATGGTG	134	(Yates et al., 2016)
	R: TGCTTCACGGGCTTGTAGGTG		
18S rRNA	F: GTAACCCGTTGAACCCCATT	151	(Byrne et al., 2010)
	R: CCATCCAATCGGTAGTAGCG		
PPARGC1A PGC1α	F: GAGATGTGACCACCGAGAATGAG	255	(Myers et al., 2008)
	R: GCTGTTGACAAATGCTCTTCGC		
NRF1 NRF1	F: AAACACAAACACAGGCCACA	197	(Myers et al., 2015)
	R: CACCGCCGAATAATTCACTT		
MYH7 MHCI	F: GAGATGGCCGCGTTTGGGGAG	284	(Yates et al., 2016)
	R: GGCTCGTGCAGGAAGGTCAGC		
MYH2 MHCIIa	F: ACCGAAGGAGGGGCGACTCTG	110	(Yates et al., 2016)
	R: GGCTCGTGCAGGTGGGTCATC		
MYH1 MHCIIx	F: AAAGCGACCGTGCAGAGCAGG	155	(Yates et al., 2016)
	R: GGCTCGTGCAGGTGGGTCATC		
UCP2 UCP2	F: AAGGCCCACCTAATGACAGA	128	Designed using Primer Blast by Dr OR Vaughan
	R: CCCAGGGCAGAGTTCATGT		
UCP3 UCP3	F: GAAAGGAATTCTGCCCAACA	142	(Kelly et al., 2011)
	R: TCCAAAGGCAGAGACGAAGT		
SLC25A4 ANT1	F: TGGTGTCCTACCCCTTTGAC	148	(Kelly et al., 2011)
	R: CAGGCGCCTTTGAAGAAAGC		
MFN1 MFN1	F: ATTGGTGAGGTGCTGTCTC	186	Adapted using Primer Blast
	R: TTCTGTCATGAGATAGGCTTT		
MFN2 MFN2	F: CATCAGCTATACTGGCTCCAACT	68	Adapted using Primer Blast
	R: AATGAGCAAAAGTCCCAGACA		
DNM1L DRP1	F: CTGACACTTGTGGACTTGCC	277	Adapted using Primer Blast
	R: CCCTTCCCATCAATACATCC		
MCU MCU	F: TTCACCAGATGGCGTTCGAGTTG	143	Modified from (Henzi and Schwaller, 2015)
	R: GTGTTGCTGCATTTTCATGGCT		
MICU1 MICU1	F: AAACAACCAGAACACTTGGGTC	140	Modified from (Henzi and Schwaller, 2015)
	R: AGTCCACATTCTCCAAGGGTGTA		
SOD1 SOD1	F: CCGCTTCGAGGCAAAGGGAGA	167	(Mishra et al., 2016)
	R: CCTTTGGCCCACCGTGTTTT		
SOD2 SOD2	F: ATTGCTGGAAGCCATCAAAC	192	(Afolayan et al., 2016)
	R: AGCAGGGGGATAAGACCT		
THRA THRα	F: ATGGCCATGGACTTGGTTCT	74	Designed using Primer Blast
	R: CGCTCTCGGTTCTGCTCAAT		
THRB THRβ	F: CAGTGCCAGGAATGTCGCTTT	116	Designed using Primer Blast
	R: TTCTCCCGGTTCTCCTCAATG		
NR3C1 GR	F: CCCAAGGAAGGCTTGAAGAGTC	228	Modified from (Myers et al., 2008)
	R: CTCTGGGAATTCAATACTCAT		

PGC1α, peroxisome proliferator-activated receptor γ coactivator 1α; NRF1, nuclear respiratory factor 1; MHCI/IIa/IIx, myosin heavy chain I/IIa/IIx; UCP2/3, uncoupling protein 2/3; ANT1, adenine nucleotide translocase 1; MFN1/2, mitofusin 1/2; DRP1, dynamin-related protein 1; MCU, mitochondrial calcium uniporter; MICU1, mitochondrial calcium uptake 1; SOD, superoxide dismutase; THRA/B, thyroid hormone receptor A/B; GR, glucocorticoid receptor.

2.3.7 Histological analyses

2.3.7.1 Freeze fixing

Tissue samples which had been fix-frozen in isopentane (Section 2.2.4) were transferred to -20°C for 24 hours before tissues were to be sectioned as this reduced the tissue fracturing when being cut. A cryostat (OTF5030; Bright Instruments, Luton, UK) was set at a specimen temperature of -18°C. A small transverse region of the muscle was mounted using TissueTek® optimum cutting temperature (O.C.T) compound (VWR) and 10µm sections were cut and transferred to glass slides. The slides were kept at -20°C until required.

2.3.7.2 H&E staining

Slides were brought to room temperature before staining. The sections were brought through a series of xylene, 100%, 80% and 70% alcohol in order to remove excess O.C.T. and rehydrate the tissue. Slides were placed in Gill's haematoxylin (Sigma) for 10 minutes, washed in running tap water for 5 minutes and dipped twice in acid-alcohol (1% hydrochloric acid in 70% alcohol solution) for differentiation. Sections were placed in running tap water for 15 minutes to halt differentiation and to blue the sections. This was followed by 4 minutes in 1% eosin solution (made up in 76% alcohol) and excess removed by dipping in tap water. Sections were dehydrated through increasing alcohol concentrations to xylene. DPX (Sigma) was used as the mounting medium.

An Axio Imager A1 microscope (Zeiss, Cambridge, UK) was used to view the sections. Using the AxioCam MRc 5, 2 representative images were taken for each section at 40x magnification and were used to quantify the area of the field of view accounted for by fibres by using point counting on imagej. A grid of 140 points was superimposed on the image. The number of points covering fibres and their nuclei were quantified and expressed as a percentage.

2.3.7.3 Immunofluorescence

Immunohistochemistry of MHC isoforms has been previously shown to identify fibre types in developing skeletal muscle (White et al., 2001). Slides were fixed in acetone at -20°C for 5 minutes, left to air-dry and a section demarcated using a PAP pen (Agar Scientific, Stansted, UK). Sections were permeabilised for an hour in TBS containing 0.1% Tween-20 and 0.1% Triton (TBS-TT), blocked for an hour in TBS containing 5% goat serum and 2% bovine serum

albumin and incubated overnight at 4°C with a mouse anti-slow skeletal myosin heavy chain antibody (Abcam; ab11083) diluted 1:200 in TBS-TT. Excess antibody was removed in 3x10 minute washes of TBS-TT before incubation for 1 hour at room temperature with Alexa Fluor™ 488-conjugated donkey anti-mouse IgG (Abcam; ab150105) diluted 1:100 in TBS-TT. Slides were washed in TBS-TT (3x10 minute washes) and water (2x5 minute washes), and mounted using Vectashield Antifade Mounting Medium (Vector, Peterborough, UK).

An Axio Imager A1 microscope was used to take 5 images per section at 20x magnification, so as to image at least 100 fibres per sample. Cellprofiler was used to analyse the images (Carpenter et al., 2006). A pipeline was designed to identify the fibres according to threshold pixel intensity, size and spherical shape to distinguish adjacent fibres (Figure 2.3). The number, average fibre area, fibre perimeter and percentage area covered by fibres were quantified by Cellprofiler.

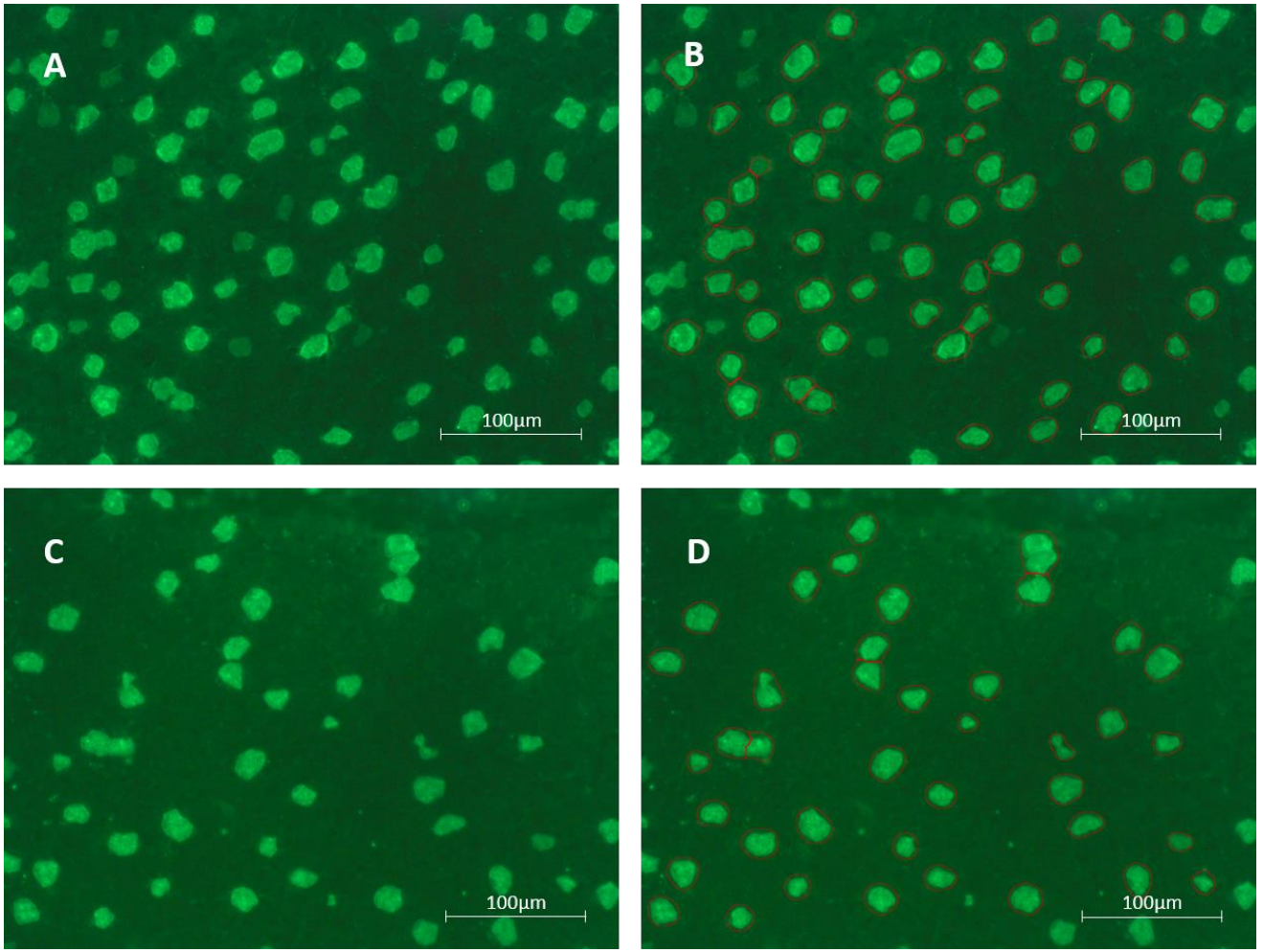

Figure 2.3 Examples of fibre outlines as determined by Cellprofiler. A&B) saline infused singleton fetus and C&D) 143dGA control twin fetus

2.4 Statistical analyses

All results are presented as mean ± standard error of the mean (SEM) and analyses were performed using GraphPad Prism Version 6.05 for Windows (www.graphpad.com). A Kolmogorov-Smirnov test was applied to test for a normal distribution. When only two groups were compared an unpaired Student's *t-test* was applied if data were normally distributed and $n \geq 5$ per group. When data sets were $n < 5$, or for data which did not fit the normal distribution a Mann-Whitney non-parametric test was used. For the comparison of more than two groups, as for comparing the age groups in the ontogeny study (Chapter 3), a one-way analysis of variance (ANOVA) was applied. When groups were compared by the parameters of age and treatment a two-way ANOVA was used. When appropriate, a Tukey's multiple comparison *post hoc* test was applied following a significant result from one- or two-way ANOVA. The Pearson product-moment correlation coefficient was used to assess linear correlation between variables and log-transformed hormone data. Partial correlation analysis was used to determine which variables had the greatest association. $P < 0.05$ was considered significant and $P < 0.1$ was considered a trend throughout. Details of the specific statistical analyses used are given in the individual results chapters.

3 Mitochondrial function in skeletal muscle: the transition from intra- to extrauterine life

3.1 Introduction

Over late gestation, maturation of fetal systems occurs to enable them to take on their new postnatal roles that ensure survival *ex utero*. Maturation of many fetal tissues involves a switch from cellular proliferation to terminal differentiation and this switch is often dependent on the maturational hormone, cortisol, which shows a prepartum surge in concentration in the fetus in most mammalian species studied to date (Fowden et al., 1998). Cortisol can directly regulate tissue maturation, while in some cases its maturational effects are mediated by other endocrine systems (Fowden et al., 1998). An example is T_3, the bioavailability of which is increased by cortisol near term (Forhead and Fowden, 2014).

In skeletal muscle over late gestation, cellular proliferation is downregulated alongside a drop in proliferative signals including IGF-I and an upregulation of myogenesis gene expression associated with terminal differentiation and tissue maturation (Brown, 2014, Forhead et al., 2002, Du et al., 2010). Thus, from late gestation, muscle growth occurs predominantly by hypertrophy and thus impaired proliferation *in utero* tends to result in a reduced muscle mass which remains into adulthood (Brown, 2014). Functional development of skeletal muscle over late gestation involves a switch from the expression of fetal myosin to the adult 'fast' and 'slow' myosin isoforms as the fibres differentiate into their fast and slow twitch phenotypes (Gambke et al., 1983). The proportion of fibre types is regulated by neural input and TH exposure (Gambke et al., 1983). The contractile phenotype also matures towards term with contraction and relaxation times of fast-twitch muscles decreasing towards term and the opposite being true in slow-twitch muscles (Javen et al., 1996). Metabolic development of muscle involves the increase in glycogen storage with gestational age, alongside an increased expression of glycogenolytic enzymes (Fowden et al., 1991). Evidently, fetal development is an energy demanding process and therefore the fetal mitochondria must be capable of generating adequate ATP. Studies on human infant muscle suggest a rise in mitochondrial activity and oxidative capacity with increasing gestational age (Sperl et al., 1992, Minai et al., 2008). Altered mitochondrial function during fetal development may impact on muscle

development and therefore may have an effect on neonatal and adult health. However, little is known about the regulation of fetal mitochondrial function.

At birth, the energy demands of tissues increase, and, as such, an increased oxygen consumption occurs in tissues including the liver and brain (Klein et al., 1983). Whilst skeletal muscle activity does occur *in utero* and activity increases with gestational age, whole body movements decrease towards term as space becomes limited (D'Elia et al., 2001). The function of muscle after birth is clearly significantly greater than beforehand, and it must be able to function immediately to enable precocial offspring, such as sheep, to be able to stand and walk within hours of birth. In addition to locomotion, skeletal muscle contraction is required for shivering. Both locomotion and thermogenesis are highly energy-consuming processes and therefore the muscle must be metabolically, as well as functionally, prepared for the challenges posed by the transition to extrauterine life.

One such challenge faced by the neonate at birth is the switch from a continuous placental to an intermittent enteral nutrient supply (Mellor and Cockburn, 1986). Thus, tissues including liver and muscle have endogenous stores of carbohydrate ready for rapid mobilisation at birth. In addition, skeletal muscle begins to metabolise lipid at birth, and fetal muscle has been shown to contain lipid deposits (Beatty and Bocek, 1970), although in the sheep, FAs metabolised by muscle postnatally are likely to come predominantly from lipolysis in the liver and adipose tissue (Mostyn et al., 2003, Hull, 1975).

As well as a change in nutrient supply at birth, the fetus must be prepared to cope with a change from a placental to a pulmonary supply of oxygen which, in turn, requires more energy to support continuous breathing. The neonate is also suddenly exposed to the much higher atmospheric pO_2 than during placental oxygen delivery and therefore it rapidly switches to use predominantly oxidative metabolism for ATP generation (Papa, 1996). Further, during the uterine contractions of labour, the fetal blood supply is no longer continuous but intermittently reduced, thereby exposing the fetus to hypoxia-reperfusion events (Rogers et al., 1998). Both these changes in oxygen exposure are associated with an increased risk of ROS production (Rogers et al., 1998, Aledo, 2014). Increased ETS activity, driving an increased PMF, is also associated with enhanced ROS production (Aledo, 2014). Therefore, the fetus is faced with the challenge of preparing for increased energy demands immediately after birth while also minimising oxidative damage over the transition period.

While interest in prenatal mitochondrial function is increasing due to the hypothesis that altered mitochondrial development *in utero* may predispose a range of adult-onset diseases (Lee et al., 2005), very few studies have investigated development of mitochondrial function in fetal skeletal muscle. Skeletal muscle is a highly metabolically active tissue, both in the fetus and the adult (Jones and Rolph, 1985, Hoppeler, 1999) so mitochondrial development in this tissue is likely to be an important component of the prepartum maturational process and essential for the successful transition to extrauterine life.

3.2 Aim

The aim of this study was to identify any changes in the oxidative capacity of the skeletal muscle over late gestation and early neonatal life, in order to provide the ATP necessary for maturation and postnatal function. An additional aim of this study was to determine whether the maturational hormones, cortisol or T_3, correlated with any of the mitochondrial parameters and, thus, may have been responsible for driving any developmental changes observed over the perinatal period.

3.3 Methods

3.3.1 Animals

For the ontogeny study, 18 Welsh Mountain ewes carrying twins of known gestational age were used. At 102-105dGA, 6 of the ewes and their fetuses were euthanised and tissue samples taken immediately as described in general methods (Section 2.2.4.1). Tissues were taken from both twins, and respirometry (general methods; section 2.3.3) was carried out. Results and subsequent analyses are only shown for one fetus from each pair of twins, selected randomly in order to try and balance males and females (Table 2.1) and an equal number of fetuses delivered first and second were selected.

The remaining 12 ewes were part of a separate study (detailed in Section 2.2). Briefly, the twin-bearing ewes underwent surgery under general anaesthesia at 102-105dGA. One of the fetuses was thyroidectomised while the second was sham-operated. Pregnancy continued until 125-129dGA (n=6 ewes) or 140-145dGA (n=6 ewes) when ewes and fetuses were euthanised and tissues collected (Section 2.2.4.1). It was randomised whether the TX or sham-operated fetus was delivered first. The sham-operated fetuses were used for this ontogeny study.

In addition, 6 newborn twin lambs were studied at 1-2 days old. They were euthanised and tissues collected (Section 2.2.4.2). Again only 1 lamb from a set of twins was used for this study. The average ages for the 4 groups are given in Table 3.1.

Table 3.1 Ages for the 4 groups used in the ontogeny study

Group name:	104dGA	127dGA	143dGA	Newborn
Age:	104±0.5dGA	127±0.7dGA	143±0.9dGA	1±0.2 days

Mean±SEM ages. dGA, days of gestational age. N=6 in each group.

Details of surgery, tissue collection and experimental protocols used in this chapter are given in Chapter 2.

3.3.2 Statistical Analyses

To compare age groups, a one-way ANOVA was applied. Following a significant result from the one-way ANOVA, a Tukey's multiple comparison *post hoc* test was applied in order to determine which groups were significantly different from each other. Whilst a normal distribution and equal variance are assumptions of an ANOVA, the test has been shown to be robust to violations of these assumptions so long as the group sizes have $n \geq 5$ (Maxwell and Delaney, 1990). Therefore, nonparametric tests were not performed in place of ANOVAs except in the cases when groups had $n<5$, for example due to samples being necessarily excluded from the respirometry datasets. When this was the case a Kruskal-Wallis non-parametric test was performed and a Dunn's multiple comparisons test used to determine which groups were significantly different from one another.

Relationships between variables and cortisol and T_3 were determined using Pearson's correlation using log-transformed hormone data. Partial correlation analyses were used to determine which variables had the greatest association. $P<0.05$ was considered significant throughout.

3.4 Results

3.4.1 Fetal and neonatal measurements

Plasma hormone concentrations

The fetal plasma cortisol and T_3 concentrations showed a prepartum rise (P<0.0001 for cortisol and P<0.05 for T_3 by one-way ANOVA considering only the 3 fetal ages; Figure 3.1 A&B). The concentration at 143dGA was significantly higher than at 104dGA in both cases. Applying a one-way ANOVA to all 4 groups there was a significant effect of age (P<0.0001 in both cases), with the concentration of both cortisol and T_3 being significantly higher in the newborn lambs than at the 3 gestational ages studied (Figure 3.1 A&B). Cortisol and T_3 showed a significant positive correlation when the data from all the fetal and newborn animals were combined (r=0.8468, n=23, P<0.0001). There was no difference in T_4 concentration between the 4 age groups (Figure 3.1 C).

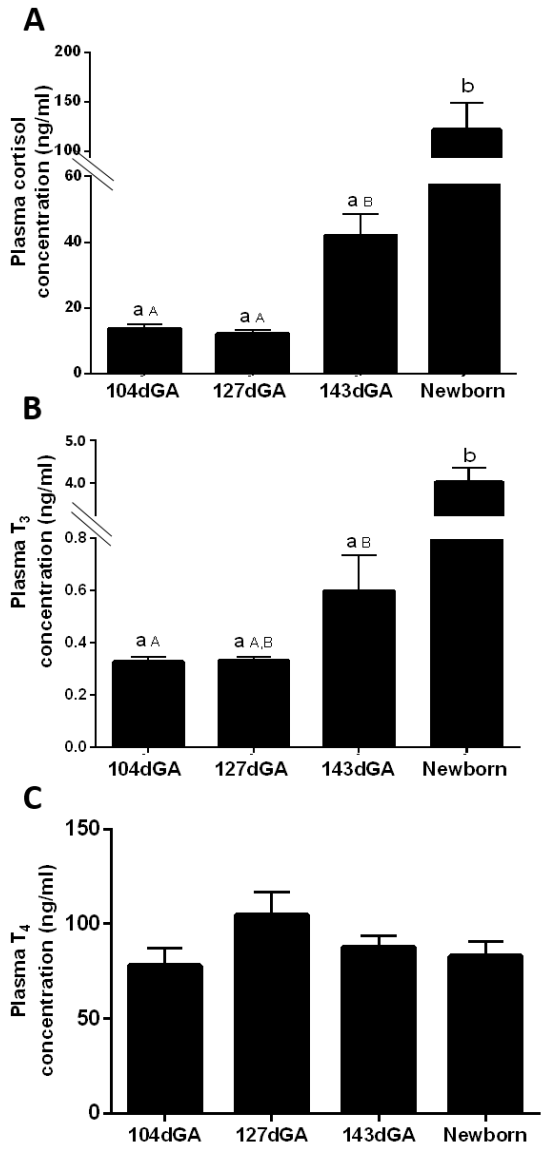

Figure 3.1 Mean±SEM plasma A) cortisol, B) T_3 and C) T_4 concentrations in fetuses at 104 (n=6), 127 (n=6) and 143 (n=5) days of gestational age (dGA) and newborn lambs (n=6). Different letters are significantly different to each other (P<0.05 by Tukey's post hoc test following one-way ANOVA). Lower case letters include all 4 age groups, upper case letters include 104-143dGA groups only.

Fetal biometry and muscle biochemical composition

Increasing age had a significant effect on body weight, fetal length and femur, tibia and metatarsus lengths ($P<0.0001$ in all cases except tibia length where $P<0.05$; Table 3.2). The weights of the individual muscles also increased significantly with age ($P<0.0001$ in all cases; Table 3.2). Age did not affect the ratio of muscle:body weight in the BF or ST, but the ratio of SDF:body weight was affected by age ($P<0.05$) and was significantly higher in the newborns than at 127dGA (Table 3.2).

In all 3 muscles studied, age had a significant effect on muscle glycogen content ($P<0.01$). In general, the glycogen content was higher in late gestation than at 104dGA, but were lower in the newborn lambs (Table 3.2). Lipid content was only measured in the BF. Here, there was a significant effect of age ($P<0.05$), but unlike glycogen, lipid content in the newborn lambs was higher than at 104 and 127dGA (Table 3.2). Additionally, there was a significant effect of age on water content, which decreased with age ($P<0.0001$ in all muscles) and on protein content which increased with age ($P<0.0001$ in BF and $P<0.01$ in SDF; Table 3.2).

As water content differed with age, the protein, glycogen and lipid content of the muscles are also expressed per mg dry weight (Table 3.2) and there remained a significant effect of age on all 3 biochemical measurements ($P<0.0001$ for protein and $P<0.01$ for lipid and glycogen content). However, the increase in lipid and protein content per gram wet weight of the muscles with age was no longer apparent when the water content was taken into account (Table 3.2).

Table 3.2 Biometric and biochemical measurements.

	104dGA	127dGA	143dGA	Newborn
Body weight (kg)	1.19±0.17 [a]	2.54±0.10 [b]	3.49±0.26 [c]	3.34±0.14 [c]
Crown-rump length (cm)	31.5±0.9 [a]	41.8±0.8 [b]	45.0±0.5 [c]	49.6±1.0 [d]
Femur (cm)	5.8±0.4 [a]	9.3±0.4 [b]	10.3±0.3 [b]	12.8±0.5 [c]
Tibia (cm)	8.8±0.3 [a]	12.3±0.3 [a,b]	14.5±0.5 [b]	12.4±0.3 [b]
Metatarsus (cm)	10.0±0.3 [a]	14.3±0.3 [a,b]	16.3±0.3 [b,c]	17.5±0.3 [c]
	Biceps femoris			
Weight (g)	5.46±0.40 [a]	11.02±0.46 [b]	13.91±1.65 [b,c]	15.39±1.20 [c]
Muscle:body weight ratio (g:kg x10^3)	4.86±0.45	4.34±0.08	3.96±0.15	4.61±0.31
Water content (%)	86.8±0.4 [a]	83.3±0.5 [b]	79.3±0.6 [c]	78.6±0.3 [c]
Protein content (mg/g wet wt)	44.5±1.2 [a]	45.7±0.7 [a]	48.3±2.4 [a]	59.6±1.9 [b]
(mg/mg dry wt)	0.34±0.02 [a]	0.28±0.01 [b,c]	0.23±0.01 [b]	0.28±0.1 [c]
Glycogen content (mg/g wet wt)	19.6±1.2 [a]	34.5±2.2 [b]	33.4±2.0 [b]	15.2±1.7 [a]
(mg/mg dry wt)	0.15±0.01 [a]	0.21±0.01 [b]	0.16±0.01 [a]	0.07±0.01 [c]
Lipid content (mg/g wet wt)	23.5±1.8 [a]	22.8±1.6 [a]	25.5±1.3 [a,b]	30.1±1.8 [b]
(mg/mg dry wt)	0.18±0.02 [a]	0.14±0.01 [b]	0.12±0.01 [b]	0.14±0.01 [a,b]
	Semitendinosus			
Weight (g)	1.99±0.12 [a]	3.90±0.23 [b]	5.37±0.47 [c]	6.83±0.48 [d]
Muscle:body weight ratio (g:kg x10^3)	1.83±0.22	1.53±0.05	1.54±0.07	2.05±0.13
Water content (%)	86.1±0.2 [a]	81.7±0.5 [b]	79.1±0.4 [c]	78.4±0.2 [c]
Protein content (mg/g wet wt)	47.9±2.2	43.8±1.8	47.7±1.1	52.7±3.2
(mg/mg dry wt)	0.34±0.01 [a] (n=5)	0.24±0.01 [b]	0.23±0.01 [b]	0.24±0.01 [b]
Glycogen content (mg/g wet wt)	24.8±3.5 [a,b]	44.4±5.8 [c]	36.9±2.8 [a,c]	20.3±2.7 [b]
(mg/mg dry wt)	0.18±0.03 [a,b] (n=5)	0.24±0.03 [a] (n=5)	0.18±0.02 [a,b] (n=5)	0.09±0.01 [b]
	Superficial digital flexor			
Weight (g)	0.76±0.07 [a]	1.57±0.05 [b]	2.29±0.17 [c]	2.87±0.18 [d]
Muscle:body weight ratio (g:kg x10^3)	0.70±0.09 [a,b]	0.62±0.02 [a]	0.66±0.02 [a,b]	0.86±0.05 [b]
Water content (%)	85.9±0.3 [a]	82.2±0.3 [b]	78.6±0.7 [c]	78.3±0.3 [c]
Protein content (mg/g wet wt)	45.9±1.1 [a]	44.5±1.4 [a]	51.2±3.3 [a,b]	55.4±2.2 [b]
(mg/mg dry wt)	0.33±0.01 [a]	0.25±0.01 [b]	0.24±0.01 [b]	0.26±0.01 [b]
Glycogen content (mg/g wet wt)	9.5±2.3 [a,b]	22.5±3.8 [a,b]	24.4±3.1 [a]	5.6±2.1 [b]
(mg/mg dry wt)	0.07±0.02 [a,b] (n=4)	0.12±0.02 [b] (n=4)	0.12±0.02 [b] (n=4)	0.03±0.01 [a] (n=4)

Data are presented as mean±SEM of fetuses at 104, 127 and 143 days of gestational age (dGA) and newborn lambs. N=6 in all groups unless stated otherwise. Different letters are significantly different to each other (P<0.05).

3.4.2 Functional oxidative capacity

Respirometry was carried out in order to determine whether the capacity for fat and carbohydrate-driven oxidative metabolism changed over late gestation. Pyruvate and PC were added as substrates, and the ADP-coupled oxygen consumption (state 3 respiration) is shown in Figure 3.2 and Figure 3.3 respectively. Age had a significant effect on Py-supported oxidative capacity in all 3 muscles (P<0.0001 in the BF and SDF and P<0.01 in ST by one-way ANOVA including all 4 ages). BF and SDF from newborn lambs had a higher Py-supported oxygen consumption than the 3 fetal age groups studied, and ST from newborns had a significantly higher oxygen consumption than the 104dGA and 127dGA groups (Figure 3.2 A-C). Age had a significant effect on the PC-driven oxygen consumption in all 3 muscles (P<0.05 in BF and ST and P<0.01 in the SDF), and in the ST and SDF the newborn lambs had a higher oxygen consumption than the two youngest fetal age groups studied (Figure 3.3 A-C).

Applying the one-way ANOVA to the respirometry data to only the 3 fetal age groups, prevented the high value of the newborns from obscuring any prepartum gestational changes. Analysis of the fetal values alone showed that there was a significant effect of age on the Py-supported oxygen consumption in the SDF (P<0.05) where oxygen consumption at 143dGA was significantly higher than at 104dGA (Figure 3.2 C).

Combining the data from all 4 age groups, the Py- and PC-supported, ADP-coupled oxygen consumption values were plotted against the plasma cortisol and T_3 concentrations (Figure 3.2 and Figure 3.3). There was a significant positive correlation in all 3 muscles between cortisol and Py- (P<0.0001 in BF, P<0.01 in ST and P<0.001 SDF; r values given in Figure 3.2 D-F) and PC-driven oxygen consumption (P<0.05 in BF, P<0.01 in ST and P<0.001 in SDF; r values given in Figure 3.3 D-F). T_3 significantly correlated in all muscles with Py- (P<0.001 for BF, P<0.01 for ST and P<0.0001 in SDF; r values given in Figure 3.2 G-I) and PC-supported oxygen consumption (P<0.05 in BF, P<0.01 in ST and P<0.001 in SDF; r values given in Figure 3.3 G-I). Partial correlation analyses suggest T_3 may be the more important hormone in regulating Py-supported oxygen consumption in the SDF (P<0.05; Table 3.3). There was no significant correlation of Py- or PC- supported respirometry data in any of the muscles with T_4 (data not shown).

Following the measurement of PC-supported, ADP-coupled oxygen consumption, Py was added. The contribution of PC to the total oxygen consumption (PC:PC+Py ratio) is given in Figure 3.4. There was no effect of age on this value in any muscle studied.

Oxygen consumption upon the addition of substrate before ADP was added into the chamber, a measure of leak state respiration, was recorded. Py-supported respiration was influenced by age in BF (P<0.01) and ST (P<0.0001) and in both cases the rate of oxygen consumption was significantly higher in the newborns than in the fetuses (Table 3.4). PC-supported oxygen consumption was also affected by age in the BF (P<0.05) and ST (P<0.001), with the newborn value being significantly higher than 127dGA (Table 3.4). The concomitant change in oxygen consumption before and after the addition of ADP meant that RCR did not show a trend to increase or decrease with age with Py or PC in any of the muscles.

In addition to respirometry, the capacity for fat metabolism was further investigated in the BF by measuring the activity of the β-oxidation enzyme, HOAD. Age had a significant effect on HOAD activity (P<0.0001 by one-way ANOVA) with activity increasing during late gestation to be higher by term and in the newborn than 104-127dGA (Figure 3.5 A). When data from all groups were combined there was a strong positive correlation between HOAD activity and both cortisol and T_3 (P<0.0001 in both cases; Figure 3.5). Applying partial correlation analysis shows that cortisol may contribute more to HOAD regulation than T_3 (P<0.001; Table 3.3).

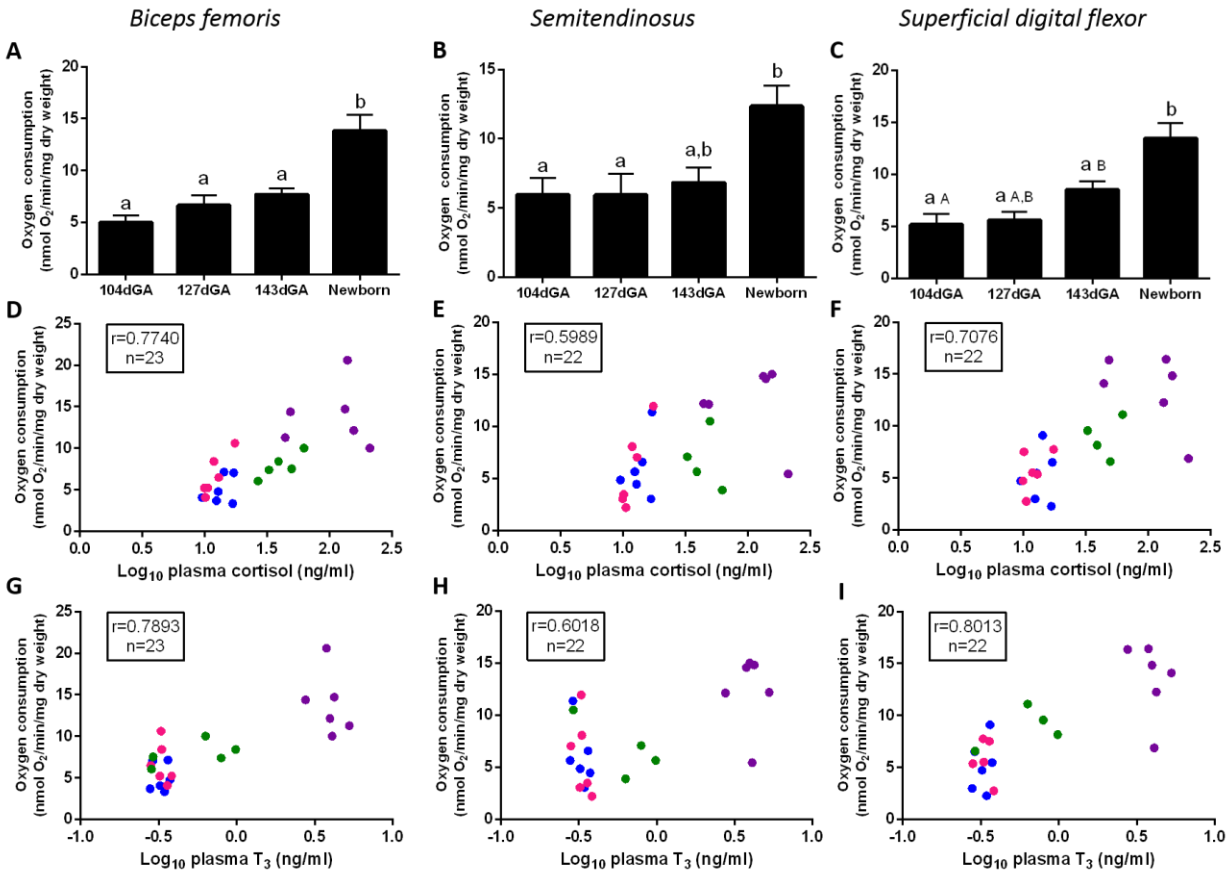

Figure 3.2 Pyruvate-supported, ADP-coupled oxygen consumption. A-C) Mean±SEM oxygen consumption of fetuses at 104 (n=6; blue), 127 (n=6; pink) and 143 (n=5-6; green) days of gestational age (dGA) and newborn lambs (n=6; purple); different letters are significantly different to each other (P<0.05 by Tukey's post hoc test following one-way ANOVA). Lower case letters include all 4 age groups, upper case letters include 104-143dGA groups only. Oxygen consumption plotted against plasma D-F) cortisol and G-I) T_3 in D&G) biceps femoris, E&H) semitendinosus and F&I) superficial digital flexor. N numbers and r values are given on each graph; 104dGA blue, 127dGA pink and 143dGA green and newborn lambs purple.

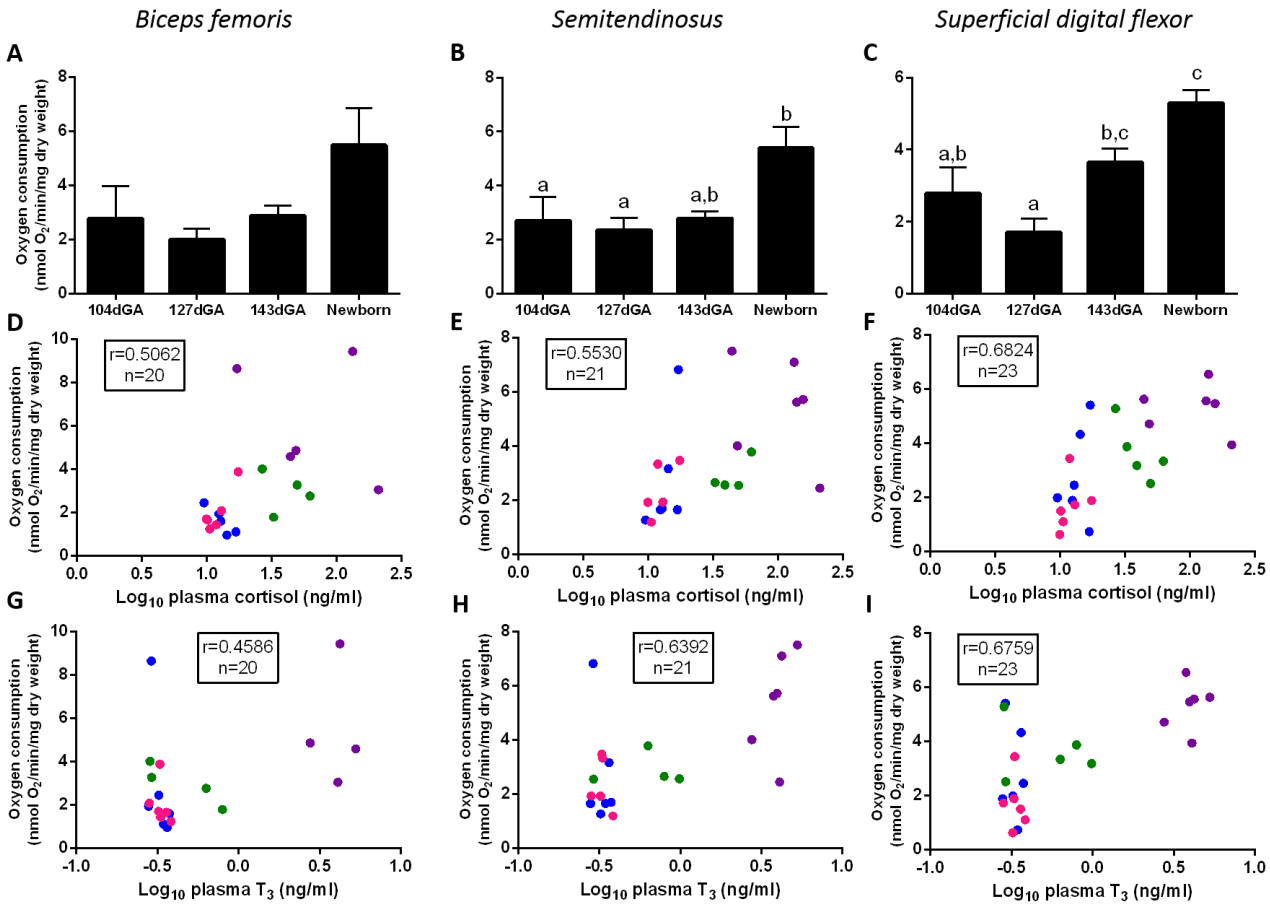

Figure 3.3 Palmitoylcarnitine-supported, ADP-coupled oxygen consumption. A-C) Mean±SEM oxygen consumption of fetuses at 104 (n=6), 127 (n=5-6) and 143 (n=5-6) days of gestational age (dGA) and newborn lambs (n=4-6); different letters are significantly different to each other (P<0.05 by Tukey's post hoc test following one-way ANOVA). Oxygen consumption plotted against plasma D-F) cortisol and G-I) T_3 in D&G) biceps femoris, E&H) semitendinosus and F&I) superficial digital flexor. N numbers and r values are given on each graph; 104dGA blue, 127dGA pink and 143dGA green and newborn lambs purple.

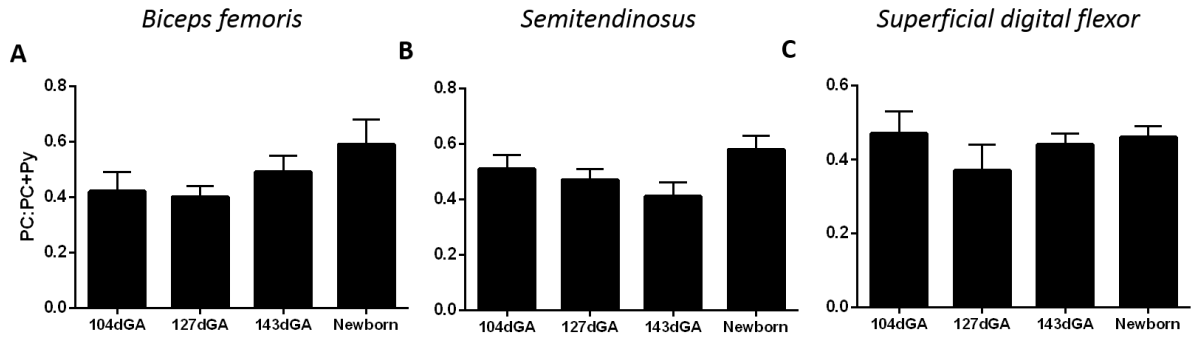

Figure 3.4 The ratio of ADP-coupled PC-supported:PC+Py-supported oxygen consumption, presented as mean±SEM in A) biceps femoris, B) semitendinosus and C) superficial digital flexor of fetuses at 104 (n=6), 127 (n=5-6) and 143 (n=5-6) days of gestational age (dGA) and newborn lambs (n=4-6).

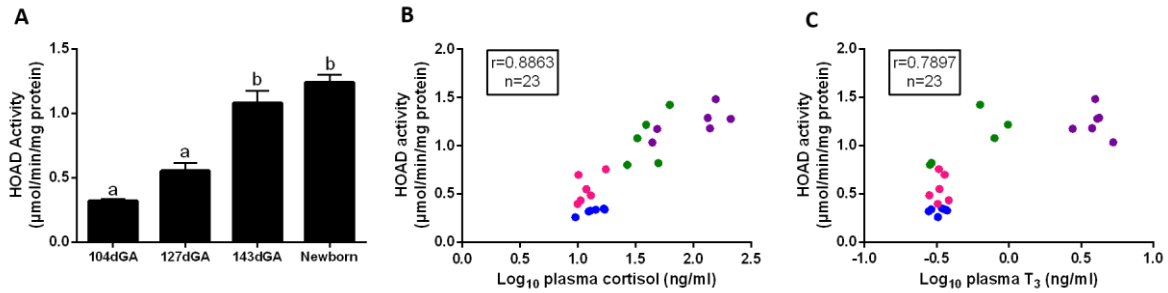

Figure 3.5 β-hydroxyacyl-CoA dehydrogenase (HOAD) activity. A) Mean±SEM HOAD activity in biceps femoris of fetuses at 104, 127 and 143 days of gestational age (dGA) and newborn lambs (n=6 for all ages); different letters are significantly different to each other (P<0.05 by Tukey's post hoc test following one-way ANOVA). B&C) HOAD activity plotted against plasma B) cortisol and C) T_3. N numbers and r values are given on each graph; 104dGA blue, 127dGA pink and 143dGA green and newborn lambs purple.

Table 3.3 Partial correlation analyses of cortisol and T_3 with respirometry data and HOAD activity.

	Biceps femoris	Semitendinosus	Superficial digital flexor
	Pyruvate-supported state III respiration		
Cortisol	0.323	0.210	0.091
T_3	0.397	0.222	**0.538**
	Palmitoylcarnitine state III respiration		
Cortisol	0.249	0.028	0.281
T_3	0.065	0.386	0.252
	HOAD activity		
Cortisol	**0.667**	/	/
T_3	0.159	/	/
	Glutamate and succinate state III respiration		
Cortisol	0.043	-0.141	0.210
T_3	**0.436**	0.497	0.378

R values given and significant correlations highlighted in bold. N=20-23. β-hydroxyacylCoA dehydrogenase (HOAD) activity was not measured in semitendinosus and superficial digital flexor (/).

Table 3.4 Leak state respiration

Leak state respiration ($nmolO_2$/min/mg dry weight)	104dGA	127dGA	143dGA	Newborn
	Biceps femoris			
Pyruvate	0.91±0.29 (n=5) [a]	1.29±0.54 [a]	1.13±0.13 [a]	3.34±0.74 [b]
Palmitoyl-carnitine	0.81±0.28 (n=4) [a,b]	0.39±0.06 [a]	1.36±0.39 (n=5) [a,b]	2.57±0.53 (n=4) [b]
Glutamate	1.12±0.24 [a]	0.82±0.12 (n=5) [a]	2.71±0.95 (n=5) [a,b]	3.07±0.42 [b]
	Semitendinosus			
Pyruvate	1.28±0.36 [a]	1.07±0.19 [a]	1.38±0.34 (n=5) [a]	4.68±0.77 [b]
Palmitoyl-carnitine	1.25±0.47 [a]	0.66±0.05 (n=5) [a]	1.23±0.17 (n=5) [a]	3.00±0.31 [b]
Glutamate	1.15±0.31 (n=4) [a]	1.12±0.09 (n=3) [a]	2.05±0.34 (n=4) [a,b]	3.44±0.41 [b]
	Superficial digital flexor			
Pyruvate	0.77±0.17 (n=5)	1.42±0.39	1.70±0.37 (n=5)	1.80±0.37
Palmitoyl-carnitine	0.78±0.24	1.17±0.20	1.25±0.21	1.49±0.28
Glutamate	0.73±0.14 (n=5) [a]	1.07±0.31 (n=5) [a]	1.85±0.38 [a,b]	2.97±0.54 [b]

Data are presented as mean±SEM. N=6 unless stated otherwise; different letters are significantly different to each other (P<0.05).

Total ADP-coupled oxygen consumption was measured upon the addition of glutamate and succinate, which drive oxphos through CI and CII respectively. There was a significant effect of age on oxygen consumption in BF and SDF muscles (P<0.01 for both muscles). The oxidative capacity of the newborn lambs was significantly higher than at any fetal age in the BF and SDF (Figure 3.6).

There was a significant correlation between total ADP-coupled oxygen consumption with cortisol in BF (P<0.01) and SDF (P<0.001) and T_3 in all 3 muscles (P<0.001 in BF, P<0.01 in ST and P<0.0001 in SDF; r values given in Figure 3.6). T_3 appears to play a predominant role in regulating total oxygen consumption in BF as shown by partial correlation analyses (P<0.05; Table 3.3).

Glutamate supported leak state respiration was affected by age in all 3 muscles (P<0.05 in BF and P<0.01 in ST and SDF). The oxygen consumption was significantly higher in the newborn than at 104 and 127dGA in all 3 muscles studied (Table 3.4). RCR did not change with age in any of the muscles.

There was no significant difference in any respirometry data between the different muscles at any age.

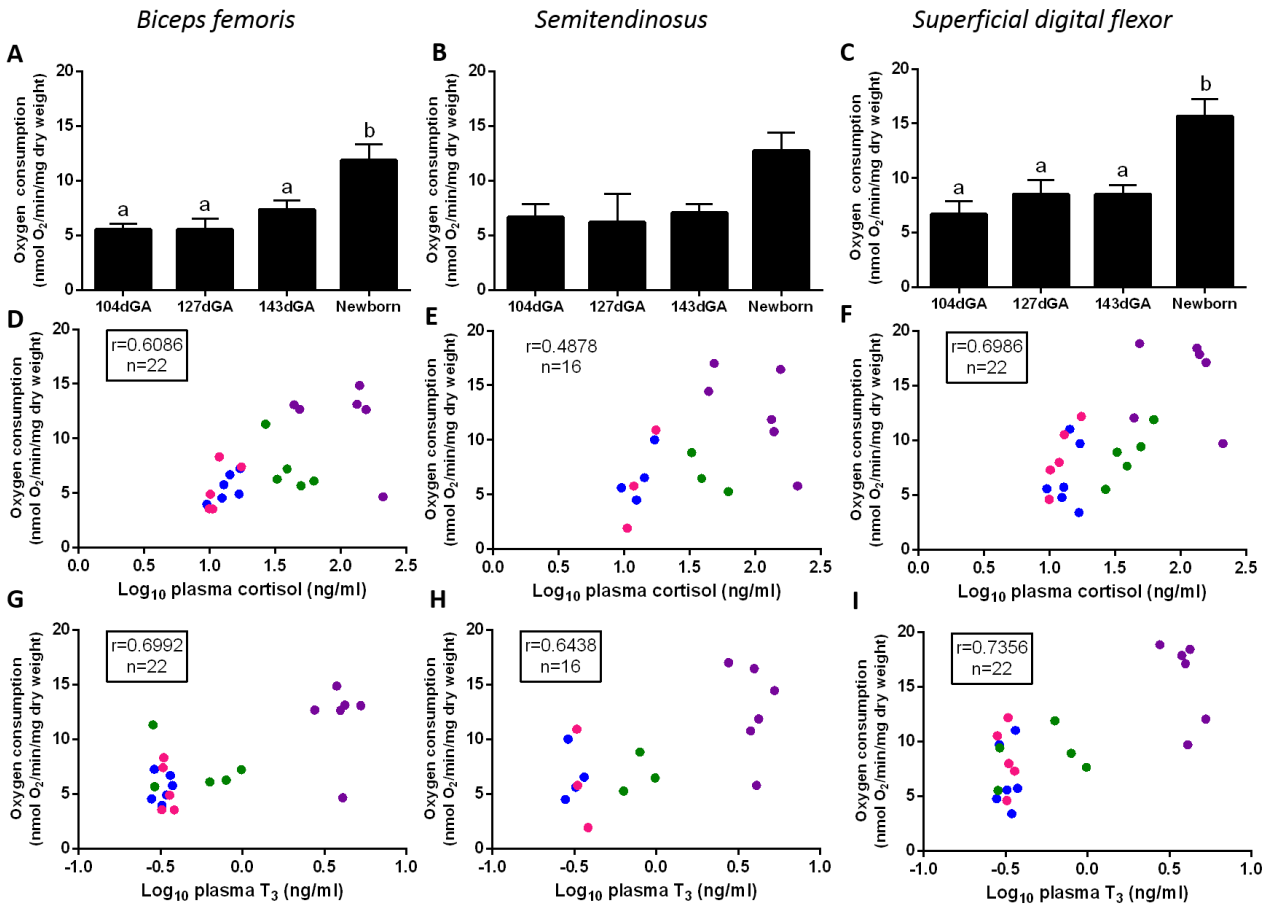

Figure 3.6 Total (glutamate and succinate supported) ADP-coupled oxygen consumption. A-C) Mean±SEM oxygen consumption of fetuses at 104 (n=4-6), 127 (n=3-5) and 143 (n=4-6) days of gestational age (dGA) and newborn lambs (n=6); different letters are significantly different to each other (P<0.05 by Tukey's post hoc test following one-way ANOVA). Oxygen consumption plotted against plasma D-F) cortisol and G-I) T_3 in D&G) biceps femoris, E&H) semitendinosus and F&I) superficial digital flexor. N numbers and r values are given on each graph; significant correlations are given in a box. 104dGA blue, 127dGA pink and 143dGA green and newborn lambs purple.

The graphs shown in Figure 3.2, 3.3, 3.5 and 3.6 suggest that the neonatal data may heavily influence the correlations between mitochondrial parameters and hormone concentrations. Determination of the correlations following the removal of the neonate data points (Table 3.5) reveals that there remains a strong correlation of HOAD activity with both cortisol and T_3 concentrations. Additionally the correlation of total ADP-coupled oxygen consumption in the BF significantly correlated with fetal plasma cortisol concentration, and in the SDF with both T_3 and cortisol when newborn data was removed, but all other respirometry data no longer correlated with the hormones. Thus, in these datasets, the newborn data is important in driving the significant correlations.

Table 3.5 Correlations of cortisol and T_3 with respirometry data and HOAD activity when neonatal data is omitted.

	Biceps femoris	**Semitendinosus**	**Superficial digital flexor**
	Pyruvate-supported state III respiration		
Cortisol	0.392	0.233	0.410
T_3	0.034	0.017	0.197
	Palmitoylcarnitine state III respiration		
Cortisol	0.257	0.307	0.429
T_3	-0.249	0.015	0.161
	Glutamate and succinate state III respiration		
Cortisol	**0.600**	0.272	**0.634**
T_3	0.387	-0.209	**0.586**
	HOAD activity		
Cortisol	**0.844**	/	/
T_3	**0.738**	/	/

R values given and significant correlations highlighted in bold. N=20-23. β-hydroxyacylCoA dehydrogenase (HOAD) activity was not measured in semitendinosus and superficial digital flexor (/).

3.4.3 Regulating oxidative capacity

3.4.3.1 Mitochondrial density and biogenesis

Mitochondrial oxidative function increased over the perinatal period and in order to investigate the factors that may be regulating this, markers of mitochondrial oxidative capacity were measured. Firstly, CS activity, a putative marker of mitochondrial density, was shown to significantly increase with age in all 3 muscles (P<0.0001 by one-way ANOVA in all cases; Figure 3.7 A-C). In all muscles, CS activity was significantly higher at 143dGA than the younger fetal age groups and then was higher still in the newborn muscles (Figure 3.7 A-C). Additionally, when data from all groups were combined, there was a strong positive correlation between CS activity in all 3 muscles and both cortisol and T_3 (P<0.0001 in all cases; r numbers are given in Figure 3.7). Partial correlation analyses suggest that T_3 strongly influences CS activity in all 3 muscles (P<0.01 in BF and P<0.001 in ST and SDF; Table 3.6). In addition, cortisol significantly correlated with CS activity in the BF when controlling for the effect of T_3 using partial correlation analysis, suggesting both hormones play a regulatory role in this muscle (P<0.01; Table 3.6).

The gene expression of PGC1α, a key regulatory protein in mitochondrial biogenesis, was only significantly affected by age in the SDF (P<0.001; Figure 3.8 A-C). In contrast, gene expression of NRF1, normally considered to be downstream of PGC1α, was negatively affected by age in ST (P<0.05) and SDF (P<0.0001; Figure 3.8 D-F).

In order to determine whether the oxidative capacity of the muscle increased in parallel with the increase in mitochondrial density, or whether the function per unit of mitochondrial mass changed with age, the respirometry data were normalised to CS activity. CS activity was initially converted to activity/mg dry weight for a direct normalisation. Py- and PC-supported and total (glutamate and succinate), ADP-coupled oxygen consumption normalised to CS activity is shown in Figure 3.9. There was a significant effect of age on Py-supported and total oxygen consumption per mitochondrial unit in the BF (P<0.001 in both cases by one-way ANOVA), both showing a lower oxidative capacity per mitochondrial unit in the newborns compared to 104-127dGA fetuses. Applying a Mann-Whitney test revealed that the PC-supported oxygen consumption in the BF and total oxygen consumption in the SDF were significantly lower per mitochondrial unit in the newborns compared with 104dGA (Figure 3.9).

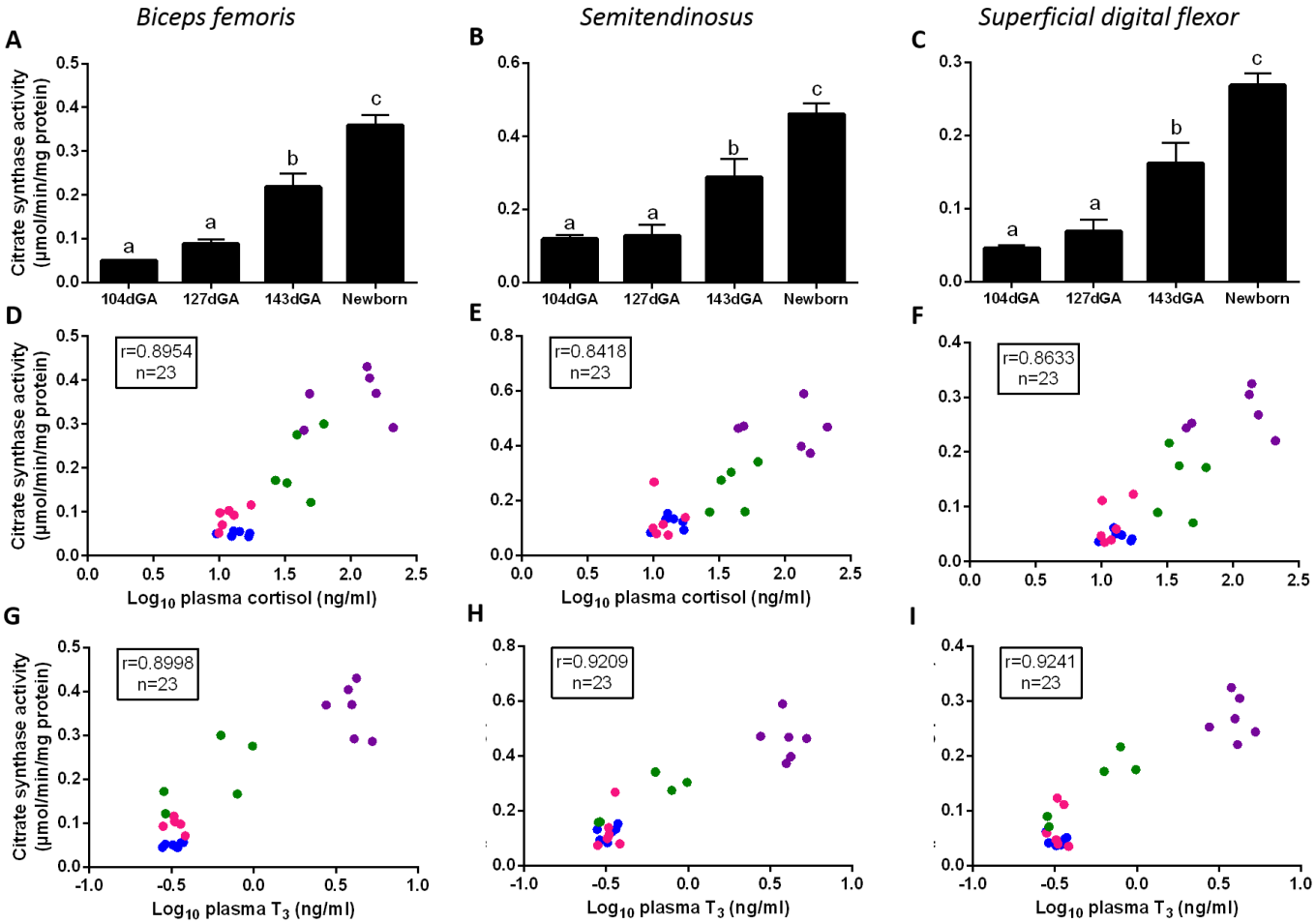

Figure 3.7 Citrate synthase activity. A-C) Mean±SEM activity of fetal muscle at 104, 127 and 143dGA and new born lambs (n=6 in each group); different letters are significantly different to each other (P<0.05 by Tukey's post hoc test following one-way ANOVA). Activity plotted against plasma D-F) cortisol and G-I) T_3 in D&G) biceps femoris, E&H) semitendinosus and F&I) superficial digital flexor. N numbers and r values are given on each graph; 104dGA blue, 127dGA pink and 143dGA green and newborn lambs purple.

Table 3.6 Partial correlation analyses of cortisol and T_3 with citrate synthase activity.

	Biceps femoris	**Semitendinosus**	**Superficial digital flexor**
Cortisol	**0.575**	0.299	0.397
T_3	**0.598**	**0.768**	**0.719**

R values given and significant correlations highlighted in bold. N=23 in each case.

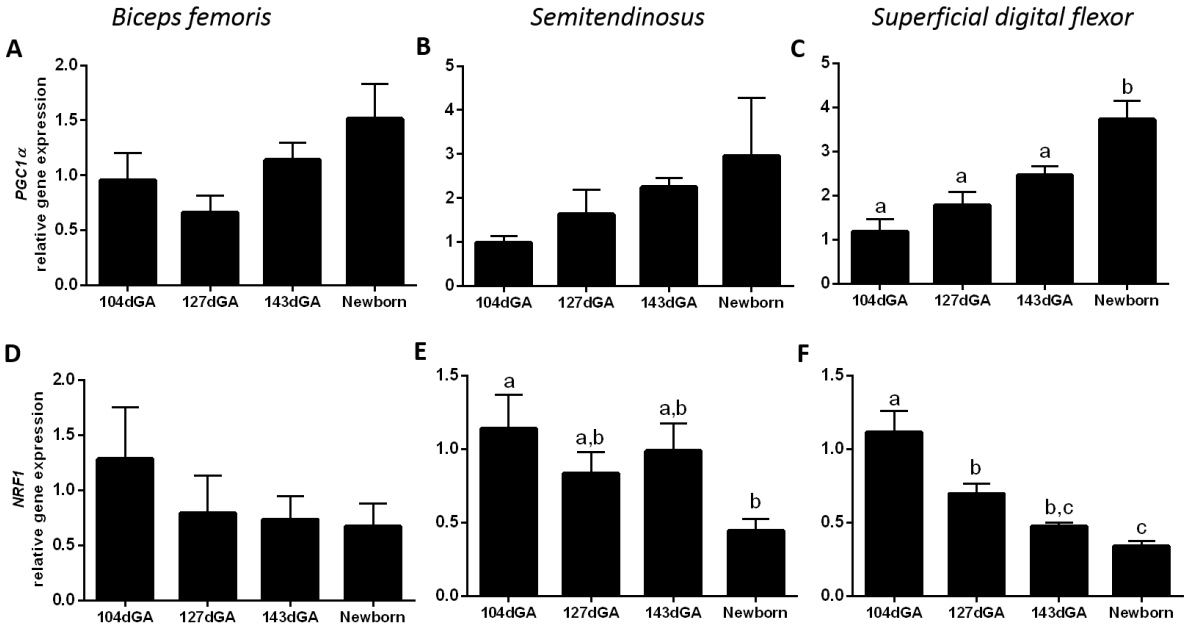

Figure 3.8 Mean±SEM relative gene expression of A-C) PGC1α and D-F) NRF1 in A&D) biceps femoris, B&E) semitendinosus and C&F) superficial digital flexor of fetuses at 104 (n=5), 127 (n=6) and 143 (n=6) days of gestational age (dGA) and newborn lambs (n=6). Different letters are significantly different to each other (P<0.05 by Tukey's post hoc test following one-way ANOVA).

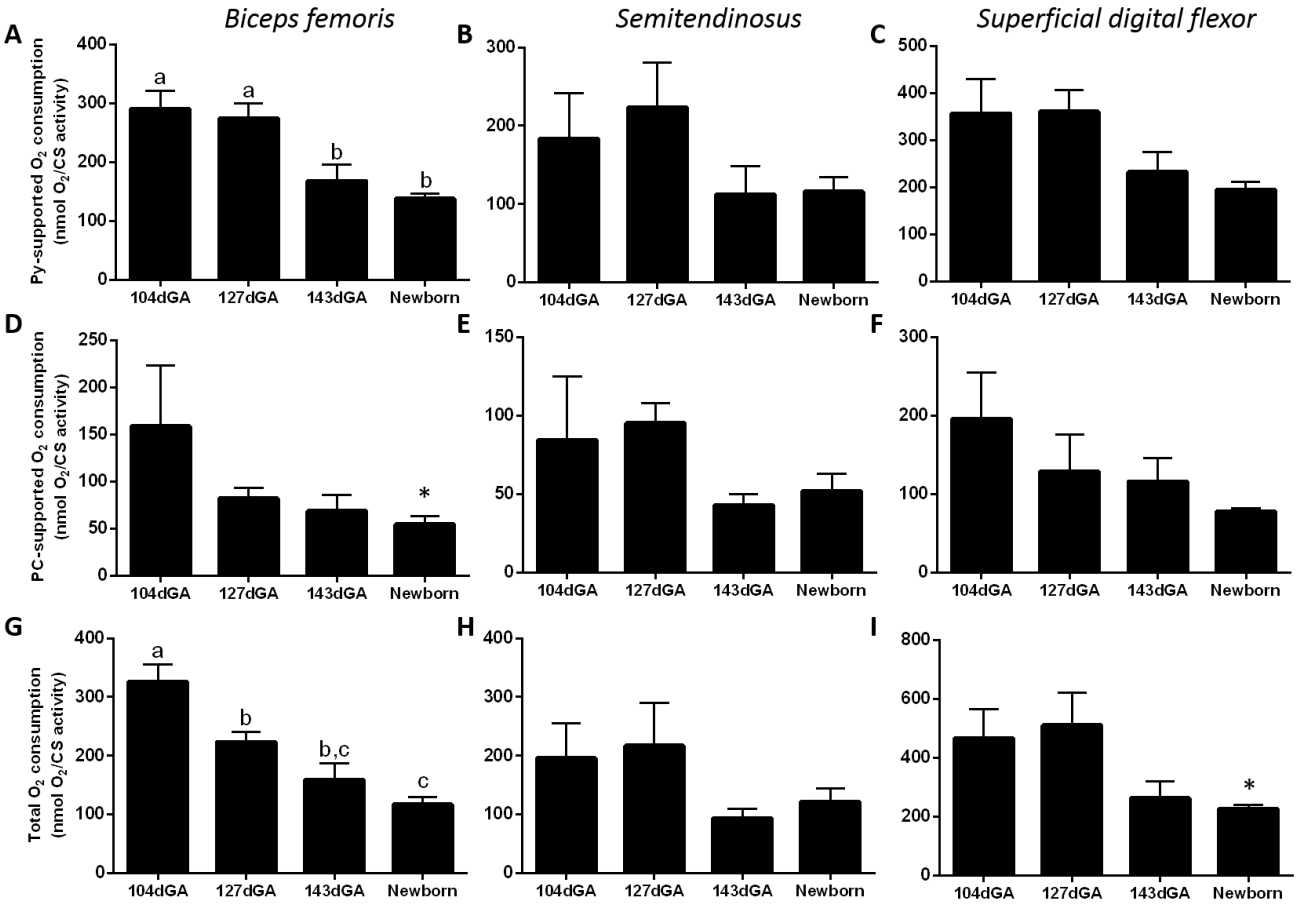

*Figure 3.9 Mean±SEM ADP-coupled, A-C) pyruvate (Py), D-F) palmitoylcarnitine (PC)-supported and G-I) total (glutamate and succinate) oxygen consumption normalised to citrate synthase (CS) activity in A,D&G) biceps femoris, B,E&H) semitendinosus and C,F&I) superficial digital flexor of fetuses at 104 (n=4-6), 127 (n=3-6) and 143 (n=4-6) days of gestational age (dGA) and newborn lambs (n=4-6). Different letters are significantly different to each other (P<0.05 by Tukey's post hoc test following one-way ANOVA). * significantly different from 104dGA (P<0.05 by Mann-Whitney test).*

3.4.3.2 Electron transfer system activity and complex abundance

Western blotting was used to measure the abundance of ETS CI-IV and ATP-synthase in BF, ST and SDF (Figure 3.10, Figure 3.11 and Figure 3.12 respectively). Age had a significant influence on CI-III and ATP-synthase in the BF ($P<0.05$ for complex I and $P<0.0001$ for CII and III and ATP-synthase), CI-IV in the ST ($P<0.001$ for CI and II and $P<0.05$ for CIII and CIV) and CI-IV in the SDF ($P<0.05$ for CI, CII and CIV and $P<0.0001$ for CIII; all by one-way ANOVA). Significant differences between complex protein abundance in the different age groups are marked on the graphs in Figure 3.10-Figure 3.12; in all cases where there was a significant effect of age, with the exception of CII abundance in the SDF, the abundance at 143dGA was significantly higher than at 104dGA.

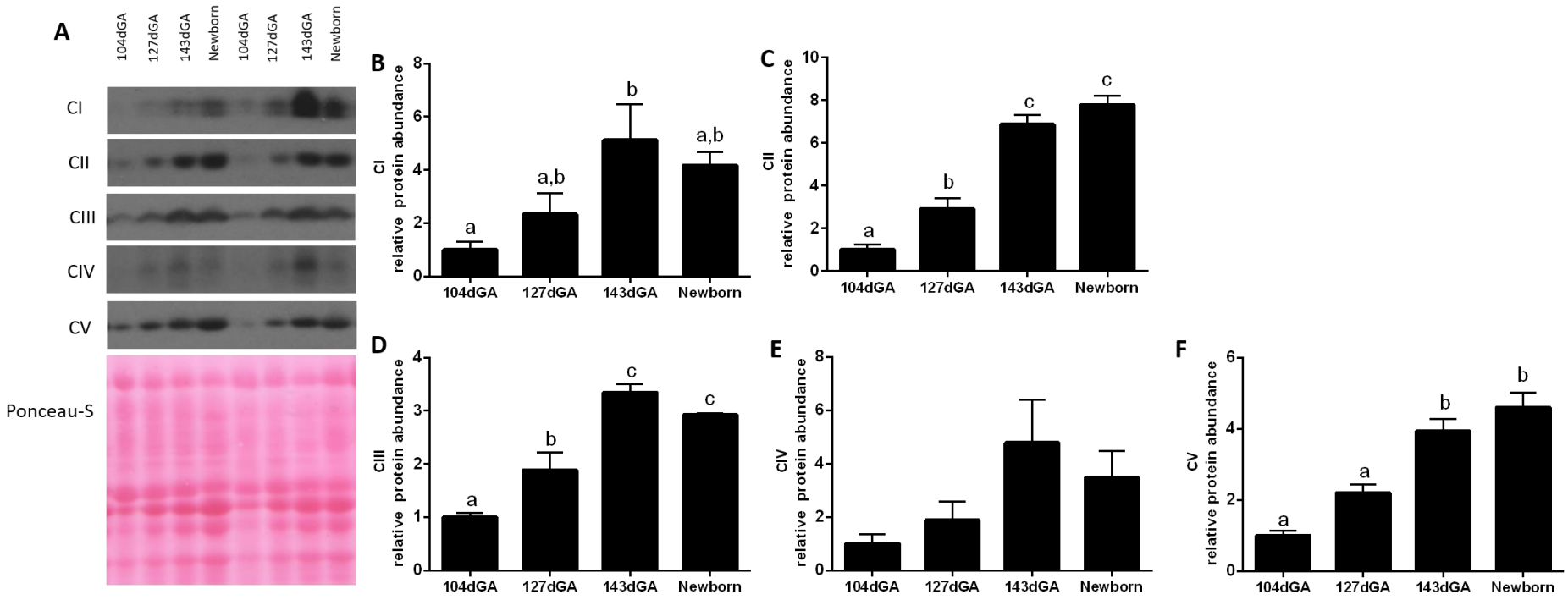

Figure 3.10 Protein expression of electron transfer system complexes I-IV (CI-IV) and ATP-synthase (CV) by western blotting in biceps femoris. A) representative blots and B-F) mean±SEM relative abundance of the complexes I-IV and ATP-synthase, as labelled, of fetuses at 104, 127 and 143 days of gestational age (dGA) and newborn lambs. N=5 in each group for CI, II, III and V; n=3-4 per group for CIV. Different letters are significantly different to each other (P<0.05 by Tukey's post hoc test following one-way ANOVA).

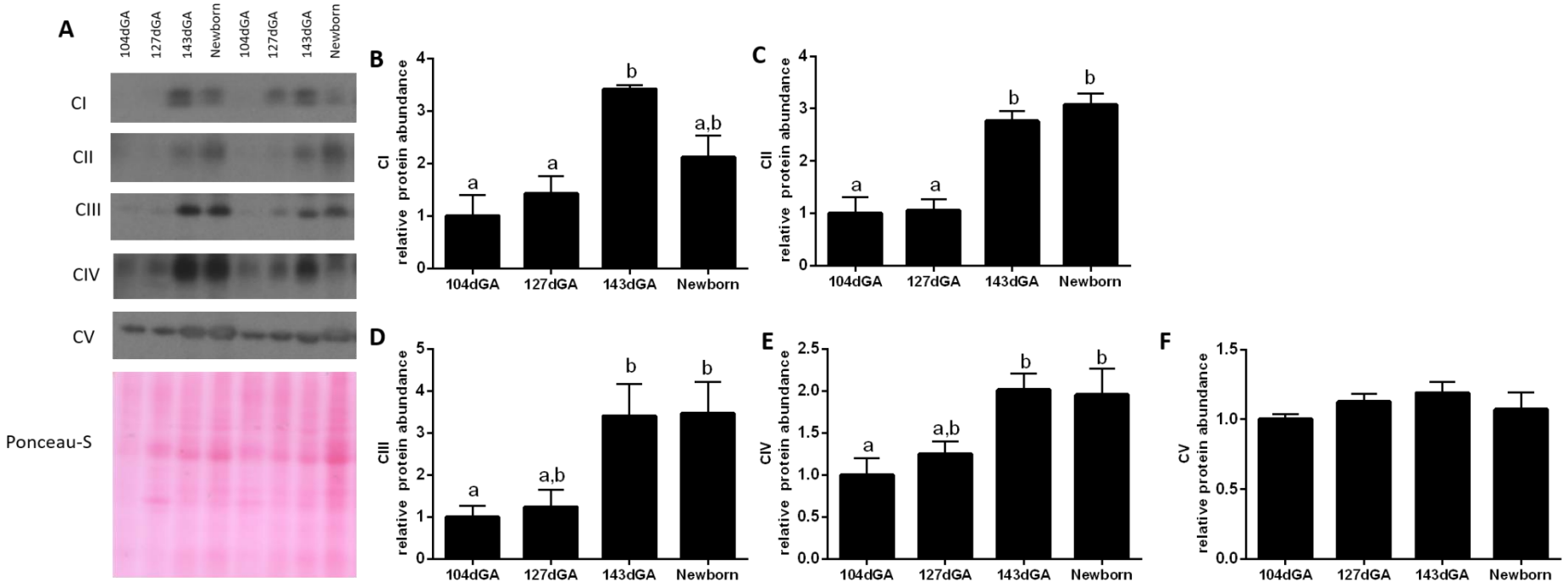

Figure 3.11 Protein expression of electron transfer system complexes I-IV (CI-IV) and ATP-synthase (CV) by western blotting in semitendinosus. A) representative blots and B-F) mean±SEM relative abundance of the complexes I-IV and ATP-synthase, as labelled, of fetuses at 104, 127 and 143 days of gestational age (dGA) and newborn lambs. N=5 in each group. Different letters are significantly different to each other (P<0.05 by Tukey's post hoc test following one-way ANOVA).

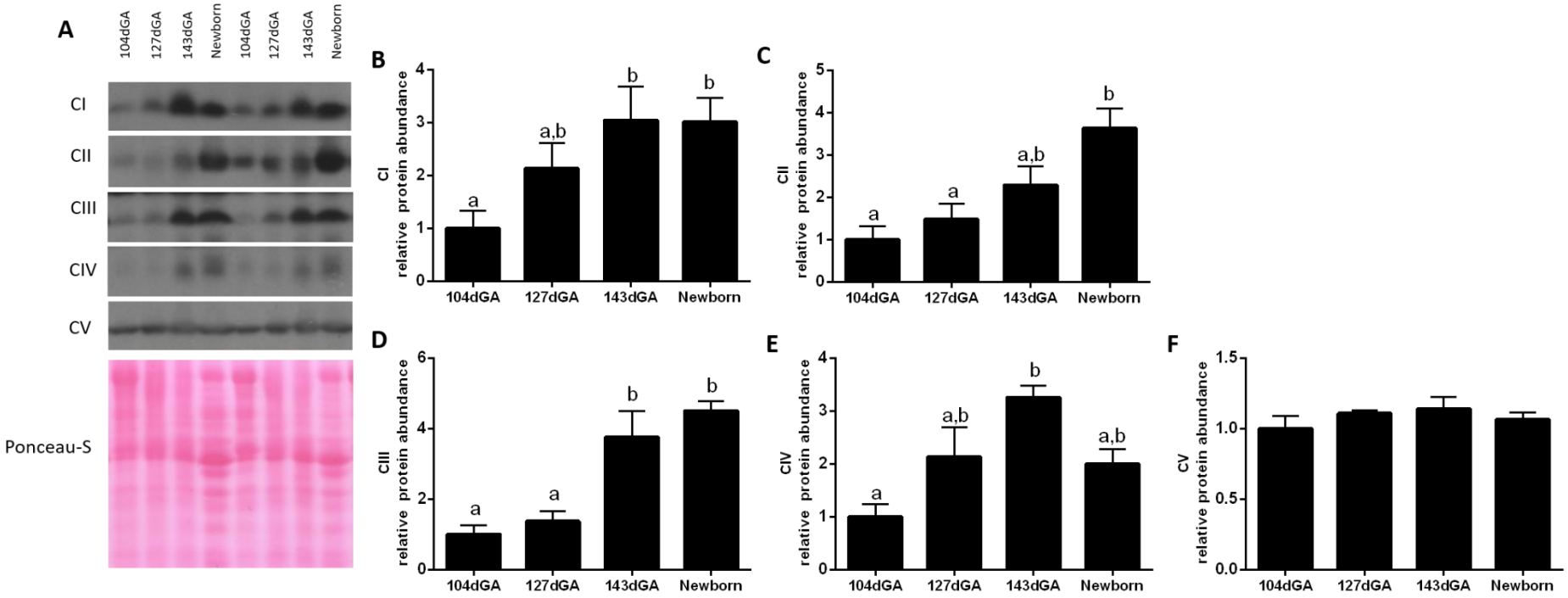

Figure 3.12 Protein expression of electron transfer system complexes I-IV (CI-IV) and ATP-synthase (CV) by western blotting in superficial digital flexor. A) representative blots and B-F) mean±SEM relative abundance of the complexes I-IV and ATP-synthase, as labelled, of fetuses at 104, 127 and 143 days of gestational age (dGA) and newborn lambs. N=5 in each group for CI-IV; n=4-5 for CV. Different letters are significantly different to each other (P<0.05 by Tukey's post hoc test following one-way ANOVA).

3.4.3.3 Uncoupling the proton gradient

Oxidative ATP production relies on the maintenance of the proton gradient across the IMM. The expression of components of the IMM known to be involved in dissipating this gradient, UCP2 and 3 and ANT1, were quantified. Age had a significant effect on the gene expression of UCP2 ($P<0.01$ in BF and ST and $P<0.0001$ in SDF) and UCP3 ($P<0.001$ in BF and $P<0.0001$ in ST and SDF by one-way ANOVA). The expression of both *UCP2* and *UCP3* was dramatically upregulated in the newborns compared to the fetuses at all 3 gestational ages in the 3 muscles studied (Figure 3.13). Applying a one-way ANOVA to only the 3 fetal groups, such that the newborn value did not obscure any preterm differences, revealed a significant effect of age on the expression of *UCP3* in the ST ($P<0.05$) and expression at 127 and 143dGA were significantly higher than at 104dGA (Figure 3.13 E). Age had a positive influence on ANT1 gene ($P<0.0001$ in ST and SDF and $P<0.01$ in BF) and protein expression ($P<0.0001$ in all 3 muscles by one-way ANOVA; Figure 3.14). ANT1 protein expression was significantly higher at 143dGA than at 104dGA in all 3 muscles, and significantly higher still in newborns in the BF and SDF, while gene expression was significantly higher in newborns than the fetuses in all 3 muscles (Figure 3.14).

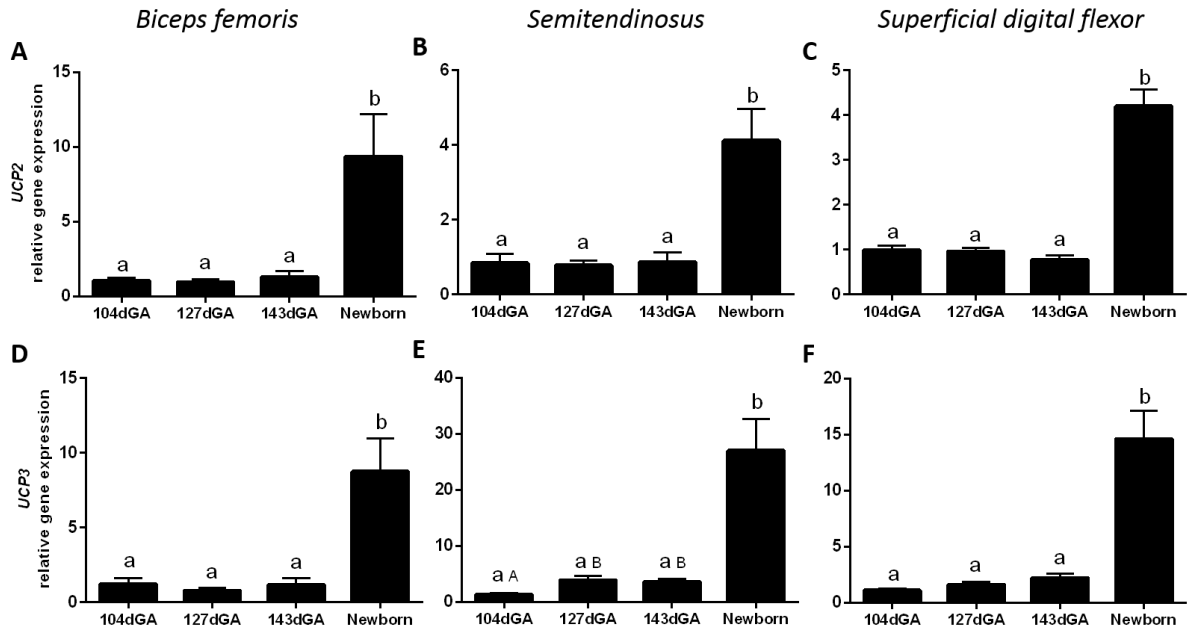

Figure 3.13 Mean±SEM relative gene expression of A-C) uncoupling proteins (UCP) 2 and D-F) UCP3 in A&D) biceps femoris, B&E) semitendinosus and C&F) superficial digital flexor of fetuses at 104 (n=5), 127 (n=4-6) and 143 (n=6) days of gestational age (dGA) and newborn lambs (n=6). Different letters are significantly different to each other (P<0.05). Lower case letters include all 4 age groups, upper case letters include 104-143dGA groups only.

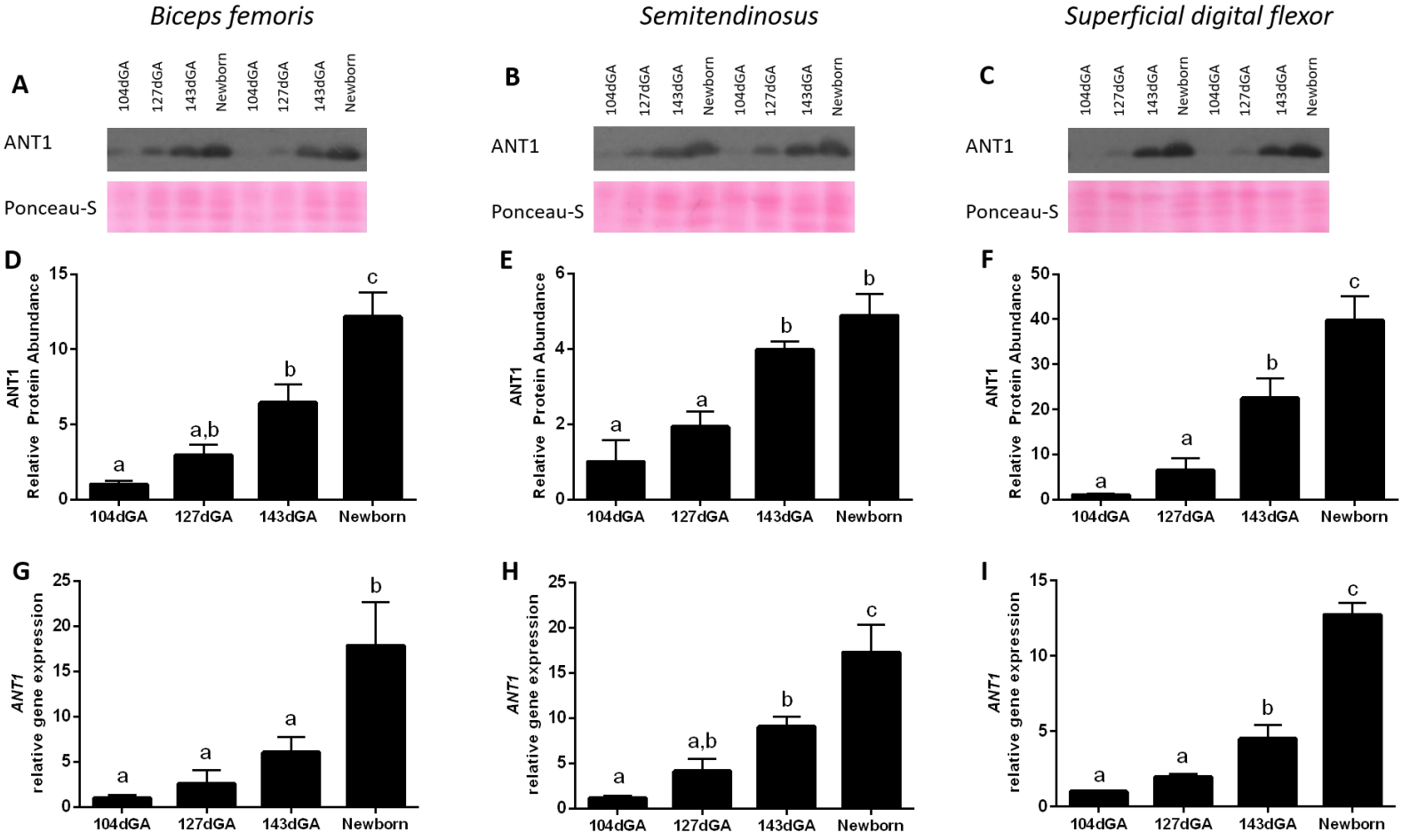

Figure 3.14 Protein and mRNA levels of adenine nucleotide translocase 1 (ANT1) A-C) representative western blots, D-F) mean±SEM protein abundance (n=5 in each group) and G-I) gene expression (n=5-6 in each group) in A,D&G) biceps femoris, B,E&H) semitendinosus and C,F&I) superficial digital flexor of fetuses at 104, 127 and 143 days of gestational age (dGA) and newborn lambs. Different letters are significantly different to each other (P<0.05 by Tukey's post hoc test following one-way ANOVA).

3.4.3.4 Mitochondrial fusion and fission

The extent of mitochondrial network fusion and fragmentation is associated with energy supply and demand (Schrepfer and Scorrano, 2016). Gene expression of fusion proteins, MFN1 and MFN2, and fission protein, DRP1, were quantified using qRT-PCR (Figure 3.15). Age had a significant influence on expression of *MFN1* in the SDF ($P<0.05$) and *MFN2* in BF ($P<0.05$) and SDF ($P<0.0001$ by one-way ANOVA). In these cases there was a general increase in expression with age, such that the expression in the newborn was higher than 127dGA (Figure 3.15 C,D&F). Age affected the expression of *DRP1* in the SDF ($P<0.01$). In this case, however, expression was lower at 127 and 143dGA than 104dGA and the newborn lambs (Figure 3.15 I).

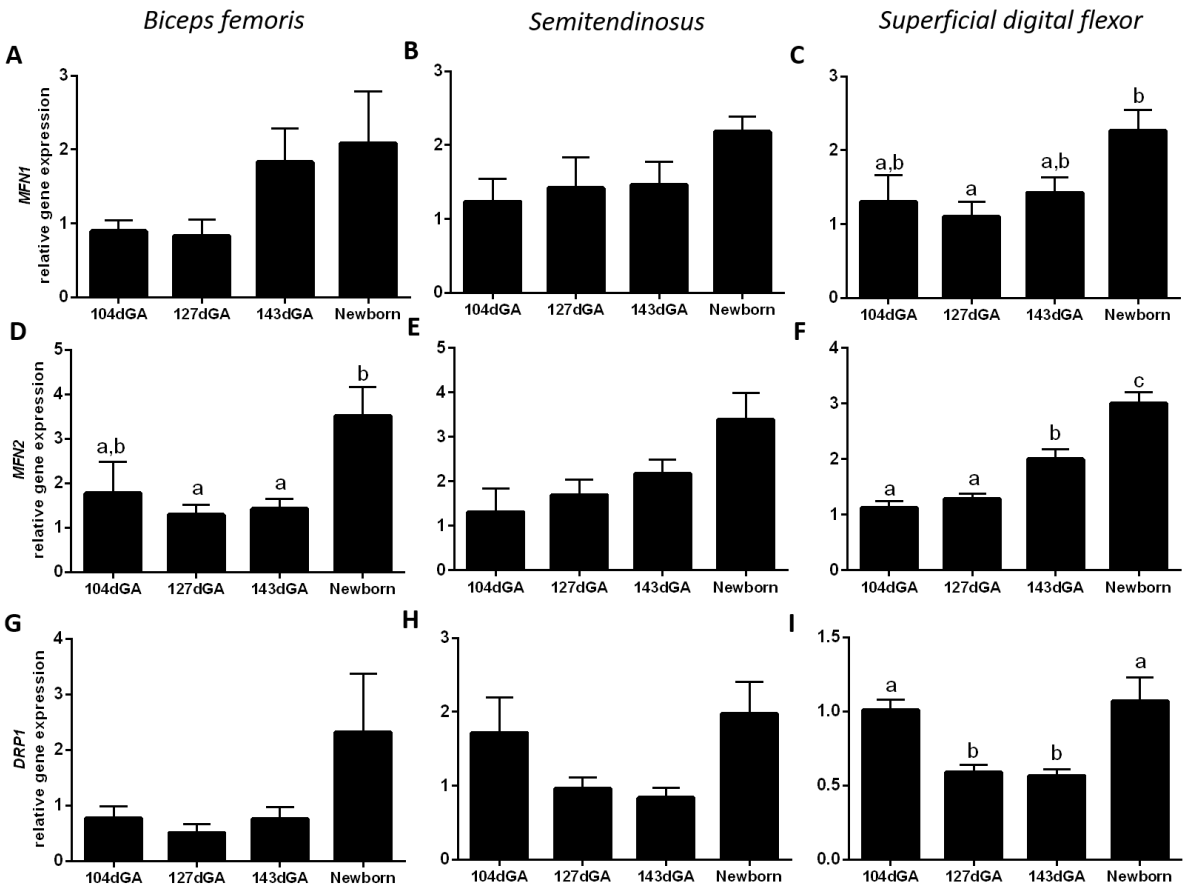

Figure 3.15 Mean±SEM relative gene expression of A-C) mitofusin (MFN) 1 D-F) MFN2 and G-I) dynamin-related protein 1 (DRP1), in A,D&G) biceps femoris, B,E&H) semitendinosus and C,F&I) superficial digital flexor of fetuses at 104 (n=3-5), 127 (n=6) and 143 (n=6) days of gestational age (dGA) and newborn lambs (n=6). Different letters are significantly different to each other (P<0.05 by Tukey's post hoc test following one-way ANOVA).

3.4.3.5 Monitoring cellular energy status

AMPK signalling is important for the cellular response to an increased energy demand or a lower ATP content. The abundance of AMPKα and its phosphorylated form, pAMPKα, was measured by western blotting (Figure 3.16). There was a significant effect of age on the abundance of AMPKα in the SDF (P<0.001 by one-way ANOVA; Figure 3.16 I) with abundance higher near term and in the newborn lambs than at 104dGA. However, there was no significant effect of age on AMPKα abundance in BF or ST, nor on pAMPKα in any of the 3 muscles studied. The ratio of pAMPKα:AMPKα shows a significant decrease with age in the SDF (P<0.05, one-way ANOVA), but no differences were seen in the BF or ST (Figure 3.17).

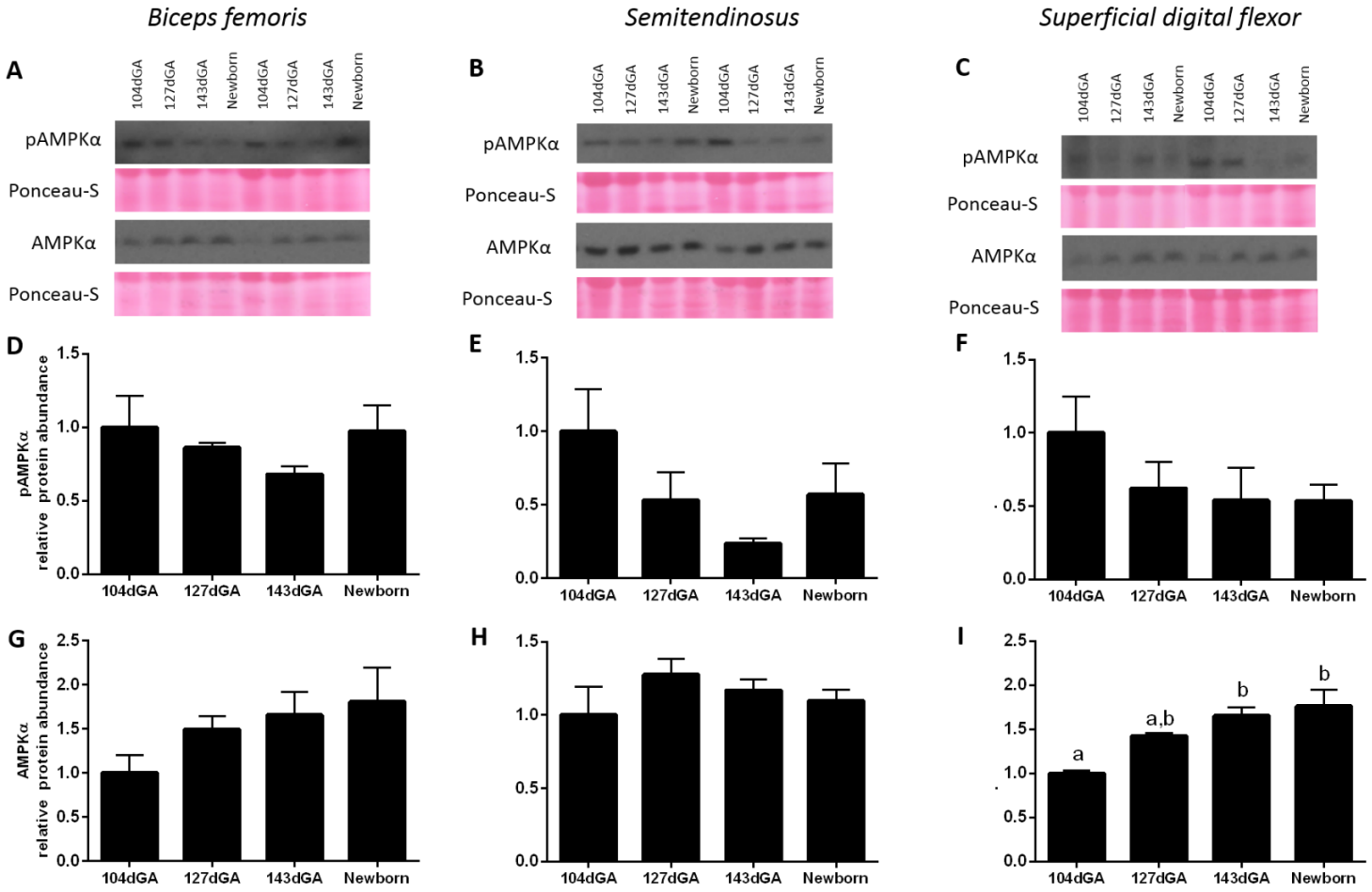

Figure 3.16 Protein expression of (phosphorylated) AMP-activated protein kinase α ((p)AMPKα) by western blotting. A-C) representative blots and D-F) mean±SEM relative abundance of pAMPKα and G-I) AMPKα in A,D&G) biceps femoris, B,E&H) semitendinosus and C,F&I) superficial digital flexor of fetuses at 104, 127 and 143 days of gestational age (dGA) and newborn lambs. N=5 in each group except BF pAMPKα with n=3 per group. Different letters are significantly different to each other (P<0.05 by Tukey's post hoc test following one-way ANOVA).

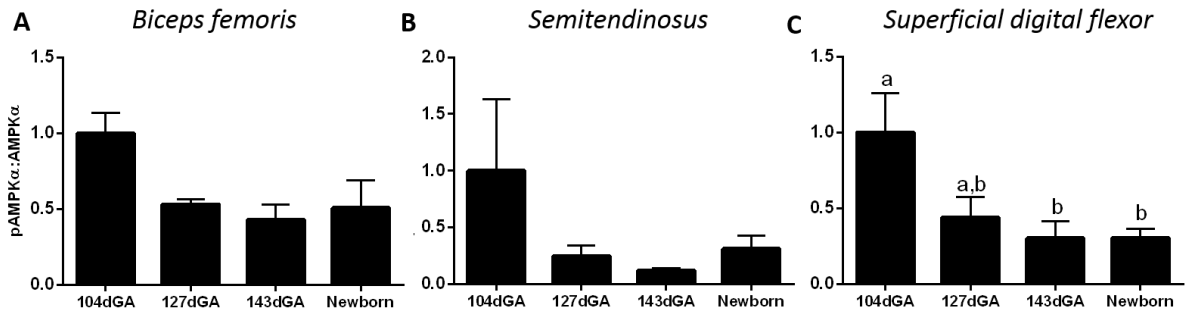

Figure 3.17 Mean±SEM ratio between phosphorylated AMP-activated protein kinase α (pAMPKα) and AMPKα in A) biceps femoris, B) semitendinosus and C) superficial digital flexor of fetuses at 104, 127 and 143 days of gestational age (dGA) and newborn lambs. N=5 per group, except BF with n=3 per group. Different letters are significantly different to each other (P<0.05 by Tukey's post hoc test following one-way ANOVA).

3.4.4 Skeletal muscle structure and type I fibres

The reported increase in skeletal muscle mitochondrial density may reflect an increase in proportion of oxidative type I muscle fibres. In order to determine whether this was the case, the total fibre density was quantified using H&E stained muscle sections (Figure 3.18). There was a significant effect of age (P<0.01 in BF and P<0.0001 in ST and SDF by one-way ANOVA), with fibres accounting for a greater proportion of the muscle area in the older age groups (Table 3.7). Type I fibres were then stained (Figure 3.19) and the fibre number, area and perimeter measured. Age had a significant positive effect on all parameters measured in the BF and ST, as shown in Table 3.7 (P<0.05 by one-way ANOVA). The high density of stained fibres in the SDF of 143dGA and newborn animals meant the individual fibres were difficult to separate, and thus the average fibre area, perimeter and fibre number have not been given for these groups. Expressing the area of type I fibres as a percentage of total fibre area shows the proportion of type I fibres increases with age (P<0.01 in BF and SDF and P<0.05 in ST by one-way ANOVA; Table 3.7). Comparing the 3 muscles, the SDF had a significantly higher MHCI proportion of fibre area than the ST at both 143dGA and newborn lambs.

To gain further insight into the ontogeny of fibre type characteristics, the gene expression of MHCI, IIa and IIx was quantified and data are shown in Figure 3.20. *MHCI* significantly increased with age in the SDF (P<0.0001). Similarly, age only significantly influenced *MHCIIa* in SDF (P=0.0001). *MHCIIx* was positively influenced by age in all muscles studied (P<0.001 in BF and ST; P<0.05 in SDF by one-way ANOVA). When a one-way ANOVA and Tukey's multiple comparisons test were applied only to the data from the 3 fetal ages, there was a significant effect of age on *MHCI* expression in the BF, and on *MHIIa* expression in the ST (P<0.001) where expression at 127 and 143dGA was significantly higher than 104dGA (Figure 3.20).

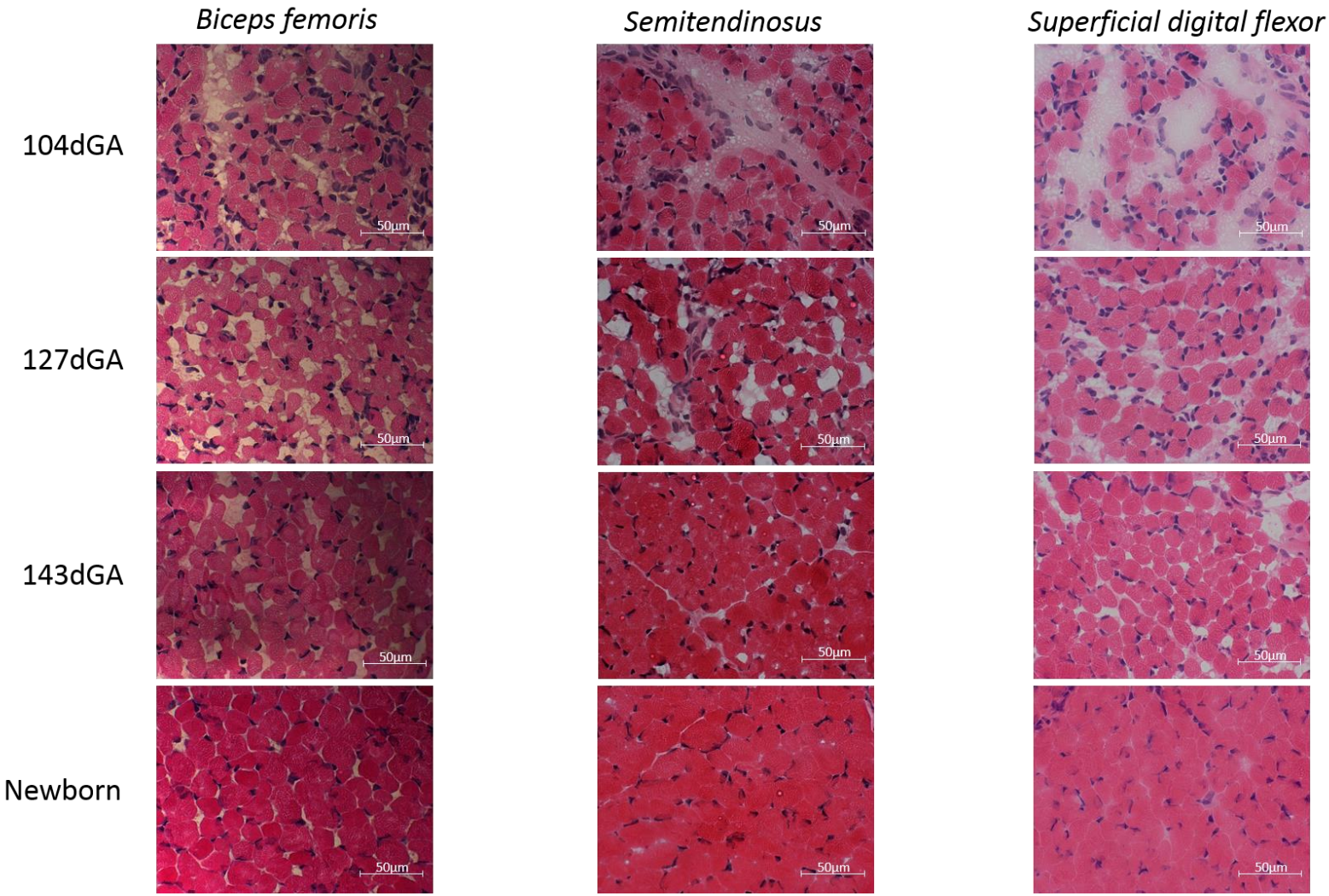

Figure 3.18 Representative H&E stained sections at 40x magnification in biceps femoris, semitendinosus and superficial digital flexor of fetuses at 104, 127 and 143 days of gestational age (dGA) and newborn lambs, as labelled.

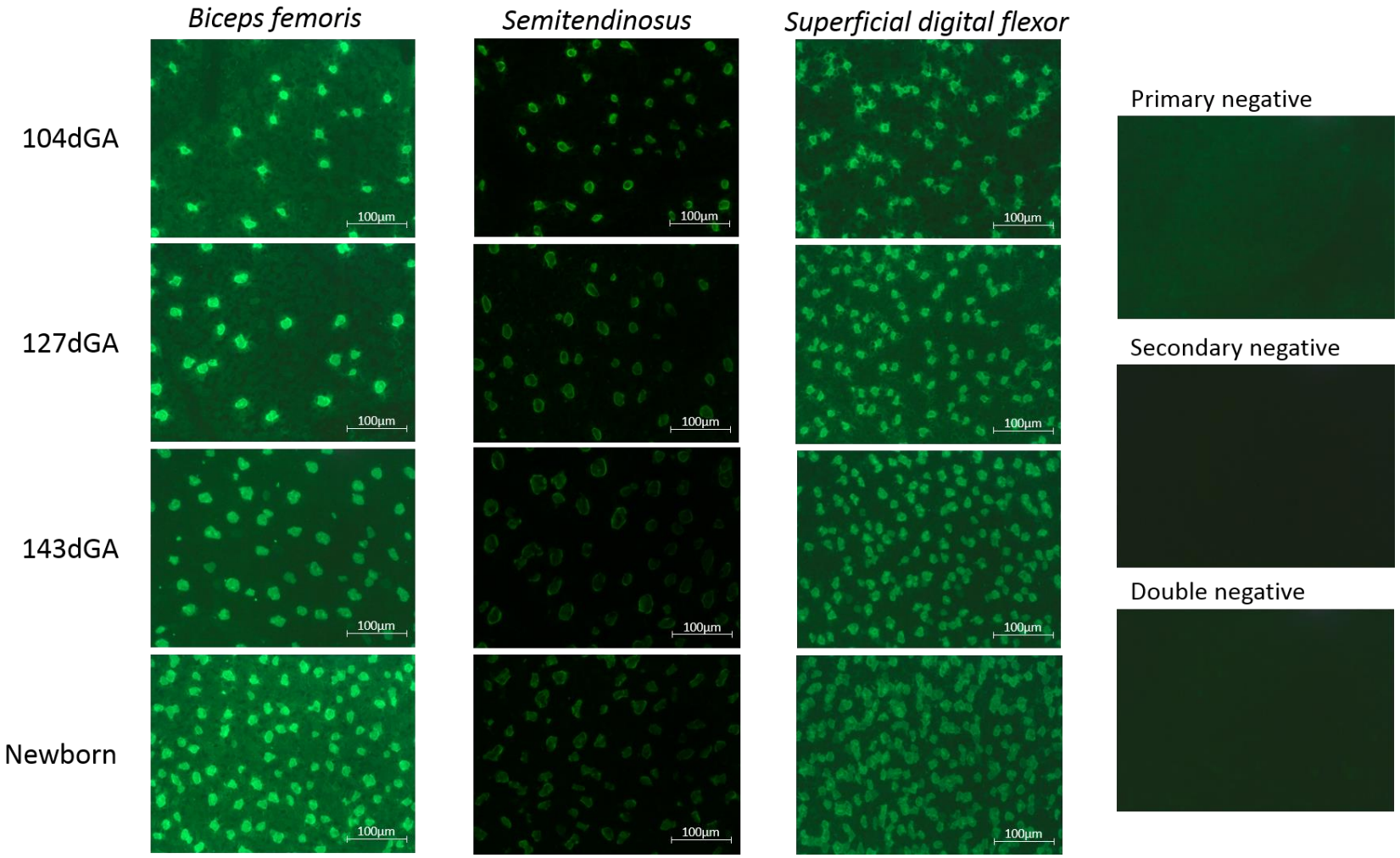

Figure 3.19 Representative MHCI stained sections at 20x magnification in biceps femoris, semitendinosus and superficial digital flexor of fetuses at 104, 127 and 143 days of gestational age (dGA) and newborn lambs, as labelled. Contemporaneous primary, secondary and double negative controls are shown (sections are 104dGA biceps femoris).

Table 3.7 Type I fibre analyses.

	104dGA	127dGA	143dGA	Newborn
	Biceps femoris			
Proportion of total area accounted for by fibres (%)	64.1±2.5 [a] (n=5)	77.6±5.6 [a,b] (n=6)	85.3±3.6 [b] (n=6)	85.2±2.7 [b] (n=6)
Number of type I fibres/mm^2	166±6	286±84	467±71	444±62
Average fibre cross-sectional area (µm^2)	274.1±30.3 [a]	364.9±34.7 [a,b]	419. ±25.6 [a,b]	454.6±44.0 [b]
Average fibre perimeter (µm)	61.9±3.6 [a]	71.6±3.5 [a,b]	78.0±2.4 [a,b]	82.0±4.2 [b]
Proportion of total area accounted for by type I fibres (%)	4.5±0.4 [a]	10.3±3.0 [a,b]	19.5±3.0 [b]	19.2±0.8 [b]
Proportion of fibre area accounted for by type I fibres (%)	7.2±0.9 [a]	11.9±3.1 [a,b]	23.2±3.6 [b]	23.0±0.5 [a,b]
	Semitendinosus			
Proportion of total area accounted for by fibres (%)	54.3±2.3 [a] (n=6)	75.1±1.8 [b] (n=6)	90.1±1.3 [c] (n=6)	89.8±1.6 [c] (n=6)
Number of type I fibres/mm^2	173±25 [a]	270±47 [a,b]	318±21 [a,b]	366±18 [b]
Average fibre cross-sectional area (µm^2)	265.3±25.6 [a]	422.2±22.7 [a,b]	481.4±13.6 [b]	417.6±19.2 [a,b]
Average fibre perimeter (µm)	61.3±3.0 [a]	78.0±2.2 [a,b]	84.4±1.3 [b]	78.7±2.0 [a,b]
Proportion of total area accounted for by type I fibres (%)	4.4±0.5 [a]	11.5±2.3 [a,b]	15.3±1.1 [b]	15.3±1.2 [b]
Proportion of fibre area accounted for by type I fibres (%)	7.8±0.8	15.8±3.2	17.0±1.1	17.0±1.4
	Superficial digital flexor			
Proportion of total area accounted for by fibres (%)	55.0±5.8 [a]	64.8±3.5 [a] (n=5)	75.1±4.7 [a,b] (n=6)	92.9±1.4 [b] (n=6)
Number of type I fibres/mm^2	312±50	465±92	n.q.	n.q.
Average fibre cross-sectional area (µm^2)	274.7±31.5	302.9±43.4	n.q.	n.q.
Average fibre perimeter (µm)	63.1±3.7	35.9±4.7	n.q.	n.q.
Proportion of total area accounted for by type I fibres (%)	8.3±1.1 [a]	13.1±1.2 [a,b]	27.6±3.1 [a,b]	33.6±2.7 [b]
Proportion of fibre area accounted for by type I fibres (%)	16.2±4.0 [a]	20.2±1.2 [a,b]	33.6±2.7 [a,b]	36.1±3.4 [b]

Data are presented as mean±SEM in biceps femoris, semitendinosus and superficial digital flexor of fetuses at 104, 127 and 143 days of gestational age (dGA) and newborn lambs. N=4 in each group unless stated otherwise. Different letters are significantly different to each other (P<0.05). n.q. not quantifiable.

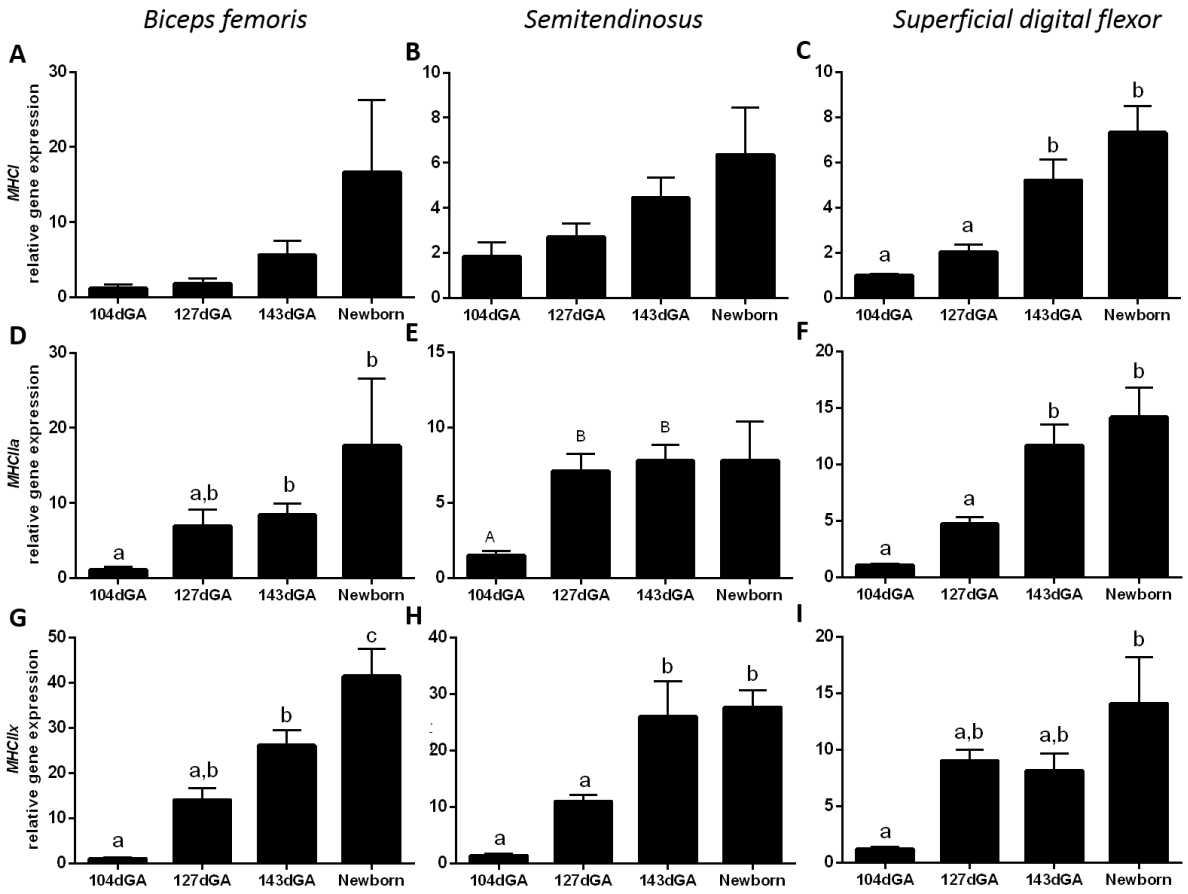

Figure 3.20 Mean±SEM gene expression of A-C) MHCI, D-F) MHCIIa and G-I) MHCIIx in A,D&G) biceps femoris, B,E&H) semitendinosus and C,F&I) superficial digital flexor of fetuses at 104 (n=5), 127 (n=5-6) and 143 (n=6) days of gestational age (dGA) and newborn lambs (n=4-6). Different letters are significantly different to each other (P<0.05). Lower case letters include all 4 age groups, upper case letters include 104-143dGA groups only.

3.5 Discussion

This study demonstrated that in 3 hind limb skeletal muscles, mitochondrial oxidative capacity increased significantly with age in a muscle- and substrate-dependent manner, with the oxygen consumption often significantly higher in neonatal than fetal muscles. Over late gestation there was an increase in mitochondrial abundance and expression of proteins involved in oxidative ATP production and transport, including ETS complexes and ANT1. The gene expression of UCP2 and UCP3 also show a significant postnatal upregulation. The fetal concentrations of cortisol and T_3 were clearly correlated with oxidative capacity and mitochondrial abundance in the 3 muscles studied.

3.5.1 Fetal and neonatal development

Total body weight increased significantly over late gestation, almost tripling between 104 and 143dGA, known to be a period of significant fetal growth (Mellor and Matheson, 1979). Similarly, fetal crown-rump length increased significantly between each age group studied, with values in accordance with previously reported values in Welsh Mountain twin and singleton fetuses (Lanham et al., 2011, Fowden et al., 1989). The rate of growth was higher between 104 and 127dGA than between 127 and 143dGA as previously shown (Fowden et al., 1989). Hind-limb length increased with age over late gestation; the late gestation period is important for the growth of the hind-limb skeleton (Lanham et al., 2011). In addition, the mass of the 3 skeletal muscles studied increased with age, with the mass of the ST and SDF being significantly different between each age group. This coincided with an increased fibre density with age in all 3 muscles. The type I fibre analyses suggest that, for type I fibres at least, this increased muscle mass and fibre density may be due to both hyperplasia and hypertrophy as both the number and cross sectional area of fibres were significantly influenced by age in the BF and ST. Maturation of muscle fibres is believed to occur during the last third of gestation, with hyperplasia contributing little to muscle growth from around 75% of the way through gestation in sheep (Du et al., 2010). As such, hypertrophy of both type I and type II muscle fibres has been shown to occur over the last third of gestation in ovine soleus, medial gastrocnemius and flexor digitorum longus, resulting in no change in the proportion of type I to type II fibres reported with gestational age (Javen et al., 1996). Consequently, the increase in number of type I fibres with age shown in the current study, may reflect an increased

number of fibres maturing to take on the type I fibre phenotype and express MHCI, rather than a continuation of fibre proliferation.

The water, lipid, glycogen and protein content of the fetal and neonatal muscles were analysed, and results expressed per wet weight fit the trends previously reported in biochemical composition of fetal muscle of rhesus monkeys during the second half of gestation (Kerr et al., 1971). Water content of all 3 muscles decreased significantly over late gestation with content not significantly different between 143dGA and the newborns lambs. In contrast, protein content increased with age, and was significantly greater in the newborns than at 127dGA in the BF and SDF.

Development of fuel reserves in skeletal muscle involves the deposition of glycogen and lipid in preparation for the immediate postpartum period when the continuous placental supply of maternal nutrients ceases (Fowden et al., 1998). In the current study muscle glycogen increased from 104dGA and reached the level seen at term by 127dGA, an ontogenic profile similar to that shown previously for ovine BF muscle (Forhead et al., 2009). Glycogen content then fell postnatally, to be significantly lower in newborns compared with 143dGA fetuses in all 3 muscles. This fall in glycogen content, reflects its rapid mobilisation and metabolism to supply the increased energy requirement of the neonatal muscle (Mellor and Cockburn, 1986). Fetal lipid deposition during late gestation is also important to provide metabolic substrates to tissues including neonatal cardiac and skeletal muscle (Beatty and Bocek, 1970). Hepatic and adipose tissue account for the majority of fetal lipid stores at term (Hull, 1975). In this study, lipid content was measured only in the BF, but content did increase with the highest value measured in the newborn lambs. Plasma free fatty acid concentration was not measured in this cohort, but previously has been shown to rise rapidly after birth in sheep (Vanduyne et al., 1965). In adult muscle, lipid droplets are situated near the mitochondria as an easily accessible fuel store (Hoppeler, 1999). Our results in the BF suggest that in the first day of neonatal life, muscle lipid does not provide a source of circulating FAs, nor a local metabolite for oxphos as lipid content was not lower in neonatal than fetal muscle. However, muscle mitochondria over late gestation are capable of using FAs for oxidative metabolism and this is discussed below.

3.5.2 Mitochondrial oxidative metabolism

In the current study, ovine fetal muscle has been shown to be capable of oxidative metabolism throughout the last third of gestation, supporting previous studies (Morriss et al., 1973). Throughout late gestation and in the neonates, skeletal muscle was capable of oxidative metabolism of both carbohydrate and lipid substrates. The contribution of lipids to fetal metabolism is a matter of debate, but this current study demonstrates that in sheep, as in primates, the fetal muscle has the capacity to carry out FA oxidation (Beatty and Bocek, 1970). However, fetal sheep are relatively lean and under normal circumstances *in vivo* are thought to be reliant predominantly on glucose metabolism (Hay, 2006, James et al., 1971). Similarly, immediately after birth, glucose is the preferred metabolic substrate, although circulating lipids rise early in neonatal life and reliance on FA for metabolism increases postnatally (Mellor and Cockburn, 1986, Vanduyne et al., 1965). In agreement with these observations, our results suggest that when PC was the available substrate oxygen consumption was around 2-3 times lower than when Py was used. This was true in all 3 muscles at all ages studied.

Using Py or PC as the substrate, there was a general trend for state 3 respiration to increase with age, reaching significance for Py-supported oxygen consumption in all 3 muscles, and in the ST and SDF for PC-supported oxygen consumption. Similarly, there was an increased oxygen consumption with the combined substrate combination of succinate and glutamate with age in BF and SDF. However, except for Py-supported respiration in the SDF, oxygen consumption was not significantly higher at 143dGA than 104dGA. These data complement reports that total fetal oxygen consumption over the second half of gestation does not vary with age, and skeletal muscle is thought to account for a significant proportion of total fetal oxygen consumption (Acheson et al., 1957, Fowden and Silver, 1995). The oxygen consumption of the newborn muscle was often significantly higher than the fetal muscle at all 3 fetal ages studied as shown for Py-supported respiration in all 3 muscles and combined glutamate- and succinate-supported oxygen consumption in the BF and SDF. These data suggest that, as hypothesised, the oxidative capacity was higher after birth in order to cope with the increased energy demands compared to those *in utero*. Tissue specific changes in oxygen consumption have been observed; the kidney did not show a significant change across the perinatal period, while liver and brain oxygen consumption was significantly increased postnatally compared with the near-term fetus (Klein et al., 1983). Results of the current study

suggest that the oxygen consumption of skeletal muscle increases at birth, as this tissue immediately takes on its new energetically demanding roles.

3.5.3 Mitochondrial density and morphology changed over the perinatal period

Following on from the finding that mitochondrial function increased with age, mitochondrial parameters that may contribute to the oxidative capacity were studied. Over late gestation there was an increase in mitochondrial density, abundance of ETS complexes and, in the SDF, mitochondrial fusion, in preparation for the increased demand for ATP production after birth.

3.5.3.1 Mitochondrial biogenesis

Citrate synthase activity, used as a marker of mitochondrial density, was significantly higher at term than earlier in gestation, and further increased in the newborn lambs in all 3 muscles studied. Histological studies on rabbit hearts have shown a similar increase in mitochondrial density over the perinatal period (Smith and Page, 1977). Alongside an increase in mitochondrial density, there was a significant increase in the abundance of ETS complexes I-IV in all muscles with gestational age, with the exception of CIV in the BF where this trend did not reach significance. However, the abundance of all ETS complexes in the 3 muscles was not significantly different in the neonate compared with at 143dGA, so upregulation of ETS oxidative capacity occurred in advance of birth even though oxygen consumption *per se* did not increase significantly until after delivery.

PGC1α and NRF1 are known to be involved in driving mitochondrial biogenesis. However, in the current study, *PGC1α* expression was only significantly higher in the newborns compared with the fetuses in the SDF and *NRF1* decreased with age, reaching significance in the ST and SDF. Therefore, the gene expression results suggest that this pathway may not be responsible for the increased mitochondrial density in late gestation. That being said, and although PGC1α and its coactivators are regulated at the level of mRNA and protein, signalling via PGC1α is highly regulated at the post-translational level (Scarpulla et al., 2012). For example, PGC1α-mediated gene expression is increased due to phosphorylation by AMPK (Scarpulla et al., 2012). There may, therefore, be downstream modulation of PGC1α signalling over late gestation, which has been missed by measuring only mRNA abundance. If PGC1α in SDF is not regulating mitochondrial biogenesis via NRF1, its upregulation in the SDF may be affecting

other downstream components. For example, NRF2 is also implicated in global mitochondrial regulation involved in upregulating numerous mitochondrial genes and increasing mitochondrial oxidative function (Scarpulla, 2011). In the current study, the expression of NRF2 has not been determined and its expression may more closely follow that of PGC1α than NRF1, and may be acting downstream of PGC1α to drive biogenesis.

Alternatively, the increase in *PGC1α* in the SDF may be regulating pathways other than mitochondrial biogenesis. PGC1α is also known to drive more acute responses preceding a detectable increase in mitochondrial number including preserving existing glycogen stores through increasing the capacity for FA oxidation (Smiles and Camera, 2015, Baar et al., 2002, Wende et al., 2007). At birth, the rapid drop in glycogen alongside the increase in muscle contraction, may be involved in upregulating lipid metabolism, both by driving the postnatal increase in PGC1α in the SDF or directly via PPAR signalling in the neonates (Philp et al., 2013). The increase in PGC1α expression in the SDF at birth may, therefore, be more important in regulating substrate usage, than mitochondrial biogenesis. Further investigation should involve measuring the abundance of PPARs.

PGC1α-independent pathways for increasing mitochondrial density may also exist and would be interesting to investigate (Philp et al., 2010). For example, an increase in mitochondrial biogenesis in skeletal muscle was seen with dexamethasone treatment without upregulation of the NRF pathway (Weber et al., 2002). These authors suggest that this may be due to the synthetic GC binding directly to the mitochondrial GR to drive biogenesis independently of nuclear factors. Additionally, a mitochondrial specific THR is known to play a key role in mediating TH-dependent mitochondrial responses, including biogenesis (Marin-Garcia, 2010). Therefore, as these hormones rise over the perinatal period, they may have a direct effect on the muscle mitochondria. Alternatively, glycolytic activity in the skeletal muscle may play a regulatory role as pyruvate has been shown to increase mitochondrial biogenesis despite decreasing PGC1α in cultured myoblasts: an effect which may be due to the concomitant rise in PGC1α-related coactivator (PRC) a known stimulant of mitochondrial biogenesis (Philp et al., 2010). Overall, there is an increased mitochondrial density, but the mechanism regulating the biogenesis requires further investigation.

3.5.3.2 Fission and fusion

In addition to the mitochondrial density and protein levels, mitochondrial morphology is believed to play a role in regulating oxidative function. An increased energy demand is associated with increased fusion and enhanced ATP production (Schrepfer and Scorrano, 2016). The expression of *MFN1* and *MFN2* in the SDF and *MFN2* in the BF increased significantly during the perinatal period. This suggests that there may be an increased incidence of mitochondrial fusion, particularly in the SDF with increasing age. The expression of *MFN1* and *2* are regulated, in part, by PGC1α which was increased in the SDF (Zorzano and Claret, 2015). Interestingly, this is the only muscle which had an increased AMPKα protein expression with age, generally associated with increased rate of fission (Zhang and Lin, 2016).

The fact that in BF and ST there seemed to be little change in expression of fusion and fission markers over late gestation and the perinatal period may suggest that network dynamics are of little importance in regulating the oxidative function at this time. However, only gene expression was measured. DRP1 activity, including its translocation from the cytosol to the mitochondria, is highly regulated by post-transcriptional processes including phosphorylation and nitrosylation and, therefore, it is perhaps unlikely that transcriptional regulation plays a large role in modulating the rate of fission (Zorzano et al., 2010, Cereghetti et al., 2008, Cribbs and Strack, 2007). Similarly, MFN1 and 2 are regulated post-translationally, in particular by ubiquitination (Zorzano and Claret, 2015). Gene expression may give a preliminary insight into the possible mitochondrial network dynamics over this period, but further investigation is required for a more reliable conclusion.

Mitofusins are known to play additional roles in the cell, which might be important during the perinatal period. *Mfn1*-knockout cells showed long-term altered mitochondrial calcium handling and membrane potential, implying a role of MFN1-driven fusion in regulating the muscle excitation-contraction coupling (Eisner et al., 2014). MFN2 is thought to directly regulate metabolism and energy balance (Hernandez-Alvarez et al., 2010). *Mfn2* repression in myotubes has been shown to result in a reduced oxygen consumption and expression of ETS complexes and ATP synthase, with a compensatory increase in glycolysis (Bach et al., 2003, Pich et al., 2005). The increase in *MFN1* and 2 expression in neonatal SDF may, therefore, be directly critical to the function and energy balance of the postnatal muscle.

3.5.4 The increase in mitochondrial density and protein abundance precede the increase in mitochondrial respiratory capacity

For all the respirometry data, an important consideration is that the oxygen consumption is measured with saturating concentrations of substrates and therefore gives a measure of maximal capacity of the muscle mitochondria (Pesta and Gnaiger, 2012). This may not represent what occurs *in vivo* but gives an interesting consideration, as the maximal rates of oxygen consumption measured do not simply follow the increase in mitochondrial abundance and ETS protein levels. A similar disparate result has been observed in cultured myoblasts, where an increase in abundance of mitochondrial proteins was not accompanied by an increase in functional capacity (Philp et al., 2010). Furthermore, when oxygen consumption was normalised to mitochondrial abundance, there was a general downward trend across all muscles, reaching significance in the BF for Py- and total oxygen consumption. The significant drop in Py-supported oxygen consumption per mitochondrial unit in the BF was between 127 and 143dGA, which supports the theory that activity is specifically repressed around birth. However, this was not seen so clearly in the other muscles or upon delivery of the other substrates.

The discrepancy between the ontogenic profiles of mitochondrial abundance and oxidative capacity poses the question of which regulatory mechanisms may drive the increased activity at birth (or conversely remove prenatal inhibition) independently of upregulating mitochondrial density and protein abundance. Numerous pathways have been suggested to regulate activity of the mitochondrial oxphos machinery. The increased ATP consumption after birth may increase the activity of the ETS, as ATP binding to CIV has been shown to interfere with its interaction with cytochrome c (Huttemann et al., 2007). In this way, CIV regulation balances energy supply and demand. ETS subunits can be phosphorylated, the most-studied being CIV which is strongly inhibited upon phosphorylation (Huttemann et al., 2007). Interestingly, hypoxia induces phosphorylation of CIV in neonatal cardiomyocytes (Ogbi and Johnson, 2006). The increased pO_2 exposure after birth may, therefore, be responsible for driving the increased mitochondrial activity, possibly in part via ETS dephosphorylation. Additionally, the low oxygen availability during fetal development may, via hypoxia-inducible factor (HIF) signalling, reduce the activity of pyruvate dehydrogenase and ETS complexes as has been reported to occur during hypoxia in adult tissues (Solaini et al., 2010, Chandel et al., 1997). At birth, this hypoxia-mediated inhibition would be lifted. Finally, the intracellular

electrolyte balance may play a role. An example is calcium which will fluctuate postnatally upon increased muscle contraction; calcium is known to increase activity of the TCA cycle, and also calcium-activated phosphatases may remove inhibitory ETS complex phosphorylation (Huttemann et al., 2007).

In agreement with the initial hypothesis, there is an increase in mitochondrial density and mitochondrial protein abundance towards term in preparation for the increased postnatal energy demand. However, oxidative function of the muscle mitochondria appears to be held back in preparation for the transition to neonatal life. Thus, there may be a mechanism in place to reduce the maximal activity of the ETS near term both to limit the oxygen demand *in utero* when the supply is limited and to minimise the risk of excessive ROS production during labour and delivery when oxygen availability fluctuates widely.

3.5.5 Uncoupling the proton gradient

Age had a significant effect on the expression of *UCP2* and *3* and ANT1 in skeletal muscle, with an increase over the perinatal period. This may explain the increased leak state respiration reported with age in all 3 muscles. Although proton leak is thought to reduce the efficiency of oxphos, a study in hyperthyroid rats showed an increased ATP synthesis despite an increase in UCP expression suggesting that UCP-mediated uncoupling is of negligible importance when oxphos is working at maximal capacity (Short et al., 2001). Alternatively, other factors may be involved in regulating the rate of UCP activity for example, inhibition by guanosine diphosphate (GDP) binding (Short et al., 2001, Simonyan et al., 2001). The upregulation of ANT1 and UCPs in this study, therefore, may be related to an increased necessity of alternative roles of these proteins, without impacting on the efficiency of ATP production.

ANT1 showed a significant increase in both protein and mRNA expression over late gestation, with a further rise after birth. Previously, an increase in ANT abundance in rat liver has been reported during the last 3 days of fetal development which continued to rise postnatally in association with the maturation of mitochondrial oxidative capacity (Schönfeld et al., 1993). Considering the role of ANT in transporting ATP out and ADP into the mitochondria, the rise in abundance with age supports the theory that the fetus is preparing for the increased energy demand at birth. ANT1 carries out its transport role via utilisation of the PMF, thereby dissipating the proton gradient and 50-60% of proton leak has been attributed to the presence

of ANT proteins (Brand et al., 2005). An alternative explanation for the ANT1 increment may be in preventing PMF rising too rapidly, thereby minimising the risk of excessive ROS production during the transition from intra- to extrauterine life.

UCPs also uncouple the proton gradient from ATP generation and increased significantly with age over the perinatal period studied. However, expression of *UCP2* and *UCP3* in all 3 muscles showed a very different profile to that of *ANT1*, with rapid upregulation of mRNA abundance in the newborns compared to any fetal values over late gestation. The primary roles of UCP2 and 3 are currently uncertain. One field of thought is that the key function of UCP2 is in metabolic regulation, with increased expression associated with an increased metabolic rate (Barbe et al., 2001) and low abundance associated with obesity (Nordfors et al., 1998). However, in the immediate postnatal period, when substrate stores are being depleted and an increase in ATP is required, increasing UCP2 for the key purpose of increasing metabolic rate through futile proton cycling is, perhaps, unlikely. As with ANT1, UCPs in neonatal skeletal muscle might be important in regulating ROS production. One theory for the primary role of UCP2 is in minimising ROS production, as macrophages from *Ucp2*-knockout mice showed an 80% increase in ROS production compared to wild-type mice (Arsenijevic et al., 2000). The widespread expression profile means UCP2 could be crucial in minimising oxidative stress throughout the organism (Pecqueur et al., 2001, Pierelli et al., 2017).

As with UCP2, the primary function of UCP3 is a matter of debate. UCP3 is upregulated in hypoxic skeletal muscle and is activated, in part, by superoxide (Echtay et al., 2002). Therefore, its upregulation may be driven by ROS produced during labour as a direct response to prevent excess oxidative damage (Yamada et al., 2003). There are 2 other theories which may explain the rapid upregulation of UCP3 expression at birth. Firstly, UCP3 has been hypothesised to play a role in skeletal muscle mediated thermogenesis (Simonsen et al., 1993, Astrup et al., 1985). An upregulation of skeletal muscle UCP3 gene and protein expression has been reported in rodents and humans upon the induction of thermogenesis, mediating a short-term response to cold-exposure (Simonyan et al., 2001, Barbe et al., 2001, Gong et al., 1997, Boss et al., 1997). The tissues in this current study have been taken only one day after the lambs would have been exposed to cold, and thus the increase in *UCP3* may be important in non-shivering thermogenesis. A second apparent function of UCP3 is in the regulation of lipid metabolism; an upregulation of UCP3 expression has been reported in response to a high fat diet (Schrauwen et al., 2001, Gong et al., 1999). In the current study, *UCP3* expression may be

higher in the newborn than the fetuses either in preparation for, or in response to, an increase in circulating FA concentration.

3.5.6 Muscle specific differences

For the majority of the mitochondrial parameters measured in this study the 3 muscles showed a very similar profile with age. However, in some cases including AMPKα abundance and expression of the markers of fusion, fission and biogenesis, significance was reached only in the SDF. This may be due to differences in the proportion of fibre types; the SDF was the only muscle to show a significant rise in expression of *MHCI* with age and had a higher percentage area of MHCI fibres than the ST shown by immunostaining. In turn, the different structural phenotypes may reflect the different roles of the muscles; the SDF carries out a more sustained contraction, generating a greater force than the BF and ST, therefore requiring a greater abundance of oxidative fibres.

Studies investigating the characteristics of mitochondria from different pig muscle fibres have shown that mitochondria from oxidative fibres have a higher abundance of β-oxidation proteins and a higher PC-supported respiration, with no difference in Py- or glutamate-oxidation in comparison to mitochondria from glycolytic fibres (Glancy and Balaban, 2011). These authors suggest that the increased metabolic demand of oxidative muscles is matched by an increased mitochondrial density rather than by changes to the mitochondria themselves. In the current study there were no differences between respirometry data obtained from the 3 muscles studied, however, whether there is a greater increase in HOAD activity in the SDF than the BF would be interesting to investigate.

3.5.7 Endocrine regulation

Maturational hormones, cortisol and T_3, rose in fetal plasma concentrations significantly towards term. Both hormones showed a further increase postnatally. There was a significant correlation of both cortisol and T_3 with numerous mitochondrial parameters measured including oxygen consumption, CS activity and HOAD activity. Partial correlation analyses indicate that T_3 may be the more important of the two hormones in regulating mitochondria, in particular mitochondrial density. The importance of THs and cortisol in regulating mitochondrial function will be explored further in Chapters 4 and 5.

3.5.8 Conclusion

In conclusion, over late gestation there is an increase in mitochondrial parameters including biogenesis and abundance of ETS proteins. This increase is, however, unlikely to be driven by PGC1α which also rises with age in the SDF. Instead, PGC1α may be playing a role in regulating substrate utilisation postnatally, or controlling the mitochondrial fusion in this muscle. Oxidative function appears to increase postnatally in the BF, ST and SDF. Preventing the increase in oxidative function until after birth might reflect a protective mechanism, in which the mitochondria and its protein components are put in place before birth, but the activity of the ETS is held back to minimise the risk of oxidative damage during the process of labour and delivery. Further, the increased *UCP* expression at birth may play a protective role against excessive ROS production upon sudden exposure to an increased pO_2 and the increased rate of oxidative ATP production.

4 The role of thyroid hormones in fetal skeletal muscle mitochondrial development

4.1 Introduction

Thyroid hormones play a key role in regulating metabolism in the adult. They are associated with an increased metabolic rate and regulate thermogenesis by increasing mitochondrial number as well as upregulating abundance of ETS complexes, TCA cycle enzymes, UCPs and ANT in a variety of adult tissues including liver, heart and skeletal muscle (Winder, 1979, Clement et al., 2002, Barbe et al., 2001, Dummler et al., 1996, Harper and Seifert, 2008, Branco et al., 1999). Additionally, they regulate metabolism by promoting the oxidation of lipids in adult rat and human skeletal muscle (Clement et al., 2002, Lombardi et al., 2009, Irrcher et al., 2008).

Fetal whole body oxygen consumption is also sensitive to TH regulation (Fowden and Silver, 1995, Lorijn et al., 1980). Previous studies of fetal sheep in late gestation have reported a positive correlation between the whole body rate of oxygen consumption and plasma T_4 concentrations (Fowden and Silver, 1995). The data in Chapter 3 also shows a positive correlation between maximal oxygen consumption of skeletal muscle *in vitro* and plasma T_3 *in vivo* in fetal sheep during the perinatal period. In addition to their role in regulating fetal oxidative metabolism, THs have previously been shown to be important for growth and development of the fetus as a whole and its individual organs during late gestation (Shields et al., 2011, Forhead and Fowden, 2014). Inducing hypothyroidism during development resulted in impaired growth and decreased mineral content of the skeleton, reduced mass of the heart, lungs, gastro-intestinal tract and subcutaneous fat, increased abundance of perirenal fat and in altered hepatic and renal carbohydrate metabolism (Erenberg et al., 1974, Forhead et al., 1998, Lanham et al., 2011, Forhead et al., 2009, Forhead et al., 2003, Harris et al., 2017). Importantly, THs are also essential for the development of skeletal muscle in the ovine fetus; hypothyroidism is associated with reduced muscle glycogen, protein and DNA content, altered structural integrity, decreased IGF-I expression, reduced growth-hormone receptor abundance and a decreased proportion of type I to type II fibres (Erenberg et al., 1974, Forhead et al., 2002, Forhead et al., 2009, Finkelstein et al., 1991).

Near term, specific developmental processes occur in order to mature tissues sufficiently to take on new roles at birth. As shown in Chapter 3, this includes the increase in mitochondrial oxidative capacity of ovine fetal skeletal muscle in preparation for the increased energy demand at birth. Several maturational processes during late gestation are regulated by hormones including T_3 which rises in a cortisol-dependent manner in the fetal circulation just before term (Fowden et al., 1998). Specifically in skeletal muscle, THs are thought to play a role in downregulating proliferative signals and inducing terminal differentiation, as shown in ovine fetal muscle and a murine cell line respectively (Carnac et al., 1992, Forhead et al., 2002). TH-dependent development continues postnatally; an increase in proportion of type I fibres was reported in 14 day old hypothyroid piglets compared to euthyroid controls (Harrison et al., 1996).

Despite the well-known role of THs in adult metabolism, few studies have investigated the role of THs on fetal mitochondria. The limited available data suggest that THs increase mitochondrial function and protein expression in fetal tissues including the liver, adipose tissue and skeletal muscle (Herpin et al., 1996, Schermer et al., 1996, Gnanalingham et al., 2005b). THs continue to rise significantly postnatally (Breall et al., 1984) and during the perinatal period, THs are crucial in driving non-shivering thermogenesis, predominantly by uncoupling the mitochondrial proton gradient via UCP1 in brown adipose tissue (Clarke et al., 1997). Additionally, the postnatal TH surge is important in the switch in myocardial substrate preference from carbohydrate to predominantly fatty acid shortly after birth (McClure et al., 2005). Whether THs regulate mitochondrial parameters before birth and drive the ontogenic changes in metabolism in skeletal muscle is not known.

4.2 Aim

The aim of this study was to investigate the role of THs during late gestation on the mitochondrial oxidative capacity of ovine skeletal muscle. The aim was to determine whether removing THs from the developing sheep fetus during late gestation would prevent the normal ontogenic rise in skeletal muscle mitochondrial function, and whether preterm T_3-infusion would prematurely increase oxidative function, mimicking the normal changes seen in preparation for birth in Chapter 3.

4.3 Methods

4.3.1 Animals

Seventeen twin-bearing ewes underwent surgery for this study. Of these, 12 ewes carried fetuses which underwent surgery at 102-105dGA in which 1 fetus was thyroidectomised (TX) and its twin sham-operated (Section 2.2.2.1). Pregnancy continued until 125-129dGA (n=6 ewes) or 140-145dGA (n=6 ewes) when ewes and fetuses were euthanised and tissues collected as described in Section 2.2.4.1. The remaining 5 ewes and their fetuses were catheterised at 116-119dGA (Section 2.2.2.2) and following at least 5 days post-operative recovery one was infused with T_3 (8-12µg/kg/day; n=5 fetuses) and its twin with saline (n=4 fetuses) for a 5 day period until euthanasia and tissue collection at 127-130dGA (Section 2.2.3.2).

Details of surgery, tissue collection and experimental protocols used in this chapter are given in Chapter 2.

4.3.2 Statistical Analyses

A two-way ANOVA was applied to data from control and TX fetuses at 127dGA and 143dGA to determine whether there was a significant effect of TX and/or age when all groups were considered. As in Chapter 3, the ANOVA was applied in all cases when all groups had n≥5 (Maxwell and Delaney, 1990). A Tukey's multiple comparison *post hoc* test was used following a significant two-way ANOVA result. Additionally, and in cases when n<5, a *t*-test or Mann-Whitney non-parametric test was used to compare control and TX values at the same age.

For comparison of saline and T_3-infused groups the sample sizes were too small to be able to test for a normal distribution and, therefore, a Mann-Whitney non-parametric test was used to detect differences between treatment groups. $P<0.05$ was considered significant and $P<0.1$ was considered a trend throughout.

4.4 Results: Effects of thyroidectomy

4.4.1 Fetal measurements

Fetal plasma hormone concentrations

There was no evidence of thyroid tissue remaining in any of the TX fetuses at the time of tissue collection. The effectiveness of the TX was confirmed by significantly lower levels of both fetal plasma T_3 (P<0.01) and T_4 (P<0.0001; Table 4.1) in the TX relative to the sham operated twin at both gestational ages (Table 4.1). TX did not significantly alter fetal cortisol concentrations (Table 4.1). There was a significant effect of age on fetal plasma cortisol (P<0.001) and T_3 (P<0.05) with no change in plasma T_4 with age (Table 4.1). TX prevented the normal increment in plasma concentration of T_3 and cortisol with increasing gestational age (Table 4.1).

Table 4.1 Fetal plasma hormone concentrations

	127dGA control	**127dGA TX**	**143dGA control**	**143dGA TX**
Cortisol (ng/ml)	12.1±1.2	14.0±2.6	42.1±6.3†	25.7±6.5
T_3 (ng/ml)	0.33±0.01	0.21±0.03*	0.60±0.1†	0.24±0.01‡
T_4 (ng/ml)	104.9±11.7	n.d.‡	87.8±6.2	13.4±6.6‡

*Mean±SEM fetal plasma hormone concentrations of control and TX fetuses at 127 days of gestational age (dGA; n=6) and 143dGA (n=5). N.d. not detectable. ‡ are significantly different from controls at the same gestational age and † are significantly different from 127dGA in the same treatment group (P<0.05 Tukey's post hoc test following two-way ANOVA). * are significantly different from controls at the same gestational age (P<0.05 by t-test).*

Fetal biometry and muscle biochemical composition

TX did not significantly affect fetal body weight, crown-rump length or the lengths of the femur and tibia (Table 4.2). However, there was a significant effect of TX on metatarsus length (P<0.0001) with significantly shorter lengths in TX animals compared to controls at both gestational ages (Table 4.2). There was no effect of TX on the weights of any of the 3 muscles studied, nor the muscle:body weight ratio at either gestational age (Table 4.2). TX did have a significant effect on the muscle water content (P<0.0001 in all 3 muscles) and protein content (P<0.05 in BF and P<0.0001 in ST; Table 4.2). Water content was significantly higher at both 127 and 143dGA in all 3 muscles of TX fetuses compared to controls. Protein content was significantly lower in the ST of TX fetuses compared with controls at both ages and in BF at 127dGA. A significant interaction between age and TX was seen in glycogen content of the BF (P<0.05) and glycogen was significantly lower in BF of TX fetuses compared to controls at 127dGA (Table 4.2). Lipid content was only measured in the BF and was significantly lower in TX than controls at 143dGA (Table 4.2).

As water content differed with treatment, the protein, glycogen and lipid content of the muscles are also expressed per mg dry weight (Table 4.2). After correction for the water content, there was a significant effect of TX on the protein content in the SDF, with content being significantly higher in the TX than control fetuses at both ages (Table 4.2). Glycogen content was higher in TX than controls at 143dGA in the BF whereas lipid content per mg dry weight BF did not differ with treatment (Table 4.2).

Table 4.2 Biometric and biochemical measurements.

	127dGA control	127dGA TX	143dGA control	143dGA TX
Body weight (kg)	2.54±0.10	2.33±0.14	3.49±0.26†	3.25±0.19†
Crown-rump length (cm)	41.8±0.8	40.0±0.5	45.0±0.5†	44.0±0.5†
Femur (cm)	9.3±0.4	8.8±0.2	10.3±0.3	9.8±0.3
Tibia (cm)	12.3±0.3	11.7±0.2	14.5±0.5†	13.3±0.5
Metatarsus (cm)	14.3±0.2	13.0±0.3‡	16.3±0.3†	14.7±0.3†‡
	Biceps femoris			
Weight (g)	11.02±0.46	10.92±0.89	13.91±1.35	13.97±0.78
Muscle:body weight ratio (g:kg x10^3)	4.34±0.08	4.71±0.35	3.96±0.15	4.30±0.08
Water content (%)	83.3±0.5	85.8±0.4‡	79.3±0.6†	83.5±0.8‡
Protein content (mg/g wet weight)	45.7±0.7	40.3±2.1*	48.3±2.4	45.1±1.9
(mg/mg dry weight)	0.28±0.01	0.28±0.01	0.23±0.01	0.28±0.02
Glycogen content (mg/g wet wt)	34.5±2.2	26.7±1.3‡	33.4±2.0	34.9±2.0†
(mg/mg dry wt)	0.21±0.01	0.19±0.01	0.16±0.01	0.21±0.01*
Lipid content (mg/g wet wt)	22.8±1.6	22.3±1.9	25.5±1.3	21.5±0.9*
(mg/mg dry wt)	0.14±0.01	0.16±0.01	0.12±0.01	0.13±0.004
	Semitendinosus			
Weight (g)	3.90±0.23	3.98±0.28	0.37±0.47†	4.98±0.32
Muscle:body weight ratio (g:kg x10^3)	1.53±0.04	1.71±0.08	1.54±0.07	1.33±0.27
Water content (%)	81.7±0.5	84.4±0.3‡	79.1±0.4†	83.4±0.6‡
Protein content (mg/g wet weight)	43.8±1.8	37.9±1.3‡	47.7±1.1	40.2±0.9‡
(mg/mg dry weight)	0.24±0.01	0.24±0.01	0.23±0.01	0.24±0.01
Glycogen content (mg/g wet wt)	44.4±5.8	37.1±5.1	36.9±2.8	43.8±5.8
(mg/mg dry wt)	0.24±0.03 (n=5)	0.24±0.03	0.18±0.01 (n=5)	0.26±0.03
	Superficial digital flexor			
Weight (g)	1.57±0.05	1.48±0.10	2.29±0.17†	2.19±0.20†
Muscle:body weight ratio (g:kg x10^3)	0.62±0.02	0.63±0.02	0.66±0.02	0.67±0.03
Water content (%)	82.2±0.3	84.8±0.3‡	78.6±0.7†	84.0±0.4‡
Protein content (mg/g wet weight)	44.5±1.4	44.9±1.4	51.2±3.3	44.1±1.8
(mg/mg dry weight)	0.25±0.01	0.30±0.01‡	0.24±0.01	0.28±0.01*
Glycogen content (mg/g wet wt)	22.5±3.8	17.3±2.3	24.4±3.1	17.4±4.9
(mg/mg dry wt)	0.12±0.02 (n=4)	0.11±0.01 (n=4)	0.12±0.02 (n=4)	0.11±0.03 (n=4)

*Data are presented as mean±SEM of control and TX fetuses at 127 days of gestational age (dGA) and 143dGA; n=6 per group unless stated otherwise. ‡ are significantly different from controls at the same gestational age and † are significantly different from 127dGA in the same treatment group (P<0.05 Tukey's post hoc test following two-way ANOVA). * are significantly different from controls at the same gestational age (P<0.05 by t-test).*

4.4.2 Functional oxidative capacity

Respirometry was used to measure the ADP-coupled oxygen consumption of permeabilised muscle fibres with Py or PC as substrates. Also total ADP-coupled oxygen consumption stimulated by both glutamate and succinate was measured. Data are shown in Figure 4.1 with significant two-way ANOVA results shown on the graphs. Py- and PC-supported oxygen consumption in the BF was significantly lower in TX than controls at 143dGA and for Py at 127dGA (Figure 4.1 A&D). Further, total oxygen consumption was significantly lower in BF of TX than control fetuses at 143dGA (Figure 4.1 G). In the ST PC-supported oxygen consumption was lower in TX than controls at 127dGA but not at 143dGA (Figure 4.1 E). In the SDF at 143dGA, oxygen consumption using all 3 substrate protocols was lower in TX than control fetuses (Figure 4.1 C,F&I). Total oxygen consumption of the SDF was also significantly lower in TX compared to controls at 127dGA (Figure 4.1 I). There was a significant effect of age only on the PC-supported oxygen uptake in the SDF ($P<0.05$ by two-way ANOVA) although the increase was seen only between control fetuses at 143 compared to 127dGA and was prevented by TX (Figure 4.1 F).

Py was added following PC and ADP, and thus the PC contribution to the combined PC- and Py-stimulated oxygen uptake could be calculated and is shown in Figure 4.2. There is no significant effect of treatment or age on this ratio. Oxygen consumption after the addition of substrates but before ADP was added, as a measure of leak state, was not affected by age or TX in any of the muscles studied (data not shown). The RCR was unaffected by TX in all cases except PC-supported RCR in the ST at 127dGA where TX values were significantly lower than their sham-operated controls ($P<0.05$ by *t*-test; data not shown).

HOAD activity was measured only in the BF. The control value was significantly higher at 143dGA than at 127dGA, and the TX value was significantly lower than the control at both 127 and 143dGA (Figure 4.3). The normal ontogenic increase in HOAD activity was prevented by TX (Figure 4.3).

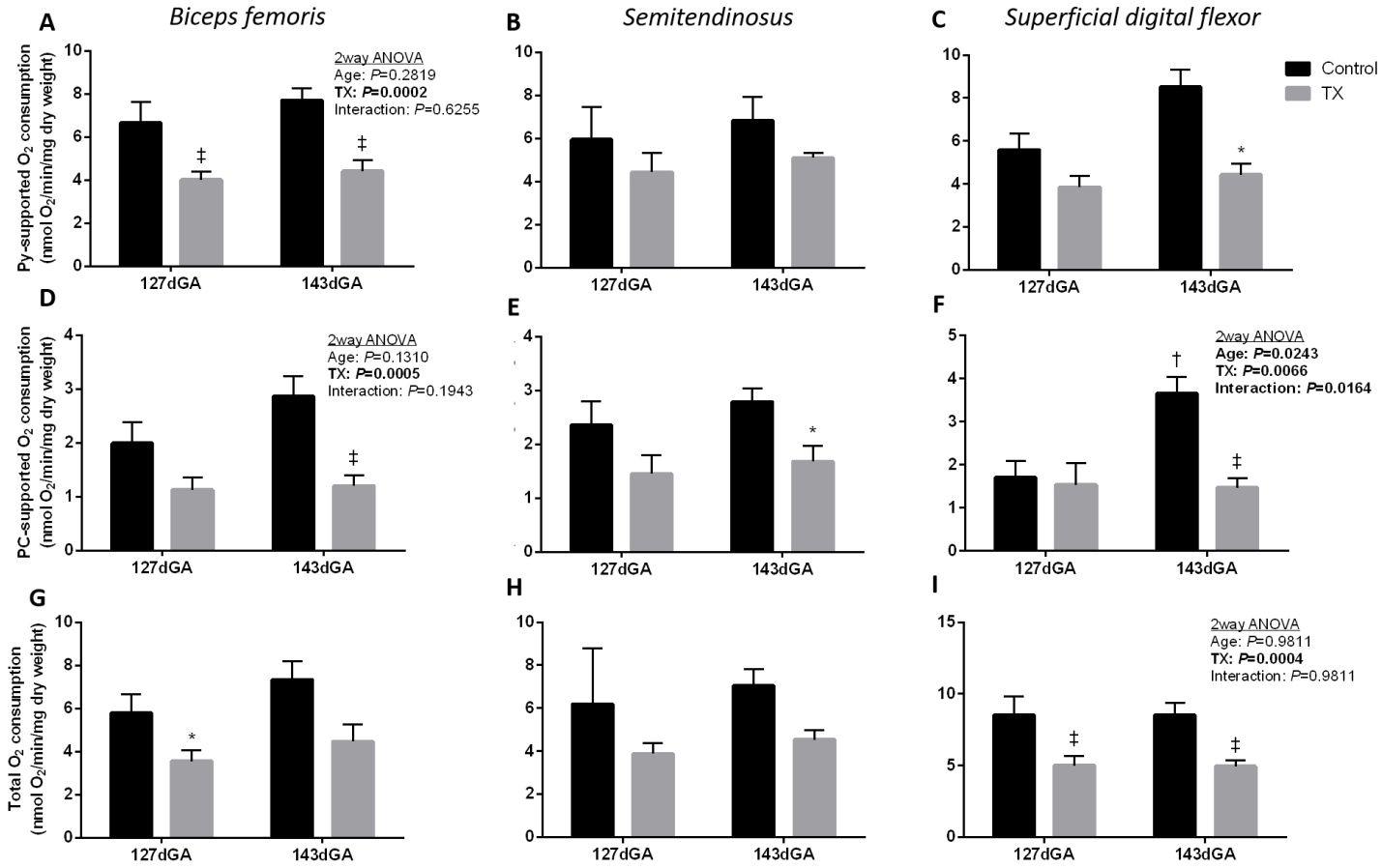

*Figure 4.1 Mean±SEM ADP-coupled, A-C) pyruvate (Py), D-F) palmitoylcarnitine (PC) and G-I) glutamate and succinate stimulated (total) oxygen consumption in A,D&G) biceps femoris, B,E&H) semitendinosus and C,F&I) superficial digital flexor of control (n=3-6; black bars) and TX (n=4-6; grey bars) fetuses at 127 and 143dGA. ‡ are significantly different from controls at the same gestational age and † are significantly different from 127dGA in the same treatment group (P<0.05 Tukey's post hoc test following two-way ANOVA). * are significantly different from controls at the same gestational age (P<0.05 by t-test or Mann-Whitney test).*

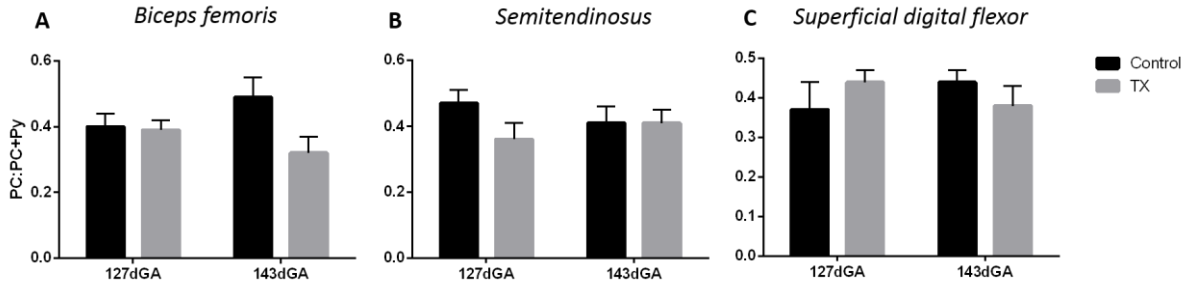

Figure 4.2 The ratio of ADP-coupled PC-supported:PC+Py-supported oxygen consumption, presented as mean±SEM in A) biceps femoris, B) semitendinosus and C) superficial digital flexor of control (n=5-6; black bars) and TX (n=4-6; grey bars) fetuses at 127dGA and 143dGA.

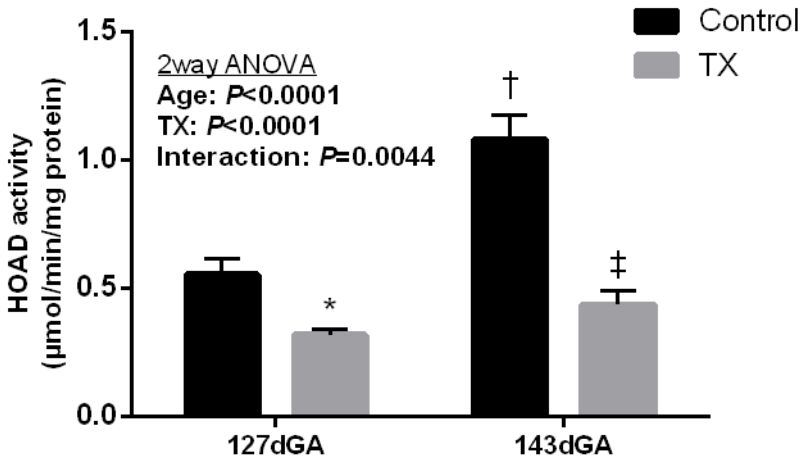

*Figure 4.3 Mean±SEM β-hydroxyacyl-CoA dehydrogenase (HOAD) activity in biceps femoris muscle of control (black bars) and TX (grey bars) fetuses at 127dGA and 143dGA. N=6 in each group. ‡ are significantly different from controls at the same gestational age and † are significantly different from 127dGA in the same treatment group (P<0.05 Tukey's post hoc test following two-way ANOVA). * are significantly different from controls at the same gestational age (P<0.05 by t-test).*

4.4.3 Regulating oxidative capacity

4.4.3.1 Mitochondrial density and biogenesis

Citrate synthase activity was measured as a putative marker of mitochondrial density and is given with two-way ANOVA analyses of the effect of treatment and age in Figure 4.4 A-C. In all 3 muscles, CS activity was significantly lower in TX than control fetuses at 143dGA. The TX values were also significantly lower than controls at 127dGA in the BF and ST but not the SDF. The normal increase in CS activity with age was prevented by TX in all 3 muscles (Figure 4.4).

Gene expression of mitochondrial biogenesis markers, PGC1α (Figure 4.4 D-F) and NRF1 (Figure 4.4 G-I), was measured. In the ST, *PGC1α* expression was significantly lower in TX than control at 127dGA and expression of *NRF1* was significantly higher in the TX fetuses compared to controls at 143dGA ($P<0.05$). There were no differences in *PGC1α* and *NRF1* expression between TX and control values in the BF and SDF.

In order to determine whether the oxidative capacity of the muscle followed the change in mitochondrial density oxygen consumption was normalised to CS activity/mg dry weight (Figure 4.5). Py-supported oxygen consumption was significantly higher in the BF of TX than controls ($P<0.05$ by two-way ANOVA). Normalised total oxygen consumption was significantly higher at 143dGA in ST of TX than control fetuses (Figure 4.5). In all other cases, there was no difference in oxygen consumption per mitochondrial unit (Figure 4.5).

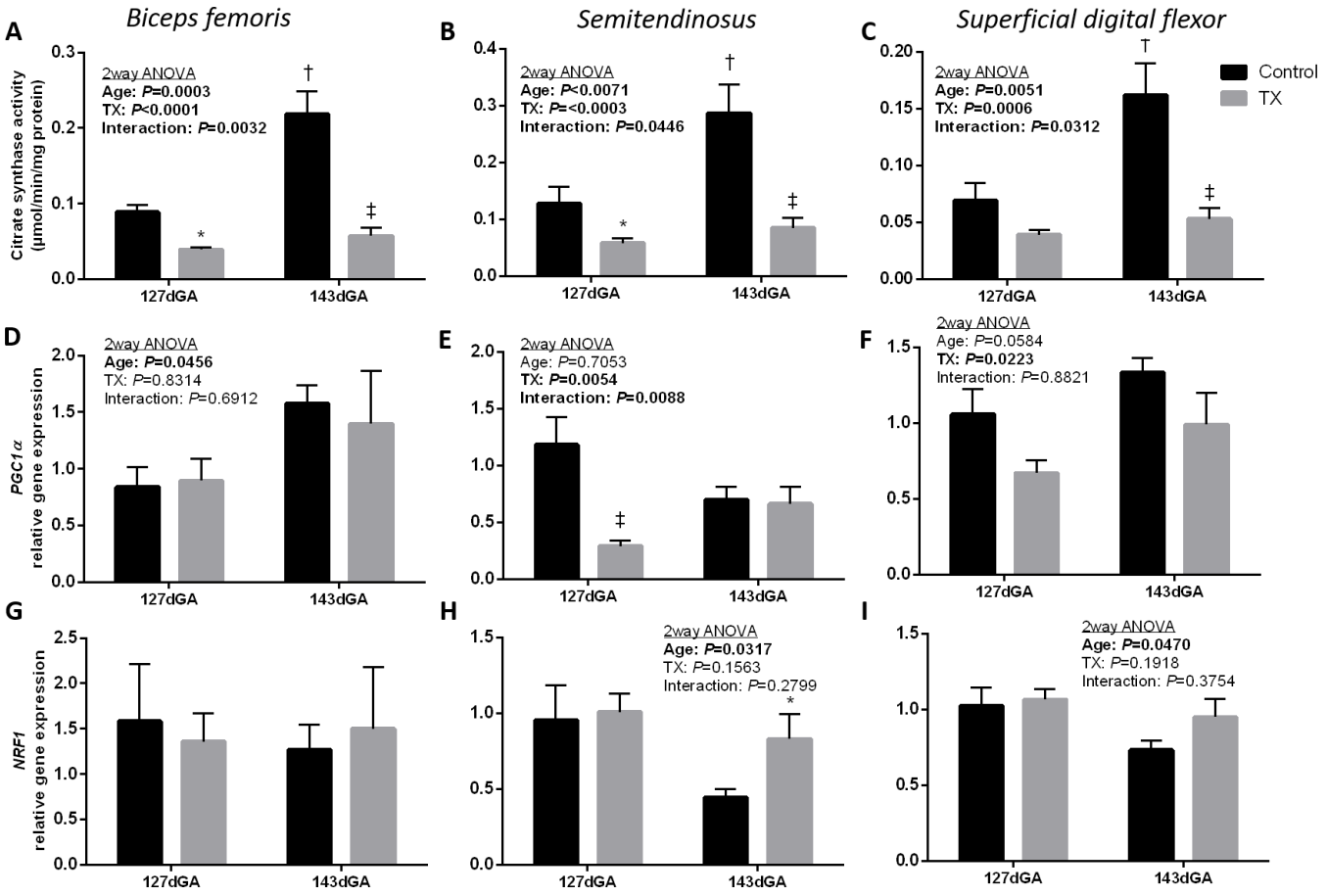

*Figure 4.4 Mean±SEM A-C) citrate synthase activity and normalised gene expression of D-F) PGC1α and G-I) NRF1 in A,D&G) biceps femoris, B,E&H) semitendinosus and C,F&I) superficial digital flexor of control (n=4-6; black bars) and TX (n=5-6; grey bars) fetuses at 127 and 143dGA. ‡ are significantly different from controls at the same gestational age and † are significantly different from 127dGA in the same treatment group (P<0.05 Tukey's post hoc test following two-way ANOVA). * are significantly different from controls at the same gestational age (P<0.05 by t-test).*

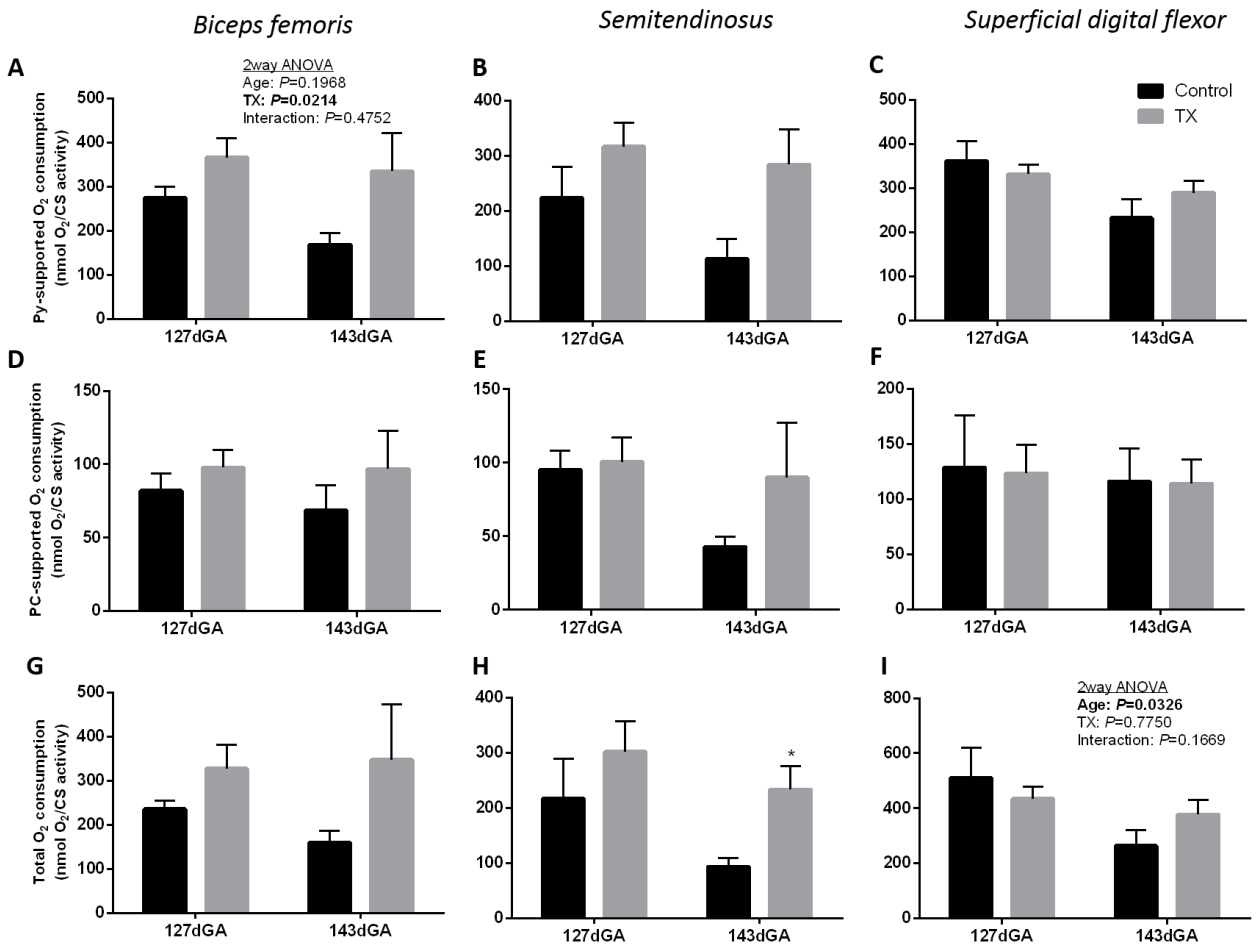

*Figure 4.5 Mean±SEM ADP-coupled, A-C) pyruvate (Py), D-F) palmitoylcarnitine (PC)-supported and G-I) total (glutamate and succinate-stimulated) oxygen consumption normalised to citrate synthase (CS) activity in A,D&G) biceps femoris, B,E&H) semitendinosus and C,F&I) superficial digital flexor of control (n=3-6; black bars) and TX (n=4-6; grey bars) fetuses at 127 and 143dGA. * are significantly different from controls at the same gestational age (P<0.05 by t-test).*

4.4.3.2 ETS abundance

The protein abundance of complexes I-IV and ATP-synthase were measured using western blotting and the data are presented for the BF, ST and SDF in Figure 4.6, Figure 4.7 and Figure 4.8 respectively. There was a significant effect of TX in all 3 muscles; the abundance of several complexes were significantly lower in muscle of TX fetuses compared with controls at both ages (Figure 4.6-Figure 4.8). There was a significant effect of age on ETS complex abundance in the controls with significantly higher values at 143dGA than 127dGA for most of the complexes with the exception of CIV in all 3 muscles (Figure 4.6-Figure 4.8). However, TX prevented these ontogenic increases in ETS complex abundance (Figure 4.6-Figure 4.8).

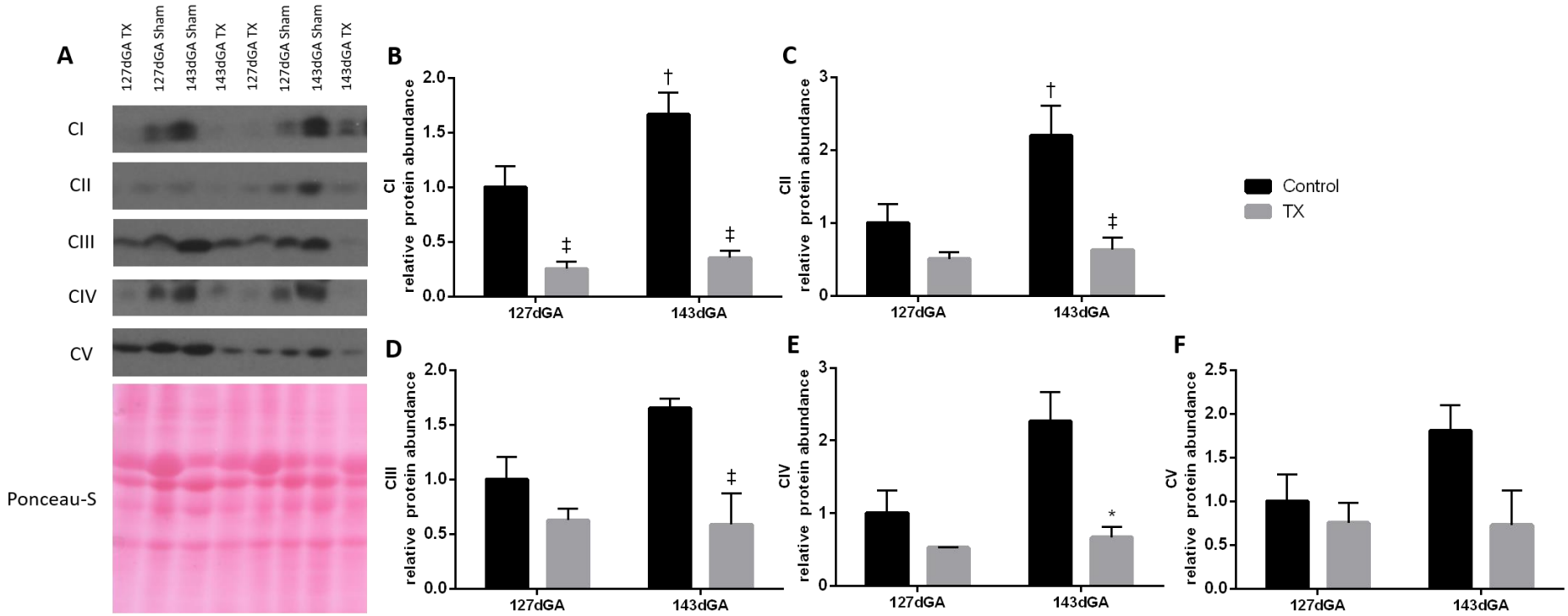

*Figure 4.6 Protein expression of electron transfer system complexes I-IV (CI-IV) and ATP-synthase (CV) by western blotting in biceps femoris. A) representative blots and B-F) mean±SEM relative abundance of the complexes I-IV and ATP-synthase, as labelled, of control (black bars) and TX (grey bars) fetuses at 127 and 143dGA. N=5 in each group for CI, II, III and V; n=4-5 for CIV. ‡ are significantly different from controls at the same gestational age and † are significantly different from 127dGA in the same treatment group (P<0.05 Tukey's post hoc test following two-way ANOVA). * are significantly different from controls at the same gestational age (P<0.05 by t-test).*

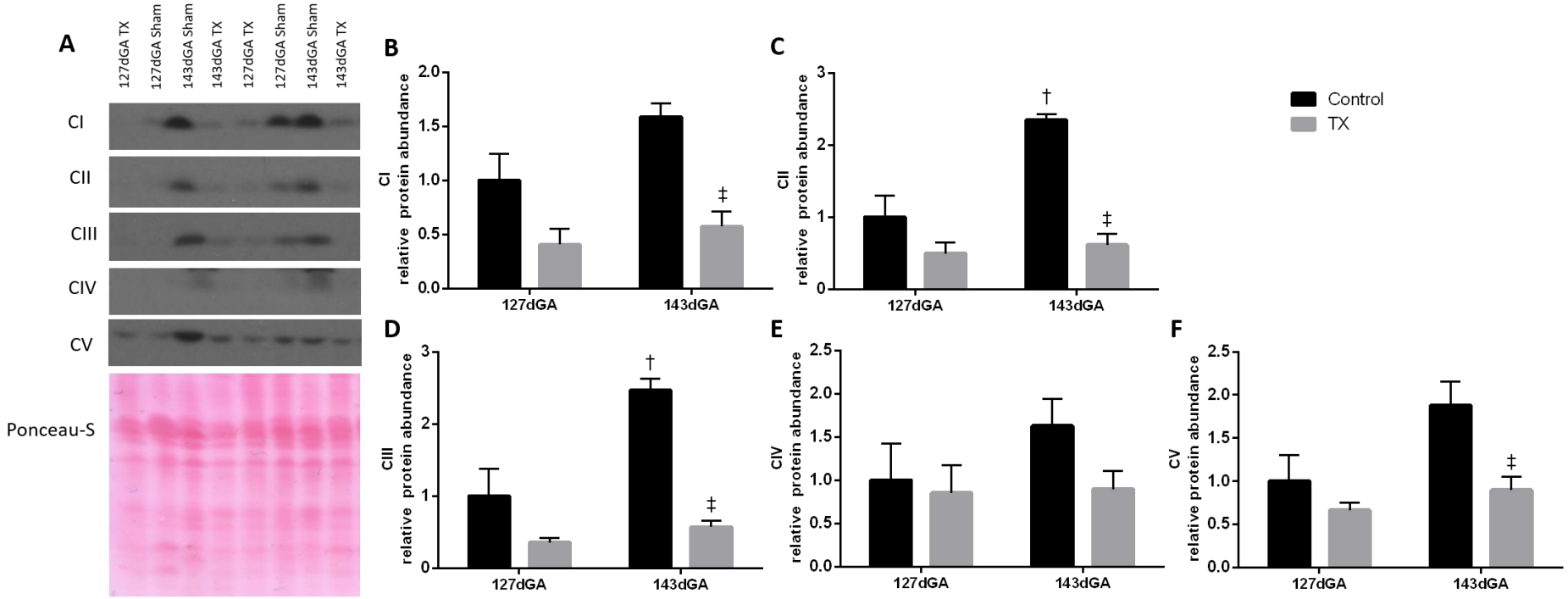

Figure 4.7 Protein expression of electron transfer system complexes I-IV (CI-IV) and ATP-synthase (CV) by western blotting in semitendinosus. A) representative blots and B-F) mean±SEM relative abundance of the complexes I-IV and ATP-synthase, as labelled, of control (black bars) and TX (grey bars) fetuses at 127 and 143dGA. N=5 in each case. ‡ are significantly different from controls at the same gestational age and † are significantly different from 127dGA in the same treatment group (P<0.05 Tukey's post hoc test following two-way ANOVA).

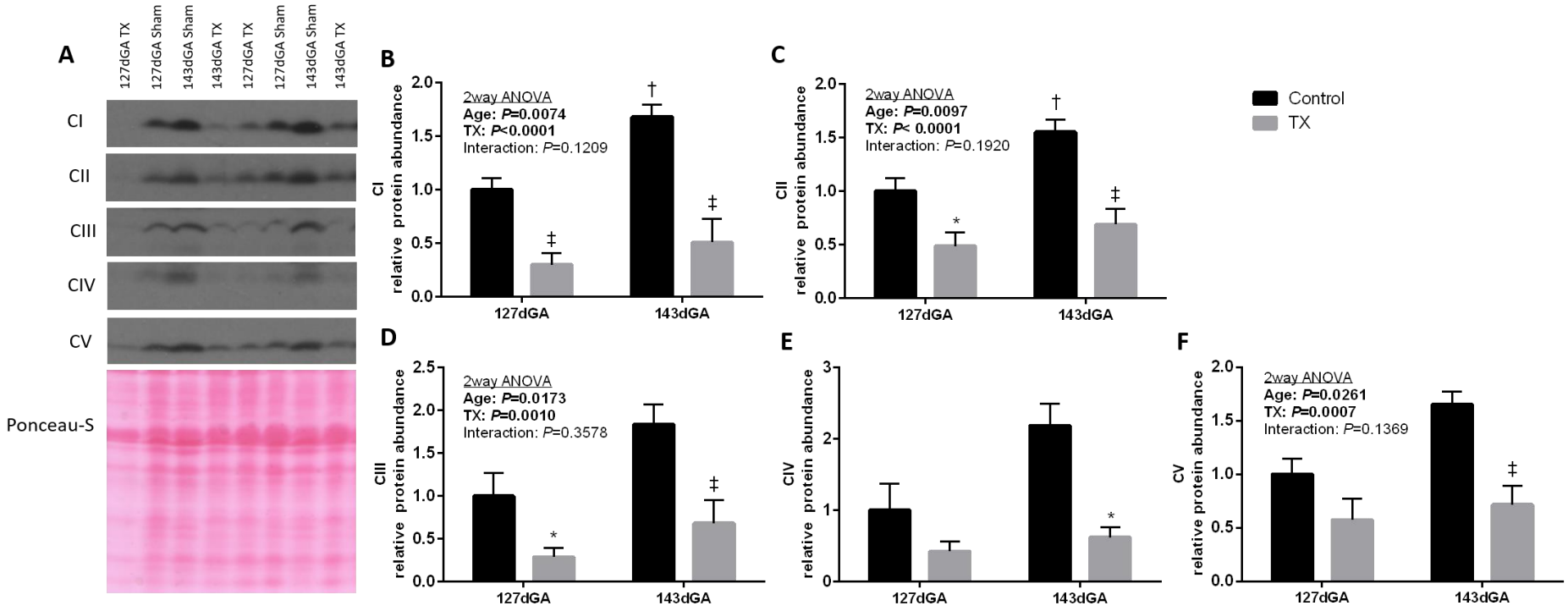

*Figure 4.8 Protein expression of electron transfer system complexes I-IV (CI-IV) and ATP-synthase (CV) by western blotting in superficial digital flexor. A) representative blots and B-F) mean±SEM relative abundance of the complexes I-IV and ATP-synthase, as labelled, of control (black bars) and TX (grey bars) fetuses at 127 and 143dGA. N=5 in each group for CI, II, III and V; n=4-5 for CIV. ‡ are significantly different from controls at the same gestational age and † are significantly different from 127dGA in the same treatment group (P<0.05 Tukey's post hoc test following two-way ANOVA). * are significantly different from controls at the same gestational age (P<0.05 by t-test or Mann-Whitney test).*

4.4.3.3 Uncoupling the proton gradient

In the ST and SDF there was a significant effect of TX on the mRNA abundance of UCP2 (Figure 4.9 A-C) and UCP3 (Figure 4.9 D-F). *UCP2* expression was significantly lower in TX than controls in all 3 muscles at 127dGA and in the SDF at 143dGA. *UCP3* expression was significantly lower in TX than controls of ST and SDF at 143dGA and in SDF at 127dGA. There was no significant effect of age on *UCP2* or *UCP3* expression in any muscle of either control or TX fetuses (Figure 4.9).

ANT1 expression was significantly affected by TX, both at the protein (Figure 4.10 A-F) and mRNA level (Figure 4.10 G-I). Protein expression was significantly lower in all 3 muscles of TX fetuses compared to their controls at both ages (Figure 4.10 D-F). Additionally, *ANT1* gene expression was lower in all 3 muscles from TX fetuses at 143dGA compared with controls and ST and SDF at 127dGA (Figure 4.10 G-I). ANT1 protein expression in all 3 muscles and gene expression in ST and SDF was significantly higher in control muscles at 143dGA compared with 127dGA. Again, TX prevented the ontogenic increase in ANT1 gene and protein expression seen in the controls (Figure 4.10).

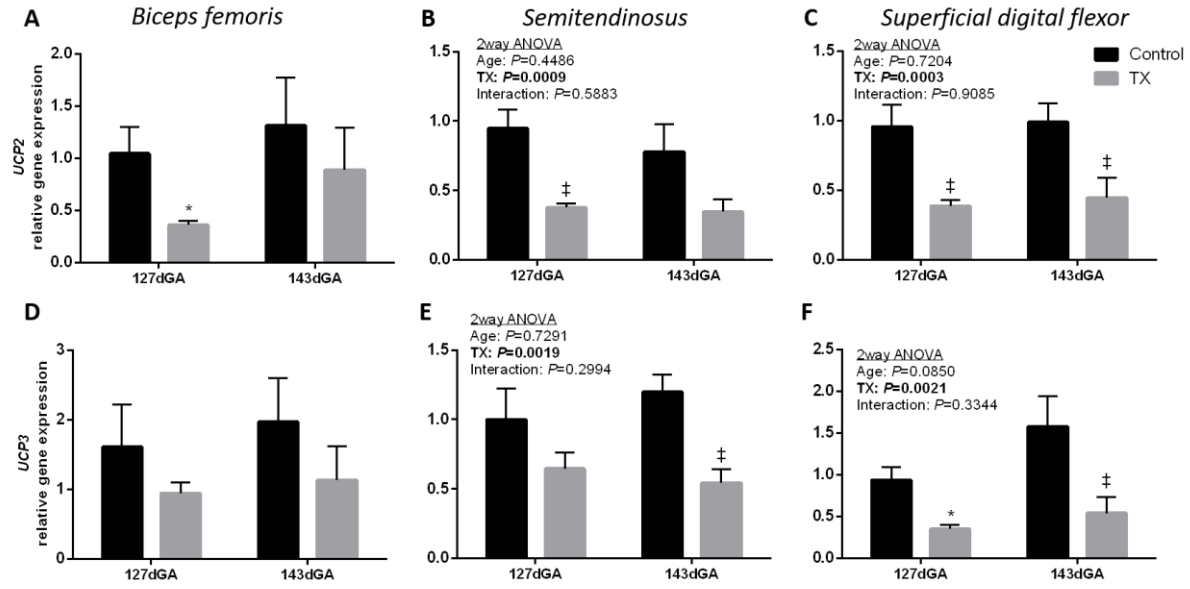

*Figure 4.9 Mean±SEM relative gene expression of A-C) uncoupling protein (UCP) 2 and D-F) UCP3 in A&D) biceps femoris, B&E) semitendinosus and C&F) superficial digital flexor of control (n=5-6; black bars) and TX (n=6; grey bars) fetuses at 127dGA and 143dGA. ‡ are significantly different from controls at the same gestational age (P<0.05 Tukey's post hoc test following two-way ANOVA). * are significantly different from controls at the same gestational age (P<0.05 by t-test or Mann-Whitney test).*

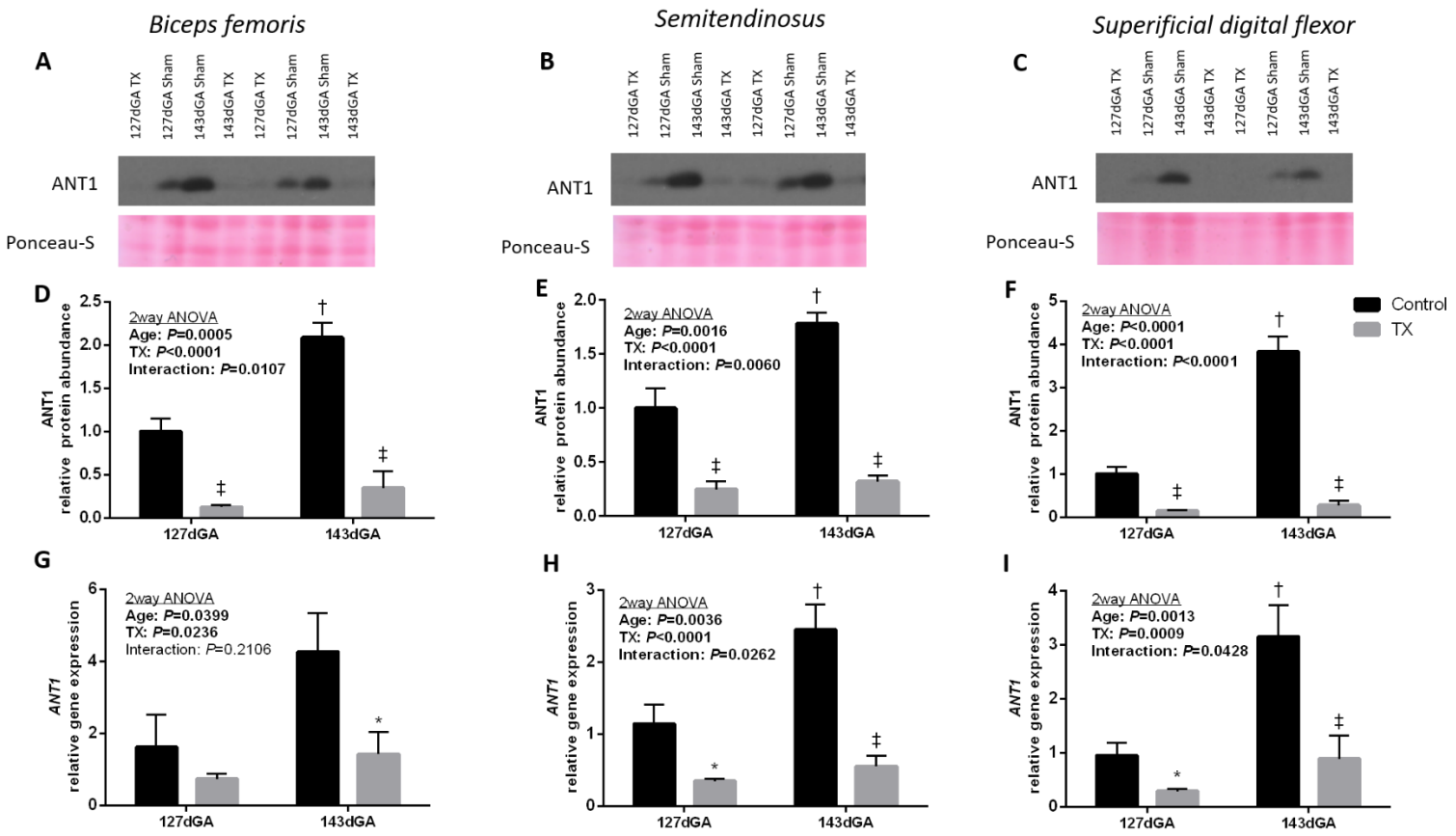

*Figure 4.10 Protein and mRNA levels of adenine nucleotide translocase 1 (ANT1) A-C) representative western blots, D-F) mean±SEM protein abundance (n=5 in each group) and G-I) gene expression (n=5-6 in each group) in A,D&G) biceps femoris, B,E&H) semitendinosus and C,F&I) superficial digital flexor of control (black bars) and TX (grey bars) fetuses at 127 days of gestational age (dGA) and 143dGA. ‡ are significantly different from controls at the same gestational age and † are significantly different from 127dGA in the same treatment group (P<0.05 Tukey's post hoc test following two-way ANOVA). * are significantly different from controls at the same gestational age (P<0.05 by t-test or Mann-Whitney test).*

4.4.3.4 Fusion and fission

qRT-PCR was used to quantify mRNA levels for proteins involved in mitochondrial fusion, MFN1 and MFN2, and fission, DRP1. There was a significant effect of TX on *MFN1* in BF and SDF and *MFN2* expression in all 3 muscles but not on *DRP1* expression (Figure 4.11). Comparing TX and control values at the same gestational age, *MFN1* expression was significantly lower in TX compared with controls in SDF and ST at both ages, and *MFN2* was significantly lower in TX compared with controls in all 3 muscles at 127dGA and in the ST and SDF at 143dGA (Figure 4.11).

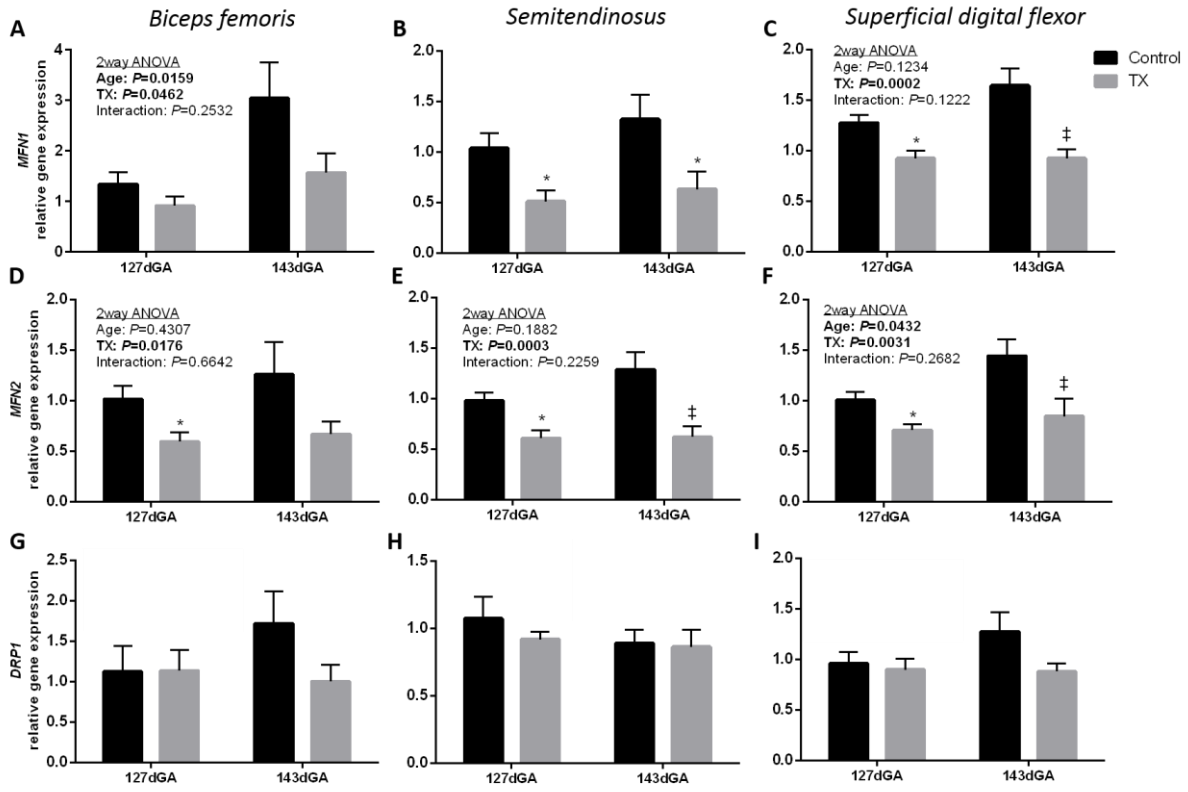

*Figure 4.11 Mean±SEM relative gene expression of A-C) mitofusin (MFN) 1 D-F) MFN2 and G-I) dynamin-related protein 1 (DRP1), in A,D&G) biceps femoris, B,E&H) semitendinosus and C,F&I) superficial digital flexor of control (black bars) and TX (grey bars) fetuses at 127dGA (n=3-6) and 143dGA (n=6). ‡ are significantly different from controls at the same gestational age (P<0.05 Tukey's post hoc test following two-way ANOVA). * are significantly different from controls at the same gestational age (P<0.05 by t-test).*

4.4.3.5 Monitoring cellular energy status

Protein abundance of AMPKα and pAMPKα were measured using western blotting. There was a significant effect of TX on pAMPKα abundance in BF with abundance significantly higher in TX than control fetuses at 143dGA (P<0.05; Figure 4.12). There was no effect of TX on pAMPKα in ST or SDF, nor of AMPKα abundance in any of the 3 muscles studied (Figure 4.12). The ratio of pAMPKα:AMPKα in BF was significantly affected by TX with a significantly higher ratio in TX compared with control fetuses at 127dGA (Figure 4.13). This ratio did not differ with TX in the other 2 muscles.

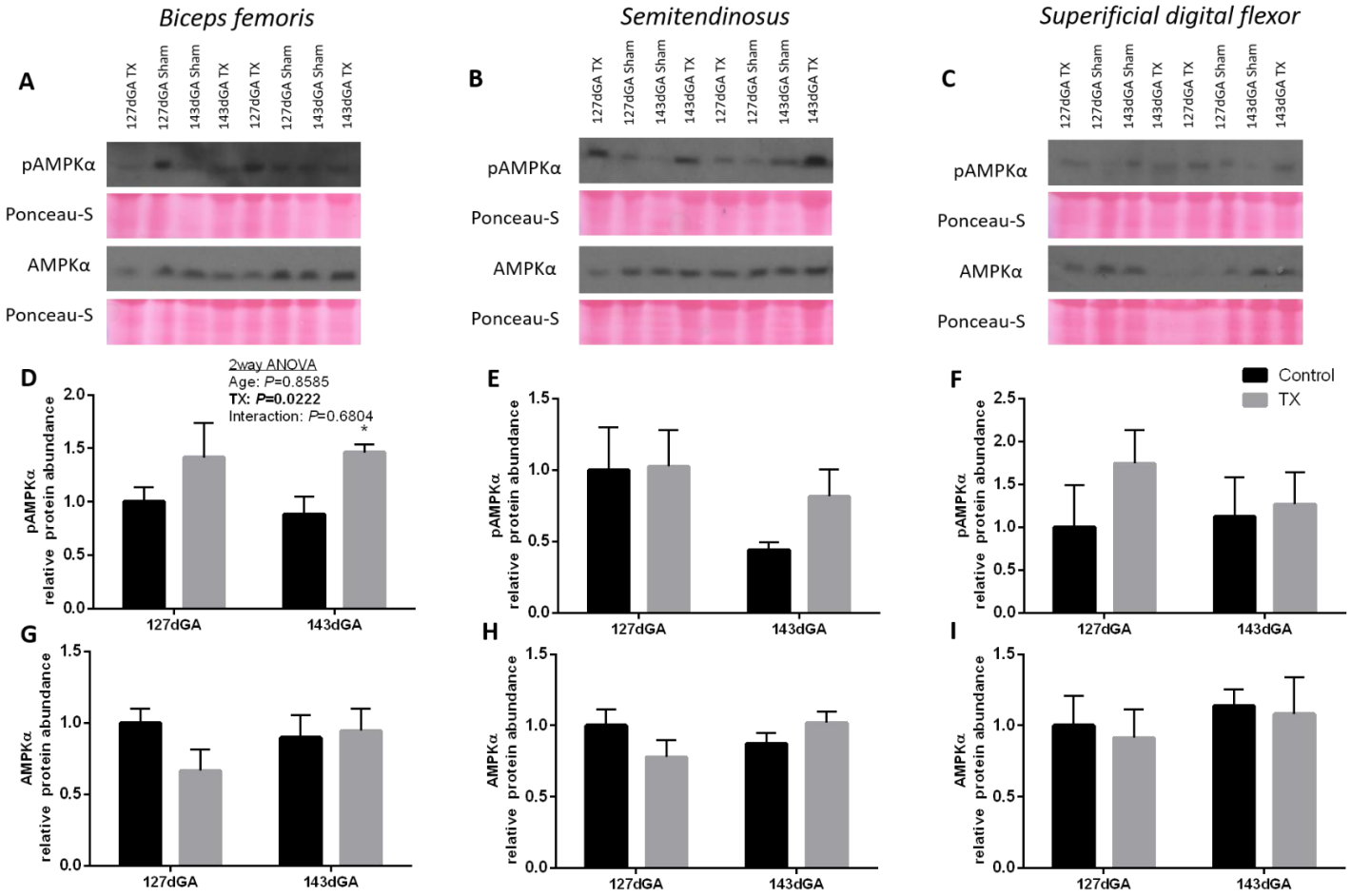

*Figure 4.12 Protein expression of (phosphorylated) AMP-activated protein kinase α ((p)AMPKα) by western blotting. A-C) representative blots and D-I) mean±SEM relative abundance of pAMPKα and AMPKα in A,D&G) biceps femoris, B,E&H) semitendinosus and C,F&I) superficial digital flexor of control (black bars) and TX (grey bars) fetuses at 127 days of gestational age (dGA) and 143dGA. N=5 per group, except ST AMPKα with n=3-4 per group. * are significantly different from controls at the same gestational age (P<0.05 by t-test).*

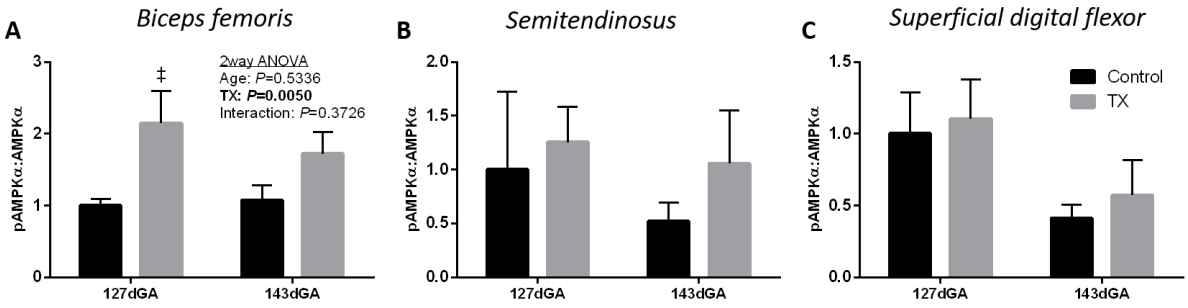

Figure 4.13 Mean±SEM ratio between phosphorylated AMP-activated protein kinase α (pAMPKα) and AMPKα in A) biceps femoris (n=5), B) semitendinosus (n=3-4) and C) superficial digital flexor (n=5) of control (black bars) and TX (grey bars) fetuses at 127dGA and 143dGA. ‡ are significantly different from controls at the same gestational age (P<0.05 Tukey's post hoc test following two-way ANOVA).

4.4.4 Skeletal muscle structure and type I fibres

In order to determine whether changes in mitochondrial parameters measured reflected a change in density of oxidative type I fibres, muscle sections were stained with H&E to determine total fibre density (Figure 4.14), and immunostained to allow quantification of the proportion of type I fibres (Figure 4.15). In addition, the number, average cross-sectional area and perimeter of the type I fibres were calculated and these data are presented in Table 4.3. There was a significant effect of TX on total fibre density in BF and ST (P<0.001 by two-way ANOVA). Fibre density was significantly lower in TX BF compared with controls at 143dGA, and in the TX ST compared with controls at both ages (Table 4.3). At 143dGA in the ST, the number, cross-sectional area and perimeter of type I fibres were all significantly lower in TX compared with controls, as was the area accounted for by type I fibres (Table 4.3). As in Chapter 3, the high density of fibres in control SDF at 143dGA resulted in the fibres being difficult to separate so the number, area and perimeter are not given for this group. The percentage area accounted for by MHCI fibres was significantly lower in TX than controls at 143dGA in the SDF and ST.

Further insight into the fibre phenotypes was gained through quantifying mRNA levels of MHC isoforms MHCI, IIa and IIx (Figure 4.16). TX significantly affected the expression of all 3 isoforms in all 3 muscles with the significant differences between TX and control values shown in Figure 4.16. Age had an effect on MHC expression in a muscle specific manner; *MHCIIx* was increased with age in ST and BF, whereas *MHCI* and *MHCIIa* expression were increased in the SDF (P<0.05). MHC expression was not different between TX fetuses at the 2 ages.

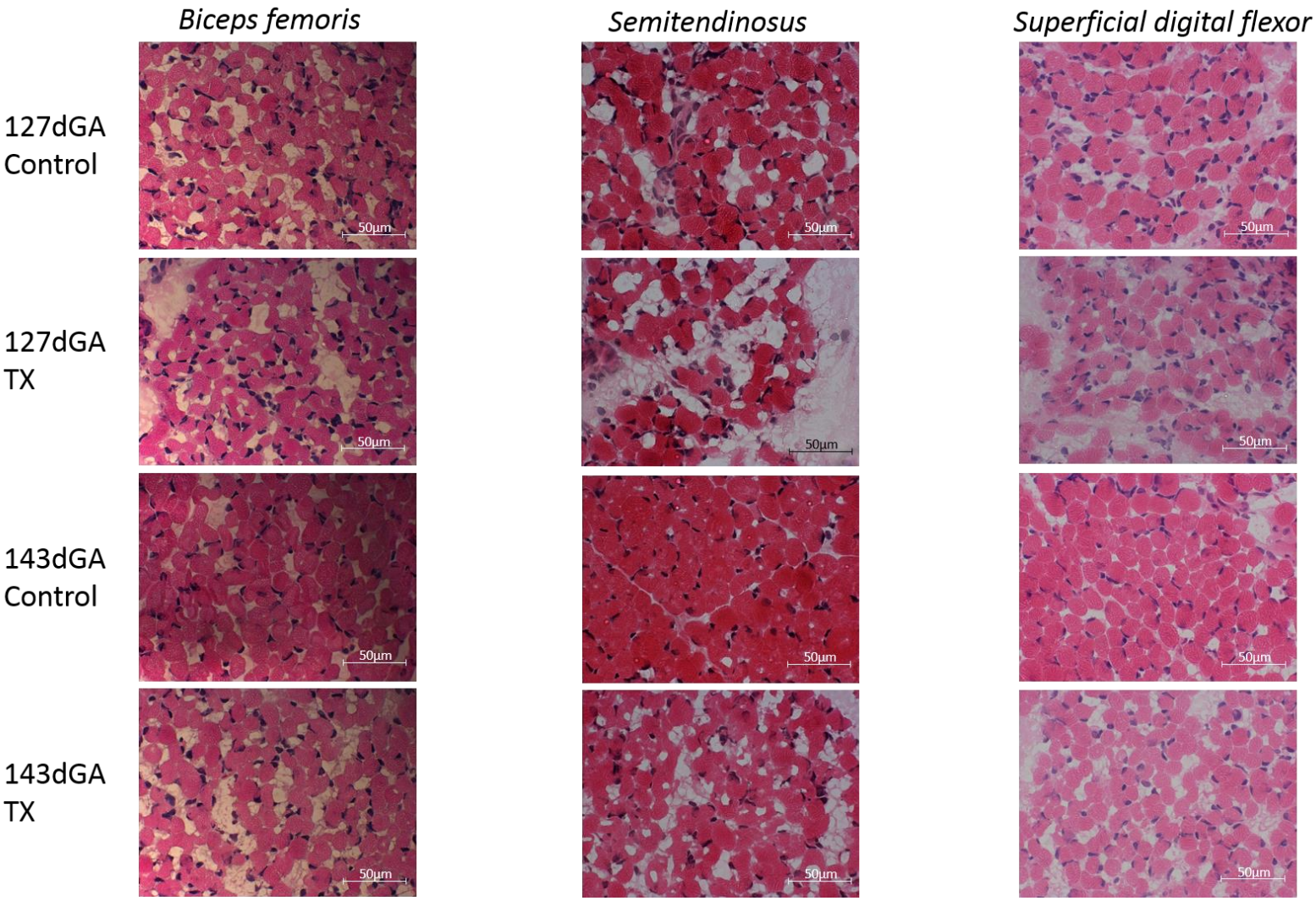

Figure 4.14 Representative H&E stained sections at 40x magnification in biceps femoris, semitendinosus and superficial digital flexor of control and TX fetuses at 127 and 143 days of gestational age (dGA), as labelled.

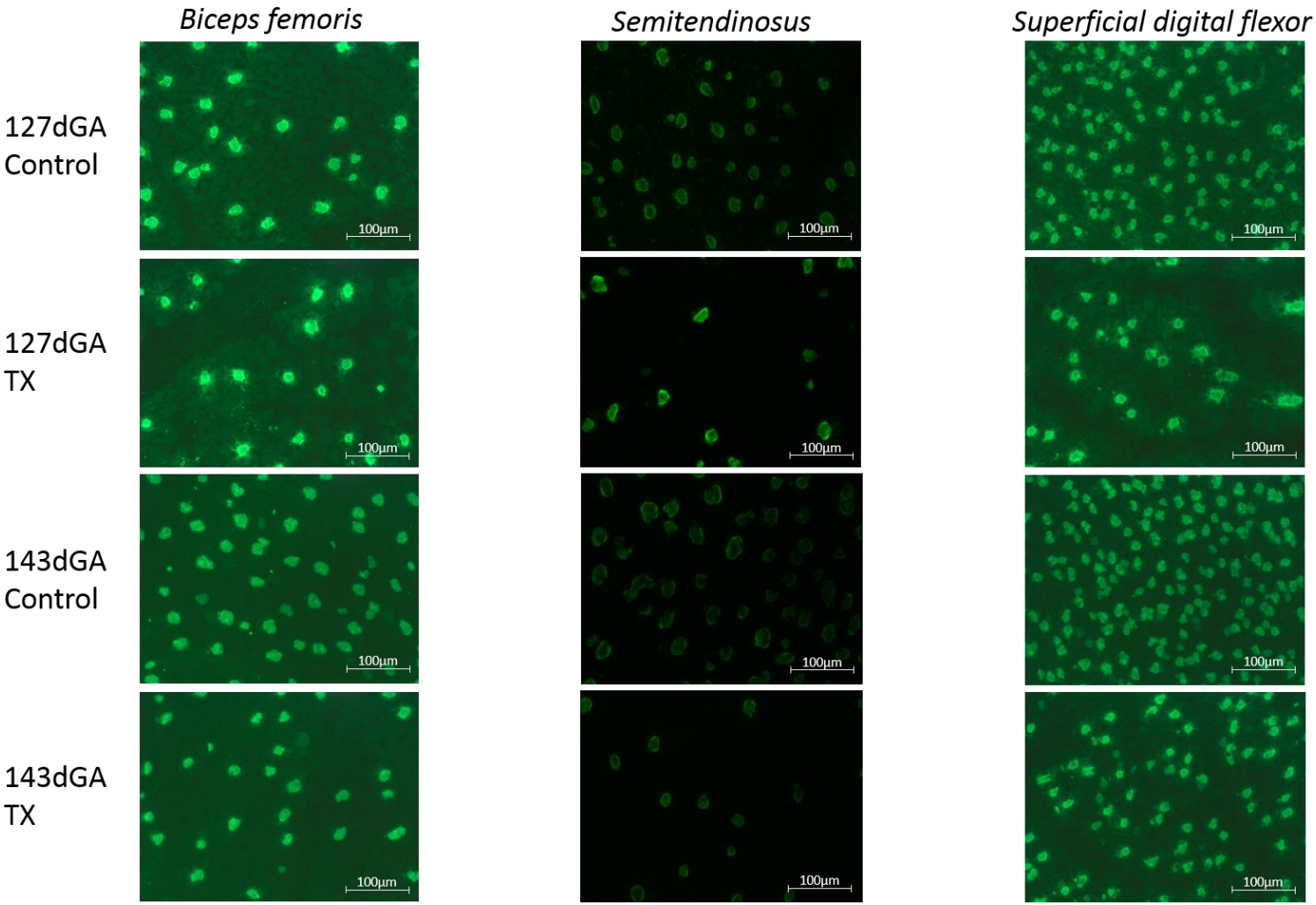

Figure 4.15 Representative MHCI stained sections at 20x magnification in biceps femoris, semitendinosus and superficial digital flexor of control and TX fetuses at 127 and 143 days of gestational age (dGA), as labelled.

Table 4.3 Type I fibre analyses.

	127dGA Control	127dGA TX	143dGA Control	143dGA TX
	Biceps femoris			
Proportion of total area accounted for by fibres (%)	77.6±5.6 (n=6)	63.8±3.3 (n=6)	85.3±3.6 (n=6)	63.9±4.8‡ (n=6)
Number of type I fibres/mm^2	286±84	178±20	467±71	225±48
Average fibre cross-sectional area (µm^2)	364.9±34.7	318.6±14.0	419. ±25.6	369.5±14.4
Average fibre perimeter (µm)	71.6±3.5	66.7±1.6	78.0±2.4	72.0±1.5
Proportion of total area accounted for by type I fibres (%)	10.3±3.0	5.8±0.9	19.5±3.0	8.2±1.8
Proportion of fibre area accounted for by type I fibres (%)	11.9±3.1	9.0±1.4	23.2±3.6	12.9±3.9
	Semitendinosus			
Proportion of total area accounted for by fibres (%)	75.1±1.8 (n=6)	51.1±3.3‡ (n=6)	90.1±1.3† (n=6)	63.3±3.1†‡ (n=6)
Number of type I fibres/mm^2	270±47	133±34	318±21	86±5*
Average fibre cross-sectional area (µm^2)	422.2±22.7	403.8±22.1	481.4±13.6	375.3±7.0*
Average fibre perimeter (µm)	78.0±2.2	76.2±2.2	84.4±1.3	73.5±0.6*
Proportion of total area accounted for by type I fibres (%)	11.5±2.3	5.3±1.2	15.3±1.1	3.3±0.1*
Proportion of fibre area accounted for by type I fibres (%)	15.8±3.2	9.9±2.2	17.0±1.1	5.1±0.3*
	Superficial digital flexor			
Proportion of total area accounted for by fibres (%)	64.8±3.5	55.1±4.3	75.1±4.7	67.1±3.2
Number of type I fibres/mm^2	465±92	424±66	n.q.	383±107
Average fibre cross-sectional area (µm^2)	302.9±43.4	300.0±23.0	n.q.	295.0±13.7
Average fibre perimeter (µm)	65.9±4.7	65.6±2.5	n.q.	65.3±1.4
Proportion of total area accounted for by type I fibres (%)	13.1±1.2	12.5±1.6	27.6±3.1	11.0±2.9#
Proportion of fibre area accounted for by type I fibres (%)	20.2±1.2	22.5±1.9	34.6±1.9	16.2±4.2*

*Data are presented as mean±SEM in biceps femoris, semitendinosus and superficial digital flexor of control and TX fetuses at 127 and 143 days of gestational age (dGA). N=4 in each group, unless stated otherwise. ‡ are significantly different from controls at the same gestational age and † are significantly different from 127dGA in the same treatment group (P<0.05 Tukey's post hoc test following two-way ANOVA). * are significantly different from controls at the same gestational age (P<0.05 by Mann-Whitney test). n.q. not quantifiable.*

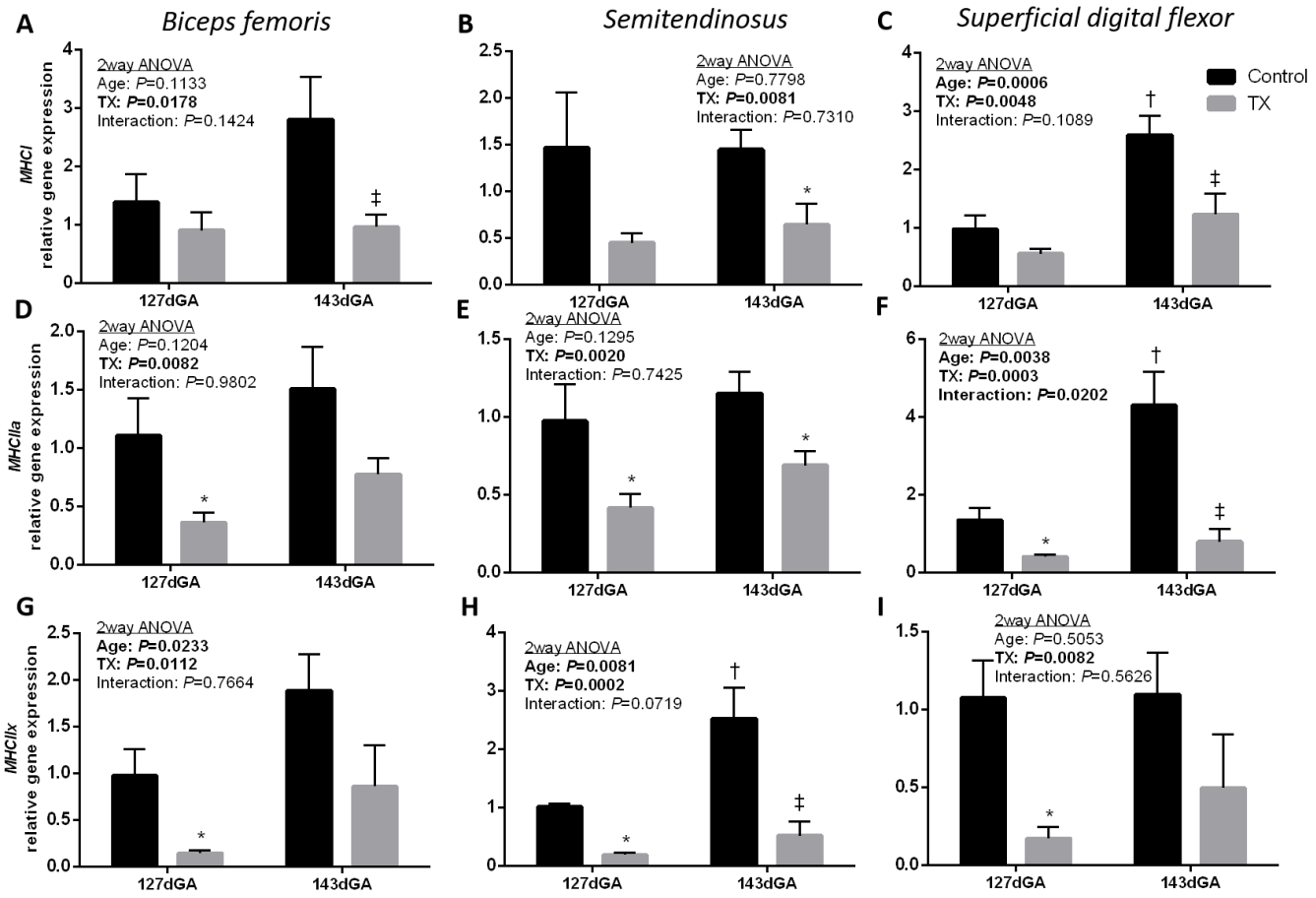

*Figure 4.16 Mean±SEM gene expression of A-C) MHCI, D-F) MHCIIa and G-I) MHCIIx in A,D&G) biceps femoris, B,E&H) semitendinosus and C,F&I) superficial digital flexor of control (black bars) and TX (grey bars) fetuses at 127 (n=5-6 per group) and 143 days of gestational age (dGA; n=6 per group). ‡ are significantly different from controls at the same gestational age and † are significantly different from 127dGA in the same treatment group (P<0.05 Tukey's post hoc test following two-way ANOVA). * are significantly different from controls at the same gestational age (P<0.05 by t-test or Mann-Whitney test).*

4.5 Results: Effects of T_3-infusion

4.5.1 Fetal measurements

Fetal blood measurements

The 5-day T_3 infusion protocol resulted in a lower T_4 plasma concentration compared with controls, although T_3 concentrations were not significantly different to controls due to wide inter-animal variation in the T_3 infused fetuses (Table 4.4, Figure 4.17A). The fetal plasma T_3 and T_4 concentrations throughout the infusion period in both control and T_3-infused fetuses are shown in Figure 4.17. The T_3 infusion did significantly raise the T_3 concentration compared to day 0 of the infusion (P<0.05, paired t-test, n=5), whereas the T_3 concentration was not different between day 0 and day 5 of the saline-infused fetuses. The weight of the fetal thyroid gland showed a trend to be lower in T_3-infused (0.45±0.03g) than control fetuses (0.58±0.05g; P<0.1 by Mann-Whitney test). Infusion of T_3 had no effect on fetal cortisol concentrations (Table 4.4). There were also no differences in blood pH, pO_2, pCO_2, HCO_3, haemoglobin, oxygen saturation, glucose or lactate between cohorts at the start of the infusion period (data not shown) through to day 5 of infusion in either group of fetuses (data shown in Table 4.5).

Table 4.4 Fetal plasma hormone concentrations

	Control	**T_3-infused**
Cortisol (ng/ml)	11.0±1.6	14.5±1.5
T_3 (ng/ml)	0.41±0.06	1.73±0.56
T_4 (ng/ml)	124.2±6.0	53.9±16.2*

*Data are presented as mean±SEM of control (n=4) and T_3-infused fetuses (n=5). * are significantly different from controls (P<0.05 by Mann-Whitney test).*

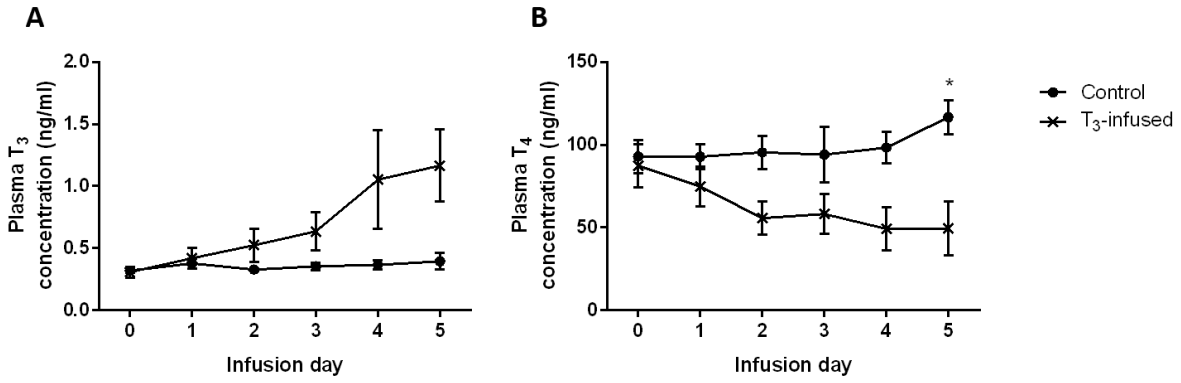

*Figure 4.17 Mean±SEM fetal plasma A) T_3 and B) T_4 concentrations over the 5-day T_3 infusion period of control (n=4; circles) and T_3-infused (n=5; crosses) fetuses. * are significantly different between control and T_3-infused fetuses (P*<0.05 by Mann-Whitney test*).*

Table 4.5 Fetal arterial blood parameters on day 5 of infusion.

		Control	T_3-infused
Fetal arterial blood parameters	pH	7.40±0.02	7.37±0.02
	pO_2 (mmHg)	17.8±0.8	18.6±1.0
	pCO_2 (mmHg)	51.0±0.8	50.7±1.1
	HCO_3 (mmol/L)	29.6±0.9	27.5±0.5
	Haemoglobin (g/dL)	10.4±0.3 (n=3)	10.2±0.5 (n=4)
	$\%O_2$ saturation	55.6±3.5 (n=2)	57.5±2.9 (n=3)
	Glucose (mmol/L)	0.69±0.07	0.67±0.07
	Lactate (mmol/L)	0.96±0.04	1.02±0.07

Data are presented as mean±SEM of control (n=4 unless stated otherwise) and T_3-infused (n=5 unless stated otherwise).

Fetal biometry and muscle biochemical composition

The 5-day T_3-infusion did not result in a significant difference in fetal body weight, body measurements, muscle weights, muscle:body weight ratios or muscle glycogen, lipid and protein content compared with the saline-infused control fetuses (Table 4.6). There was a trend for a lower water content in all 3 muscles of T_3-infused fetuses compared with controls (Table 4.6). When expressed per mg dry weight, the glycogen content of BF of T_3-infused fetuses tended to be lower than controls (Table 4.6).

Table 4.6 Biometric and biochemical measurements.

	Control	T_3-infused
Body weight (kg)	2.54±0.10	2.33±0.14
CRL (cm)	43.0±1.2	43.4±0.9
Femur (cm)	8.8±0.3	8.8±0.3
Tibia (cm)	12.6±0.4	13.0±0.2
Metatarsus (cm)	14.9±0.4	15.1±0.3
	Biceps femoris	
Weight (g)	11.02±0.46	10.92±0.89
Muscle:body weight ratio (g:kg x10^3)	4.34±0.08	4.71±0.35
Water content (%)	82.3±0.4 (n=3)	80.6±0.2 (n=4) #
Protein content (mg/g wet wt)	46.7±2.8	47.6±2.5
(mg/mg dry wt)	0.25±0.02 (n=3)	0.23±0.01 (n=4)
Glycogen content (mg/g wet wt)	40.8±2.4 (n=3)	37.8±2.4 (n=4)
(mg/mg dry wt)	0.23±0.19 (n=3)	0.19±0.01 (n=4) #
Lipid content (mg/g wet wt)	38.8±3.8 (n=3)	40.1±3.1 (n=4)
(mg/mg dry wt)	0.22±0.03 (n=3)	0.21±0.02 (n=4)
	Semitendinosus	
Weight (g)	3.90±0.23	3.98±0.28
Muscle:body weight ratio (g:kg x10^3)	1.53±0.04	1.71±0.08
Water content (%)	82.1±0.3 (n=3)	80.6±0.3 (n=4) #
Protein content (mg/g wet wt)	45.6±3.9	47.8±4.0
(mg/mg dry wt)	0.26±0.03 (n=3)	0.25±0.02 (n=4)
Glycogen content (mg/g wet wt)	32.9±4.7	28.0±3.6
(mg/mg dry wt)	0.16±0.05	0.12±0.03
	Superficial digital flexor	
Weight (g)	1.57±0.05	1.48±0.10
Muscle:body weight ratio (g:kg x10^3)	0.62±0.02	0.63±0.02
Water content (%)	82.6±80.7 (n=3)	80.6±0.4 #
Protein content (mg/g wet wt)	45.4±48.5	48.5±1.7
(mg/mg dry wt)	0.27±0.01 (n=3)	0.24±0.004 (n=4)
Glycogen content (mg/g wet wt)	29.2±1.0	29.5±5.1 (n=4)
(mg/mg dry wt)	0.14±0.04 (n=3)	0.14±0.04 (n=4)

Data are presented as mean±SEM of control (n=4 unless stated otherwise) and T_3-infused fetuses (n=5 unless stated otherwise). # trend to differ from control values (P<0.1 by Mann-Whitney test).

4.5.2 Oxidative capacity

The oxygen consumption of permeabilised muscle fibres was measured using respirometry. There was no difference in ADP-coupled oxygen consumption between control and T_3-infused cohorts using Py, PC or glutamate and succinate as substrates in any muscle (Figure 4.18). There was also no difference in the ratio of PC-supported:PC plus Py-supported state 3 respiration in the 3 skeletal muscles from T_3-infused fetuses compared with controls (Figure 4.19). Leak state respiration and RCR values using Py, PC or glutamate were not affected by T_3 infusion (data not shown). HOAD activity was measured only in the BF and there was no significant difference between T_3-infused and control fetuses (Figure 4.20).

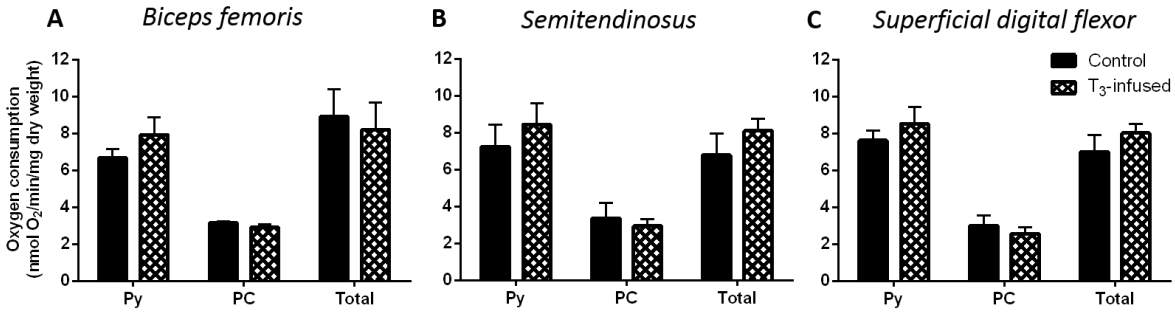

Figure 4.18 Mean±SEM ADP-coupled, pyruvate (Py), palmitoylcarnitine (PC) and glutamate and succinate stimulated (total) oxygen consumption in A) biceps femoris, B) semitendinosus and C) superficial digital flexor of control (n=3-4; black bars) and T_3-infused (n=4-5; cross-hatched bars) fetuses.

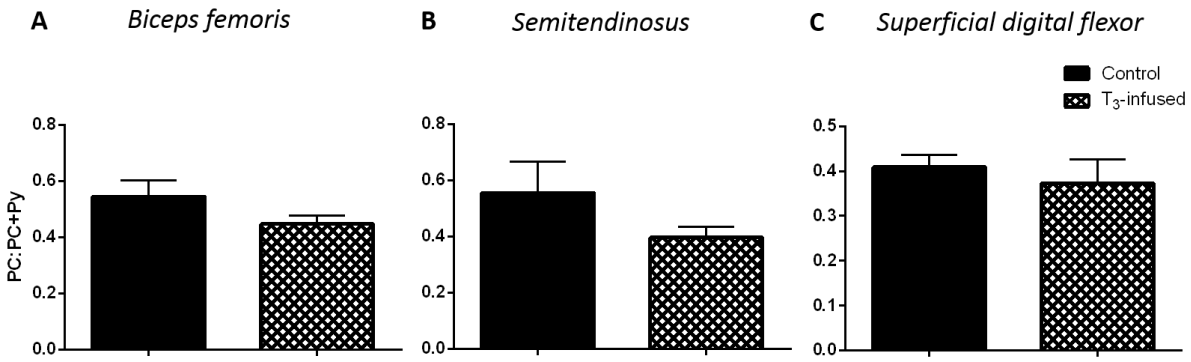

Figure 4.19 Mean±SEM ratio of ADP-coupled palmitoylcarnitine (PC)-supported:PC+pyruvate (Py)-supported oxygen consumption in A) biceps femoris, B) semitendinosus and C) superficial digital flexor of control (n=3-4; black bars) and T_3-infused (n=4-5; cross-hatched bars) fetuses.

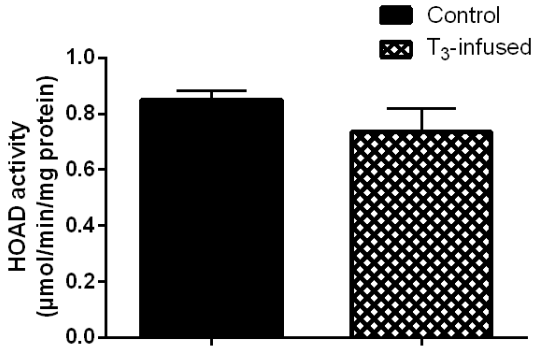

Figure 4.20 Mean±SEM β-hydroxyacyl-CoA dehydrogenase (HOAD) activity in biceps femoris muscle of control (n=3; black bars) and cortisol-infused (n=3; cross-hatched bars) fetuses.

4.5.3 Regulating oxidative capacity

4.5.3.1 Mitochondrial abundance

The mitochondrial density, as assessed by CS activity, was not affected by T_3-infusion in BF or SDF, although tended to be higher in ST of T_3-infused than control fetuses (Figure 4.21 A-C). When the Py- and PC-supported and total ADP-coupled oxygen consumption were normalised to CS activity, there was no difference in oxygen consumption per mitochondrial unit in any of the muscles studied (data not shown). The gene expression of mitochondrial biogenesis markers, PGC1α and NRF1, was not different in any of the muscles studied of T_3-infused fetuses compared with controls (Figure 4.21 D-F).

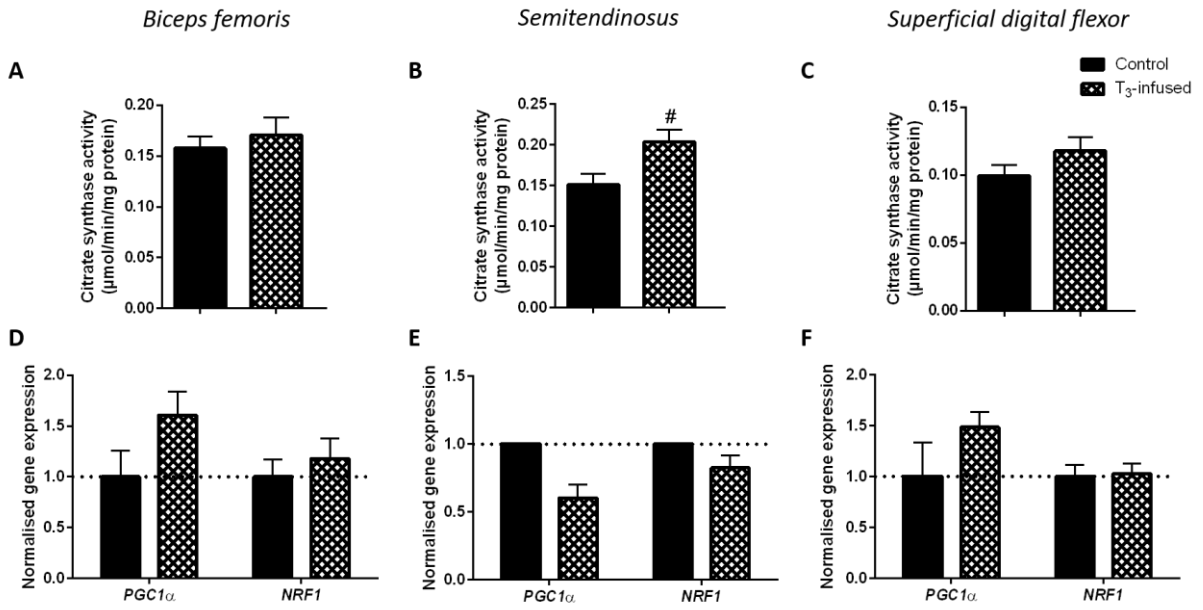

Figure 4.21 Mean±SEM A-C) citrate synthase activity and D-F) normalised gene expression of PGC1α and NRF1 in A&D) biceps femoris, B&E) semitendinosus and C&F) superficial digital flexor of control (n=2-4; black bars) and T_3-infused (n=3-5; cross-hatched bars) fetuses. # trend to differ from controls (P<0.1 by Mann-Whitney test).

4.5.3.2 ETS abundance

The protein abundance of ETS complexes I-IV and ATP-synthase were measured by western blotting (Figure 4.22). ATP-synthase showed a trend to be higher in the SDF of T_3-infused fetuses compared with controls. T_3 infusion did not have a significant effect on abundance of the other ETS complexes in any of the muscles studied. When considering all complexes and performing a two-way ANOVA (complex and treatment), there was a significant effect of T_3-infusion on ETS complex abundance in the BF (P<0.01) but not in the ST or SDF.

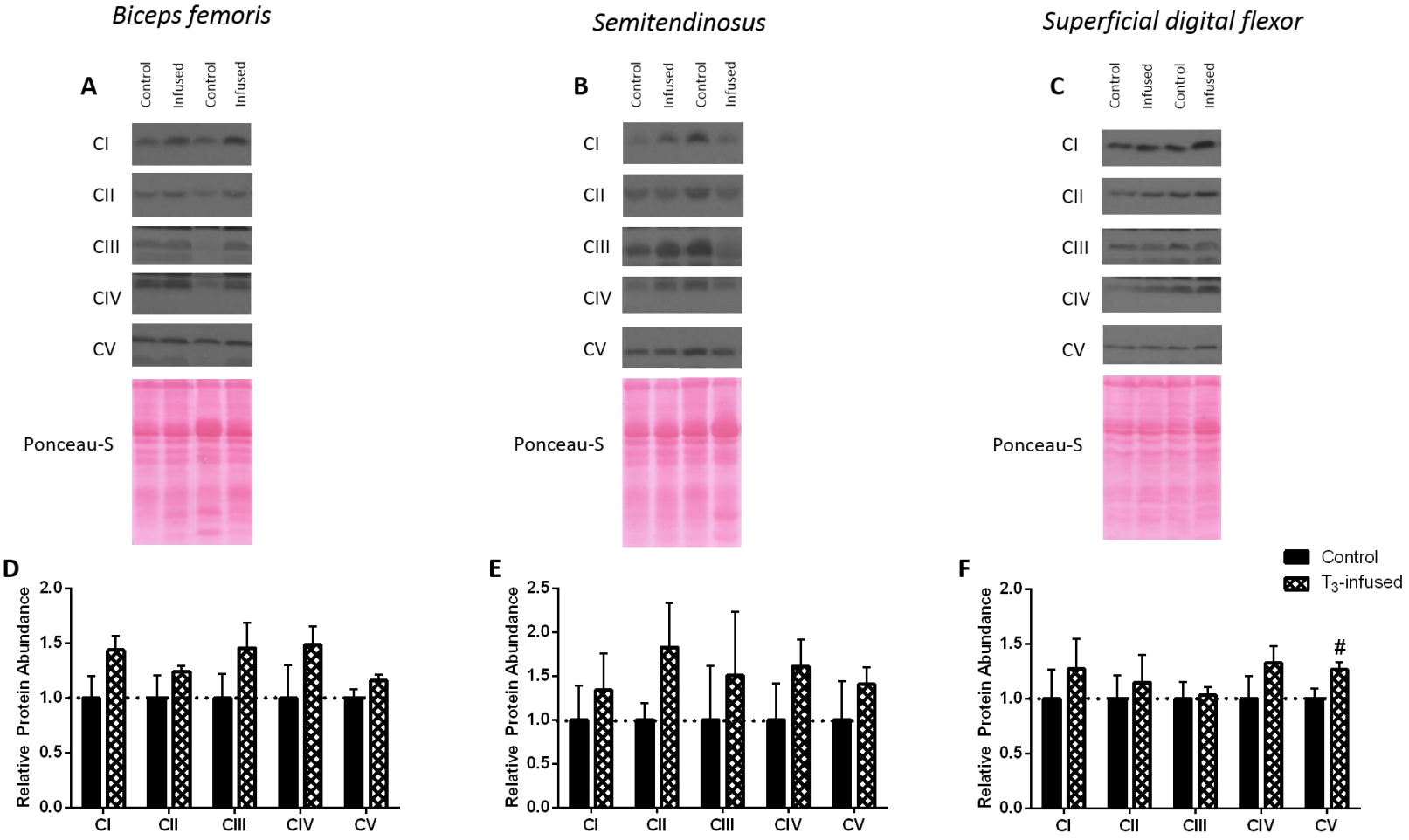

Figure 4.22 Protein expression of electron transfer system complexes I-IV (CI-IV) and ATP-synthase (CV) by western blotting. A-C) representative blots and D-F) mean±SEM relative abundance of the complexes in A&D) biceps femoris, B&E) semitendinosus and C&F) superficial digital flexor of control (n=4; black bars) and T_3-infused (n=5; cross-hatched bars) fetuses. # trend to differ from control (P<0.1 by Mann-Whitney test).

4.5.3.3 Uncoupling the proton gradient

There was no significant difference in the gene expression of UCP2 or UCP3 between control and T_3-infused fetuses in any of the 3 muscles studied (Figure 4.23). The protein abundance of ANT1 shows a trend to be higher in the SDF of T_3-infused fetuses compared with controls but no difference was seen in the BF or ST (Figure 4.24). ANT1 gene expression was also unaffected by T_3 infusion in all 3 muscles (Figure 4.24).

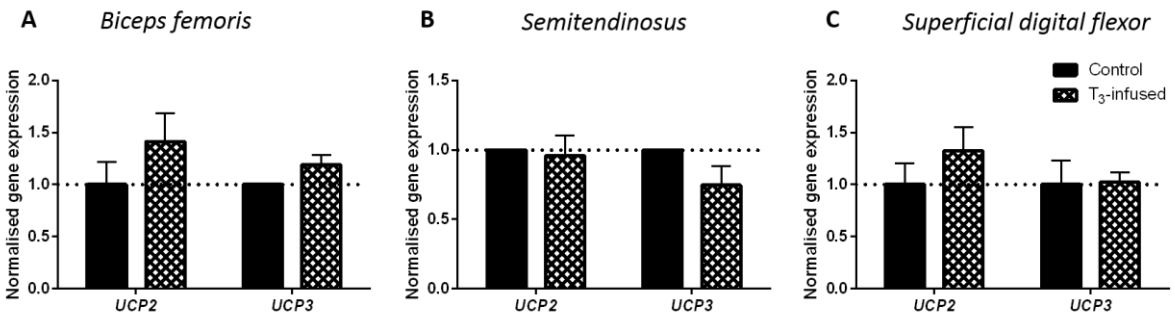

Figure 4.23 Mean±SEM normalised gene expression of uncoupling proteins (UCP) 2 and 3 in A) biceps femoris, B) semitendinosus and C) superficial digital flexor of control (n=2-3; black bars) and T_3-infused (n=5; crosshatched bars) fetuses.

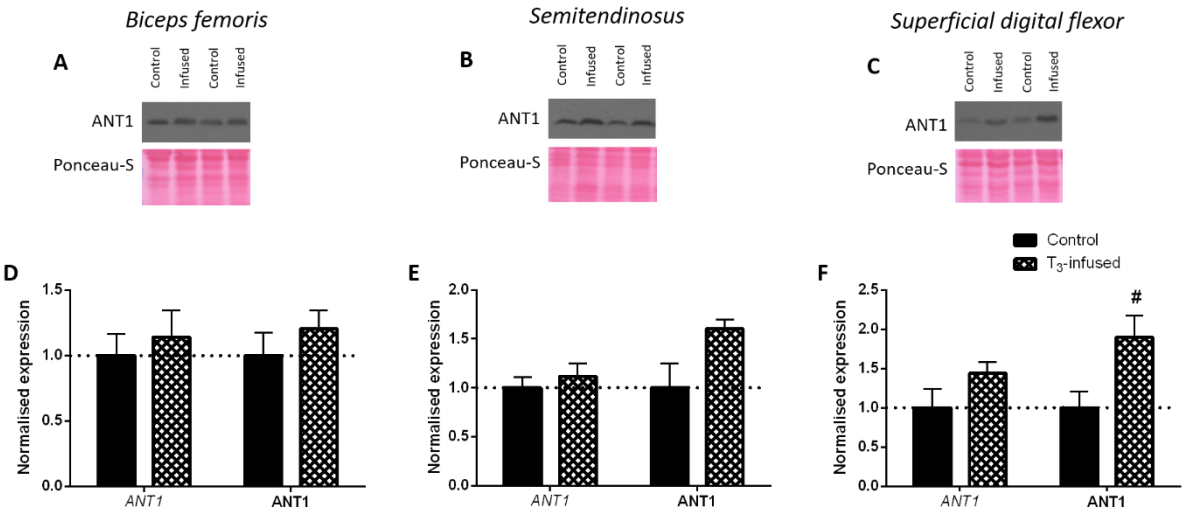

Figure 4.24 Protein and mRNA levels of adenine nucleotide translocase 1 (ANT1) A-C) representative western blots and D-F) mean±SEM normalised gene expression and protein abundance in A&D) biceps femoris, B&E) semitendinosus and C&F) superficial digital flexor of control (n=2-4; black bars) and T_3-infused (n=4-5; crosshatched bars) fetuses. # trend to differ from control (P<0.1 by Mann-Whitney test).

4.5.3.4 Fusion and fission

T_3 infusion did not significantly affect gene expression of the fusion and fission proteins, MFN1, MFN2 or DRP1, in any muscle studied, although *DRP1* showed a trend to be lower in ST of T_3-infused fetuses compared with controls (Figure 4.25).

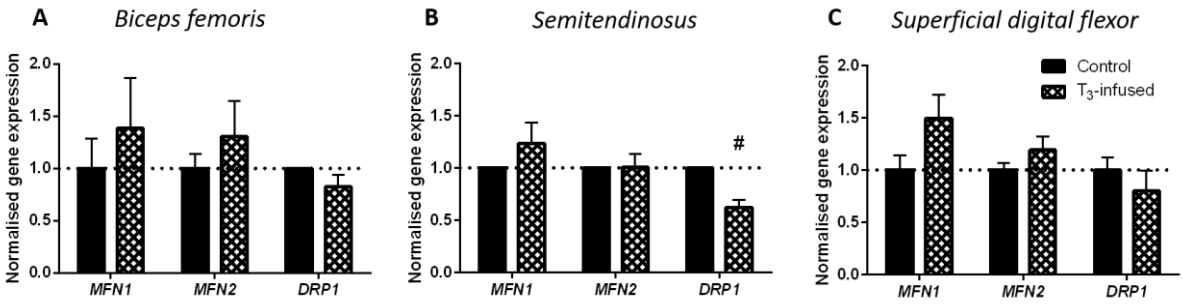

Figure 4.25 Mean±SEM normalised gene expression of mitofusins (MFN) 1 and 2 and dynamin-related protein 1 (DRP1) in A) biceps femoris, B) semitendinosus and C) superficial digital flexor of control (n=4-6; black bars) and T_3-infused (n=6; crosshatched bars) fetuses. # trend to differ from control (P<0.1 by Mann-Whitney test).

4.5.4 Skeletal muscle structure and type I fibres

Muscle sections were stained with H&E to quantify fibre density (Figure 4.26), and MHCI was stained fluorescently in order to identify type I muscle fibres (Figure 4.27). T_3-infusion did not affect total fibre density, nor type I fibre parameters including density, cross sectional area, perimeter or number in any muscle (Table 4.7), or gene expression of MHCI, IIa and IIx in any muscle studied (Figure 4.28).

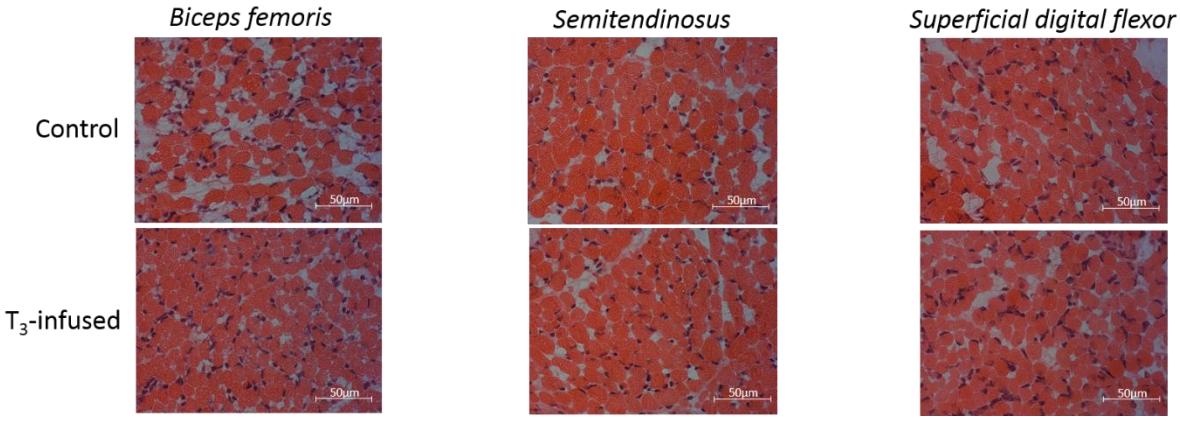

Figure 4.26 Representative H&E stained sections at 40x magnification in biceps femoris, semitendinosus and superficial digital flexor of control and T_3-infused fetuses, as labelled.

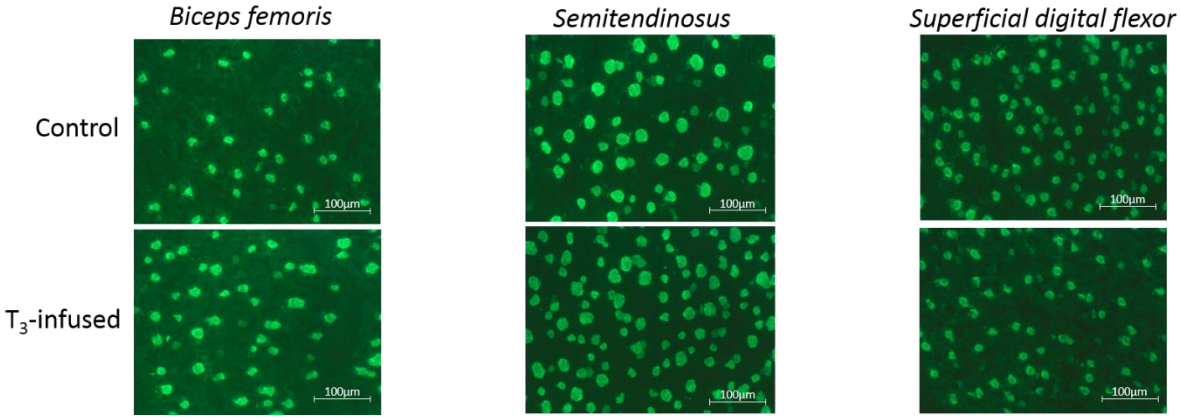

Figure 4.27 Representative MHCI stained sections at 20x magnification in biceps femoris, semitendinosus and superficial digital flexor of control and T_3-infused fetuses, as labelled.

Table 4.7 Type I fibre analyses.

	Control	T_3-infused
	Biceps femoris	
Proportion of total area accounted for by fibres (%; n=6)	69.8±6.1	74.9±3.1
Number of type I fibres/mm²	322±55	523±61
Average fibre area (µm²)	342.4±44.6	331.9±16.1
Average fibre perimeter (µm)	69.3±4.7	69.4±1.7
Proportion of total area accounted for by type I fibres (%)	11.0±2.5	17.0±1.6
Proportion of fibre area accounted for by type I fibres (%)	15.3±2.5	24.0±5.1
	Semitendinosus	
Proportion of total area accounted for by fibres (%; n=6)	83.6±4.3	88.5±2.9
Number of type I fibres/mm²	239±41	314±58
Average fibre area (µm²)	388.7±44.2	397.6±6.3
Average fibre perimeter (µm)	73.5±4.2	75.0±0.4
Proportion of total area accounted for by type I fibres (%)	9.8±2.6	12.4±2.2
Proportion of fibre area accounted for by type I fibres (%)	13.8±2.8	16.2±3.9
	Superficial digital flexor	
Proportion of total area accounted for by fibres (%; n=6)	70.9±3.6	74.4±2.2
Number of type I fibres/mm²	534±65	505±52
Average fibre area (µm²)	294.8±12.0	295.2±21.5
Average fibre perimeter (µm)	65.3±1.4	65.0±2.2
Proportion of total area accounted for by type I fibres (%)	15.5±1.4	14.5±1.0
Proportion of fibre area accounted for by type I fibres (%)	21.9±2.5	19.4±2.2

Data are presented as mean±SEM in biceps femoris, semitendinosus and superficial digital flexor of control and T_3-infused fetuses. N=4 in each group unless stated otherwise).

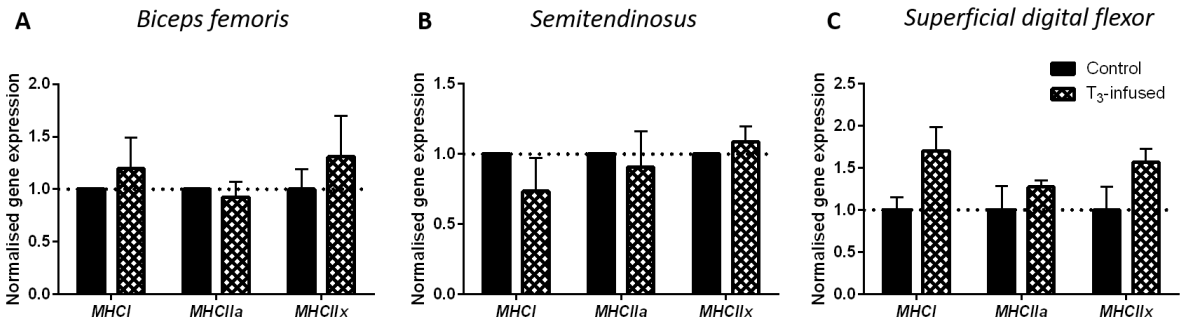

Figure 4.28 Mean±SEM gene expression of MHCI, MHCIIa and MHCIIx in A) biceps femoris, B) semitendinosus and C) superficial digital flexor of control and T_3-infused fetuses. N=3-5 in each group.

4.6 Discussion

This study demonstrates that THs are important for regulating several aspects of mitochondrial development in skeletal muscle of fetal sheep during late gestation. Hypothyroidism during late gestation resulted in skeletal muscle having a significantly lower mitochondrial density and abundance of proteins involved in oxidative ATP production at term, as well as delaying maturation of the muscle structure and leading to a higher water content and lower fibre density relative to sham operated controls. Muscle-specific reductions in mitochondrial oxidative capacity and in *UCP* and *MFN* expression were also evident, particularly close to term, in response to TX earlier in gestation. Fetal hypothyroidism also prevented the normal ontogenic changes in mitochondrial function seen towards term. However, the 5-day T_3 infusion did not prematurely increase the functional oxidative capacity of the muscle, nor significantly affect any of the mitochondrial parameters measured.

4.6.1 Effectiveness of the hormone manipulation protocols; impact on fetal development

TX was performed at 102-105dGA and the hormone levels measured 24-40 days post-surgery at ~127 and ~143dGA. Previous studies using this protocol have reported no detectable fetal plasma T_3 or T_4 at both ages (Forhead et al., 1998). However, in this cohort of animals, excluding T_4 at 127dGA, the concentrations of the THs were close to, but did not fall below the limit of detection of the RIA. Concentrations of both T_3 and T_4 were significantly lower in TX fetuses than the age-matched controls at both 127 and 143dGA. In individual pairs of twins, the TX fetus always had a much lower concentration of T_4, suggesting that cross-circulation was unlikely to be responsible for THs detected in the TX fetuses.

T_3 has been reported in the circulation of TX fetuses at ~127dGA following cortisol infusion, suggesting that there is still a source of THs present following TX (Forhead et al., 1998). This may be partly due to the presence of T_3 sulphate which has been shown to remain in the circulation after TX and has been suggested to contribute to the plasma and tissue T_3 concentrations following desulphation (Wu et al., 1993). Additionally, T_4 levels may be buffered by binding protein in the plasma, delaying their removal from the circulation (Hoffenberg and Ramsden, 1983). Any remaining T_4 may then be converted locally to T_3 resulting in some residual T_3. TX performed at a similar timing to our protocol resulted in a tissue-specific effect on deiodinase activity with increased D2 activity in the brain, whereas TX later in gestation resulted in additional downregulation of D1 in the liver (Polk et al., 1988).

These results suggest that when TH levels are low, the fetal response is to spare T_3 for the more vital development of the brain. Whether fetal muscle D2 is regulated by thyroid status has not been investigated, although in adult human muscle, activity and abundance of D2 is not changed in response to hypothyroidism (Heemstra et al., 2009). Measuring the deiodinase abundance in the muscles may give an idea of the local exposure to T_3.

A further comment on the measurement of THs in this study is that only total levels of both hormones have been considered. Only approximately 0.3% T_3 and 0.03% T_4 circulate unbound in the plasma and are immediately available for cellular uptake (Hoffenberg and Ramsden, 1983). Further insight into the bioavailability of THs may come from measuring levels of the TH binding globulins and free TH.

Although the TH levels did not fall to undetectable levels, biometric measurements and fetal observations match those previously reported following ovine TX at the same point in gestation (Harris et al., 2017). In particular, the metatarsus length has been previously reported to be shorter in TX fetuses than age-matched controls (Lanham et al., 2011).

For this study aspects of skeletal muscle structure and biochemistry were analysed. There was no significant difference in muscle weight of any of the muscles studied between TX and control fetuses. A previous study has reported a lower muscle mass due to TX, however, in this case TX was performed earlier in gestation, 70-75dGA, and tissues taken at term (Finkelstein et al., 1991). The body weight of TX fetuses were not significantly different to controls as has been shown before (Erenberg et al., 1974). As shown previously, the muscle mass:body weight ratio was not different in TX and control fetuses (Finkelstein et al., 1991).

The biochemical composition of the muscles showed muscle specific changes in response to TX. The glycogen content was lower at 127dGA in BF of TX compared to control fetuses, but by term this difference was no longer observed. These results are in agreement with a previous study on the BF of TX fetuses (Forhead et al., 2009). However, glycogen content of the ST and SDF were not different at either time point between treatment groups. Previously, protein content of TX muscle has been shown to be lower than controls, although the muscle was not specified in the previous study (Erenberg et al., 1974). In the current study, protein content was lower in TX than control ST at both ages studied, and the BF at 127dGA. In addition, a lower muscle DNA content has been reported previously alongside a normal ratio of protein:DNA was normal (Erenberg et al., 1974). These authors hypothesised that this may

be due to an increased water content of the fibres and/or a decrease in fibre number. Here, the data shows that either hypothesis may explain their observations. All 3 muscles of TX fetuses had a significantly higher water content than controls at both ages studied. Additionally, the fibre density of the BF and ST was lower in TX than control fetuses at term.

T_3-infusion in this cohort resulted in a significantly lower T_4 circulating concentration which may reflect the T_3 negative feedback on the HPT axis which has been previously reported in some, but not all, studies using this protocol (Forhead et al., 2003, Forhead et al., 1998, Lorijn et al., 1980). There was also a trend for a decrease in fetal thyroid gland mass in the T_3-infused fetuses compared with controls, reflecting the previously identified reduction in blood flow to this organ and the potential reduction in TSH (Lorijn et al., 1980).

4.6.2 Thyroidectomy prevented the normal prepartum development of mitochondrial function in skeletal muscle

The importance of THs for development of mitochondrial function in skeletal muscle is shown not only by the reduction in many of the mitochondrial parameters measured in the muscles after TX, but also by the lack of any increment in these values between 127 and 143dGA as seen in their sham operated twins. As shown in Chapter 3, and replicated in this chapter, gestational age has a significant effect on the mitochondrial density and abundance of some of the ETS complexes and ANT1. TX suppressed the normal ontogenic rise in all of these parameters. Similarly, maturation of the skeletal muscle adult phenotype over late gestation, for example the increase in expression of MHCI and MHCIIa in the SDF, is not apparent in the muscle of TX fetuses. Therefore, THs are essential for the normal metabolic development of skeletal muscle mitocondria during late gestation in preparation for birth.

4.6.2.1 Oxidative capacity

This study has shown that in fetal skeletal muscle, as in adult tissue, THs are important metabolic regulators. The mitochondrial density in TX fetal muscle at term was lower than in controls coinciding with lower oxygen consumption in a muscle- and substrate-specific manner. Interestingly, when Py-supported state 3 respiration was normalised to CS activity, oxidative function per mitochondrion was higher in the TX fetuses than controls. Similarly, total ADP-coupled oxygen consumption per mitochondrial unit in the ST at 143dGA was higher

in TX than control fetuses. These results suggest there may be a compensatory mechanism in place to help maintain mitochondrial function when mitochondrial density is prevented from increasing towards term in the hypothyroid environment. THs may be regulating metabolism by controlling abundance of ETS complexes and ATP-synthase, several of which were lower in TX than control fetal muscle. Additionally, results presented here support a role of THs in increasing fetal metabolism through MFN1 and MFN2-driven mitochondrial fusion. THs have previously been shown to increase fetal metabolic rate and the results of this study support the hypothesis that this may be largely due to an increase in skeletal muscle metabolism (Fowden and Silver, 1995, Forhead and Fowden, 2014).

4.6.2.2 Uncoupling the gradient

THs in the adult increase metabolic rate, in part through decreasing the efficiency of oxphos by increasing the abundance of proteins known to dissipate the proton gradient. In the current study, THs have been shown to play a similar role in the fetus, with expression of ANT1 significantly lower in all 3 muscles from TX than control fetuses at both 127 and 143dGA. Similarly, both *UCP2* and *UCP3* were lower in TX SDF than controls, and *UCP3* expression was lower in ST at 143dGA and *UCP2* was reduced at 127dGA in BF and ST. At birth, there is an increased requirement for ATP and therefore, the efficiency of oxphos should be critical for neonatal survival. As discussed in Chapter 3, we hypothesise that increased UCP and ANT expression at birth is perhaps a protective mechanism against excessive ROS production, or in order to carry out additional roles, for example in thermogenesis.

Over the perinatal period, one key role of THs is in thermogenesis (Clarke et al., 1997). T_3 is crucial for increasing the UCP1-mediated non-shivering thermogenesis in brown adipose tissue. Further, TH-driven thermogenesis has been associated with an upregulation of skeletal muscle UCP3 in humans and rodents (Barbe et al., 2001, Gong et al., 1997). The TH-dependency of *UCP3* expression in ST and SDF at term may reflect this role of THs in preparation for neonatal cold exposure and the immediate requirement for thermogenesis.

This study has also shown that ANT1 expression, especially at the protein level, is dependent on the presence of circulating THs. A study on rats suggests that increased ANT expression may, at least in part, explain the TH-driven increase in metabolism in the liver and the heart (Dummler et al., 1996). Additionally, postnatal cardiac maturation has been shown to require

a T_3-dependent increase in ANT abundance (Portman et al., 2000). However, in adult rats, ANT1 expression in the heart is not sensitive to T_3 (Dummler et al., 1996). In this study, there was a trend for higher ANT1 protein abundance in the SDF of T_3-infused fetuses compared to controls, but no difference in the BF or ST. In the sheep fetus, therefore, ANT1 expression seems to be sensitive to TH availability, but as in the rat, may not be directly responsive to the hormone.

4.6.3 Physiological impact of TX; indirect effects on skeletal muscle development

The THR is expressed in developing pig skeletal muscle and a compensatory upregulation of the THR has been reported to occur in response to hypothyroidism, therefore THs may play a direct role in regulating the expression of mitochondrial genes (White et al., 2001, Duchamp et al., 1994). However, TX may also downregulate mitochondrial function indirectly by affecting the expression of other pathways in skeletal muscle, altering the tissue availability of, and tissue responsiveness to, other hormones or even affecting the development of other organs which in turn impact on muscle development.

Although not measured in this study, TX ovine fetuses have been previously shown to have significantly higher circulating leptin and insulin concentrations, by both 129 and 143dGA (Harris et al., 2017). Leptin has been shown to play a role in some aspects of fetal maturation and negatively correlates to fetal weight, whereas insulin is a growth factor *in utero* (Buchbinder et al., 2001, Fowden et al., 1989, Forhead et al., 2008). The leptin receptor has been identified in fetal sheep tissues including skeletal muscle, however, to date a role of leptin in skeletal muscle maturation is unknown (Forhead et al., 2008, Buchbinder et al., 2001). Fetal insulin, on the other hand, plays an important role in glucose uptake, oxidation and storage in fetal muscle (Hay, 2006). Cortisol in our cohort was lower, although not significantly, whereas in previous studies, conflicting data has been presented on the effect of TX on cortisol concentration ranging from having no effect to preventing the normal rise in cortisol at term (Harris et al., 2017, Forhead et al., 2002). The discrepancy may be due to the timing of tissue collection being just before or after a delayed cortisol surge in the TX fetuses. In addition, TX results in a diminished growth hormone receptor abundance in ovine skeletal muscle (Forhead et al., 2002). The muscle expression of IGF-I, a fetal growth factor, is lower in TX fetuses compared to controls, although circulating IGF-I and IGF-II is not different (Forhead et al., 2002, Harris et al., 2017). The dysregulation of numerous endocrine systems in the TX animals

may be involved in the diminished metabolism of the TX skeletal muscle, although the roles of the individual hormones are not clear.

THs are essential for the normal development of the brain, with hypothyroidism associated with reduced neuronal density, branching and synaptic contacts and myelination (Horn and Heuer, 2010). Neuronal stimulation and TH are both responsible for determining the proportions of skeletal muscle fibre types (Gambke et al., 1983). In the current study, TX caused a decreased proportion of type I fibres in the ST and reduced the expression of *MHCI*, *MHCIIa* and *MHCIIx* in all muscles studied. Similarly, a decreased proportion of type I fibres due to TX has been reported previously in the gastrocnemius and extensor digitorum longus muscles and may be, in part, due to impaired neuronal development (Finkelstein et al., 1991). Indeed, the axonal conduction velocity of the nerve stimulating the gastrocnemius was significantly slower in TX than control fetuses at term resulting in a delayed maturation of the muscle contractile properties (Finkelstein et al., 1991). In a separate study, removal of the pituitary gland did not alter fibre type proportions, although it did reduce the average fibre cross-sectional area as shown in the current study for type I fibres in the ST (Javen et al., 1996). Although removal of the pituitary gland affects both the HPT and HPA axes, the negative impact on skeletal muscle development was less severe than after TX which may be due to a slower decline in TH availability, or due to the central nervous system development being less impaired (Javen et al., 1996).

TX clearly affects numerous aspects of development at the cellular, tissue and whole body level and it is difficult to separate out the roles of individual components when considering the whole physiological system.

4.6.4 T_3 infusion is not sufficient to drive prepartum skeletal muscle maturation

Despite the striking phenotype associated with TX, infusion of T_3 for 5 days did not affect skeletal muscle structural and mitochondrial maturation. Of the parameters measured, water content of the 3 muscles showed a trend to decrease with T_3-infusion, ANT1 and ATP synthase protein abundance showed a trend to be higher in SDF of T_3-infused than control fetuses and mitochondrial density was higher in the ST of T_3-infused than control fetuses but again this did not reach significance. Previously, developmental pathways in fetal tissues including skeletal

muscle have been reported to be impaired by TX but not prematurely driven by T_3 infusion (Forhead et al., 2002, Forhead et al., 1998).

As discussed above, TX was performed early in gestation, giving up to 40 days of an altered endocrine environment. During this time the development of numerous physiological systems is affected which may interact to impair skeletal muscle development. The T_3 infusion protocol, however, alters the endocrine environment over a much shorter time-scale. The predominant action of THs are long-term effects mediated through altered gene expression (Wu and Koenig, 2000). Therefore, 5 days may not be sufficient to up- or down-regulate target pathways in time to have a measurable effect, although T_3-infusion has been shown to stimulate maturational changes in other tissues (Forhead et al., 2003, Forhead et al., 2006, Lorijn et al., 1980).

Removal of the thyroid gland in the sheep fetus means that, apart from minimal local TH stores and sulphated THs, the concentration of THs are low and there is little the organism can do to compensate for this. Conversely, T_3-infusion can have a direct negative feedback on the HPT axis, and this seemed to be occurring in this cohort as we measured a decreased circulating T_4 concentration, and the thyroid gland tended to be smaller in the infused fetuses compared to controls. A further consideration here is that the lack of T_3 effects may be due to the concomitant decrease in T_4. Certainly, the total oxygen consumption of the fetus was more closely correlated to T_4 than T_3 (Fowden and Silver, 1995). Alternatively, although circulating T_3 was higher at the end of the infusion period than at the start, the skeletal muscle local bioavailability and activity has not been determined; T_3-infusion may affect the deiodinase activity and abundance of the THR. In mouse muscle cell lines, a decrease in D3 and increase in D2 is associated with the terminal differentiation stage of myogenesis, although whether this is TH-regulated is not clear (Bloise et al., 2017, Dentice et al., 2010). However, in the sheep fetal liver the activity of D1 increases with T_3-infusion, suggesting that near term, there is a positive feedback of T_3 upregulating the conversion of T_4 to T_3 (Forhead et al., 2006). Determining the iodinase activity in ovine fetal skeletal muscle in response to T_3 would give further insight into the potential for a T_3 response.

Perhaps the most likely explanation as to why T_3-infusion did not have a significant effect on mitochondrial parameters measured is that its infusion alone was insufficient to drive maturation without all the other changes normally experienced by the fetus in the prepartum period. One of the key drivers of maturation is cortisol, which was unaffected by T_3-infusion,

but as shown in Chapter 3, correlated to numerous aspects of mitochondrial development and tended to be lower in TX than control fetuses at term. Therefore, a delayed prepartum rise in cortisol may be part of the potential explanation for the lack of skeletal muscle maturation near term in TX fetuses. In the next chapter the role of cortisol in driving fetal skeletal muscle metabolic maturation will be discussed.

4.6.5 Conclusion

THs are essential permissive factors for the development of mitochondrial function in ovine skeletal muscle over late gestation but T_3 alone is insufficient to prematurely induce the maturational changes in mitochondrial function seen close to term in preparation for birth.

5 The role of cortisol in fetal skeletal muscle mitochondrial development

5.1 Introduction

In precocial species, skeletal muscle is required immediately at birth to take on the roles of locomotion and thermogenesis. Its energy requirement therefore increases rapidly. During late gestation maturation of skeletal muscle occurs in preparation for these new roles and the increased energy demands, in part by alterations in mitochondrial activity. As previously shown in Chapter 3, there is an age-related increase in mitochondrial number, oxidative capacity and expression of a variety of mitochondrial genes over the perinatal period in ovine skeletal muscle. These changes are occurring in parallel with a surge in fetal plasma cortisol which is known to drive prepartum maturation in other fetal tissues (Fowden et al., 1998). Additionally, a rise in cortisol before term due to stresses, including malnutrition, also has an impact on fetal development (Jensen et al., 2002). However, whether cortisol regulates energetic aspects of skeletal muscle maturation is unknown.

In the adult, the predominant roles of glucocorticoids are in regulation of glucose metabolism and immunosuppression in response to stress (Newton, 2000). However, some studies have implicated glucocorticoids in upregulating overall metabolic rate by increasing mitochondrial number and function in adult rat skeletal muscle as well as in various cell lines in culture including mouse muscle cells (Morgan et al., 2016, Scheller et al., 2000, Weber et al., 2002). This is likely to be driven predominantly via altered nuclear gene expression, but may be coordinated in part by direct glucocorticoid interaction with mitochondrial DNA to modify its transcription rate (Marin-Garcia, 2010, Scheller et al., 2000, Demonacos et al., 1995). In the fetus, an increased cortisol concentration associated with fetal hypoxaemia was suggested to increase the expression of mitochondrial proteins in the lung and brown adipose tissue, although whether cortisol is the predominant driving factor in this situation remains unclear (Gnanalingham et al., 2005a, Mostyn et al., 2003). Cortisol does, however, play a role in fetal metabolism. In the liver it is required for the deposition of glycogen and the increase in glycogenolytic and gluconeogenic enzyme activities over late gestation, thereby ensuring a supply of glucose to the neonate immediately after birth (Barnes et al., 1978, Fowden et al.,

1993). However, cortisol infusion in the sheep fetus does not alter its total rate of oxygen consumption (Ward et al., 2004).

In order to determine whether cortisol plays a role in regulating mitochondrial function in fetal skeletal muscle, ovine fetuses were catheterised at ~118dGA and infused with cortisol at a constant rate for a 5-day period until ~130dGA. This well-established protocol has been shown previously to elevate fetal cortisol levels up to values seen close to term and to lead to morphological and functional changes in a range of fetal tissues that mimic the prepartum maturational processes essential for neonatal survival (Fowden et al., 1996). This 5-day cortisol infusion has been shown to slow fetal growth (Fowden et al., 1996) and reduce placental glucose transport (Ward et al., 2004). In skeletal muscle, the 5-day cortisol infusion protocol has been shown to significantly downregulate IGF-I expression consistent with the inhibitory effect of cortisol on fetal growth (Forhead et al., 2002, Li et al., 2002). Additionally, cortisol affects the insulin signalling pathway in fetal skeletal muscle with potential effects on growth and glucose metabolism (Jellyman et al., 2012). Finally, cortisol infusion has been shown to affect mitochondria in fetal adipose tissue through changes in the expression of uncoupling proteins (Gnanalingham et al., 2005b) but little is known of the effects of cortisol on mitochondria in fetal skeletal muscle.

5.2 Aim

The aim of this study was to determine whether preterm cortisol infusion upregulates mitochondrial biogenesis and oxidative function in skeletal muscle of fetal sheep, thereby mimicking the maturational changes seen in skeletal muscle as cortisol levels rise close to term.

5.3 Methods

5.3.1 Animals

Twelve ewes carrying singleton fetuses were used for this study. Eleven ewes and fetuses were catheterised at 118-119dGA (Section 2.2.2.2). Six of the fetuses were infused with cortisol (2-3mg/kg/day) and 5 with saline for a 5-day period until 128-131dGA when both ewe and fetus were euthanised and tissues collected (Section 2.2.4.1). The remaining ewe and fetus underwent a sham surgery without catheterisation or infusion. Euthansia and tissue collection took place at 130dGA and results from this animal were included with the saline-infused control fetuses.

Details of surgery, tissue collection and experimental protocols used in this chapter are given in Chapter 2.

5.3.2 Statistical Analyses

A Kolmogorov-Smirnov test was applied to test for a normal distribution. A *t*-test was used to compare the data from cortisol and saline-infused fetuses if data were normally distributed. If the assumption of normality was not realised, or the number of samples was too small to determine whether the data followed a normal distribution, a Mann-Whitney non-parametric test was used. $P<0.05$ was considered significant and $P<0.1$ was considered a trend throughout.

5.4 Results

5.4.1 Fetal measurements

Fetal blood measurements

The fetal plasma cortisol and T_3 concentrations were significantly higher in the cortisol-infused fetuses than in controls, with no difference in fetal plasma T_4 with treatment (Table 5.1). The fetal plasma cortisol concentration throughout the infusion period in both control and cortisol-infused fetuses is shown in Figure 5.1. No differences were seen in blood pH, pO_2, pCO_2, oxygen saturation, haemoglobin, HCO_3, glucose or lactate between cortisol-infused and control groups at the start of the infusion period (data not shown). However, on day 5 of the infusion, glucose concentrations were significantly higher in cortisol-infused than control fetuses (Table 5.2).

Table 5.1 Fetal plasma hormone concentrations

	Control	**Cortisol-infused**
Cortisol (ng/ml)	8.4±1.7	49.2±2.4*
T_3 (ng/ml)	0.43±0.03	0.70±0.14*
T_4 (ng/ml)	122.0±9.5	131.6±4.0

*Data are presented as mean±SEM of control (n=6) and cortisol-infused (n=6) fetuses. * are significantly different from control fetuses (P<0.05 by t-test*).

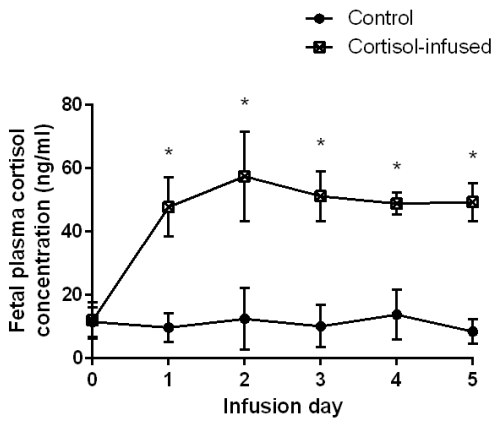

*Figure 5.1 Mean±SEM fetal plasma cortisol concentrations over the 5-day infusion period of control (n=5; circles) and cortisol-infused (n=6; squares) fetuses. * significantly different from control at the same infusion day (P<0.05 by t-test).*

Table 5.2 Fetal arterial blood parameters as measured on day 5 of infusion.

		Control	Cortisol-infused
Fetal arterial blood parameters	pH	7.34±0.02 (3)	7.39±0.01 (5)
	pO_2 (mmHg)	17.5±2.8 (3)	21.5±1.1 (5)
	pCO_2 (mmHg)	54.5±2.2 (3)	50.1±1.3 (5)
	HCO_3 (mmol/L)	27.6±2.8 (3)	28.4±0.5 (5)
	Haemoglobin (g/dL)	10.8±0.4 (3)	9.7±0.6 (4)
	$\%O_2$ saturation	56.6±2.5 (3)	56.9±3.7 (5)
	Glucose (mmol/L)	0.62±0.04 (3)	1.15±0.15 (6) *
	Lactate (mmol/L)	1.02±0.09 (3)	1.21±0.08 (6)

Data are presented as mean±SEM and the n number is given in brackets. significantly different from control fetuses at the same age (P<0.05 by Mann-Whitney test*).

Fetal biometry and muscle biochemical composition

There was no significant difference in body weight, muscle weight or the muscle to body weight ratio of any of the 3 muscles between cortisol and saline-infused fetuses (Table 5.3). There was a trend for glycogen content to be higher in the ST of cortisol-infused than control fetuses, but there were no other significant differences in glycogen content between the cortisol-infused and control fetuses in the BF or SDF, nor in lipid content which was only measured in the BF (Table 5.3). Protein content was not different in any of the muscles of cortisol-infused compared to control fetuses (Table 5.3). However, the water content of the BF and ST was significantly lower in cortisol-infused than control fetuses, with no significant difference in the SDF (Table 5.3). When the water content was taken into account by expressing data per mg dry weight, the trend for increased glycogen content in the ST with cortisol treatment was lost, whereas protein content tended to be lower in the ST of cortisol-infused than control fetuses (Table 5.3).

Table 5.3 Biometric and biochemical measurements.

	Control	Cortisol-infused
Body weight (kg)	3.05±0.12	2.96±0.15
CRL (cm)	43.3±0.6	43.8±0.5
Femur (cm)	9.9±0.7	9.2±0.3
Tibia (cm)	13.9±0.5	13.4±0.2
Metatarsus (cm)	15.6±0.3	15.3±0.3
	Biceps femoris	
Weight (g)	13.07±0.61	12.30±0.87
Muscle:body weight ratio (g:kg x10^3)	4.28±0.09	4.14±0.14
Water content (%)	82.1±0.2	80.5±0.2*
Protein content (mg/g wet wt)	44.0±1.2	47.5±2.6
(mg/mg dry wt)	0.25±0.01	0.24±0.02
Glycogen content (mg/g wet wt)	34.6±2.0	37.8±0.8
(mg/mg dry wt)	0.19±0.01	0.19±0.01
Lipid content (mg/g wet wt)	38.8±0.5	39.5±1.1
(mg/mg dry wt)	0.22±0.003 (n=5)	0.20±0.01
	Semitendinosus	
Weight (g)	4.78±0.29	4.36±0.30
Muscle:body weight ratio (g:kg x10^3)	1.56±0.05	1.47±0.07
Water content (%)	81.7±0.1	79.6±0.4*
Protein content (mg/g wet wt)	47.7±1.4	48.1±1.7
(mg/mg dry wt)	0.26±0.01	0.24±0.01 #
Glycogen content (mg/g wet wt)	19.9±0.5	25.0±2.5 #
(mg/mg dry wt)	0.11±0.003	0.12±0.01
	Superficial digital flexor	
Weight (g)	2.06±0.17	1.97±0.09
Muscle:body weight ratio (g:kg x10^3)	0.67±0.03	0.67±0.03
Water content (%)	80.9±0.3	79.8±0.5
Protein content (mg/g wet wt)	51.1±2.1	50.9±2.3
(mg/mg dry wt)	0.27±0.01	0.25±0.01
Glycogen content (mg/g wet wt)	24.1±4.3	28.8±0.3
(mg/mg dry wt)	0.13±0.02 (n=4)	0.14±0.01 (n=4)

*Data are presented as mean±SEM of control and cortisol-infused fetuses (n=6 in all cases unless stated otherwise). * significantly different to control (P<0.05 by t-test) and # trend to differ from control values (P<0.1 by t-test).*

5.4.2 Oxidative capacity

Respirometry was carried out measuring the oxygen consumption of permeabilised muscle using carbohydrate (Py) or lipid (PC) as substrates and ADP. BF muscle from cortisol-infused fetuses had a significantly higher ADP-coupled, Py-supported rate of oxygen consumption than controls whereas there was no difference with PC as the substrate (Figure 5.2 A). Conversely, the capacity for ADP-coupled, PC-supported oxygen consumption was significantly higher in SDF from cortisol-infused fetuses compared with controls with a trend for a higher oxygen consumption with Py as the substrate (Figure 5.2 C). Cortisol infusion had no effect on oxidation of either substrate in ST muscle (Figure 5.2 B). An additional respirometry protocol was carried out using glutamate and succinate as substrates to measure total oxphos through ETS CI and II. The total ADP-coupled oxygen consumption was higher in SDF of cortisol-infused fetuses compared with controls but did not differ with treatment in either the BF or ST (Figure 5.2). There was no significant difference in state 3 respiration between muscle types in either treatment group.

Using a protocol in which ADP-coupled, PC-supported oxygen consumption was measured, followed by further addition of Py, the ratio of PC-supported:PC+Py-supported ADP-coupled oxygen consumption was determined and shown in Figure 5.3. There was no significant difference in this ratio between cortisol-infused and controls in any of the 3 muscles studied.

PC-supported oxygen consumption before the addition of ADP was higher in SDF of cortisol-infused than control fetuses (1.30±0.21 and 0.69±0.17nmol oxygen/minute/mg dry weight respectively; $P<0.05$) but not in the BF or ST. Py- or glutamate-supported leak state respiration did not differ with treatment in any of the 3 muscles. The RCR was not different between control and cortisol-infused fetuses using any of the substrates in any muscle studied.

HOAD activity, as a marker of β-oxidation activity, was measured only in the BF muscle and was unaffected by treatment (Figure 5.4), in line with the finding that there was no difference in PC-driven oxygen consumption in this muscle.

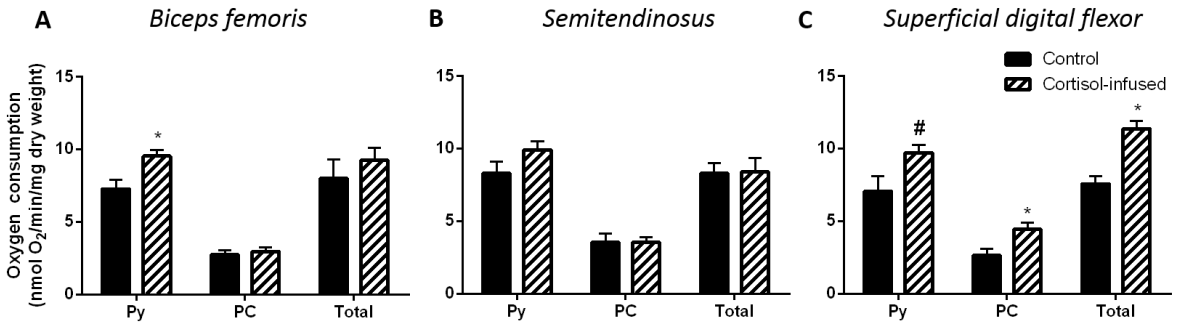

*Figure 5.2 Mean±SEM ADP-coupled, pyruvate (Py), palmitoylcarnitine (PC) and glutamate and succinate supported (total) oxygen consumption in A) biceps femoris, B) semitendinosus and C) superficial digital flexor of control (n=5-6; black bars) and cortisol-infused (n=5-6; dashed bars) fetuses. * is significantly different from controls of the same experimental protocol (P<0.05 by t-test). # trend to differ from controls of the same experimental protocol (P<0.1 by t-test).*

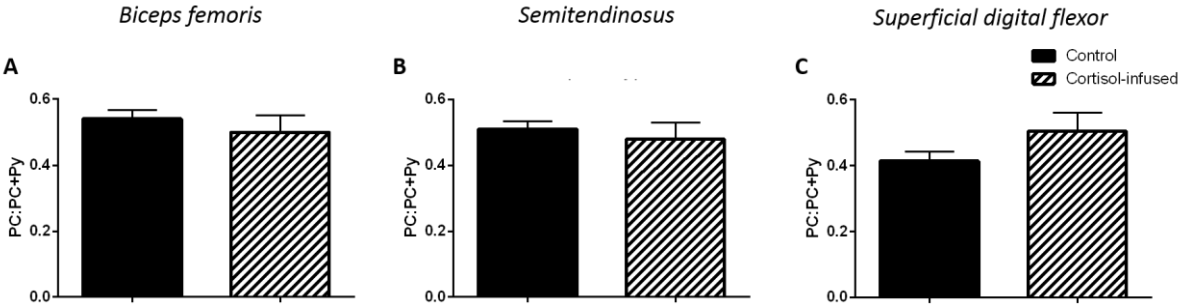

Figure 5.3 Mean±SEM ratio of ADP-coupled palmitoylcarnitine (PC)-supported:PC+pyruvate (Py) oxygen consumption in A) biceps femoris, B) semitendinosus and C) superficial digital flexor of control (n=5-6; black bars) and cortisol-infused (n=5-6; dashed bars) fetuses.

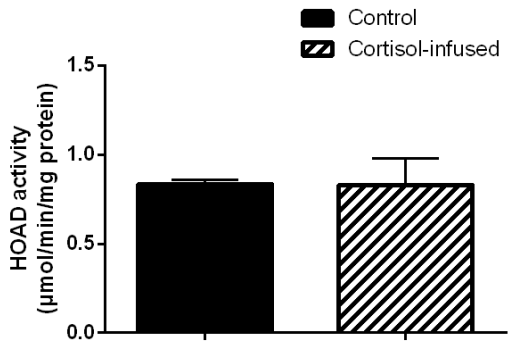

Figure 5.4 Mean±SEM β-hydroxyacyl-CoA dehydrogenase (HOAD) activity in biceps femoris muscle of control (n=6; black bars) and cortisol-infused (n=5; dashed bars) fetuses.

5.4.3 Regulating oxidative capacity

5.4.3.1 Mitochondrial density and biogenesis

In order to determine whether any changes in oxidative function reflected changes in mitochondrial density, the putative marker of mitochondrial mass, CS activity, was measured in all muscles of both treatment groups. In addition, gene expression of markers of mitochondrial biogenesis, PGC1α and NRF1, was quantified. Cortisol infusion did not alter mitochondrial density, *PGC1α* or *NRF1* in BF and ST (Figure 5.5 A,B,D,E). There was a trend for higher mitochondrial density in the SDF of cortisol infused than control fetuses (Figure 5.5 C). Gene expression of PGC1α, but not NRF1, in the SDF was significantly higher in cortisol-infused than control groups (Figure 5.5 F).

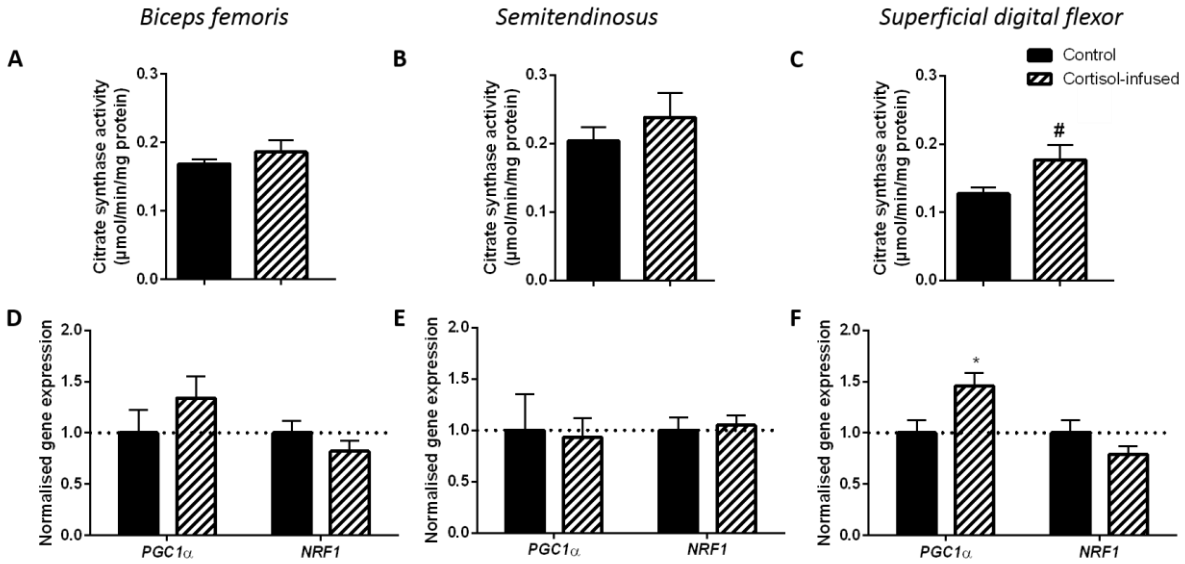

*Figure 5.5 Mean±SEM A-C) citrate synthase activity and D-F) normalised gene expression of PGC1α and NRF1 in A&D) biceps femoris, B&E) semitendinosus and C&F) superficial digital flexor of control (n=4-6; black bars) and cortisol-infused (n=5-6; dashed bars) fetuses. * significantly different to control (P<0.05 by t-test) and # trend to differ from control (P<0.1 by t-test).*

The measured protein and water content of the muscles were used to express CS activity per mg dry weight in order to normalise respirometry data to mitochondrial density. When normalised, there remained a trend for higher Py-supported oxygen consumption, but not PC-supported and total (glutamate and succinate) ADP-coupled oxygen consumption in the BF of cortisol-infused than control fetuses (Figure 5.6 A). Cortisol infusion had no effect on the normalised rates of Py and PC-supported and total (glutamate and succinate) ADP-coupled oxygen consumption in the ST and SDF (Figure 5.6 B&C).

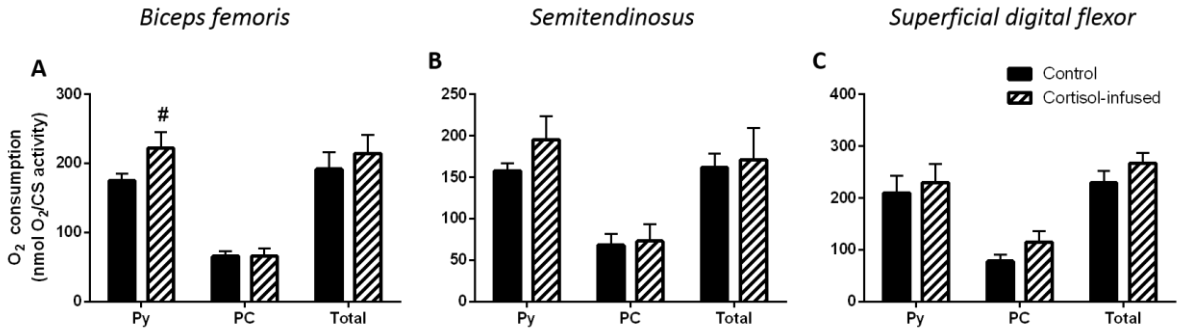

Figure 5.6 Mean±SEM ADP-coupled, pyruvate (Py), palmitoylcarnitine (PC)-supported and total (glutamate and succinate) oxygen consumption normalised to citrate synthase (CS) activity in A) biceps femoris, B) semitendinosus and C) superficial digital flexor of control (n=5-6; black bars) and cortisol-infused (n=4-6; dashed bars) fetuses. # trend to differ from control values of the same experimental protocol (P<0.1 by t-test).

5.4.3.2 Electron transfer system abundance

To further investigate the mitochondrial oxidative capacity, the abundance of the ETS complexes I-IV and ATP-synthase were measured by western blot. The abundance of CI was significantly higher in BF of cortisol-infused fetuses compared with controls, whereas none of the other complexes differed with treatment (Figure 5.7 A&D). Additionally, no differences of the abundance of any of the ETS complexes were seen between treatment groups in the ST or SDF (Figure 5.7 B,C,E&F).

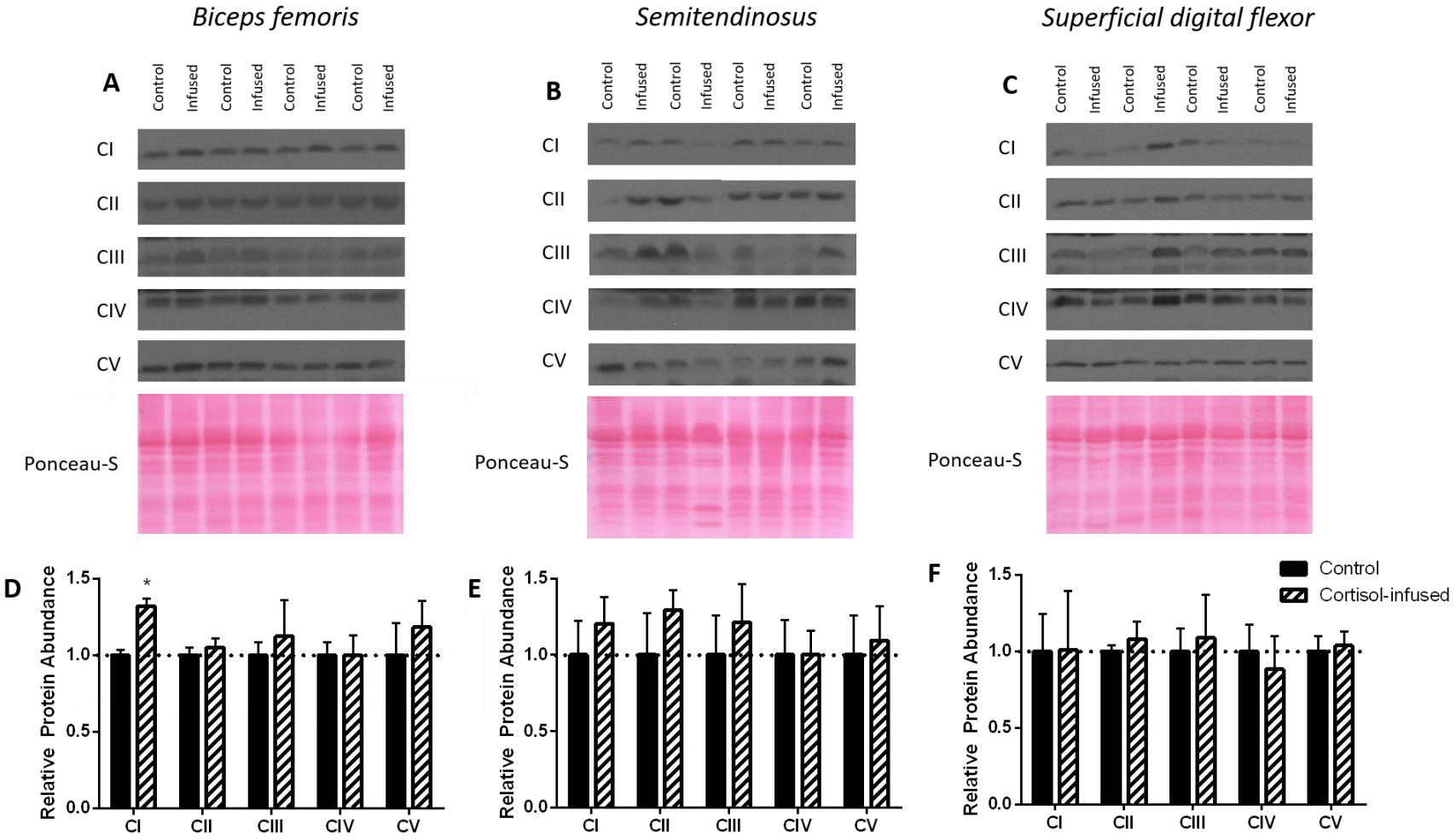

*Figure 5.7 Protein expression of electron transfer system complexes I-IV (CI-IV) and ATP-synthase (CV) by western blotting. A-C) representative blots and D-F) mean±SEM relative abundance of the complexes in A&D) biceps femoris, B&E) semitendinosus and C&F) superficial digital flexor of control (n=5-6; black bars) and cortisol-infused (n=5-6; dashed bars) fetuses. * significantly different to control (P<0.05 by t-test).*

5.4.3.3 Uncoupling the proton gradient

Despite the minimal change in mitochondrial density, cortisol may influence the efficiency of ATP production by regulating expression of IMM proteins associated with proton leak. *UCP2* and *UCP3* expression was not significantly different between control and cortisol-infused fetuses in any of the 3 muscles studied (Figure 5.8). Cortisol-infusion resulted in a significantly higher ANT1 gene expression in the ST and SDF and ANT1 protein abundance in the SDF than found in the saline infused fetuses (Figure 5.9).

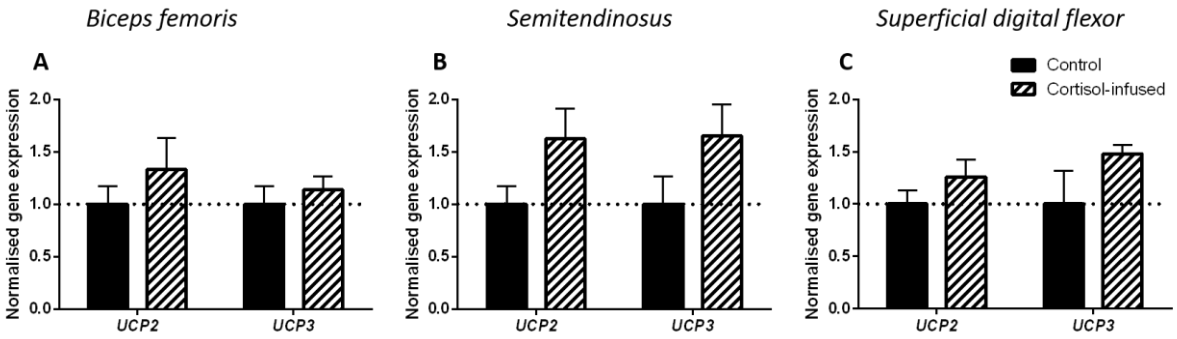

Figure 5.8 Mean±SEM normalised gene expression of uncoupling proteins (UCP) 2 and 3 in A) biceps femoris, B) semitendinosus and C) superficial digital flexor of control (n=4-6; black bars) and cortisol-infused (n=6; dashed bars) fetuses.

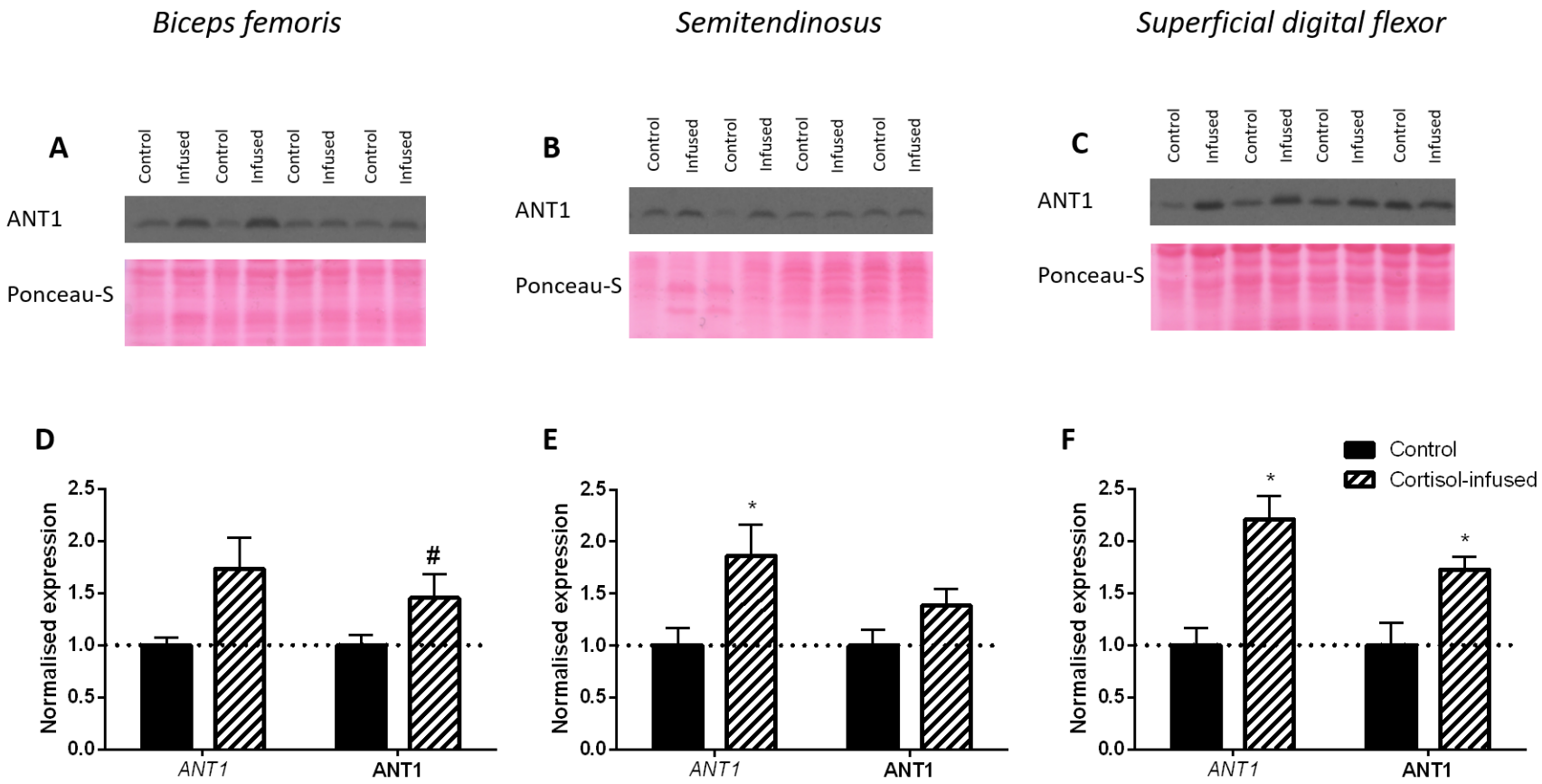

*Figure 5.9 Protein and mRNA levels of adenine nucleotide translocase 1 (ANT1) A-C) representative western blots and D-F) mean±SEM normalised gene expression and protein abundance in A&D) biceps femoris, B&E) semitendinosus and C&F) superficial digital flexor of control (n=5-6; black bars) and cortisol-infused (n=5-6; dashed bars) fetuses. * significantly different to control (P<0.05 by t-test) and # trend to differ from control values (P<0.1 by t-test).*

5.4.3.4 Mitochondrial fusion and fission

In addition to mitochondrial number, mitochondrial function is believed to be influenced by the level of fusion and fragmentation of the mitochondrial network. Thus, gene expression of MFN1, MFN2 and DRP1 were quantified. There was no difference in expression of any of these genes in BF (Figure 5.10 A). There was a trend for greater *MFN2* expression in the ST (Figure 5.10 B) and significantly higher *MFN2* expression in the SDF of cortisol-infused than control fetuses (Figure 5.10 C). Cortisol did not influence gene expression of either MFN1 or DRP1 in the 3 muscles studied.

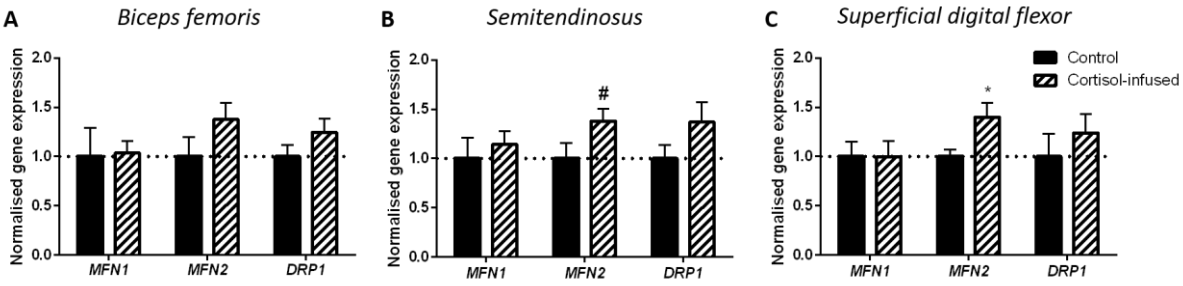

*Figure 5.10 Mean±SEM normalised gene expression of mitofusins (MFN) 1 and 2 and dynamin-related protein 1 (DRP1) in A) biceps femoris, B) semitendinosus and C) superficial digital flexor of control (n=4-6; black bars) and cortisol-infused (n=6; dashed bars) fetuses. * significantly different to control (P<0.05 by t-test) and # trend to differ from control values (P<0.1 by t-test).*

5.4.3.5 Monitoring cellular energy status

In order to determine whether the increased mitochondrial oxidative capacity in the BF and SDF were driven by changes in the AMPK signalling pathway, the protein abundance of both AMPKα and pAMPKα were measured using western blotting. There were no significant differences in these protein abundances or their ratio between the cortisol-infused and control fetuses in either muscle (Figure 5.11).

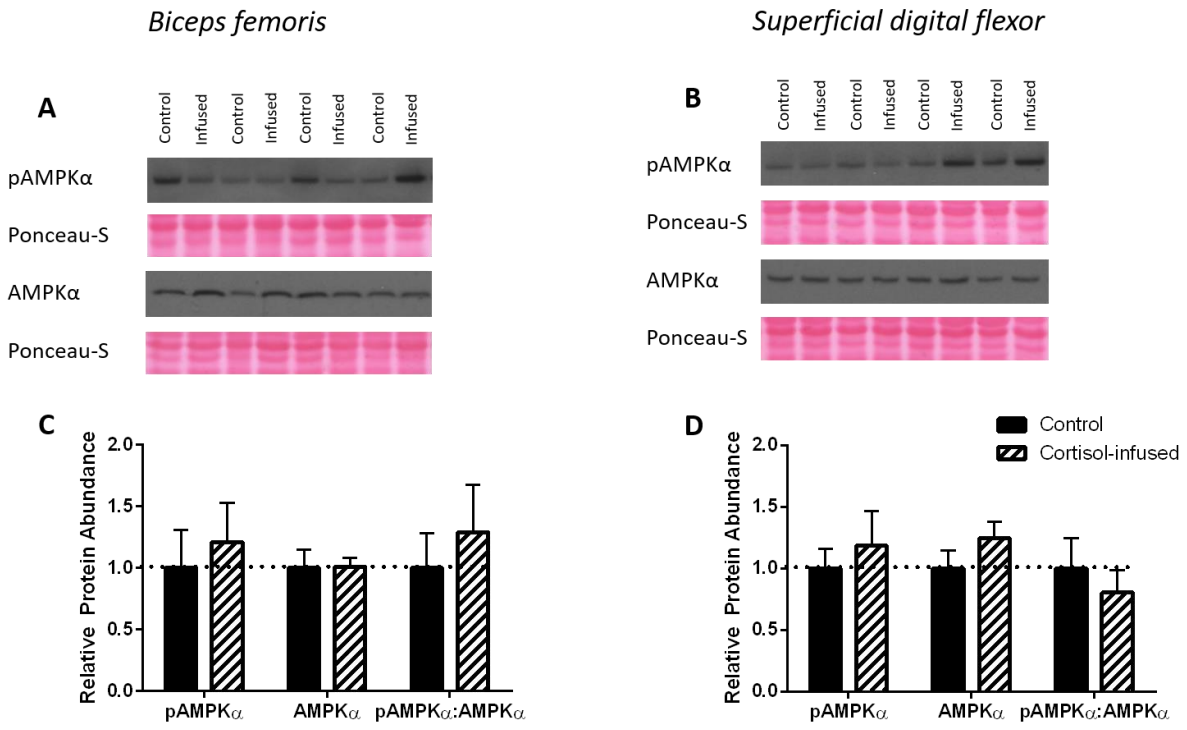

Figure 5.11 Protein expression of (phosphorylated) AMP-activated protein kinase α ((p)AMPKα) by western blotting. A-B) representative blots and C&D) mean±SEM relative abundance of the pAMPKα, AMPKα and the ratio between the two in A&C) biceps femoris, B&D) superficial digital flexor of control (n=6; black bars) and cortisol-infused (n=6; dashed bars) fetuses.

5.4.4 Skeletal muscle structure and type I fibres

Mitochondrial density may reflect the relative proportions of muscle fibre types and thus the muscle fibre density and phenotype were analysed. Sections of the 3 skeletal muscles were stained using H&E and point counting was used to determine the proportion of the field of view occupied by muscle fibres (Figure 5.12). There was a trend for higher fibre density in the SDF from the cortisol-infused fetuses compared with the controls but no differences were seen between treatment groups in the other 2 muscles (Table 5.4).

Immunohistochemistry was used to stain type I fibres (Figure 5.13). Cortisol did not affect the type I fibre number, perimeter, cross-sectional area or percentage of the total area in any of the muscles studied (Table 5.4). Gene expression of MHCI, IIa and IIx was also quantified. Gene expression of MHCIIx was higher in the BF of cortisol than saline-infused fetuses with no difference in *MHCI* or *MHCIIa* (Figure 5.14 A). There was also no difference between treatments in the expression of *MHCI*, *MHCIIa* or *MHCIIx* in the ST and SDF (Figure 5.14 B&C).

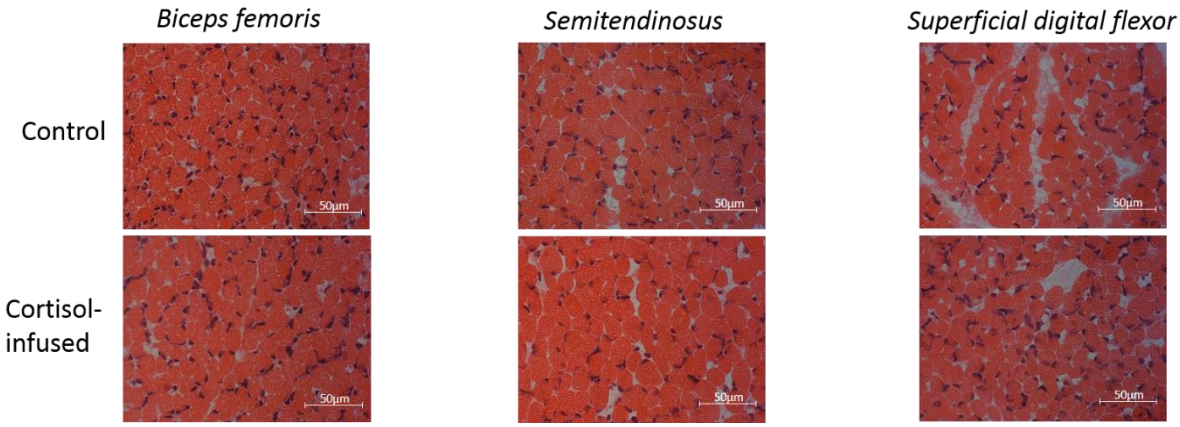

Figure 5.12 Representative H&E stained sections at 40x magnification in biceps femoris, semitendinosus and superficial digital flexor of control and cortisol-infused fetuses, as labelled.

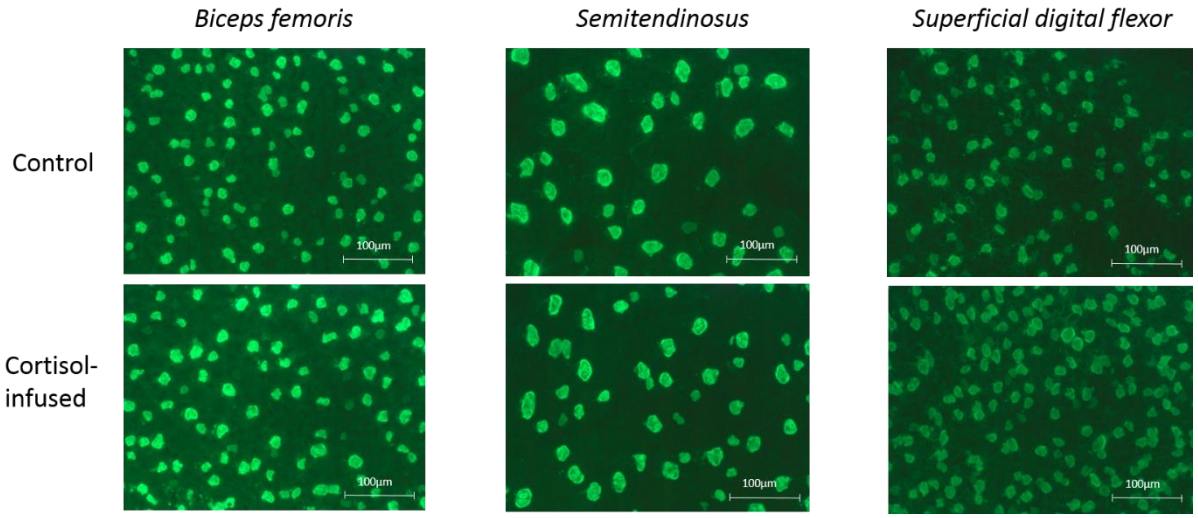

Figure 5.13 Representative MHCI stained sections at 20x magnification in biceps femoris, semitendinosus and superficial digital flexor of control and cortisol-infused fetuses, as labelled.

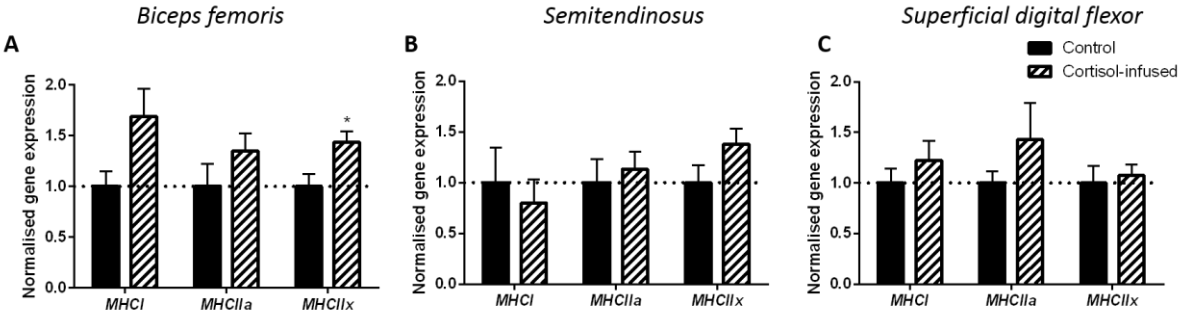

*Figure 5.14 Mean±SEM gene expression of MHCI, MHCIIa and MHCIIx in A) biceps femoris, B) semitendinosus and C) superficial digital flexor of control (n=5; black bars) and cortisol-infused (n=6; dashed bars) fetuses. * significantly different from control (P<0.05 by Mann Whitney test).*

Table 5.4 Type I fibre analyses.

	Control	**Cortisol-infused**
	Biceps femoris	
Proportion of total area accounted for by fibres (%; n=6)	78.2±4.3	86.4±1.9
Number of type I fibres/mm^2	452±89	478±71
Average fibre area (µm^2)	373.3±50.3	378.7±27.8
Average fibre perimeter (µm)	72.8±5.0	73.8±2.5
Proportion of total area accounted for by type I fibres (%)	15.5±2.0	17.4±1.6
Proportion of fibre area accounted for by type I fibres (%)	19.8±1.2	20.2±1.7
	Semitendinosus	
Proportion of total area accounted for by fibres (%; n=6)	82.1±4.0	87.8±1.7
Number of type I fibres/mm^2	346±45	282±78
Average fibre area (µm^2)	443.9±41.9	482.5±37.2
Average fibre perimeter (µm)	79.7±3.9	82.9±3.3
Proportion of total area accounted for by type I fibres (%)	15.1±1.7	13.6±3.6
Proportion of fibre area accounted for by type I fibres (%)	17.4±2.2	15.5±4.1
	Superficial digital flexor	
Proportion of total area accounted for by fibres (%; n=6)	74.5±2.6	81.4±2.6 #
Number of type I fibres/mm^2	511±16	643±97
Average fibre area (µm^2)	324.9±24.5	337.6±15.6
Average fibre perimeter (µm)	68.8±2.8	71.3±1.3
Proportion of total area accounted for by type I fibres (%)	16.1±1.1	21.3±2.8
Proportion of fibre area accounted for by type I fibres (%)	20.9±2.0	27.2±4.3

Data are presented as mean±SEM in biceps femoris, semitendinosus and superficial digital flexor of control and cortisol-infused fetuses. N=4 in each group, unless stated otherwise. # trend to differ from control values (P<0.1 by t-test).

5.5 Discussion

This study shows that cortisol regulates some aspects of mitochondrial function in a muscle specific manner during late gestation. Elevating the fetal circulating cortisol prematurely to term concentrations resulted in an increase in the oxidative function of the SDF, presumably driven by the increase in its mitochondrial density. In addition, there was an increased expression of ANT1 and *MFN2* in the SDF which may aid the increase in oxidative production of ATP through regulating its transport and the dynamics of the mitochondrial network respectively.

5.5.1 Fetal growth and muscle development

The 5-day cortisol infusion protocol resulted in cortisol levels being significantly higher than controls at each day of the protocol, and brought cortisol levels up to those reported previously in near term singleton ovine fetuses (Mostyn et al., 2003) and to the values found in the control 143dGA group of twin fetuses in Chapter 3. Cortisol infusion also raised the T_3 concentration without affecting T_4 levels as has been reported previously (Mostyn et al., 2003). Fetal blood glucose levels were higher in the cortisol-infused fetuses than controls as has been shown in some but not all previous studies of sheep (Fowden et al., 1996, Ward et al., 2004). Using the same infusion protocol as in the current study, cortisol has been shown to slow the rate of fetal growth measured individually as CRL increment (Fowden et al., 1996). However, in the current study, there were no differences in CRL or body weight between the treatment groups. This probably reflects analysis of a cohort rather than of individuals.

The mass of the 3 muscles studied also did not show any difference in response to early cortisol exposure and nor did the muscle protein or lipid content. Previous studies in fetal sheep during late gestation have reported a cortisol-driven decrease in protein accretion primarily due to increased proteolysis, however tissue-specific protein metabolism was not investigated (Milley, 1995). The ST glycogen content showed a trend to increase in response to cortisol infusion, whereas the glycogen content of the BF and SDF was unaffected by treatment. Cortisol is believed to play a role in skeletal muscle glycogen deposition over late gestation, and cortisol infusion into fetal pigs resulted in an increased glycogen levels in the psoas muscle (Fowden et al., 1985, Fowden et al., 1991). However, previous studies on fetal sheep have shown cortisol infusion to have no effect on skeletal muscle glycogen content suggesting there may be a species-specific response (Forhead et al., 2009, Barnes et al., 1978).

Water content of the BF and ST was significantly lower in the cortisol-infused than control fetuses. Cortisol, therefore, appears to have a maturational influence on the skeletal muscle structure. However, it had a minimal effect on the fibre density and proportion of type I fibres. Overall, prematurely elevating cortisol in the fetus had minimal impact on fetal growth and muscle structure, and alone is unlikely to explain the change in muscle structure observed in Chapter 3.

5.5.2 Cortisol had a muscle-specific effect on skeletal muscle mitochondria

As shown in Chapter 3, age had a significant effect on, and cortisol significantly correlated with, the mitochondrial oxidative capacity, as well as mitochondrial density and expression of several mitochondrial proteins in BF, ST and SDF during late gestation and the perinatal periods. This chapter shows that cortisol increased the oxidative capacity of the SDF in accordance with its increased mitochondrial density and expression of ANT1 and *MFN2*. These findings are consistent with previous observations of increased oxygen consumption in neonatal sheep exposed to maternally administered dexamethasone during fetal development (Clarke et al., 1998). Very few studies have looked at the SDF and therefore little is known about its developmental or its metabolic profile. However, the function of the SDF is known and, unlike the hamstring muscles, the SDF generates a high level of force through isometric contraction as it controls the positioning of the lower limb during both standing and locomotion (Biewener, 1998, McGuigan et al., 2009). The continuous use of this muscle necessitates a high oxidative capacity, and in the current study, the proportion of oxidative type I fibre area has been shown to be greater in the SDF than then ST. Perhaps the response to cortisol needs to be more rapid to ensure maturity of the postural muscles required to allow the lamb to stand after birth.

The differential effects of cortisol on the different muscles may also reflect variations in muscle GR expression. The GR abundance of the muscles studied here has not been quantified. In adult muscle, GR abundance is higher in type I than type II fibres (Perez et al., 2013). Therefore, GR abundance may be greater in the more oxidative fetal muscles including the SDF earlier in gestation than in the other muscles, explaining the more rapid response of the SDF to the cortisol infusion. Alternatively, the SDF maturation may rely predominantly on cortisol for its metabolic maturation whereas other factors may be of greater importance in the other muscles, for example THs. Postnatally, muscles with a lower content of type I fibres

have been shown to be more responsive to THs (White et al., 2001). Therefore, the SDF may be less dependent on T_3 for mitochondrial maturation than muscles with a higher proportion of fast-twitch muscle fibres.

The oxygen consumption using all 3 respirometry protocols was higher in the cortisol-treated than control SDF, although this only reached significance for PC-supported and total oxygen consumption. This suggests that cortisol may generally increase the activity of the mitochondrial oxidative pathways and play a role in upregulating FA-oxidation in this muscle. Previously, mitochondria from slow-twitch fibres have been shown to possess a higher capacity for FA oxidation (Glancy and Balaban, 2011), and the current results suggest this may be regulated by cortisol *in utero*. HOAD activity was only measured in the BF where PC-supported oxygen consumption was not upregulated by cortisol. Measuring HOAD activity in the SDF would help to determine whether β-oxidation is upregulated by cortisol in the SDF. The abundance of ETS complexes I-IV was not different in the SDF of cortisol infused compared with control fetuses which suggests that the cortisol-induced increase in oxidative capacity is not due to changes in complex abundance although there may be cortisol-dependent mechanisms by which ETS activity is enhanced. In contrast to the SDF, only Py-supported oxygen consumption was increased with cortisol treatment in the BF, as was the expression of CI, suggesting carbohydrate metabolism may be of greater importance in the BF postnatally. However, this increase in oxygen consumption was not associated with an increase in mitochondrial density as occurred in the SDF. This suggests that cortisol acts through a different mechanism in regulating mitochondrial oxidative capacity in the 2 muscles.

Overall, cortisol regulates some aspects of mitochondrial function in the SDF and BF, but cannot fully explain the ontogenic rise in skeletal muscle mitochondrial respiratory capacity, particularly in the ST. Potential explanations are discussed below.

5.5.3 Cortisol does not drive mitochondrial development in late gestation in all muscles

Few previous studies have looked at the effects of GCs on mitochondria, but those which have suggest GCs upregulate mitochondrial activity in skeletal muscle (Weber et al., 2002). However, in this previous study the synthetic GC, dexamethasone was used, which is more potent than natural GCs and can bind to mineralocorticoid receptors as well as GRs (Jellyman et al., 2012). Importantly, dexamethasone and cortisol are known to have differential effects

on the insulin signalling pathway in developing sheep skeletal muscle (Jellyman et al., 2012). Therefore, whether GCs play a metabolic role *in vivo* cannot be assumed from dexamethasone studies. Additionally, the previous study was carried out on adult rat quadriceps and soleus muscles, and the sheep fetal muscles in the current study may not necessarily respond in the same way. A model of developing muscle has been studied, in which mitochondria from a developing mouse muscle cell line were shown to respond to dexamethasone (Weber et al., 2002). However, conclusions drawn from *in vivo* and *in vitro* results across different species are variable. GC treatment on a human hepatic cell line and adult rat liver suggest that GCs are likely to act directly on the mitochondria to increase transcription, however, no increase in mitochondrial protein abundance or activity was reported in a separate study on adult rat liver *in vivo* (Weber et al., 2002, Scheller et al., 2000, Mansour and Nass, 1970). In addition to species differences, tissue differences are apparent in the mitochondrial response to cortisol in the fetus; in the current study there was no difference in *UCP* expression in the skeletal muscle, whereas *UCP2* increased in the perirenal adipose tissue of fetal sheep using the same cortisol infusion protocol (Gnanalingham et al., 2005b). These tissue specific effects of cortisol on the mitochondria may explain why cortisol infusion has little effect on the total fetal oxygen consumption by the sheep (Ward et al., 2004) and emphasise that further work is needed to fully understand the role of GCs on fetal oxidative metabolism.

The response to cortisol is primarily via regulating gene expression. However, cortisol is also known to influence post-transcriptional processes and translation (Newton, 2000). Therefore, the fact that cortisol has been shown to have limited effect on the mRNA abundance of the genes of interest studied here does not rule out the possibility of it playing a regulatory role on these pathways, although any cortisol-driven activation or inhibition of downstream pathways did not manifest in a measurable change in oxygen consumption in the BF or ST. An example of a GC-target protein is the GR itself, the transcription of which is reduced and the rate of degradation increased upon dexamethasone treatment in rat adult liver (Dong et al., 1988). Cortisol-driven downregulation of the GR may be in part responsible for repressing the HPA negative feedback in the lead up to term in the sheep fetus (Challis et al., 2001). However, in the fetal perirenal adipose tissue, cortisol infusion has been shown to upregulate expression of the GR, perhaps to amplify the maturational effects of cortisol near term (Gnanalingham et al., 2005b). Whether cortisol regulates expression of its receptor in fetal skeletal muscle has not been reported. Through potentially altering the abundance of functional GR protein,

cortisol infusion may be minimising the effect of premature GC-signalling when other factors, normally altered near term, are not present.

The lack of effect of cortisol in muscles such as ST may be due to insufficient time to activate the downstream pathways as cortisol levels normally rise over 10-15 days before term in the sheep (Silver and Fowden, 1988). This may affect both the direct and indirect actions of cortisol in stimulating tissue maturation. As well as increasing the bioavailability of T_3, cortisol regulates numerous other endocrine systems in the lead up to term. These include increasing the circulating catecholamine concentrations and decreasing skeletal muscle IGF-I expression (Fowden et al., 1998). Additionally, there is altered hormone signalling, for example cortisol has been shown to increase the abundance of the leptin-receptor in the fetal lung and β-adrenenoreceptors in the fetal liver (De Blasio et al., 2015, Apatu et al., 1990). Cortisol may play a role in regulating mitochondrial function but 5 days of cortisol infusion alone may be insufficient to induce mitochondrial maturation without the other changes which occur alongside the cortisol surge near term.

5.5.4 Conclusion

Overall, this study shows that cortisol can upregulate specific aspects of mitochondrial function and density in a muscle-specific manner. This variable responsiveness of muscles to cortisol may reflect the density of type I fibres, the sensitivity to cortisol *per se* or the independency on direct versus indirect maturational actions of cortisol.

6 General Discussion

6.1 Overall summary

The results of this thesis support the initial hypothesis that the oxidative capacity of skeletal muscle would increase during the perinatal period to meet the extra energy demands of the new muscular activities required after birth. In the 3 ovine hind limb muscles studied, the BF, ST and SDF, the oxidative function was higher in the neonate than earlier in gestation. This occurred in association with an ontogenic increase in mitochondrial density, abundance of ETS complexes and expression of ANT1 and UCPs in these muscles over the perinatal period. The later changes in ANT1 and UCPs would also help minimise excessive ROS production during the fluctuations in oxygen availability associated with labour, delivery and exposure to atmospheric oxygen levels for the first time.

In Chapter 3, skeletal muscle mitochondrial oxidative capacity and density from control fetuses were correlated positively with the plasma concentrations of both cortisol and T_3 during the perinatal period. When fetal hypothyroidism was induced by thyroidectomy, mitochondrial density was reduced both at 127dGA and near term in all 3 hind limb muscles studied, and respiratory capacity was also lowered particularly near term. In addition, thyroidectomy prevented the normal ontogenic increase in several mitochondrial parameters towards term, including mitochondrial density, ETS complex abundance and ANT1 expression. However, raising the T_3 concentration prematurely before term did not affect mitochondrial function in any of the muscles. In contrast, elevation of fetal cortisol concentration to term values earlier in gestation did affect some aspects of muscle mitochondrial function, albeit in a tissue specific manner. The BF and SDF of cortisol infused fetuses showed an increased capacity for oxidative metabolism of carbohydrates and FAs respectively, whereas the ST was unaffected by treatment consistent with its lower density of oxidative type I fibres. When data from all groups across the 3 chapters were combined, irrespective of age and treatment, both the concentrations of cortisol and T_3 retained a significant positive correlation with oxygen consumption and with CS activity in all 3 muscles and with HOAD activity, measured only in the BF (Table 6.1). CS activity correlations are presented in Figure 6.1, and partial correlation analyses of these data suggest that both cortisol and T_3 are important in regulating activity in all 3 muscles studied. In support of the initial hypothesis, the results collectively suggest that both maturational hormones are important regulators of mitochondrial development and

function in ovine skeletal muscle during the perinatal period, consistent with their known roles as maturational signals in the preparation for the transition from intra- to extrauterine life in other fetal tissues (Fowden et al., 1998).

Table 6.1 Correlation analyses of cortisol and T_3 with respirometry data and HOAD activity.

	Biceps femoris	**Semitendinosus**	**Superficial digital flexor**
	Pyruvate-supported state III respiration		
Log_{10}Cortisol (ng/ml)	r=0.6158 *P*<0.0001	r=0.4122 *P*<0.01	r=0.5244 *P*<0.0001
Log_{10} T_3 (ng/ml)	r=0.7171 *P*<0.0001	r=0.6232 *P*<0.0001	r=0.7269 *P*<0.0001
	Palmitoylcarnitine state III respiration		
Log_{10}Cortisol (ng/ml)	r=0.3325 *P*<0.05	r=0.3640 *P*<0.05	r=0.5401 *P*<0.0001
Log_{10} T_3 (ng/ml)	r=0.5043 *P*<0.001	r=0.5715 *P*<0.0001	r=0.6436 *P*<0.0001
	Glutamate and succinate state III respiration		
Log_{10}Cortisol (ng/ml)	r=0.4311 *P*<0.01	r=0.3972 *P*<0.01	r=0.6397 *P*<0.0001
Log_{10} T_3 (ng/ml)	r=0.5439 *P*<0.0001	r=0.6290 *P*<0.0001	r=0.6931 *P*<0.0001
	HOAD activity		
Log_{10}Cortisol (ng/ml)	r=0.6237 *P*<0.0001	/	/
Log_{10} T_3 (ng/ml)	r=0.7652 *P*<0.0001	/	/

N=47-55. β-hydroxyacylCoA dehydrogenase (HOAD) activity was not measured in semitendinosus and superficial digital flexor (/).

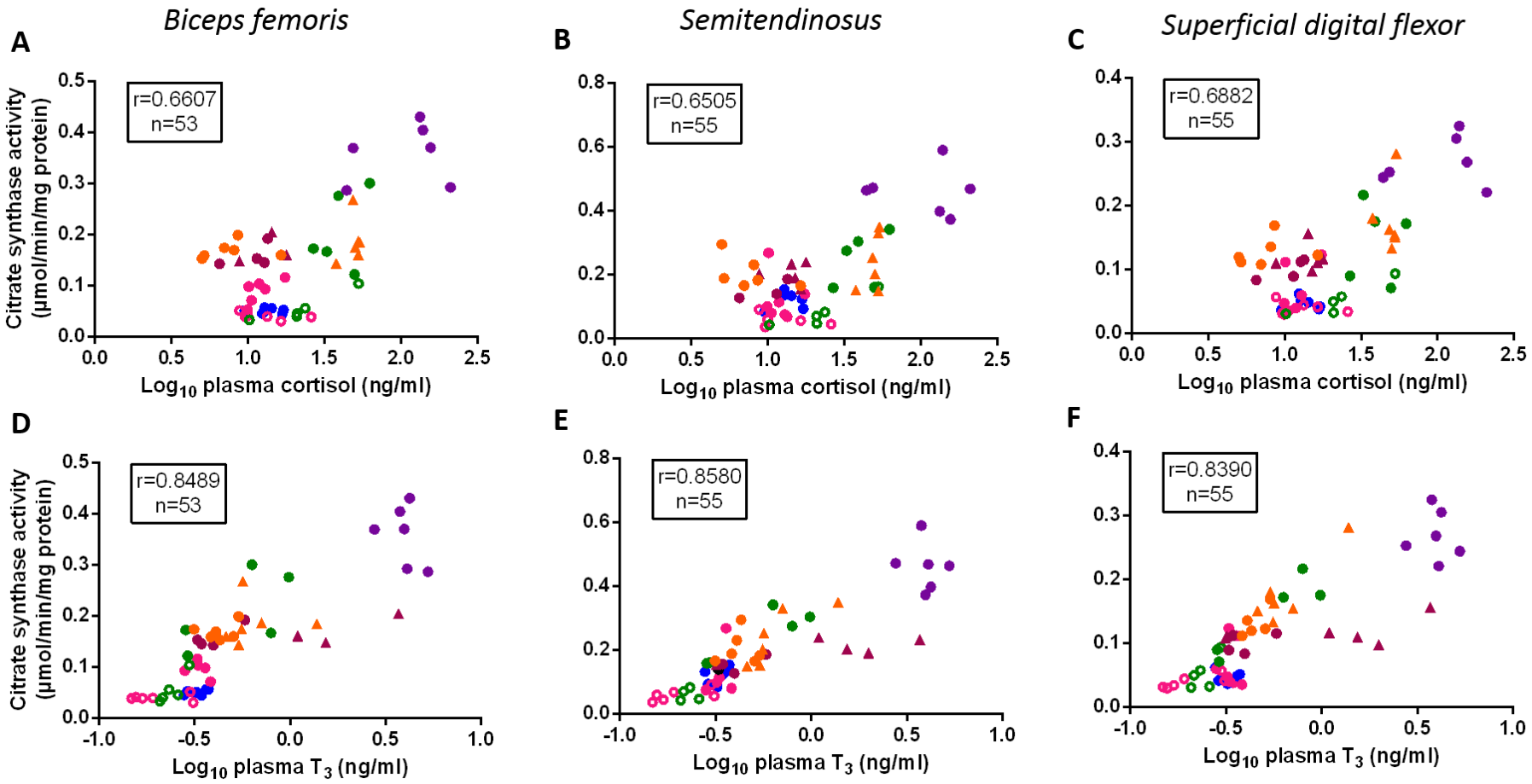

Figure 6.1 Citrate synthase activity plotted against plasma A-C) cortisol and D-F) T_3 in A&D) biceps femoris, B&E) semitendinosus and C&F) superficial digital flexor. N numbers and r values are given on each graph. 104dGA blue, 127dGA pink (sham, full circle; TX, empty circle), 143dGA green (sham, full circle; TX, empty circle), 130dGA catheterised twins maroon (saline-infused, circles; T_3-infused, triangles), 130dGA catheterised singletons (saline-infused, circles; cortisol-infused, triangles) and newborn lambs purple.

6.2 Limitations of the study

Most studies and analytical techniques have their limitations and the data presented in this thesis is no exception. The respirometry protocol used in this study follows a well-established methodology, previously published for skeletal muscle (Pesta and Gnaiger, 2012, Kuznetsov et al., 2008). Using permeabilised muscle fibres allows for mitochondrial function to be measured while the cellular system is kept intact, maintaining mitochondrial interactions with the cytoskeleton and endoplasmic reticulum. This approach also permits ATP consumers to remain present in the system which allows coupling of ATP consumption with production and, hence, an assessment of total oxidative function most closely resembling that *in vivo* (Kuznetsov et al., 2008). However, the physiological relevance of the high pO_2, and saturating concentrations of substrates used in this protocol for fetal metabolism is perhaps more debateable. This protocol will give the maximal rates of oxygen consumption of the tissues (Pesta and Gnaiger, 2012) and the data obtained therefore gives information on any changes in maximal oxidative capacity over the perinatal period.

With permeabilisation, the substrates used in the respirometry protocols can be directly transported into the mitochondria and feed into the TCA cycle or β-oxidation. Therefore, only the internal mitochondrial oxidative pathways could be studied with no allowance for changes in cytosolic pathways or cellular transport mechanisms which may influence the availability of substrates in intact fibres (Jorgensen et al., 2017). In particular, the rate of glycolysis may have an important role in determining the substrate availability for mitochondrial oxphos. Indeed, there may be a greater reliance on anaerobic glycolysis for ATP production in the fetal muscle towards term as there was minimal upregulation of oxidative function of the muscle despite the increase in mitochondrial density in the current study.

Throughout this study, CS activity was used as a marker of mitochondrial density, as has shown to be a good marker in adult human skeletal muscle (Larsen et al., 2012). However, this may not be the case in the fetus. Citrate synthase catalyses the first step in the TCA cycle, and therefore activity may rise over the perinatal period in accordance with our hypothesis of increasing the activity of mitochondrial metabolic pathways (Marin-Garcia et al., 2000). A limitation of this study, therefore, is that there is not an additional marker of mitochondrial density to confirm the assumption that CS activity correlates with density in developing ovine skeletal muscle.

Within a muscle there are regional differences in mitochondrial parameters; deeper regions have been associated with a more oxidative phenotype and a higher CS activity in the pig semitendinosus and rat quadriceps respectively (Markham et al., 2009, Kohn and Myburgh, 2007). Additionally, there are differences in the MHC expression along the length of the rat quadriceps; in the deeper region of the muscle there was a lower MHCI content at the distal than at the proximal end (Kohn and Myburgh, 2007). Throughout the study, care was taken to study a central region of muscle for the respirometry and histology, and where possible for assays on the remaining frozen muscle. In addition to variation across the muscle, there are intracellular differences in the mitochondria within the myocytes with 2 functionally distinct subpopulations, subsarcolemmal (SS) and intermyofibrillar (IMF) responsible for sustaining activity of membrane transporters and contractile machinery respectively (Kuznetsov et al., 2006, Lundby and Jacobs, 2016). In adult muscle, the SS mitochondria are the smaller population but have a higher oxidative state, calcium content and capacity for FA oxidation (Kuznetsov et al., 2006, Hoppeler, 1999). Both populations show plasticity, for example, the density of both increase in response to exercise with a greater fold-increase reported in SS mitochondria (Hoppeler et al., 1985, Samjoo et al., 2013, Lundby and Jacobs, 2016). Thus, changes in the relative size of the 2 populations may have contributed to ontogenic and hormonally induced changes in mitochondrial function observed in the fetal skeletal muscles, although respirometry of permeabilised fibres does not allow the subpopulations to be studied separately (Kuznetsov et al., 2008). Fractionation of the subpopulations of muscle mitochondria would be required to address this but study of isolated mitochondria provides little information about their physiological function *in vivo*.

A further limitation of this study is the small sample sizes which can ethically be considered when using larger animal species, such as the sheep, for experimental research. This can influence the conclusions drawn; in particular a non-significant result may reach significance if the sample size were greater. Power calculations (such as in Equation 6.1) can be applied to data in order to give the sample size which would be required in order to reject the null hypothesis. Using the pyruvate-supported oxygen consumption of cortisol compared to saline-infused fetuses (Figure 5.2) as an example, the value for the cortisol-infused fetuses were higher in all muscles compared with controls. This difference reached significance in the BF, however was not significant in the ST and showed only a trend in the SDF. Power calculations suggest that the difference between the means, at the standard deviation of the

dataset, would be sufficient to reject the null hypothesis if there were 18 samples in each group for the ST and the example power calculation for the ST is given below (Chow et al., 2008).

$$n = (1 + \frac{1}{k})(\sigma \frac{z_{1-\alpha/2} + z_{1-\beta}}{\mu_A - \mu_B})^2$$

Where: k=ratio of sample sizes of the 2 groups (k=1 in our case)

σ=standard deviation

μ=mean

α=type I error=0.05

β=type II error. 1-β=power=0.8

Equation 6.1 Power calculation in order to determine the sample size required to compare 2 means for a 2-tailed t-test.

In the case of Py-supported, ADP-coupled oxygen consumption in the ST:

$$n = 2\left(1.7 \cdot \frac{1.96 + 0.84}{9.91 - 8.30}\right)^2$$

$$n = 18$$

6.3 Future studies

6.3.1 Endocrine regulation of mitochondrial oxidative capacity

Overall, the results suggest that both cortisol and T_3 are involved in the developmental regulation of mitochondrial function in ovine skeletal muscle. However, the relative importance and the individual effects of the two hormones in these regulatory processes is difficult to establish with the current data. Neither cortisol nor T_3 infusion between 125 and 130 days of gestation fully recapitulated the developmental changes in mitochondrial density and expression of key genes and proteins seen towards term, despite the increased T_3 concentrations in the cortisol infused fetuses. In addition, cortisol concentrations have been shown to be lower in TX than control fetuses at term (Harris et al, 2017) similar to the trend seen in the current study. Studying mitochondrial function both in term fetuses adrenalectomised to prevent the normal prepartum rise in cortisol and T_3 and after combined infusion of the two hormones before term may help to identify whether the developmental

effects of these hormones are independent or are primarily dependent on cortisol but effected in part by the cortisol induced rise in T_3. Similar cortisol-dependent, T_3 mediated maturational effects are seen with other processes in fetal ovine tissues such as the liver and lungs (Fowden et al., 2001, Forhead et al., 2000, Forhead and Fowden, 2002).

Preliminary measurements of the expression of GR and THR in some of the muscles may help to understand variabilities observed between treatment and age groups. The mRNA abundance of THRα and THRβ isoforms in the ST over the perinatal period showed no effect of age on the gene expression of THRα (Figure 6.2 A). However, THRβ mRNA levels increased with age (P<0.05 by one-way ANOVA) with the expression in the newborns significantly higher than at 104dGA (Figure 6.2 B). These results are in agreement with a study on skeletal muscle in fetal pigs, in which the THRβ expression increased over late gestation and continued to increase postnatally with expression correlating with plasma cortisol concentration over the perinatal period (White et al., 2001). In the brain, this late upregulation of THRβ has also been reported and was associated with the TH-sensitive period of neuronal maturation (Forrest et al., 1991). Preliminary data from the BF, however, suggests there was no difference between expression of either THR isoform when comparing control and T_3-infused fetuses (Figure 6.3). Similarly, the GR gene expression was measured across the 4 age groups in the SDF and there was no effect of age (Figure 6.2 C). Further investigation of the ontogenic and hormone dependence of the tissue specific abundance of these receptors may help explain the effects of cortisol and T_3 on mitochondrial function in the different muscles.

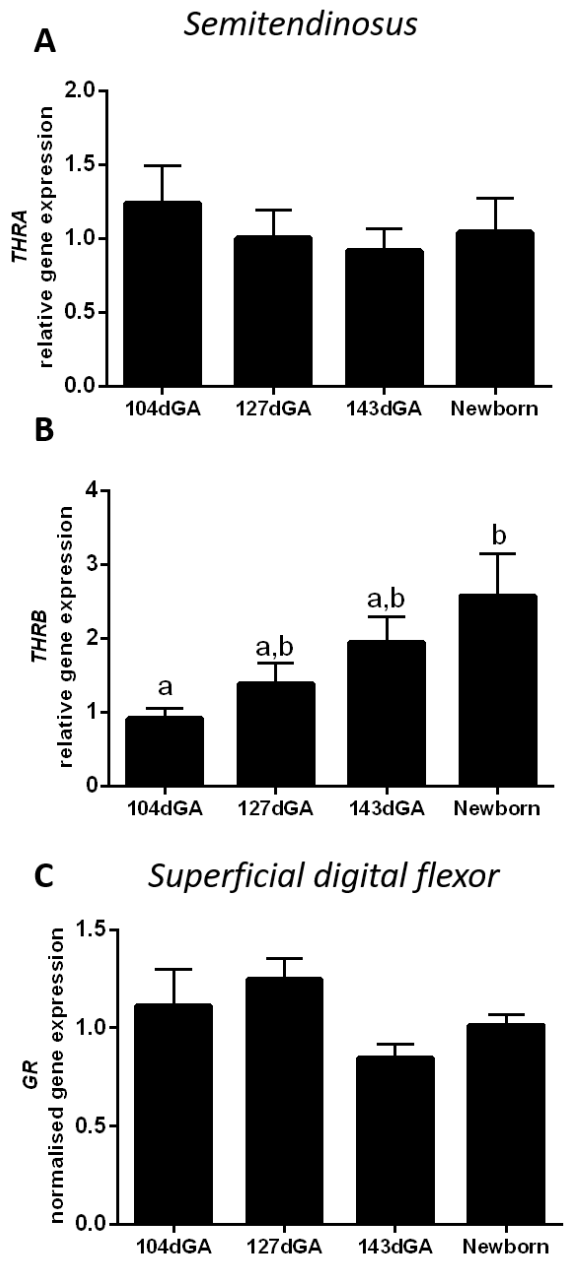

Figure 6.2 Mean±SEM normalised gene expression of A) thyroid hormone receptor α (THRA) B) THRB in the semitendinosus and C) glucocorticoid receptor (GR) of fetuses at 104 (n=5), 127 (n=5-6) and 143 (n=6) days of gestational age (dGA) and newborn lambs (n=6). Different letters are significantly different to each other (P<0.05 by Tukey's post hoc test following one-way ANOVA).

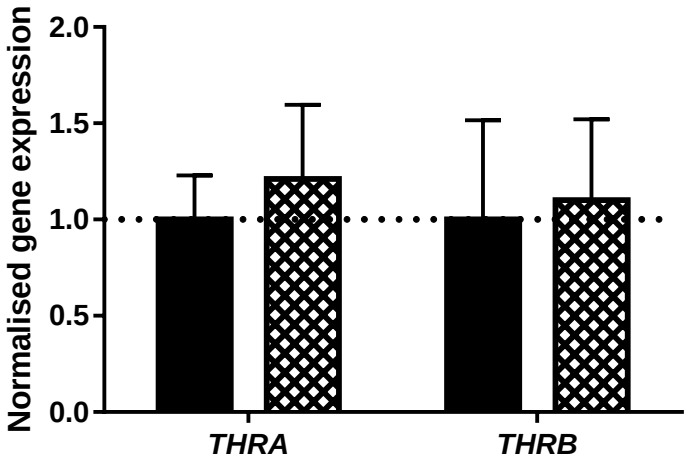

Figure 6.3 Mean±SEM normalised gene expression of thyroid hormone receptor α (THRA) and THRB in biceps femoris, of control (n=3; black bars) and T_3-infused (n=4-5; crosshatched bars) fetuses.

Altered abundance of the GR and THR, alongside plasma hormone binding proteins will affect the levels of hormone available to the skeletal muscle. Determining a method of assessing the bioavailability of the hormones to the tissue, independently of the parameters measured in this study, would be useful for future analyses to understand the extent to which the endocrine manipulation protocols are able to impact on muscle physiology. In adult muscle, cortisol is known to play a role in regulating nutrient availability during stress and thus acts to decrease glucose uptake and induce protein catabolism (Salehzadeh et al., 2009, Tarpenning et al., 2001), and well-characterised transcriptional targets of GCs include monamine oxidase A and apolipoprotein D (Wang et al., 2010). However, age and tissue specific profiles of co-activator and co-repressor expression, required in order to ensure an appropriate cellular response means that whether this is also true in fetal muscle at this particular time in development has not been shown (Rousseau, 1984, Oakley et al., 1996). Thus, this information cannot be directly applied to the current study. Upon hormone binding to the cytosolic GR or THR, the complexes translocate to the nucleus and, following a decreased hormonal signal, the receptors are then exported to the cytosol over a period of hours (Walther et al., 2003). A potential alternative method of monitoring cellular hormonal bioavailability could be to determine the fraction of receptor present in the nucleus compared with the cytosol either by histological or biochemical methods. Therefore, monitoring the fraction of nuclear receptors may be representative of the hormone abundance.

In twins, activation of the HPA axis occurs later in gestation than in singleton sheep fetuses (Gardner et al., 2004, Edwards and McMillen, 2002). Fetal concentrations of cortisol therefore rise later in gestation in twins than singleton fetuses (Edwards and McMillen, 2002). Twins also have a lower birthweight than singletons which is partly explained by the physical space restriction *in utero* and the division of the maternal nutrient supply (Gardner et al., 2007, Brown, 2014). However, there is now evidence that physiological differences between twins and singletons begin early on in gestation and pre-determine the fetal growth resulting in a smaller birthweight for twins (Hancock et al., 2012). The restriction on fetal growth may have implications on skeletal muscle development and in the current study, the body and muscle weights were lower in control twins than singletons at ~130dGA from Chapters 4 and 5. When the maternal nutrient supply is divided between two growing fetuses, the skeletal muscle development may be particularly vulnerable to impaired nutrient supply (Brown, 2014). As well as a suppressed function of the HPA axis which may be due to reported hypothalamic epigenetic modifications, twinning has been associated with a lower basal insulin concentration over late gestation (Begum et al., 2012, Rumball et al., 2008b, Green et al., 2011, Rumball et al., 2008a, Gardner et al., 2004). The different endocrine environment may represent a mechanism by which twin physiology may impact on skeletal muscle growth and development.

In the current study, correlations between the mitochondrial parameters and the concentrations of cortisol and T_3 were more significant when the smaller number of singleton fetuses were excluded which suggests that there are differences in mitochondrial development between singletons and twins (Figure 6.1 and Table 6.2). More detailed analyses of the mitochondrial data from the control singleton and twin animals at ~130dGA in Chapters 4 and 5 indicate that muscle from twins and singletons does differ significantly in certain aspects of mitochondrial function. These differences are present despite similar fetal concentrations of cortisol and T_3 in the two groups at this age (Table 4.1, Table 4.4 and Table 5.1; $P>0.05$). The CS activity was significantly higher in the singletons than the twins in the SDF ($P<0.05$ by *t*-test) and tended to be higher in the BF and ST as well (Figure 6.4 A-C). In addition, the abundance of some of the ETS complexes were different between the singletons and twins (Figure 6.4 D-F). Applying a two-way ANOVA to the protein abundance of the ETS complexes, singletons were significantly different than twins for the BF ($P<0.0001$) and ST ($P<0.05$). Individually, the CI and CIII abundance of the BF was significantly higher in the singletons than

twins (*P*<0.05 by Mann-Whitney test). There was no difference in the oxygen consumption rates, nor protein abundance of ANT1 in the muscles from twins compared with singletons, although ANT1 gene expression was significantly higher in the BF of singletons than twins (*P*<0.05; data not shown). The extent and muscle specific nature of the differences in mitochondrial development between twins and singletons need to be investigated further.

Table 6.2 Hormone correlations with CS activity combining all twin fetal data.

	Biceps Femoris	**Semitendinosus**	**Superficial Digital Flexor**
Log_{10}plasma cortisol (ng/ml)	r=0.7724 n=41	r=0.7652 n=43	r=0.7788 n=43
Log_{10}plasma T_3 (ng/ml)	r=0.8765 N=41	r=8783 n=43	r=0.8718 n=43

r and n numbers are given; P<0.0001 in each case.

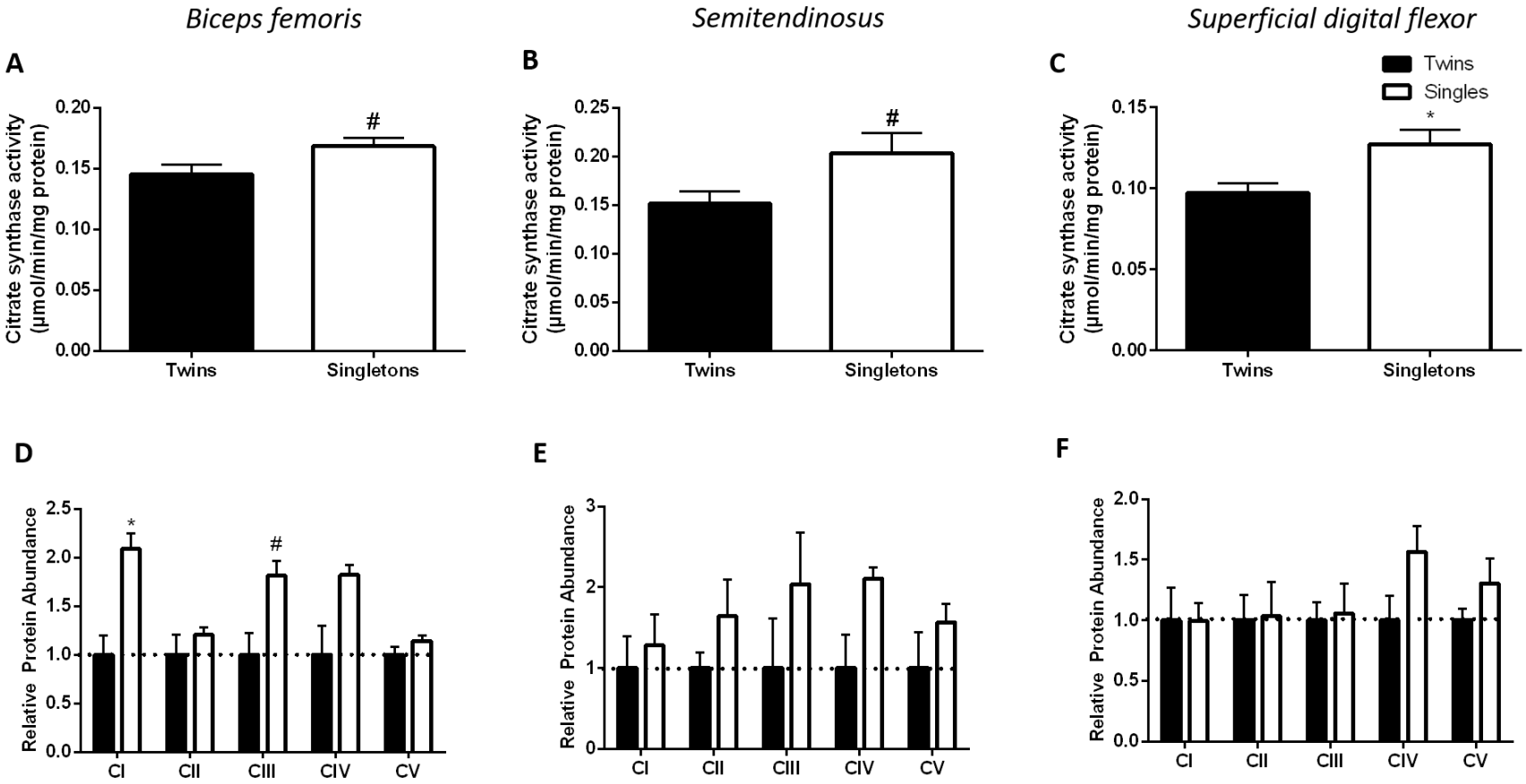

*Figure 6.4 Mean±SEM A-C) citrate synthase activity and D-F) protein expression of electron transfer system complexes I-IV (CI-IV) and ATP-synthase (CV) in A&D) biceps femoris, B&E) semitendinosus and C&F) superficial digital flexor of twins (black bars; n=3-4) and singletons (white bars; n=3-5). * significantly different from twins (P<0.05); # trend to differ from twins (P<0.1).*

In adults, there are major differences in skeletal muscle metabolism between the sexes which have been related to difference in sex steroid concentrations (Green et al., 1984a, Simoneau et al., 1985). Sex of the fetus and the sex-combination of the twins are also known to have an effect on the growth and development of a number of physiological systems *in utero* with males often being heavier than females throughout gestation (Luke et al., 2005, Gardner et al., 2007). Sex of the fetus has also been shown to affect fetal responses to environmental challenges during late gestation (Giussani et al., 2011, Clark et al., 2007, Gonzalez-Bulnes et al., 2015). In the current study, an effort was made to balance males and females in all groups (Table 2.1) but the only group large enough to directly compare males and females was a group of control twins formed by combining sham-operated and saline-infused fetuses from Chapter 4 (n=3 females and n=7 males). In this cohort, males tended to be heavier than females ($P<0.1$ by Mann-Whitney test) but there were no differences between the sexes in CS activity, total oxidative capacity or biochemical measurements in any of the muscles studied. Further studies are needed to establish whether mitochondrial function is sex-linked during intrauterine development.

6.3.2 Development of other aspects of muscle mitochondrial function

Protection against oxidative stress at birth

Although the capacity for oxidative metabolism is put in place before birth, activity is rapidly upregulated after birth. One of the key hypotheses of this thesis is that the delay in activating oxidative function is perhaps as a protective mechanism, to prevent the excessive ROS production and tissue oxidative damage over the perinatal period. Markers of oxidative damage were not measured in this cohort, however, previously an increased lipid peroxidation has been reported in cord blood during parturition in humans (Rogers et al., 1998). Future work should include looking at markers of tissue oxidative stress, including markers of protein and lipid oxidation (Horscroft et al., 2015, Tarry-Adkins et al., 2013). This would confirm the necessity for protective mechanisms and determine whether manipulating the endocrine environment impacts on the tissue oxidative damage.

Further protection from oxidative stress may also be provided in fetal tissues by the availability of ROS-detoxifying enzymes, SODs and catalase. SOD1 and SOD2 are both expressed in skeletal muscle; SOD1 is located primarily in the cytoplasm whereas SOD2 is mitochondrial-

specific (Fukai and Ushio-Fukai, 2011). The expression of SODs, in particular SOD2, has been shown to remain low throughout gestation in fetal rat tissues, including brain, liver and limb tissues until birth when their hepatic expression rose over the first few weeks of life (Mackler et al., 1998, Pittschieler et al., 1991). Preliminary data from the fetal and neonatal lambs in the current study showed no effect of age on the mRNA abundance of SOD1 (measured only in BF; Figure 6.5 A). However, SOD2 expression did increase with age (measured only in SDF where $P<0.0001$ by one-way ANOVA; Figure 6.5 B), where expression was significantly higher at 143dGA compared with earlier in gestation, and further increased in the newborn lambs. This suggests that expression of the mitochondrial SOD may be raised before birth in preparation for the increase in ROS production which would be expected in response to labour and exposure to a higher pO_2 postnatally.

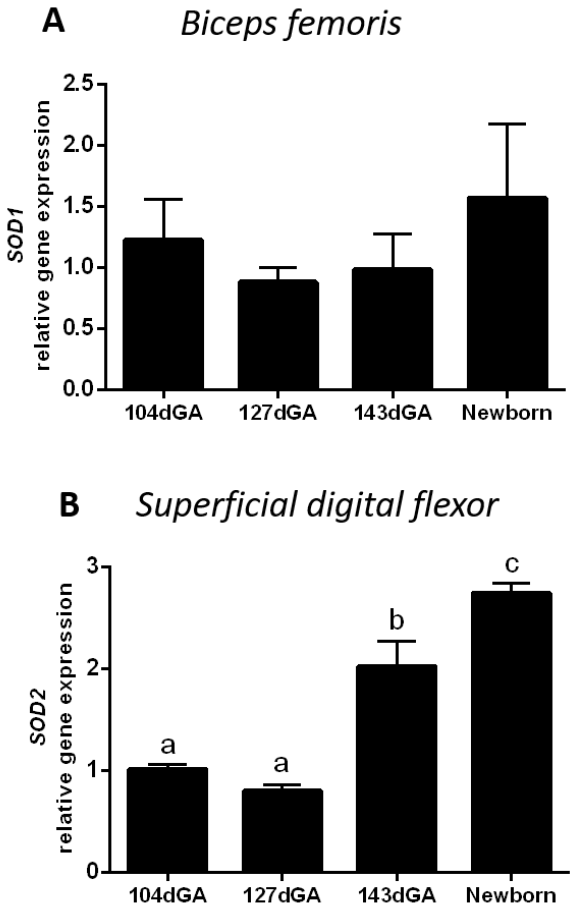

Figure 6.5 Mean±SEM normalised gene expression of A) superoxide dismutase (SOD) 1 in biceps femoris and B) SOD2 in superficial digital flexor of fetuses at 104 (n=5), 127 (n=6) and 143 (n=6) days of gestational age (dGA) and newborn lambs (n=6). Different letters are significantly different to each other (P<0.05 by Tukey's post hoc test following one-way ANOVA).

Calcium homeostasis and signalling

Mitochondria are able to accumulate calcium which has important implications on cellular and organelle function. Mitochondrial calcium has been shown to increase oxidative capacity, to play a role in coupling energy production and requirement in muscle and has been associated with muscle growth (Mammucari et al., 2015, Duchen, 2000). However, excessive mitochondrial calcium uptake, particularly when associated with periods of oxidative stress, is associated with mitochondrial degradation and apoptosis and, in particular, plays a role in ischaemia-reperfusion injury and cell death (Duchen, 2000, Kalogeris et al., 2012). Over late gestation, whether an increase or decrease in calcium uptake into the mitochondria would be of greater benefit in skeletal muscle is difficult to predict.

Calcium is taken into the mitochondrial matrix through the mitochondrial calcium uniporter (MCU) utilising the proton circuit (De Stefani et al., 2011, Duchen, 2004). There is a huge driving force for the cations to enter the matrix and therefore cation channels need to be carefully gated. The MCU is controlled by regulatory elements in the mitochondrial calcium uptake (MICU) family. MICU1 is thought to primarily increase calcium flux through the MCU, while MICU2 limits calcium uptake (Patron et al., 2014). The interaction of the two regulates activity of the MCU, thereby controlling calcium uptake in a tissue-specific manner to prevent the adverse effects of calcium overload but guarantee the stimulation of ATP generation (Patron et al., 2014).

Preliminary data shows no effect of age on MCU gene expression in the BF (Figure 6.6 A) but age did affect the expression of MICU1 in the SDF ($P<0.0001$ by one-way ANOVA; Figure 6.6 B). The expression of MICU1 was similar in the 3 fetal age groups studied, but was significantly upregulated in the newborns compared with the fetuses (Figure 6.6), perhaps to protect against the damaging effects of calcium accumulation during the ischaemia-reperfusion events associated with labour. Postnatally, MICU1 upregulation would be beneficial as calcium may play a role not only in increasing the oxidative capacity of the muscle but also in regulating cytosolic calcium essential for muscle contraction. A more comprehensive investigation into the changes in mitochondrial calcium uptake, and the regulatory mechanisms driving them, would certainly be interesting to consider for future studies.

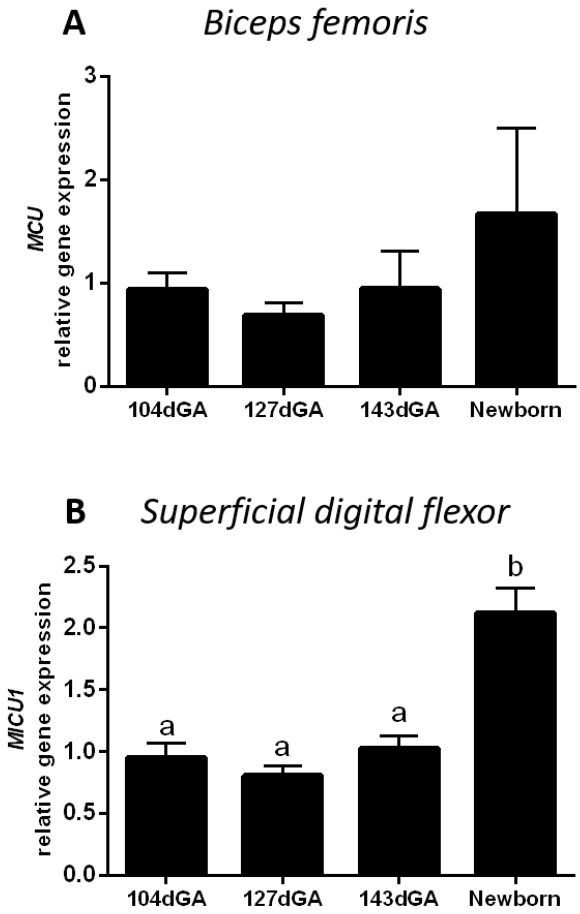

Figure 6.6 Mean±SEM relative gene expression of A) mitochondrial calcium uniporter (MCU) in the biceps femoris and B) mitochondrial calcium uptake 1 (MICU1) in superficial digital flexor of fetuses at 104 (n=5), 127 (n=6) and 143 (n=5-6) gays of gestational age (dGA) and newborn lambs (n=6). Different letters are significantly different to each other (P<0.05 by Tukey's post hoc test following one-way ANOVA).

6.3.3 Developmental programming of mitochondrial dysfunction

The overall aim of this project was to research the normal development of mitochondrial function *in utero* and provide some insight into how these functional changes may influence the health of the offspring later in life. For this research, the skeletal muscle was chosen, as a highly metabolically active tissue and a tissue in which altered energetics is associated with metabolic syndrome (Brown, 2014). Animal models of suboptimal fetal growth have been shown to predispose symptoms of the metabolic syndrome (Bertram and Hanson, 2001), as well as programme mitochondrial dysfunction, as was summarised in Table 1.1. In addition, stressful pregnancies resulting in suboptimal fetal growth, are associated with lower than normal fetal T_3 levels, but higher than normal fetal cortisol concentrations, either from maternal or fetal origin (Forhead and Fowden, 2014, Bertram and Hanson, 2001). Therefore, results from our endocrine manipulation protocols may provide a mechanism by which suboptimal conditions *in utero* may programme an altered metabolic profile.

Results from Chapter 4 suggest that a reduced TH availability, associated with compromised pregnancy, may have a severe detrimental impact on the development of mitochondrial function *in utero*. In addition, hypothyroidism was associated with delayed maturation of the muscle structure. Thus, in such cases, even at birth the cellular metabolic status may be affected. With additional stress during the offspring's lifetime and the effect of aging which is known to be associated with reduced mitochondrial function (Sun et al., 2016), any complication arising prenatally may be worsened such that offspring may be at greater risk of disease in adulthood. Fetal exposure to high cortisol may initially be beneficial, as shown in Chapter 5. Exposing the fetus to higher cortisol upregulated some aspect of mitochondrial function in particular in the SDF. However, problems arise when the pre- and postnatal environments do not align and the modifications set *in utero* are inappropriate postnatally. Impaired cellular energetics will affect all metabolic processes including, for example, the insulin signalling response and the transport of GLUTs to the sarcolemma. As skeletal muscle accounts for the greatest proportion of insulin-stimulated glucose uptake (Brown, 2014), this impaired mitochondrial function due to exposure to an altered endocrine environment *in utero* may manifest as symptoms of metabolic syndrome. A future continuation of this study will involve measuring mitochondrial oxidative capacity in the skeletal muscle of adult offspring which were exposed to elevated cortisol during late gestation, with the aim being to

determine whether altered muscle mitochondrial function associated with metabolic disease begins *in utero* and persists into adulthood.

6.4 General conclusion

Taken together, the results suggest that the capacity for ATP production increased *in utero* in advance of the extra energy requirement at birth by increasing the number of muscle mitochondria in a hormone-dependent manner. However, there is little evidence for any increase in rate of oxygen consumption *per se* until after delivery and the actual oxidative capacity per mitochondrial unit appears to decline during the perinatal period. This may be a mechanism to control ROS production more effectively in fluctuating oxygen availability during the transition to extrauterine life. Further investigation into the signalling pathways and regulatory mechanisms controlling the independent increase in mitochondrial number and oxidative capacity is crucial to understanding the strategy of coping with the transition from intra- to extrauterine life, which may present the biggest metabolic challenge faced by an organism in its lifetime.

References

Acheson, G. H., Dawes, G. S. and Mott, J. C. (1957) Oxygen consumption and the arterial oxygen saturation in foetal and new-born lambs. *J Physiol* **135**(3): 623-43.

Afolayan, A. J., Eis, A., Alexander, M., Michalkiewicz, T., Teng, R. J., Lakshminrusimha, S. and Konduri, G. G. (2016) Decreased endothelial nitric oxide synthase expression and function contribute to impaired mitochondrial biogenesis and oxidative stress in fetal lambs with persistent pulmonary hypertension. *Am J Physiol Lung Cell Mol Physiol,* **310**(1): L40-9.

Aguilar, M., Bhuket, T., Torres, S., Liu, B. and Wong, R. J. (2015) Prevalence of the metabolic syndrome in the united states 2003-2012. *JAMA* **313**(19): 1973-4.

Akana, S. F., Shinsako, J. and Dallman, M. F. (1985) Closed-loop feedback control of the nyctohemeral rise in adrenocortical system function. *Fed Proc* **44**(1 Pt 2): 177-81.

Aken, B. L., Ayling, S., Barrell, D., Clarke, L., Curwen, V., Fairley, S., Fernandez Banet, J., Billis, K., García Girón, C., Hourlier, T., Howe, K., Kähäri, A., Kokocinski, F., Martin, F. J., Murphy, D. N., Nag, R., Ruffier, M., Schuster, M., Tang, Y. A., Vogel, J.-H., White, S., Zadissa, A., Flicek, P. and Searle, S. M. J. (2016) The Ensembl gene annotation system. *Database (Oxford)* **2016**: baw093.

Al-Hasan, Y. M., Pinkas, G. A. and Thompson, L. P. (2014) Prenatal hypoxia reduces mitochondrial protein levels and cytochrome c oxidase activity in offspring guinea pig hearts. *Reprod Sci* **21**(7): 883-91.

Alberti, K. G., Zimmet, P. and Shaw, J. (2005) The metabolic syndrome--a new worldwide definition. *Lancet* **366**(9491): 1059-62.

Aledo, J. C. (2014) Life-history constraints on the mechanisms that control the rate of ROS production. *Curr Genomics* **15**(3): 217-30.

Almeida, A., Bolanos, J. P. and Moncada, S. (2010) E3 ubiquitin ligase APC/C-Cdh1 accounts for the Warburg effect by linking glycolysis to cell proliferation. *Proc Natl Acad Sci U S A* **107**(2): 738-41.

Antoun, G., McMurray, F., Thrush, A. B., Patten, D. A., Peixoto, A. C., Slack, R. S., McPherson, R., Dent, R. and Harper, M. E. (2015) Impaired mitochondrial oxidative phosphorylation and supercomplex assembly in rectus abdominis muscle of diabetic obese individuals. *Diabetologia* **58**(12): 2861-6.

Anyetei-Anum, C. S., Roggero, V. R., Allison, L. A. (2018) Thyroid hormone receptor localization in target tissues. *J Endocrinol* **237**(1):R19-34.

Apatu, R. S. K., Barnes, R. J. and Martin, B. R. (1990) The effects of cortisol and ACTH on the concentration of adrenoreceptors in membrane preparations from fetal sheep livers. *J Physiol* **426**: 27P.

Arsenijevic, D., Onuma, H., Pecqueur, C., Raimbault, S., Manning, B. S., Miroux, B., Couplan, E., Alves-Guerra, M. C., Goubern, M., Surwit, R., Bouillaud, F., Richard, D., Collins, S. and Ricquier, D. (2000) Disruption of the uncoupling protein-2 gene in mice reveals a role in immunity and reactive oxygen species production. *Nat Genet* **26**(4): 435-9.

Astrup, A., Bulow, J., Madsen, J. and Christensen, N. J. (1985) Contribution of BAT and skeletal muscle to thermogenesis induced by ephedrine in man. *Am J Physiol* **248**(5 Pt 1): e507-15.

Baar, K., Wende, A. R., Jones, T. E., Marison, M., Nolte, L. A., Chen, M., Kelly, D. P. and Holloszy, J. O. (2002) Adaptations of skeletal muscle to exercise: rapid increase in the transcriptional coactivator PGC-1. *FASEB J* **16**(14): 1879-86.

Bach, D., Pich, S., Soriano, F. X., Vega, N., Baumgartner, B., Oriola, J., Daugaard, J. R., Lloberas, J., Camps, M., Zierath, J. R., Rabasa-Lhoret, R., Wallberg-Henriksson, H., Laville, M.,

Palacin, M., Vidal, H., Rivera, F., Brand, M. and Zorzano, A. (2003) Mitofusin-2 determines mitochondrial network architecture and mitochondrial metabolism. A novel regulatory mechanism altered in obesity. *J Biol Chem* **278**(19): 17190-7.

Ballabio, M., Nicolini, U., Jowett, T., Ruiz de Elvira, M. C., Ekins, R. P. and Rodeck, C. H. (1989) Maturation of thyroid function in normal human foetuses. *Clin Endocrinol (Oxf)* **31**(5): 565-71.

Barbe, P., Larrouy, D., Boulanger, C., Chevillotte, E., Viguerie, N., Thalamas, C., Oliva Trastoy, M., Roques, M., Vidal, H. and Langin, D. (2001) Triiodothyronine-mediated up-regulation of UCP2 and UCP3 mRNA expression in human skeletal muscle without coordinated induction of mitochondrial respiratory chain genes. *FASEB J* **15**(1): 13-15.

Barker, D. J., Eriksson, J. G., Forsen, T. and Osmond, C. (2002) Fetal origins of adult disease: strength of effects and biological basis. *Int J Epidemiol* **31**(6): 1235-9.

Barker, D. J. and Osmond, C. (1986) Infant mortality, childhood nutrition, and ischaemic heart disease in England and Wales. *Lancet* **1**(8489): 1077-81.

Barker, D. J., Winter, P. D., Osmond, C., Margetts, B. and Simmonds, S. J. (1989) Weight in infancy and death from ischaemic heart disease. *Lancet* **2**(8663): 577-80.

Barnes, R. J., Comline, R. S. and Silver, M. (1978) Effect of cortisol on liver glycogen concentrations in hypophysectomized, adrenalectomized and normal foetal lambs during late or prolonged gestation. *J Physiol* **275**: 567-79.

Barth, E., Albuszies, G., Baumgart, K., Matejovic, M., Wachter, U., Vogt, J., Radermacher, P. and Calzia, E. (2007) Glucose metabolism and catecholamines. *Crit Care Med* **35**(Suppl 9): S508-18.

Bartlett, K. and Eaton, S. (2004) Mitochondrial beta-oxidation. *Eur J Biochem* **271**(3): 462-9.

Beatty, C. H. and Bocek, R. M. (1970) Metabolism of palmitate by fetal, neonatal, and adult muscle of the rhesus monkey. *Am J Physiol* **219**(5): 1311-6.

Beauchamp, B., Ghosh, S., Dysart, M., Kanaan, G. N., Chu, A., Blais, A., Rajamanickam, K., Tsai, E. C., Patti, M.-E. and Harper, M.-E. (2015a) Low birth weight is associated with adiposity, impaired skeletal muscle energetics, and weight loss resistance in mice. *Int J Obes (2005)* **39**(4): 702-11.

Beauchamp, B., Thrush, A B., Quizi, J., Antoun, G., McIntosh, N., Al-Dirbashi, Osama Y., Patti, M.-E. and Harper, M.-E. (2015b) Undernutrition during pregnancy in mice leads to dysfunctional cardiac muscle respiration in adult offspring. *Biosci Rep* **35**(3): e00200.

Begum, G., Stevens, A., Smith, E. B., Connor, K., Challis, J. R. G., Bloomfield, F. and White, A. (2012) Epigenetic changes in fetal hypothalamic energy regulating pathways are associated with maternal undernutrition and twinning. *FASEB J* **26**(4): 1694-703.

Behrman, R. E. and Butler, A. S. (2007) Preterm Birth: Causes, Consequences, and Prevention. *Washington, DC: The National Academies Press.*

Bergeron, R., Ren, J. M., Cadman, K. S., Moore, I. K., Perret, P., Pypaert, M., Young, L. H., Semenkovich, C. F. and Shulman, G. I. (2001) Chronic activation of AMP kinase results in NRF-1 activation and mitochondrial biogenesis. *Am J Physiol Endocrinol Metab* **281**(6): e1340-6.

Bertram, C. E. and Hanson, M. A. (2001) Animal models and programming of the metabolic syndromeType 2 diabetes. *Br Med Bull* **60**(1): 103-21.

Biewener, A. A. (1998) Muscle function in vivo: A comparison of muscles used for elastic energy savings versus muscles used to generate mechanical power. *Amer Zool.* **38**(4): 703-17.

Bloise, F. F., Cordeiro, A. and Ortiga-Carvalho, T. M. (2018) Role of thyroid hormone in skeletal muscle physiology. *J Endocrinol* **236**(1): R57-68

Boirie, Y., Short, K. R., Ahlman, B., Charlton, M. and Nair, K. S. (2001) Tissue-specific regulation of mitochondrial and cytoplasmic protein synthesis rates by insulin. *Diabetes* **50**(12): 2652-8.

Borengasser, S. J., Faske, J., Kang, P., Blackburn, M. L., Badger, T. M. and Shankar, K. (2014) In utero exposure to prepregnancy maternal obesity and postweaning high-fat diet impair regulators of mitochondrial dynamics in rat placenta and offspring. *Physiol Genomics* **46**(23): 841-850.

Boss, O., Samec, S., Paoloni-Giacobino, A., Rossier, C., Dulloo, A., Seydoux, J., Muzzin, P. and Giacobino, J. P. (1997) Uncoupling protein-3: a new member of the mitochondrial carrier family with tissue-specific expression. *FEBS Lett* **408**(1): 39-42.

Boushel, R., Gnaiger, E., Schjerling, P., Skovbro, M., Kraunsoe, R. and Dela, F. (2007) Patients with type 2 diabetes have normal mitochondrial function in skeletal muscle. *Diabetologia* **50**(4): 790-6.

Boveris, A. and Chance, B. (1973) The mitochondrial generation of hydrogen peroxide. General properties and effect of hyperbaric oxygen. *Biochem J* **134**(3): 707-16.

Branco, M., Ribeiro, M., Negrao, N. and Bianco, A. C. (1999) 3,5,3'-Triiodothyronine actively stimulates UCP in brown fat under minimal sympathetic activity. *Am J Physiol* **276**(1 Pt 1): e179-87.

Brand, M. D., Chien, L. F., Ainscow, E. K., Rolfe, D. F. and Porter, R. K. (1994) The causes and functions of mitochondrial proton leak. *Biochim Biophys Acta* **1187**(2): 132-9.

Brand, M. D. and Nicholls, D. G. (2011) Assessing mitochondrial dysfunction in cells. *Biochem J* **435**(2): 297-312.

Brand, M. D., Pakay, J. L., Ocloo, A., Kokoszka, J., Wallace, D. C., Brookes, P. S. and Cornwall, E. J. (2005) The basal proton conductance of mitochondria depends on adenine nucleotide translocase content. *Biochem J* **392**(2): 353-62.

Breall, J. A., Rudolph, A. M. and Heymann, M. A. (1984) Role of thyroid hormone in postnatal circulatory and metabolic adjustments: *J Clin Invest* **73**(5): 1418-24.

Brent, G. A. (2012) Mechanisms of thyroid hormone action. *J Clin Invest* **122**(9): 3035-43.

Bricker, D. K., Taylor, E. B., Schell, J. C., Orsak, T., Boutron, A., Chen, Y. C., Cox, J. E., Cardon, C. M., Van Vranken, J. G., Dephoure, N., Redin, C., Boudina, S., Gygi, S. P., Brivet, M., Thummel, C. S. and Rutter, J. (2012) A mitochondrial pyruvate carrier required for pyruvate uptake in yeast, Drosophila, and humans. *Science* **337**(6090): 96-100.

Brookes, P. S., Hulbert, A. J. and Brand, M. D. (1997) The proton permeability of liposomes made from mitochondrial inner membrane phospholipids: no effect of fatty acid composition. *Biochim Biophys Acta* **1330**(2): 157-64.

Brown, G. C. and Borutaite, V. (2012) There is no evidence that mitochondria are the main source of reactive oxygen species in mammalian cells. *Mitochondrion* **12**(1): 1-4.

Brown, L. D. (2014) Endocrine regulation of fetal skeletal muscle growth: impact on future metabolic health. *J Endocrinol* **221**(2): R13-29.

Buchbinder, A., Lang, U., Baker, R. S., Khoury, J. C., Mershon, J. and Clark, K. E. (2001) Leptin in the ovine fetus correlates with fetal and placental size. *Am J Obstet Gynecol* **185**(4): 786-91.

Burgueno, A. L., Cabrerizo, R., Gonzales Mansilla, N., Sookoian, S. and Pirola, C. J. (2013) Maternal high-fat intake during pregnancy programs metabolic-syndrome-related phenotypes through liver mitochondrial DNA copy number and transcriptional activity of liver PPARGC1A. *J Nutr Biochem* **24**(1): 6-13.

Burns, N., Finucane, F., Hatunic, M., Gilman, M., Murphy, M., Gasparro, D., Mari, A., Gastaldelli, A. and Nolan, J. (2007) Early-onset type 2 diabetes in obese white subjects is

characterised by a marked defect in beta cell insulin secretion, severe insulin resistance and a lack of response to aerobic exercise training. *Diabetologia* **50**(7): 1500-8

Butcher, M. T., Chase, P. B., Hermanson, J. W., Clark, A. N., Brunet, N. M. and Bertram, J. E. A. (2010) Contractile properties of muscle fibers from the deep and superficial digital flexors of horses. *Am J Physiol Regul Integr Comp Physiol* **299**(4): R996-1005.

Byrne, K., Vuocolo, T., Gondro, C., White, J. D., Cockett, N. E., Hadfield, T., Bidwell, C. A., Waddell, J. N. and Tellam, R. L. (2010) A gene network switch enhances the oxidative capacity of ovine skeletal muscle during late fetal development. *BMC Genomics* **11**: 378.

Cardaci, S. and Ciriolo, M. R. (2012) TCA cycle defects and cancer: When metabolism tunes redox state. *Int J Cell Biol* **2012**: 161837.

Carnac, G., Albagli-Curiel, O., Vandromme, M., Pinset, C., Montarras, D., Laudet, V. and Bonnieu, A. (1992) 3,5,3'-Triiodothyronine positively regulates both MyoD1 gene transcription and terminal differentiation in C2 myoblasts. *Mol Endocrinol* **6**(8): 1185-94.

Carpenter, A. E., Jones, T. R., Lamprecht, M. R., Clarke, C., Kang, I. H., Friman, O., Guertin, D. A., Chang, J. H., Lindquist, R. A., Moffat, J., Golland, P. and Sabatini, D. M. (2006) CellProfiler: image analysis software for identifying and quantifying cell phenotypes. *Genome Biol* **7**(10): R100.

Castro, M. I., Valego, N. K., Zehnder, T. J. and Rose, J. C. (1992) The ratio of plasma bioactive to immunoreactive ACTH-like activity increases with gestational age in the fetal lamb. *J Dev Physiol* **18**(4): 193-201.

Cereghetti, G. M., Stangherlin, A., de Brito, O. M., Chang, C. R., Blackstone, C., Bernardi, P. and Scorrano, L. (2008) Dephosphorylation by calcineurin regulates translocation of Drp1 to mitochondria. *Proc Natl Acad Sci U S A* **105**(41): 15803-8.

Challis, J. R., Sloboda, D., Matthews, S. G., Holloway, A., Alfaidy, N., Patel, F. A., Whittle, W., Fraser, M., Moss, T. J. and Newnham, J. (2001) The fetal placental hypothalamic-pituitary-adrenal (HPA) axis, parturition and post natal health. *Mol Cell Endocrinol* **185**(1-2): 135-44.

Chan, S. Y., Vasilopoulou, E. and Kilby, M. D. (2009) The role of the placenta in thyroid hormone delivery to the fetus. *Nat Clin Pract Endocrinol Metab* **5**(1): 45-54.

Chandel, N. S., Budinger, G. R., Choe, S. H. and Schumacker, P. T. (1997) Cellular respiration during hypoxia. Role of cytochrome oxidase as the oxygen sensor in hepatocytes *J Biol Chem* **272**(30): 18808-16.

Chang, T. W. and Goldberg, A. L. (1978) The metabolic fates of amino acids and the formation of glutamine in skeletal muscle *J Biol Chem* **253**(10): 3685-93.

Chaudhari, S., Otiv, M., Hoge, M., Pandit, A. and Sayyed, M. (2017) Components of metabolic syndrome at 22 years of age - Findings From Pune low birth weight study. *Indian Pediatr* **54**(6): 461-6.

Chen, H., Detmer, S. A., Ewald, A. J., Griffin, E. E., Fraser, S. E. and Chan, D. C. (2003) Mitofusins Mfn1 and Mfn2 coordinately regulate mitochondrial fusion and are essential for embryonic development. *J Cell Biol* **160**(2): 189-200.

Chen, Q. P. and Li, Q. T. (2001) Effect of cardiolipin on proton permeability of phospholipid liposomes: the role of hydration at the lipid-water interface. *Arch Biochem Biophys* **389**(2): 201-6.

Chow. S., Shao. J. and Wang, H. (2008) Sample size calculations in clinical research. Second Edition: Chapman and Hall/CRC Biostatistics Series.

Christie, W. W., Calvert, D. T., Shand, J. H. and Noble, R. C. (1985) The metabolism of palmitic acid in the fetal lamb. *Comp Biochem Physiol B Comp Biochem* **80**(3): 617-621.

Cipolat, S., Martins de Brito, O., Dal Zilio, B. and Scorrano, L. (2004) OPA1 requires mitofusin 1 to promote mitochondrial fusion. *Proc Natl Acad Sci U S A* **101**(45): 15927-32.

Clapham, J. C., Arch, J. R., Chapman, H., Haynes, A., Lister, C., Moore, G. B., Piercy, V., Carter, S. A., Lehner, I., Smith, S. A., Beeley, L. J., Godden, R. J., Herrity, N., Skehel, M., Changani, K. K., Hockings, P. D., Reid, D. G., Squires, S. M., Hatcher, J., Trail, B., Latcham, J., Rastan, S., Harper, A. J., Cadenas, S., Buckingham, J. A., Brand, M. D. and Abuin, A. (2000) Mice overexpressing human uncoupling protein-3 in skeletal muscle are hyperphagic and lean *Nature* **406**(6794): 415-8.

Clark, J. M., Hulme, E., Devendrakumar, V., Turner, M. A., Baker, P. N., Sibley, C. P. and D'Souza, S. W. (2007) Effect of maternal asthma on birthweight and neonatal outcome in a British inner-city population. *Paediatr Perinat Epidemiol* **21**(2): 154-162.

Clarke, I., Heasman, L. and Symonds, M. E. (1998) Influence of maternal dexamethasone administration on thermoregulation in lambs delivered by caesarean section. *J Endocrinol* **156**(2): 307-14.

Clarke, L., Bryant, M. J., Lomax, M. A. and Symonds, M. E. (1997) Maternal manipulation of brown adipose tissue and liver development in the ovine fetus during late gestation *Br J Nutr* **77**(6): 871-83.

Clement, K., Viguerie, N., Diehn, M., Alizadeh, A., Barbe, P., Thalamas, C., Storey, J. D., Brown, P. O., Barsh, G. S. and Langin, D. (2002) In vivo regulation of human skeletal muscle gene expression by thyroid hormone. *Genome Res* **12**(2): 281-91.

Cook, S., Weitzman, M., Auinger, P., Nguyen, M. and Dietz, W. H. (2003) Prevalence of a metabolic syndrome phenotype in adolescents: findings from the third National Health and Nutrition Examination Survey, 1988-1994. *Arch Pediatr Adolesc Med* **157**(8): 821-7.

Cribbs, J. T. and Strack, S. (2007) Reversible phosphorylation of Drp1 by cyclic AMP-dependent protein kinase and calcineurin regulates mitochondrial fission and cell death. *EMBO Rep* **8**(10): 939-44.

D'Elia, A., Pighetti, M., Moccia, G. and Santangelo, N. (2001) Spontaneous motor activity in normal fetuses. *Early Hum Dev* **65**(2): 139-47.

Davies, V. J., Hollins, A. J., Piechota, M. J., Yip, W., Davies, J. R., White, K. E., Nicols, P. P., Boulton, M. E. and Votruba, M. (2007) Opa1 deficiency in a mouse model of autosomal dominant optic atrophy impairs mitochondrial morphology, optic nerve structure and visual function. *Hum Mol Genet* **16**(11): 1307-18.

De Blasio, M. J., Boije, M., Vaughan, O. R., Bernstein, B. S., Davies, K. L., Plein, A., Kempster, S. L., Smith, G. C., Charnock-Jones, D. S., Blache, D., Wooding, F. B., Giussani, D. A., Fowden, A. L. and Forhead, A. J. (2015) Developmental expression and glucocorticoid control of the leptin receptor in fetal ovine lung. *PLoS One* **10**(8): e0136115.

De Stefani, D., Raffaello, A., Teardo, E., Szabò, I. and Rizzuto, R. (2011) A 40 kDa protein of the inner membrane is the mitochondrial calcium uniporter. *Nature* **476**(7360): 336-40.

Demonacos, C., Djordjevic-Markovic, R., Tsawdaroglou, N. and Sekeris, C. E. (1995) The mitochondrion as a primary site of action of glucocorticoids: the interaction of the glucocorticoid receptor with mitochondrial DNA sequences showing partial similarity to the nuclear glucocorticoid responsive elements. *J Steroid Biochem Mol Biol* **55**(1): 43-55.

Dentice, M., Marsili, A., Ambrosio, R., Guardiola, O., Sibilio, A., Paik, J. H., Minchiotti, G., DePinho, R. A., Fenzi, G., Larsen, P. R. and Salvatore, D. (2010) The FoxO3/type 2 deiodinase pathway is required for normal mouse myogenesis and muscle regeneration. *J Clin Invest* **120**(11): 4021-30.

Deveaux, V., Picard, B., Bouley, J. and Cassar-Malek, I. (2003) Location of myostatin expression during bovine myogenesis in vivo and in vitro. *Reprod Nutr Dev* **43**(6): 527-42.

Dimitriadis, G., Mitrou, P., Lambadiari, V., Maratou, E. and Raptis, S. A. (2011) Insulin effects in muscle and adipose tissue *Diabetes Res Clin Pract* **93**(Suppl 1): S52-9.

Dong, Y., Poellinger, L., Gustafsson, J. A. and Okret, S. (1988) Regulation of glucocorticoid receptor expression: evidence for transcriptional and posttranslational mechanisms. *Mol Endocrinol* **2**(12): 1256-64.

Du, M., Tong, J., Zhao, J., Underwood, K. R., Zhu, M., Ford, S. P. and Nathanielsz, P. W. (2010) Fetal programming of skeletal muscle development in ruminant animals. *J Anim Sci* **88**(Suppl 13): e51-60.

Duchamp, C., Burton, K. A., Herpin, P. and Dauncey, M. J. (1994) Perinatal ontogeny of porcine nuclear thyroid hormone receptors and its modulation by thyroid status. *Am J Physiol* **267**(5 Pt 1): e687-93.

Duchen, M. R. (2000) Mitochondria and calcium: from cell signalling to cell death. *J Physiol* **529**(1): 57-68.

Duchen, M. R. (2004) Roles of mitochondria in health and disease. *Diabetes* **53**(Suppl 1): S96-102.

Dummler, K., Muller, S. and Seitz, H. J. (1996) Regulation of adenine nucleotide translocase and glycerol 3-phosphate dehydrogenase expression by thyroid hormones in different rat tissues. *Biochem J* **317**(Pt 3): 913-8.

Ebeling, P., Koistinen, H. A. and Koivisto, V. A. (1998) Insulin-independent glucose transport regulates insulin sensitivity. *FEBS Lett* **436**(3): 301-3.

Echtay, K. S., Roussel, D., St-Pierre, J., Jekabsons, M. B., Cadenas, S., Stuart, J. A., Harper, J. A., Roebuck, S. J., Morrison, A., Pickering, S., Clapham, J. C. and Brand, M. D. (2002) Superoxide activates mitochondrial uncoupling proteins. *Nature* **415**(6867): 96-9.

Edwards, L. J. and McMillen, I. C. (2002) Impact of maternal undernutrition during the periconceptional period, fetal number, and fetal sex on the development of the hypothalamo-pituitary adrenal axis in sheep during late gestation. *Biol Reprod* **66**(5): 1562-9.

Eisner, V., Lenaers, G. and Hajnoczky, G. (2014) Mitochondrial fusion is frequent in skeletal muscle and supports excitation-contraction coupling. *J Cell Biol* **205**(2): 179-95.

Enerback, S., Jacobsson, A., Simpson, E. M., Guerra, C., Yamashita, H., Harper, M. E. and Kozak, L. P. (1997) Mice lacking mitochondrial uncoupling protein are cold-sensitive but not obese. *Nature* **387**(6628): 90-4.

Erenberg, A., Omori, K., Menkes, J. H., O, W. and Fisher, D. A. (1974) Growth and development of the thyroidectomized ovine fetus. *Pediatr Res* **8**(9): 783-9.

Fernandez, X., Lefaucheur, L. and Candek, M. (1995) Comparative study of two classifications of muscle fibres: Consequences for the photometric determination of glycogen according to fibre type in red and white muscle of the pig. *Meat Sci* **41**(2): 225-35.

Finkelstein, D. I., Andrianakis, P., Luff, A. R. and Walker, D. (1991) Effects of thyroidectomy on development of skeletal muscle in fetal sheep. *Am J Physiol* **261**(5 Pt 2): R1300-6.

Fleury, C., Neverova, M., Collins, S., Raimbault, S., Champigny, O., Levi-Meyrueis, C., Bouillaud, F., Seldin, M. F., Surwit, R. S., Ricquier, D. and Warden, C. H. (1997) Uncoupling protein-2: a novel gene linked to obesity and hyperinsulinemia. *Nat Genet* **15**(3): 269-72.

Folch, J., Lees, M. and Sloane Stanley, G. H. (1957) A simple method for the isolation and purification of total lipides from animal tissues. *J Biol Chem* **226**(1): 497-509.

Forhead, A. J., Curtis, K., Kaptein, E., Visser, T. J. and Fowden, A. L. (2006) Developmental control of iodothyronine deiodinases by cortisol in the ovine fetus and placenta near term. *Endocrinology* **147**(12): 5988-94.

Forhead, A. J., Cutts, S., Matthews, P. A. and Fowden, A. L. (2009) Role of thyroid hormones in the developmental control of tissue glycogen in fetal sheep near term. *Exp Physiol* **94**(10): 1079-87.

Forhead, A. J. and Fowden, A. L. (2002) Effects of thyroid hormones on pulmonary and renal angiotensin-converting enzyme concentrations in fetal sheep near term. *J Endocrinol* **173**(1): 143-50.

Forhead, A. J. and Fowden, A. L. (2014) Thyroid hormones in fetal growth and prepartum maturation. *J Endocrinol* **221**(3): R87-103.

Forhead, A. J., Lamb, C. A., Franko, K. L., O'Connor, D. M., Wooding, P. F. B., Cripps, R. L., Ozanne, S., Blache, D., Shen, Q. W., Du, M. and Fowden, A. L. (2008) Role of leptin in the regulation of growth and carbohydrate metabolism in the ovine fetus during late gestation. *J Physiol* **586**(9): 2393-403.

Forhead, A. J., Li, J., Gilmour, R. S., Dauncey, M. J. and Fowden, A. L. (2002) Thyroid hormones and the mRNA of the GH receptor and IGFs in skeletal muscle of fetal sheep. *Am J Physiol Endocrinol Metab* **282**(1): e80-6.

Forhead, A. J., Li, J., Gilmour, R. S. and Fowden, A. L. (1998) Control of hepatic insulin-like growth factor II gene expression by thyroid hormones in fetal sheep near term. *Am J Physiol* **275**(1 Pt 1): e149-56.

Forhead, A. J., Li, J., Saunders, J. C., Dauncey, M. J., Gilmour, R. S. and Fowden, A. L. (2000) Control of ovine hepatic growth hormone receptor and insulin-like growth factor I by thyroid hormones in utero. *Am J Physiol Endocrinol Metab* **278**(6): e1166-74.

Forhead, A. J., Poore, K. R., Mapstone, J. and Fowden, A. L. (2003) Developmental regulation of hepatic and renal gluconeogenic enzymes by thyroid hormones in fetal sheep during late gestation. *J Physiol* **548**(3): 941-7.

Forrest, D., Hallböök, F., Persson, H. and Vennström, B. (1991) Distinct functions for thyroid hormone receptors alpha and beta in brain development indicated by differential expression of receptor genes. *EMBO J* **10**(2): 269-75.

Fowden, A. L., Comline, R. S. and Silver, M. (1985) The effects of cortisol on the concentration of glycogen in different tissues in the chronically catheterized fetal pig. *Q J Exp Physiol* **70**(1): 23-35.

Fowden, A. L., Hughes, P. and Comline, R. S. (1989) The effects of insulin on the growth rate of the sheep fetus during late gestation. *Q J Exp Physiol* **74**(5): 703-14.

Fowden, A. L., Li, J. and Forhead, A. J. (1998) Glucocorticoids and the preparation for life after birth: are there long-term consequences of the life insurance? *Proc Nutr Soc* **57**(1): 113-22.

Fowden, A. L., Mapstone, J. and Forhead, A. J. (2001) Regulation of glucogenesis by thyroid hormones in fetal sheep during late gestation. *J Endocrinol* **170**(2): 461-9.

Fowden, A. L., Mijovic, J. and Silver, M. (1993) The effects of cortisol on hepatic and renal gluconeogenic enzyme activities in the sheep fetus during late gestation. *J Endocrinol* **137**(2): 213-22.

Fowden, A. L., Mundy, L., Ousey, J. C., McGladdery, A. and Silver, M. (1991) Tissue glycogen and glucose 6-phosphatase levels in fetal and newborn foals. *J Reprod Fertil Suppl* **44**: 537-42.

Fowden, A. L. and Silver, M. (1995) The effects of thyroid hormones on oxygen and glucose metabolism in the sheep fetus during late-gestation. *J Physiol (Lond)* **482**(1): 203-13.

Fowden, A. L., Szemere, J., Hughes, P., Gilmour, R. S. and Forhead, A. J. (1996) The effects of cortisol on the growth rate of the sheep fetus during late gestation. *J Endocrinol* **151**(1): 97-105.

Frandson, R. D., Wilke, W. L. and Fails, A. D. (2013) Anatomy and physiology of farm animals. 7th edn.: John Wiley & Sons.

Fraser, M., Braems, G. A. and Challis, J. R. (2001) Developmental regulation of corticotrophin receptor gene expression in the adrenal gland of the ovine fetus and newborn lamb: effects of hypoxia during late pregnancy. *J Endocrinol* **169**(1): 1-10.

Fukai, T. and Ushio-Fukai, M. (2011) Superoxide dismutases: Role in redox signaling, vascular function, and diseases. *Antioxid Redox Signal* **15**(6): 1583-606.

Gambke, B., Lyons, G. E., Haselgrove, J., Kelly, A. M. and Rubinstein, N. A. (1983) Thyroidal and neural control of myosin transitions during development of rat fast and slow muscles. *FEBS Lett* **156**(2): 335-9.

Gandre-Babbe, S. and van der Bliek, A. M. (2008) The novel tail-anchored membrane protein Mff controls mitochondrial and peroxisomal fission in mammalian cells. *Mol Biol Cell* **19**(6): 2402-12.

Gardner, D. S., Buttery, P. J., Daniel, Z. and Symonds, M. E. (2007) Factors affecting birth weight in sheep: maternal environment. *Reproduction* **133**(1): 297-307.

Gardner, D. S., Jamall, E., Fletcher, A. J., Fowden, A. L. and Giussani, D. A. (2004) Adrenocortical responsiveness is blunted in twin relative to singleton ovine fetuses. *J Physiol* **557**(3): 1021-32.

Gaster, M., Handberg, A., Beck-Nielsen, H. and Schroder, H. D. (2000) Glucose transporter expression in human skeletal muscle fibers. *Am J Physiol Endocrinol Metab* **279**(3): e529-38.

Gemmell, R. T. and Alexander, G. (1978) Ultrastructural development of adipose-tissue in fetal sheep. *Aust J Biol Sci* **31**(5): 505-15.

Gereben, B., Zavacki, A. M., Ribich, S., Kim, B. W., Huang, S. A., Simonides, W. S., Zeöld, A. and Bianco, A. C. (2008) Cellular and molecular basis of deiodinase-regulated thyroid hormone signaling. *Endocr Rev* **29**(7): 898-938.

Giussani, D. A., Fletcher, A. J. W. and Gardner, D. S. (2011) Sex differences in the ovine fetal cortisol response to stress. *Pediatr Res* **69**(2): 118-22.

Glancy, B. and Balaban, R. S. (2011) Protein composition and function of red and white skeletal muscle mitochondria. *Am J Physiol Cell Physiol* **300**(6): C1280-90.

Gnaiger, E. (2012) Mitochondrial pathways and respiratory control: An introduction to OXPHOS analysis. *Mitochondr Physiol Network 17.18.* Oroboros Instruments.

Gnanalingham, M. G., Giussani, D. A., Sivathondan, P., Forhead, A. J., Stephenson, T., Symonds, M. E. and Gardner, D. S. (2005a) Chronic umbilical cord compression results in accelerated maturation of lung and brown adipose tissue in the sheep fetus during late gestation. *Am J Physiol Endocrinol Metab* **289**(3): e456-65.

Gnanalingham, M. G., Mostyn, A., Forhead, A. J., Fowden, A. L., Symonds, M. E. and Stephenson, T. (2005b) Increased uncoupling protein-2 mRNA abundance and glucocorticoid action in adipose tissue in the sheep fetus during late gestation is dependent on plasma cortisol and triiodothyronine. *J Physiol (Lond)* **567**(1): 283-92.

Gong, D. W., He, Y., Karas, M. and Reitman, M. (1997) Uncoupling protein-3 is a mediator of thermogenesis regulated by thyroid hormone, 3-adrenergic agonists, and leptin. *J Biol Chem* **272**(39): 24129-32

Gong, D. W., He, Y. and Reitman, M. L. (1999) 'Genomic organization and regulation by dietary fat of the uncoupling protein 3 and 2 genes. *Biochem Biophys Res Commun* **256**(1): 27-32.

Gong, D. W., Monemdjou, S., Gavrilova, O., Leon, L. R., Marcus-Samuels, B., Chou, C. J., Everett, C., Kozak, L. P., Li, C., Deng, C., Harper, M. E. and Reitman, M. L. (2000) Lack of obesity

and normal response to fasting and thyroid hormone in mice lacking uncoupling protein-3. *J Biol Chem* **275**(21):16251-7.

Gonzalez-Bulnes, A., Torres-Rovira, L., Astiz, S., Ovilo, C., Sanchez-Sanchez, R., Gomez-Fidalgo, E., Perez-Solana, M., Martin-Lluch, M., Garcia-Contreras, C. and Vazquez-Gomez, M. (2015) Fetal Sex Modulates Developmental Response to Maternal Malnutrition. *PLoS One* **10**(11): e0142158.

Goodyear, L. J., Hirshman, M. F., Smith, R. J. and Horton, E. S. (1991) Glucose transporter number, activity, and isoform content in plasma membranes of red and white skeletal muscle. *Am J Physiol* **261**(5 Pt 1): e556-61.

Gray, M. W. (2012) Mitochondrial Evolution. *Cold Spring Harb Perspect Biol* **4**(9): a011403.

Green, A. S., Macko, A. R., Rozance, P. J., Yates, D. T., Chen, X., Hay, W. W. and Limesand, S. W. (2011) Characterization of glucose-insulin responsiveness and impact of fetal number and sex difference on insulin response in the sheep fetus. *Am J Physiol Endocrinol Metab* **300**(5): e817-23.

Green, H. J., Fraser, I. G. and Ranney, D. A. (1984a) Male and female differences in enzyme activities of energy metabolism in vastus lateralis muscle. *J Neurol Sci* **65**(3): 323-31.

Green, H. J., Klug, G. A., Reichmann, H., Seedorf, U., Wiehrer, W. and Pette, D. (1984b) Exercise-induced fibre type transitions with regard to myosin, parvalbumin, and sarcoplasmic reticulum in muscles of the rat. *Pflugers Arch* **400**(4): 432-8.

Greenberg, A. H., Czernichow, P., Reba, R. C., Tyson, J. and Blizzard, R. M. (1970) Observations on the maturation of thyroid function in early fetal life. *J Clin Invest* **49**(10): 1790-803.

Greenfield, P. C. and Boell, E. J. (1968) Succinic dehydrogenase and cytochrome oxidase of mitochondria of chick liver, heart, and skeletal muscle during embryonic development. *J Exp Zool* **168**(4): 491-500.

Groner, B., Hynes, N. E., Rahmsdorf, U. and Ponta, H. (1983) Transcription initiation of transfected mouse mammary tumor virus LTR DNA is regulated by glucocorticoid hormones. *Nucleic Acids Research* **11**(14): 4713-25.

Guertin, M., Baril, P., Bartkowiak, J., Anderson, A. and Belanger, L. (1983) Rapid suppression of alpha1-fetoprotein gene transcription by dexamethasone in developing rat liver. *Biochemistry* **22**(18): 4296-302

Hales, C. N., Barker, D. J., Clark, P. M., Cox, L. J., Fall, C., Osmond, C. and Winter, P. D. (1991) Fetal and infant growth and impaired glucose tolerance at age 64. *BMJ* **303**(6809): 1019-22.

Halestrap, A. P. (1978) Pyruvate and ketone-body transport across the mitochondrial membrane. Exchange properties, pH-dependence and mechanism of the carrier *Biochem J* **172**(3): 377-87.

Halestrap, A. P. and Denton, R. M. (1974) Specific inhibition of pyruvate transport in rat liver mitochondria and human erythrocytes by α-cyano-4-hydroxycinnamate. *Biochem J* **138**(2): 313-6.

Hall, K. D., Heymsfield, S. B., Kemnitz, J. W., Klein, S., Schoeller, D. A. and Speakman, J. R. (2012) Energy balance and its components: implications for body weight regulation. *Am J Clin Nutr* **95**(4): 989-94.

Han, J., Thompson, P. and Beutler, B. (1990) Dexamethasone and pentoxifylline inhibit endotoxin-induced cachectin/tumor necrosis factor synthesis at separate points in the signaling pathway. *J Exp Med* **172**(1): 391-4.

Hancock, S. N., Oliver, M. H., McLean, C., Jaquiery, A. L. and Bloomfield, F. H. (2012) Size at birth and adult fat mass in twin sheep are determined in early gestation. *J Physiol* **590**(5): 1273-85.

Harper, M. E. and Seifert, E. L. (2008) Thyroid hormone effects on mitochondrial energetics. *Thyroid* **18**(2): 145-56.

Harris, S. E., De Blasio, M. J., Davis, M. A., Kelly, A. C., Davenport, H. M., Wooding, F. B. P., Blache, D., Meredith, D., Anderson, M., Fowden, A. L., Limesand, S. W. and Forhead, A. J. (2017) Hypothyroidism in utero stimulates pancreatic beta cell proliferation and hyperinsulinaemia in the ovine fetus during late gestation. *J Physiol* **595**(11): 3331-43.

Harrison, A. P., Tivey, D. R., Clausen, T., Duchamp, C. and Dauncey, M. J. (1996) Role of thyroid hormones in early postnatal development of skeletal muscle and its implications for undernutrition. *Br J Nutr* **76**(6): 841-55.

Hay, W. W. (2006) Placental-Fetal Glucose Exchange and Fetal Glucose Metabolism. *Trans Am Clin Climatol Assoc* **117**: 321-40.

Hay, W. W., Jr., Sparks, J. W., Quissell, B. J., Battaglia, F. C. and Meschia, G. (1981) Simultaneous measurements of umbilical uptake, fetal utilization rate, and fetal turnover rate of glucose. *Am J Physiol* **240**(6): e662-8.

Heaton, G. M., Wagenvoord, R. J., Kemp, A., Jr. and Nicholls, D. G. (1978) Brown-adipose-tissue mitochondria: photoaffinity labelling of the regulatory site of energy dissipation. *Eur J Biochem* **82**(2): 515-21.

Heemstra, K. A., Soeters, M. R., Fliers, E., Serlie, M. J., Burggraaf, J., van Doorn, M. B., van der Klaauw, A. A., Romijn, J. A., Smit, J. W., Corssmit, E. P. and Visser, T. J. (2009) Type 2 iodothyronine deiodinase in skeletal muscle: effects of hypothyroidism and fasting. *J Clin Endocrinol Metab* **94**(6): 2144-50.

Hennessy, D. P., Coghlan, J. P., Hardy, K. J., Scoggins, B. A. and Wintour, E. M. (1982) The origin of cortisol in the blood of fetal sheep. *J Endocrinol* **95**(1): 71-9.

Henzi, T. and Schwaller, B. (2015) Antagonistic regulation of parvalbumin expression and mitochondrial calcium handling capacity in renal epithelial cells. *PLoS One* **10**(11): e0142005.

Hernandez, A., Martinez, M. E., Fiering, S., Galton, V. A. and St. Germain, D. (2006) Type 3 deiodinase is critical for the maturation and function of the thyroid axis. *J Clin Invest* **116**(2): 476-84.

Hernandez-Alvarez, M. I., Thabit, H., Burns, N., Shah, S., Brema, I., Hatunic, M., Finucane, F., Liesa, M., Chiellini, C., Naon, D., Zorzano, A. and Nolan, J. J. (2010) Subjects with early-onset type 2 diabetes show defective activation of the skeletal muscle PGC-1α/Mitofusin-2 regulatory pathway in response to physical activity. *Diabetes Care* **33**(3): 645-51.

Herpin, P., Berthon, D., Duchamp, C., Dauncey, M. J. and Le Dividich, J. (1996) Effect of thyroid status in the perinatal period on oxidative capacities and mitochondrial respiration in porcine liver and skeletal muscle. *Reprod Fertil Dev* **8**(1): 147-55.

Hoffenberg, R. and Ramsden, D. B. (1983) The transport of thyroid hormones. *Clin Sci (Lond)* **65**(4): 337-42.

Holman, G. D. and Cushman, S. W. (1994) Subcellular localization and trafficking of the GLUT4 glucose transporter isoform in insulin-responsive cells. *Bioessays* **16**(10): 753-9.

Hood, D. A., Irrcher, I., Ljubicic, V. and Joseph, A. M. (2006) Coordination of metabolic plasticity in skeletal muscle. *J Exp Biol* **209**(12): 2265-75.

Hood, D. A., Uguccioni, G., Vainshtein, A. and D'Souza, D. (2011) Mechanisms of exercise-induced mitochondrial biogenesis in skeletal muscle: implications for health and disease. *Compr Physiol* **1**(3): 1119-34.

Hoppeler, H. (1999) Skeletal muscle substrate metabolism. *Int J Obes Relat Metab Disord* **23**(Suppl 3): S7-10.

Hoppeler, H., Howald, H., Conley, K., Lindstedt, S. L., Claassen, H., Vock, P. and Weibel, E. R. (1985) Endurance training in humans: aerobic capacity and structure of skeletal muscle. *J Appl Physiol* **59**(2): 320-7.

Horn, S. and Heuer, H. (2010) Thyroid hormone action during brain development: more questions than answers. *Mol Cell Endocrinol* **315**(1-2): 19-26.

Horscroft, J. A., Burgess, S. L., Hu, Y. and Murray, A. J. (2015) Altered oxygen utilisation in rat left ventricle and soleus after 14 days, but not 2 days, of environmental hypoxia. *PLoS ONE* **10**(9): e0138564.

Hu, F. B. (2011) Globalization of diabetes: the role of diet, lifestyle, and genes. *Diabetes Care* **34**(6): 1249-57.

Huizing, M., Ruitenbeek, W., Thinnes, F. P., DePinto, V., Wendel, U., Trijbels, F. J., Smit, L. M., ter Laak, H. J. and van den Heuvel, L. P. (1996) Deficiency of the voltage-dependent anion channel: a novel cause of mitochondriopathy. *Pediatr Res* **39**(5): 760-5.

Hull, D. (1975) Storage and supply of fatty acids before and after birth. *Br Med Bull* **31**(1): 32-6.

Hurd, R. E., Santini, F., Lee, B., Naim, P. and Chopra, I. J. (1993) A study of the 3,5,3'-triiodothyronine sulfation activity in the adult and the fetal rat. *Endocrinology* **133**(5): 1951-5.

Huttemann, M., Lee, I., Pecinova, A., Pecina, P., Przyklenk, K. and Doan, J. W. (2008) Regulation of oxidative phosphorylation, the mitochondrial membrane potential, and their role in human disease. *J Bioenerg Biomembr* **40**(5): 445-56.

Huttemann, M., Lee, I., Samavati, L., Yu, H. and Doan, J. W. (2007) Regulation of mitochondrial oxidative phosphorylation through cell signaling. *Biochim Biophys Acta* **1773**(12): 1701-20.

Hyde, R., Taylor, P. M. and Hundal, H. S. (2003) Amino acid transporters: roles in amino acid sensing and signalling in animal cells. *Biochem J* **373**(1): 1-18.

Irrcher, I., Adhihetty, P. J., Sheehan, T., Joseph, A. M. and Hood, D. A. (2003) PPARgamma coactivator-1alpha expression during thyroid hormone- and contractile activity-induced mitochondrial adaptations. *Am J Physiol Cell Physiol* **284**(6): C1669-77.

Irrcher, I., Walkinshaw, D. R., Sheehan, T. E. and Hood, D. A. (2008) Thyroid hormone (T3) rapidly activates p38 and AMPK in skeletal muscle in vivo. *J Appl Physiol* **104**(1): 178-85.

Ishihara, N., Eura, Y. and Mihara, K. (2004) Mitofusin 1 and 2 play distinct roles in mitochondrial fusion reactions via GTPase activity. *J Cell Sci* **117**(26): 6535-46.

Ishihara, N., Nomura, M., Jofuku, A., Kato, H., Suzuki, S. O., Masuda, K., Otera, H., Nakanishi, Y., Nonaka, I., Goto, Y., Taguchi, N., Morinaga, H., Maeda, M., Takayanagi, R., Yokota, S. and Mihara, K. (2009) Mitochondrial fission factor Drp1 is essential for embryonic development and synapse formation in mice. *Nat Cell Biol* **11**(8): 958-66.

Jacobs, R. A., Young, I. R., Hollingworth, S. A. and Thorburn, G. D. (1994) Chronic administration of low doses of adrenocorticotropin to hypophysectomized fetal sheep leads to normal term labor. *Endocrinology* **134**(3): 1389-94.

Jaimes, E. A., Sweeney, C. and Raij, L. (2001) Effects of the reactive oxygen species hydrogen peroxide and hypochlorite on endothelial nitric oxide production. *Hypertension* **38**(4): 877-83.

Jakovcic, S., Haddock, J., Getz, G. S., Rabinowitz, M. and Swift, H. (1971) Mitochondrial development in liver of foetal and newborn rats. *Biochem J* **121**(2): 341-7.

James, E., Meschia, G. and Battaglia, F. C. (1971) A-V differences of free fatty acids and glycerol in the ovine umbilical circulation. *Proc Soc Exp Biol Med* **138**(3): 823-6.

Javen, I., Williams, N. A., Young, I. R., Luff, A. R. and Walker, D. (1996) Growth and differentiation of fast and slow muscles in fetal sheep, and the effects of hypophysectomy. *J Physiol* **494**(3): 839-49.

Jellyman, J. K., Martin-Gronert, M. S., Cripps, R. L., Giussani, D. A., Ozanne, S. E., Shen, Q. W., Du, M., Fowden, A. L. and Forhead, A. J. (2012) Effects of cortisol and dexamethasone on insulin signalling pathways in skeletal muscle of the ovine fetus during late gestation. *Plos One* **7**(12): e52363.

Jensen, A., Gips, H., Hohmann, M. and Künzel, W. (1988) Adrenal endocrine and circulatory responses to acute prolonged asphyxia in surviving and non-surviving fetal sheep near term. *The Endocrine Control of the Fetus: Physiologic and Pathophysiologic Aspects*. Berlin, Heidelberg: Springer Berlin Heidelberg, pp. 64-79.

Jensen, E. C., Gallaher, B. W., Breier, B. H. and Harding, J. E. (2002) The effect of a chronic maternal cortisol infusion on the late-gestation fetal sheep. *J Endocrinol* **174**(1): 27-36.

Jeoung, N. H., Wu, P., Joshi, M. A., Jaskiewicz, J., Bock, C. B., Depaoli-Roach, A. A. and Harris, R. A. (2006) Role of pyruvate dehydrogenase kinase isoenzyme 4 (PDHK4) in glucose homoeostasis during starvation. *Biochem J* **397**(3): 417-25.

Jin, S. M. and Youle, R. J. (2012) PINK1- and Parkin-mediated mitophagy at a glance. *J Cell Sci* **125**(4): 795-9.

Jones, C. T. and Rolph, T. P. (1985) Metabolism during fetal life: a functional assessment of metabolic development. *Physiol Rev* **65**(2): 357-430.

Jorgensen, W., Rud, K. A., Mortensen, O. H., Frandsen, L., Grunnet, N. and Quistorff, B. (2017) Your mitochondria are what you eat: a high-fat or a high-sucrose diet eliminates metabolic flexibility in isolated mitochondria from rat skeletal muscle. *Physiol Rep* **5**(6) e13207.

Jousse, C., Muranishi, Y., Parry, L., Montaurier, C., Even, P., Launay, J. M., Carraro, V., Maurin, A. C., Averous, J., Chaveroux, C., Bruhat, A., Mallet, J., Morio, B. and Fafournoux, P. (2014) Perinatal protein malnutrition affects mitochondrial function in adult and results in a resistance to high fat diet-induced obesity. *PLoS One* **9**(8): e104896.

Jäger, S., Handschin, C., St.-Pierre, J. and Spiegelman, B. M. (2007) AMP-activated protein kinase (AMPK) action in skeletal muscle via direct phosphorylation of PGC-1α. *Proc Natl Acad Sci U S A* **104**(29): 12017-22.

Kalogeris, T., Baines, C. P., Krenz, M. and Korthuis, R. J. (2012) Cell Biology of Ischemia/Reperfusion Injury. *Int Rev Cell Mol Biol* **298**: 229-317.

Kapoor, A., Dunn, E., Kostaki, A., Andrews, M. H. and Matthews, S. G. (2006) Fetal programming of hypothalamo-pituitary-adrenal function: prenatal stress and glucocorticoids. *J Physiol* **572**(1): 31-44.

Kaur, J. (2014) A Comprehensive Review on Metabolic Syndrome. *Cardiol Res Pract* **2014**: 943162.

Kelley, D. E., He, J., Menshikova, E. V. and Ritov, V. B. (2002) Dysfunction of mitochondria in human skeletal muscle in type 2 diabetes. *Diabetes* **51**(10): 2944-50.

Kelly, A. K., Waters, S. M., McGee, M., Fonseca, R. G., Carberry, C. and Kenny, D. A. (2011) mRNA expression of genes regulating oxidative phosphorylation in the muscle of beef cattle divergently ranked on residual feed intake. *Physiol Genomics* **43**(1): 12-23.

Kerr, G. R., Campbell, J. A., Helmuth, A. C. and Waisman, H. A. (1971) Growth and Development of the Fetal Rhesus Monkey. II. Total Nitrogen, Protein, Lipid, Glycogen, and Water Composition of Major Organs. *Pediatr Res* **5**(4): 151-8.

Kimber, N. E., Heigenhauser, G. J. F., Spriet, L. L. and Dyck, D. J. (2003) Skeletal muscle fat and carbohydrate metabolism during recovery from glycogen-depleting exercise in humans. *J Physiol* **548**(3): 919-27.

Klein, A. H., Reviczky, A., Padbury, J. F. and Fisher, D. A. (1983) Effect of changes in thyroid status on tissue respiration in fetal and newborn sheep. *Am J Physiol* **244**(6): e603-6.

Kohn, T. A. and Myburgh, K. H. (2007) Regional specialization of rat quadriceps myosin heavy chain isoforms occurring in distal to proximal parts of middle and deep regions is not mirrored by citrate synthase activity. *J Anat* **210**(1): 8-18.

Kontani, Y., Wang, Y., Kimura, K., Inokuma, K. I., Saito, M., Suzuki-Miura, T., Wang, Z., Sato, Y., Mori, N. and Yamashita, H. (2005) UCP1 deficiency increases susceptibility to diet-induced obesity with age. *Aging Cell* **4**(3): 147-55.

Krebs, H. A. and Johnson, W. A. (1937) Metabolism of ketonic acids in animal tissues. *Biochem J* **31**(4): 645-60.

Kudin, A. P., Bimpong-Buta, N. Y., Vielhaber, S., Elger, C. E. and Kunz, W. S. (2004) Characterization of superoxide-producing sites in isolated brain mitochondria. *J Biol Chem* **279**(6): 4127-35.

Kuznetsov, A. V., Troppmair, J., Sucher, R., Hermann, M., Saks, V. and Margreiter, R. (2006) Mitochondrial subpopulations and heterogeneity revealed by confocal imaging: possible physiological role? *Biochim Biophys Acta* **1757**(5-6): 686-91.

Kuznetsov, A. V., Veksler, V., Gellerich, F. N., Saks, V., Margreiter, R. and Kunz, W. S. (2008) Analysis of mitochondrial function in situ in permeabilized muscle fibers, tissues and cells. *Nat Protoc* **3**(6): 965-76.

Lambert, A. J. and Brand, M. D. (2004) Superoxide production by NADH:ubiquinone oxidoreductase (complex I) depends on the pH gradient across the mitochondrial inner membrane. *Biochem J* **382**(2): 511-7.

Lane, R. H., Chandorkar, A. K., Flozak, A. S. and Simmons, R. A. (1998) Intrauterine growth retardation alters mitochondrial gene expression and function in fetal and juvenile rat skeletal muscle. *Pediatr Res* **43**(5): 563-70.

Lanham, S. A., Fowden, A. L., Roberts, C., Cooper, C., Oreffo, R. O. and Forhead, A. J. (2011) Effects of hypothyroidism on the structure and mechanical properties of bone in the ovine fetus. *J Endocrinol* **210**(2): 189-98.

Larsen, S., Nielsen, J., Hansen, C. N., Nielsen, L. B., Wibrand, F., Stride, N., Schroder, H. D., Boushel, R., Helge, J. W., Dela, F. and Hey-Mogensen, M. (2012) Biomarkers of mitochondrial content in skeletal muscle of healthy young human subjects. *J Physiol* **590**(14): 3349-60.

Larsson, L., Li, X., Teresi, A. and Salviati, G. (1994) Effects of thyroid hormone on fast- and slow-twitch skeletal muscles in young and old rats. *J Physiol* **481**(1): 149-61.

Latouche, C., Heywood, S. E., Henry, S. L., Ziemann, M., Lazarus, R., El-Osta, A., Armitage, J. A. and Kingwell, B. A. (2014) Maternal overnutrition programs changes in the expression of skeletal muscle genes that are associated with insulin resistance and defects of oxidative phosphorylation in adult male rat offspring. *J Nutr* **144**(3): 237-44.

Lee, H. K., Park, K. S., Cho, Y. M., Lee, Y. Y. and Pak, Y. K. (2005) Mitochondria-based model for fetal origin of adult disease and insulin resistance. *Ann N Y Acad Sci* **1042**: 1-18.

Lee, J. W., Kim, N. H. and Milanesi, A. (2014) Thyroid hormone signaling in muscle development, repair and metabolism. *J Endocrinol Diabetes Obes* **2**(3): 1046.

Lee, S. W., Tsou, A. P., Chan, H., Thomas, J., Petrie, K., Eugui, E. M. and Allison, A. C. (1988) Glucocorticoids selectively inhibit the transcription of the interleukin 1 beta gene and decrease the stability of interleukin 1 beta mRNA. *Proc Natl Acad Sci U S A* **85**(4): 1204-8.

Lehman, J. J., Barger, P. M., Kovacs, A., Saffitz, J. E., Medeiros, D. M. and Kelly, D. P. (2000) Peroxisome proliferator-activated receptor gamma coactivator-1 promotes cardiac mitochondrial biogenesis. *J Clin Invest* **106**(7): 847-56.

Leto, D. and Saltiel, A. R. (2012) Regulation of glucose transport by insulin: traffic control of GLUT4. *Nat Rev Mol Cell Biol* **13**(6): 383-96.

Letts, J. A., Fiedorczuk, K. and Sazanov, L. A. (2016) The architecture of respiratory supercomplexes. *Nature* **537**(7622): 644-8.

Levett, D. Z., Radford, E. J., Menassa, D. A., Graber, E. F., Morash, A. J., Hoppeler, H., Clarke, K., Martin, D. S., Ferguson-Smith, A. C., Montgomery, H. E., Grocott, M. P. and Murray, A. J. (2012) Acclimatization of skeletal muscle mitochondria to high-altitude hypoxia during an ascent of Everest. *FASEB J* **26**(4): 1431-41.

Lewis, M. R. and Lewis, W. H. (1914) Mitochondria in tissue culture. *Science* **39**(1000): 330-3.

Li, J., Forhead, A. J., Dauncey, M. J., Gilmour, R. S. and Fowden, A. L. (2002) Control of growth hormone receptor and insulin-like growth factor-I expression by cortisol in ovine fetal skeletal muscle. *J Physiol* **541**(2): 581-9.

Li, X.-b., Gu, J.-d. and Zhou, Q.-h. (2015) Review of aerobic glycolysis and its key enzymes – new targets for lung cancer therapy. *Thorac Cancer* **6**(1): 17-24.

Liggins, G. C. (1969) Premature delivery of foetal lambs infused with glucocorticoids. *J Endocrinol* **45**(4): 515-23.

Liu, J., Chen, D., Yao, Y., Yu, B., Mao, X., He, J., Huang, Z. and Zheng, P. (2012) Intrauterine growth retardation increases the susceptibility of pigs to high-fat diet-induced mitochondrial dysfunction in skeletal muscle. *PLoS ONE* **7**(4): e34835.

Lombardi, A., de Lange, P., Silvestri, E., Busiello, R. A., Lanni, A., Goglia, F. and Moreno, M. (2009) 3,5-Diiodo-L-thyronine rapidly enhances mitochondrial fatty acid oxidation rate and thermogenesis in rat skeletal muscle: AMP-activated protein kinase involvement. *Am J Physiol Endocrinol Metab* **296**(3): e497-502.

Long, Y. C. and Zierath, J. R. (2006) AMP-activated protein kinase signaling in metabolic regulation. *J Clin Invest* **116**(7): 1776-83.

Lorijn, R. H., Nelson, J. C. and Longo, L. D. (1980) Induced fetal hyperthyroidism: cardiac output and oxygen consumption. *Am J Physiol* **239**(3): H302-7.

Loschen, G., Azzi, A., Richter, C. and Flohe, L. (1974) Superoxide radicals as precursors of mitochondrial hydrogen peroxide. *FEBS Lett* **42**(1):68-72.

Lossow, W. J. and Chaikoff, I. L. (1955) Carbohydrate sparing of fatty acid oxidation. I. The relation of fatty acid chain length to the degree of sparing. II. The mechanism by which carbohydrate spares the oxidation of palmitic acid. *Arch Biochem Biophys* **57**(1): 23-40.

Luke, B., Hediger, M., Min, S. J., Brown, M. B., Misiunas, R. B., Gonzalez-Quintero, V. H., Nugent, C., Witter, F. R., Newman, R. B., Hankins, G. D., Grainger, D. A. and Macones, G. A. (2005) Gender mix in twins and fetal growth, length of gestation and adult cancer risk. *Paediatr Perinat Epidemiol* **19**(Suppl 1): 41-7.

Lundby, C. and Jacobs, R. A. (2016) Adaptations of skeletal muscle mitochondria to exercise training. *Exp Physiol* **101**(1): 17-22.

Mackler, B., Person, R. E., Nguyen, T. D. and Fantel, A. G. (1998) Studies of the cellular distribution of superoxide dismutases in adult and fetal rat tissues. *Free Radic Res* **28**(2): 125-9.

Magyar, D. M., Elsner, C. W., Fridshal, D., Eliot, J., Klein, A., Glatz, T., Lowe, K. C., Nathanielsz, P. W. and Buster, J. E. (1981) Time-trend analysis of plasma 11-desoxycorticosterone, corticosterone, cortisol, and aldosterone in fetal and maternal sheep during the last 18 days of gestation. *J Steroid Biochem* **14**(10): 1091-9.

Mai, W., Janier, M. F., Allioli, N., Quignodon, L., Chuzel, T., Flamant, F. and Samarut, J. (2004) Thyroid hormone receptor alpha is a molecular switch of cardiac function between fetal and postnatal life. *Proc Natl Acad Sci U S A* **101**(28): 10332-7.

Mammucari, C., Gherardi, G., Zamparo, I., Raffaello, A., Boncompagni, S., Chemello, F., Cagnin, S., Braga, A., Zanin, S., Pallafacchina, G., Zentilin, L., Sandri, M., De Stefani, D., Protasi,

F., Lanfranchi, G. and Rizzuto, R. (2015) The mitochondrial calcium uniporter controls skeletal muscle trophism in vivo. *Cell Rep* **10**(8): 1269-79.

Mansfield, K. D., Guzy, R. D., Pan, Y., Young, R. M., Cash, T. P., Schumacker, P. T. and Simon, M. C. (2005) Mitochondrial dysfunction resulting from loss of cytochrome c impairs cellular oxygen sensing and hypoxic HIF-α activation. *Cell Metab* **1**(6): 393-9.

Mansour, A. M. and Nass, S. (1970) In vivo cortisol action on RNA synthesis in rat liver nuclei and mitochondria. *Nature* **228**(5272): 665-7.

Marin-Garcia, J. (2010) Thyroid hormone and myocardial mitochondrial biogenesis. *Vascul Pharmacol* **52**(3-4): 120-30.

Marin-Garcia, J., Ananthakrishnan, R. and Goldenthal, M. J. (2000) Heart mitochondrial DNA and enzyme changes during early human development. *Mol Cell Biochem* **210**(1-2): 47-52.

Markham, T. C., Latorre, R. M., Lawlor, P. G., Ashton, C. J., McNamara, L. B., Natter, R., Rowlerson, A. and Stickland, N. C. (2009) Developmental programming of skeletal muscle phenotype/metabolism. *Animal* **3**(7): 1001-12.

Maxwell, S. E. and Delaney, H. D. (1990) Designing experiments and analyzing data: A model comparison approach. Second Edition.: Psychology Press.

McClelland, G. B., Dalziel, A. C., Fragoso, N. M. and Moyes, C. D. (2005) Muscle remodeling in relation to blood supply: implications for seasonal changes in mitochondrial enzymes. *J Exp Biol* **208**(3): 515-22.

McClure, T. D., Young, M. E., Taegtmeyer, H., Ning, X. H., Buroker, N. E., Lopez-Guisa, J. and Portman, M. A. (2005) Thyroid hormone interacts with PPARalpha and PGC-1 during mitochondrial maturation in sheep heart. *Am J Physiol Heart Circ Physiol* **289**(5): H2258-64.

McGarry, J. D., Mannaerts, G. P. and Foster, D. W. (1977) A possible role for malonyl-CoA in the regulation of hepatic fatty acid oxidation and ketogenesis. *J Clin Invest* **60**(1): 265-70.

McGuigan, M. P. and Wilson, A. M. (2003) The effect of gait and digital flexor muscle activation on limb compliance in the forelimb of the horse Equus caballus. *J Exp Biol* **206**(8): 1325-36.

McGuigan, M. P., Yoo, E., Lee, D. V. and Biewener, A. A. (2009) Dynamics of goat distal hind limb muscle–tendon function in response to locomotor grade. *J Exp Biol* **212**(13): 2092-194.

McMillen, I. C. and Robinson, J. S. (2005) Developmental origins of the metabolic syndrome: prediction, plasticity, and programming. *Physiol Rev* **85**(2): 571-633.

Mdaki, K. S., Larsen, T. D., Wachal, A. L., Schimelpfenig, M. D., Weaver, L. J., Dooyema, S. D. R., Louwagie, E. J. and Baack, M. L. (2016) Maternal high-fat diet impairs cardiac function in offspring of diabetic pregnancy through metabolic stress and mitochondrial dysfunction. *Am J Physiol Heart Circ Physiol* **310**(6): H681-H692.

Mellor, D. J. and Cockburn, F. (1986) A comparison of energy metabolism in the new-born infant, piglet and lamb. *Q J Exp Physiol* **71**(3): 361-79.

Mellor, D. J. and Matheson, I. C. (1979) Daily changes in the curved crown-rump length of individual sheep fetuses during the last 60 days of pregnancy and effects of different levels of maternal nutrition. *Q J Exp Physiol Cogn Med Sci* **64**(2): 119-31.

Meyuhas, O., Thompson, E. A., Jr. and Perry, R. P. (1987) Glucocorticoids selectively inhibit translation of ribosomal protein mRNAs in P1798 lymphosarcoma cells. *Mol Cell Biol* **7**(8): 2691-9.

Migeon, C. J., Bertrand, J. and Wall, P. E. (1957) Physiological Disposition of 4-C(14)-Cortisol During Late Pregnancy. *J Clin Invest* **36**(9): 1350-62.

Milanesi, A., Lee, J.-W., Kim, N.-H., Liu, Y.-Y., Yang, A., Sedrakyan, S., Kahng, A., Cervantes, V., Tripuraneni, N., Cheng, S.-y., Perin, L. and Brent, G. A. (2016) Thyroid Hormone Receptor α Plays an Essential Role in Male Skeletal Muscle Myoblast Proliferation, Differentiation, and Response to Injury. *Endocrinology* **157**(1): 4-15.

Miller, W. L. (2013) Steroid hormone synthesis in mitochondria. *Mol Cell Endocrinol* **379**(1-2): 62-73.

Milley, J. R. (1995) Effects of increased cortisol concentration on ovine fetal leucine kinetics and protein metabolism. *Am J Physiol* **268**(6 Pt 1): e1114-22.

Minai, L., Martinovic, J., Chretien, D., Dumez, F., Razavi, F., Munnich, A. and Roetig, A. (2008) Mitochondrial respiratory chain complex assembly and function during human fetal development. *Mol Gen Metab* **94**(1): 120-6.

Mishra, A., Reddy, I. J., Gupta, P. S. and Mondal, S. (2016) L-carnitine mediated reduction in oxidative stress and alteration in transcript level of antioxidant enzymes in sheep embryos produced in vitro. *Reprod Domest Anim* **51**(2): 311-21.

Mitchell, P. (1961) Coupling of phosphorylation to electron and hydrogen transfer by a chemi-osmotic type of mechanism. *Nature* **191**: 144-8.

Mitchell, P. and Moyle, J. (1969) Estimation of membrane potential and pH difference across the cristae membrane of rat liver mitochondria. *Eur J Biochem* **7**(4): 471-84.

Morgan, D. J., Poolman, T. M., Williamson, A. J., Wang, Z., Clark, N. R., Ma'ayan, A., Whetton, A. D., Brass, A., Matthews, L. C. and Ray, D. W. (2016) Glucocorticoid receptor isoforms direct distinct mitochondrial programs to regulate ATP production. *Sci Rep* **6**: 26419.

Morriss, F. H., Jr., Boyd, R. D., Makowski, E. L., Meschia, G. and Battaglia, F. C. (1973) Glucose-oxygen quotients across the hindlimb of fetal lambs. *Pediatr Res* **7**(10): 794-7.

Mostyn, A., Pearce, S., Budge, H., Elmes, M., Forhead, A. J., Fowden, A. L., Stephenson, T. and Symonds, M. E. (2003) Influence of cortisol on adipose tissue development in the fetal sheep during late gestation. *J Endocrinol* **176**(1): 23-30.

Mullur, R., Liu, Y.-Y. and Brent, G. A. (2014) Thyroid hormone regulation of metabolism. *Physiol Rev* **94**(2): 355-82.

Muoio, D. M. and Neufer, P. D. (2012) Lipid-induced mitochondrial stress and insulin action in muscle. *Cell Metab* **15**(5): 595-605.

Murphy, M. P. (2009) How mitochondria produce reactive oxygen species. *Biochem J* **417**(1): 1-13.

Murray, A. J. (2012) Oxygen delivery and fetal-placental growth: beyond a question of supply and demand? *Placenta* **33**(Suppl 2): e16-22.

Murray, A. J., Cole, M. A., Lygate, C. A., Carr, C. A., Stuckey, D. J., Little, S. E., Neubauer, S. and Clarke, K. (2008) Increased mitochondrial uncoupling proteins, respiratory uncoupling and decreased efficiency in the chronically infarcted rat heart. *J Mol Cell Cardiol* **44**(4): 694-700.

Myers, D. A., Hanson, K., Mlynarczyk, M., Kaushal, K. M. and Ducsay, C. A. (2008) Long-term hypoxia modulates expression of key genes regulating adipose function in the late-gestation ovine fetus. *Am J Physiol Regul Integr Comp Physiol* **294**(4): R1312-8.

Myers, D. A., Singleton, K., Hyatt, K., Mlynarczyk, M., Kaushal, K. M. and Ducsay, C. A. (2015) Long-term gestational hypoxia modulates expression of key genes governing mitochondrial function in the perirenal adipose of the late gestation sheep fetus. *Reprod Sci* **22**(6): 654-63.

Nafikov, R. A. and Beitz, D. C. (2007) Carbohydrate and lipid metabolism in farm animals. *J Nutr* **137**(3): 702-5.

Nakai, A., Taniuchi, Y., Asakura, H., Oya, A., Yokota, A., Koshino, T. and Araki, T. (2000) Developmental changes in mitochondrial activity and energy metabolism in fetal and neonatal rat brain. *Brain Res Dev Brain Res* **121**(1): 67-72.

Neupert, W. (1997) Protein import into mitochondria *Annu Rev Biochem* **66**: 863-917.

Newton, R. (2000) Molecular mechanisms of glucocorticoid action: what is important? *Thorax* **55**(7): 603-13.

Newton, R., Seybold, J., Kuitert, L. M., Bergmann, M. and Barnes, P. J. (1998) Repression of cyclooxygenase-2 and prostaglandin E2 release by dexamethasone occurs by transcriptional and post-transcriptional mechanisms involving loss of polyadenylated mRNA. *J Biol Chem* **273**(48): 32312-21.

Noji, H., Yasuda, R., Yoshida, M. and Kinosita, K., Jr. (1997) Direct observation of the rotation of F1-ATPase. *Nature* **386**(6622): 299-302.

Nordfors, L., Hoffstedt, J., Nyberg, B., Thorne, A., Arner, P., Schalling, M. and Lonnqvist, F. (1998) Reduced gene expression of UCP2 but not UCP3 in skeletal muscle of human obese subjects. *Diabetologia* **41**(8): 935-9.

Nunnari, J. and Suomalainen, A. (2012) Mitochondria: In sickness and in health. *Cell* **148**(6): 1145-59.

Nyirenda, M. J., Carter, R., Tang, J. I., de Vries, A., Schlumbohm, C., Hillier, S. G., Streit, F., Oellerich, M., Armstrong, V. W., Fuchs, E. and Seckl, J. R. (2009) Prenatal programming of metabolic syndrome in the common marmoset is associated with increased expression of 11β-hydroxysteroid dehydrogenase type 1. *Diabetes* **58**(12): 2873-9.

Nyirenda, M. J., Lindsay, R. S., Kenyon, C. J., Burchell, A. and Seckl, J. R. (1998) Glucocorticoid exposure in late gestation permanently programs rat hepatic phosphoenolpyruvate carboxykinase and glucocorticoid receptor expression and causes glucose intolerance in adult offspring. *J Clin Invest.* **101**(10): 2174-81.

Oakley, R. H., Sar, M. and Cidlowski, J. A. (1996) The human glucocorticoid receptor beta isoform. Expression, biochemical properties, and putative function. *J Biol Chem* **271**(16): 9550-9.

Ogbi, M. and Johnson, J. A. (2006) Protein kinase C epsilon interacts with cytochrome c oxidase subunit IV and enhances cytochrome c oxidase activity in neonatal cardiac myocyte preconditioning. *Biochem J.* **393**(1): 191-9.

Ojuka, E. O., Jones, T. E., Han, D. H., Chen, M. and Holloszy, J. O. (2003) Raising Ca2+ in L6 myotubes mimics effects of exercise on mitochondrial biogenesis in muscle. *FASEB J* **17**(6): 675-81.

Oliver, P., Sánchez, J., Caimari, A., Miralles, O., Picó, C. and Palou, A. (2007) The intake of a high-fat diet triggers higher brown adipose tissue UCP1 levels in male rats but not in females *Genes Nutr* **2**(1): 125-6.

Owens, J. A., Thavaneswaran, P., De Blasio, M. J., McMillen, I. C., Robinson, J. S. and Gatford, K. L. (2007) Sex-specific effects of placental restriction on components of the metabolic syndrome in young adult sheep. *Am J Physiol Endocrinol Metab* **292**(6): e1879.

Ozanne, S. E., Jensen, C. B., Tingey, K. J., Storgaard, H., Madsbad, S. and Vaag, A. A. (2005) Low birthweight is associated with specific changes in muscle insulin-signalling protein expression. *Diabetologia* **48**(3): 547-52.

Ozanne, S. E., Olsen, G. S., Hansen, L. L., Tingey, K. J., Nave, B. T., Wang, C. L., Hartil, K., Petry, C. J., Buckley, A. J. and Mosthaf-Seedorf, L. (2003) Early growth restriction leads to down regulation of protein kinase C zeta and insulin resistance in skeletal muscle. *J Endocrinol* **177**(2): 235-41.

Palade, G. E. (1953) An electron microscope study of the mitochondrial structure. *J Histochem Cytochem* **1**(4): 188-211.

Papa, S. (1996) Mitochondrial oxidative phosphorylation changes in the life span. Molecular aspects and physiopathological implications. *Biochim Biophys Acta* **1276**(2): 87-105.

Park, H. K., Jin, C. J., Cho, Y. M., Park, D. J., Shin, C. S., Park, K. S., Kim, S. Y., Cho, B. Y. and Lee, H. K. (2004) Changes of mitochondrial DNA content in the male offspring of protein-malnourished rats. *Ann N Y Acad Sci* **1011**: 205-16.

Park, K. S., Kim, S. K., Kim, M. S., Cho, E. Y., Lee, J. H., Lee, K. U., Pak, Y. K. and Lee, H. K. (2003) Fetal and early postnatal protein malnutrition cause long-term changes in rat liver and muscle mitochondria. *J Nutr* **133**(10): 3085-90.

Patron, M., Checchetto, V., Raffaello, A., Teardo, E., Vecellio Reane, D., Mantoan, M., Granatiero, V., Szabo, I., De Stefani, D. and Rizzuto, R. (2014) MICU1 and MICU2 finely tune the mitochondrial Ca2+ uniporter by exerting opposite effects on MCU activity. *Mol Cell* **53**(5): 726-37.

Pecqueur, C., Alves-Guerra, M. C., Gelly, C., Levi-Meyrueis, C., Couplan, E., Collins, S., Ricquier, D., Bouillaud, F. and Miroux, B. (2001) Uncoupling protein 2, in vivo distribution, induction upon oxidative stress, and evidence for translational regulation. *J Biol Chem* **276**(12): 8705-12.

Pehowich, D. J. (1999) Thyroid hormone status and membrane n-3 fatty acid content influence mitochondrial proton leak. *Biochim Biophys Acta* **1411**(1): 192-200.

Peng, T. I. and Jou, M. J. (2010) Oxidative stress caused by mitochondrial calcium overload. *Ann N Y Acad Sci* **1201**: 183-8.

Perez, M. H., Cormack, J., Mallinson, D. and Mutungi, G. (2013) A membrane glucocorticoid receptor mediates the rapid/non-genomic actions of glucocorticoids in mammalian skeletal muscle fibres. *J Physiol* **591**(20): 5171-85.

Pesta, D. and Gnaiger, E. (2012) High-resolution respirometry: OXPHOS protocols for human cells and permeabilized fibers from small biopsies of human muscle. *Methods Mol Biol* **810**: 25-58.

Petrik, J., Reusens, B., Arany, E., Remacle, C., Coelho, C., Hoet, J. J. and Hill, D. J. (1999) A low protein diet alters the balance of islet cell replication and apoptosis in the fetal and neonatal rat and is associated with a reduced pancreatic expression of insulin-like growth factor-II. *Endocrinology* **140**(10): 4861-73.

Pfaff, E. and Klingenberg, M. (1968) Adenine nucleotide translocation of mitochondria. 1. Specificity and control. *Eur J Biochem* **6**(1): 66-79.

Pfaff, E., Klingenberg, M. and Heldt, H. W. (1965) Unspecific permeation and specific exchange of adenine nucleotides in liver mitochondria. *Biochim Biophys Acta* **104**(1): 312-5.

Philp, A., Hargreaves, M. and Baar, K. (2012) More than a store: regulatory roles for glycogen in skeletal muscle adaptation to exercise. *Am J Physiol Endocrinol Metab* **302**(11): e1343-51.

Philp, A., MacKenzie, M. G., Belew, M. Y., Towler, M. C., Corstorphine, A., Papalamprou, A., Hardie, D. G. and Baar, K. (2013) Glycogen content regulates peroxisome proliferator activated receptor-ð (PPAR-ð) activity in rat skeletal muscle. *PLoS ONE* **8**(10): e77200.

Philp, A., Perez-Schindler, J., Green, C., Hamilton, D. L. and Baar, K. (2010) Pyruvate suppresses PGC1alpha expression and substrate utilization despite increased respiratory chain content in C2C12 myotubes. *Am J Physiol Cell Physiol* **299**(2): C240-50.

Pich, S., Bach, D., Briones, P., Liesa, M., Camps, M., Testar, X., Palacin, M. and Zorzano, A. (2005) The Charcot-Marie-Tooth type 2A gene product, Mfn2, up-regulates fuel oxidation through expression of OXPHOS system. *Hum Mol Genet* **14**(11): 1405-15.

Pierelli, G., Stanzione, R., Forte, M., Migliarino, S., Perelli, M., Volpe, M. and Rubattu, S. (2017) Uncoupling protein 2: A key player and a potential therapeutic target in vascular diseases. *Oxid Med Cell Longev* **2017**: 7348372.

Pileggi, C. A., Hedges, C. P., Segovia, S. A., Markworth, J. F., Durainayagam, B. R., Gray, C., Zhang, X. D., Barnett, M. P. G., Vickers, M. H., Hickey, A. J. R., Reynolds, C. M. and Cameron-Smith, D. (2016) Maternal high fat diet alters skeletal muscle mitochondrial catalytic activity in adult male rat offspring. *Front Physiol* **7**: 546.

Pitts, K. R., Yoon, Y., Krueger, E. W. and McNiven, M. A. (1999) The dynamin-like protein DLP1 is essential for normal distribution and morphology of the endoplasmic reticulum and mitochondria in mammalian cells. *Mol Biol Cell* **10**(12): 4403-17.

Pittschieler, K., Lebenthal, E., Bujanover, Y. and Petell, J. K. (1991) Levels of Cu-Zn and Mn superoxide dismutases in rat liver during development. *Gastroenterology* **100**(4): 1062-8.

Polk, D. H. (1995) Thyroid hormone metabolism during development. *Reprod Fertil Dev* **7**(3): 469-77.

Polk, D. H., Reviczky, A., Lam, R. W. and Fisher, D. A. (1991) Thyrotropin-releasing hormone in ovine fetus: ontogeny and effect of thyroid hormone. *Am J Physiol* **260**(1 Pt 1): e53-8.

Polk, D. H., Wu, S. Y., Wright, C., Reviczky, A. L. and Fisher, D. A. (1988) Ontogeny of thyroid hormone effect on tissue 5'-monodeiodinase activity in fetal sheep. *Am J Physiol* **254**(3 Pt 1): e337-41.

Portman, M. A., Xiao, Y., Qian, K., Tucker, R. L., Parish, S. M. and Ning, X. H. (2000) Thyroid hormone coordinates respiratory control maturation and adenine nucleotide translocator expression in heart in vivo. *Circulation* **102**(11): 1323-9.

Rab, M., Mader, N., Kamolz, L. P., Hausner, T., Gruber, H. and Girsch, W. (1997) Basic anatomical investigation of semitendinosus and the long head of biceps femoris muscle for their possible use in electrically stimulated neosphincter formation. *Surg Radiol Anat* **19**(5): 287-91.

Ramachandran, A. (2005) Epidemiology of diabetes in India--three decades of research. *J Assoc Physicians India* **53**: 34-8.

Ramachandran, A., Snehalatha, C., Satyavani, K., Sivasankari, S. and Vijay, V. (2003) Metabolic syndrome in urban Asian Indian adults--a population study using modified ATP III criteria. *Diabetes Res Clin Pract* **60**(3): 199-204.

Randle, P. J., Garland, P. B., Hales, C. N. and Newsholme, E. A. (1963) The glucose fatty-acid cycle. Its role in insulin sensitivity and the metabolic disturbances of diabetes mellitus. *Lancet* **1**(7285): 785-9.

Reinehr, T. (2013) Type 2 diabetes mellitus in children and adolescents. *World J Diabetes* **4**(6): 270-81.

Ricquier, D. and Bouillaud, F. (2000) The uncoupling protein homologues: UCP1, UCP2, UCP3, StUCP and AtUCP. *Biochem J* **345**(2): 161-79.

Rippe, C., Berger, K., Boiers, C., Ricquier, D. and Erlanson-Albertsson, C. (2000) Effect of high-fat diet, surrounding temperature, and enterostatin on uncoupling protein gene expression. *Am J Physiol Endocrinol Metab* **279**(2): e293-300.

Ritov, V. B., Menshikova, E. V., He, J., Ferrell, R. E., Goodpaster, B. H. and Kelley, D. E. (2005) Deficiency of subsarcolemmal mitochondria in obesity and type 2 diabetes. *Diabetes* **54**(1): 8-14.

Roelfsema, V., Gunn, A. J., Fraser, M., Quaedackers, J. S. and Bennet, L. (2005) Cortisol and ACTH responses to severe asphyxia in preterm fetal sheep. *Exp Physiol* **90**(4): 545-55.

Rogers, M. S., Mongelli, J. M., Tsang, K. H., Wang, C. C. and Law, K. P. (1998) Lipid peroxidation in cord blood at birth: the effect of labour. *Br J Obstet Gynaecol* **105**(7): 739-44.

Rojo, M., Legros, F., Chateau, D. and Lombes, A. (2002) Membrane topology and mitochondrial targeting of mitofusins, ubiquitous mammalian homologs of the transmembrane GTPase Fzo. *J Cell Sci* **115**(8): 1663-74.

Roseboom, T., de Rooij, S. and Painter, R. (2006) The Dutch famine and its long-term consequences for adult health. *Early Hum Dev* **82**(8): 485-91.

Rousseau, G. G. (1984) Control of gene expression by glucocorticoid hormones. *Biochem J* **224**(1): 1-12.

Rumball, C. W., Oliver, M. H., Thorstensen, E. B., Jaquiery, A. L., Husted, S. M., Harding, J. E. and Bloomfield, F. H. (2008a) Effects of twinning and periconceptional undernutrition on late-gestation hypothalamic-pituitary-adrenal axis function in ovine pregnancy. *Endocrinology* **149**(3): 1163-72.

Rumball, C. W. H., Harding, J. E., Oliver, M. H. and Bloomfield, F. H. (2008b) Effects of twin pregnancy and periconceptional undernutrition on maternal metabolism, fetal growth and glucose–insulin axis function in ovine pregnancy. *J Physiol* **586**(5): 1399-1411.

Russell, A. P., Somm, E., Praz, M., Crettenand, A., Hartley, O., Melotti, A., Giacobino, J.-P., Muzzin, P., Gobelet, C. and Dériaz, O. (2003) UCP3 protein regulation in human skeletal muscle fibre types I, IIa and IIx is dependent on exercise intensity. *J Physiol* **550**(3): 855-61.

Salehzadeh, F., Al-Khalili, L., Kulkarni, S. S., Wang, M., Lönngvist, F. and Krook, A. (2009) Glucocorticoid-mediated effects on metabolism are reversed by targetting 11 betahydroxysteroid dehydrogenase type 1 in human skeletal muscle. *Diabetes Metab Res Rev* **25**(3):250-8.

Salvatore, D., Simonides, W. S., Dentice, M., Zavacki, A. M. and Larsen, P. R. (2014) Thyroid hormones and skeletal muscle — new insights and potential implications. *Nature Rev Endocrinol* **10**(4):. 206-14.

Samjoo, I. A., Safdar, A., Hamadeh, M. J., Glover, A. W., Mocellin, N. J., Santana, J., Little, J. P., Steinberg, G. R., Raha, S. and Tarnopolsky, M. A. (2013) Markers of skeletal muscle mitochondrial function and lipid accumulation are moderately associated with the homeostasis model assessment index of insulin resistance in obese men. *PLoS ONE* **8**(6): e66322.

Santini, F., Chopra, I. J., Wu, S.-Y., Solomon, D. H. and Chua Teco, G. N. (1992) Metabolism of 3,5,3'-triiodothyronine sulfate by tissues of the fetal rat: A consideration of the role of desulfation of 3,5,3'-triiodothyronine sulfate as a source of T_3. *Pediatr Res* **31**(6): 541-4.

Saoud, C. J. and Wood, C. E. (1996) Ontogeny and molecular weight of immunoreactive arginine vasopressin and corticotropin-releasing factor in the ovine fetal hypothalamus. *Peptides* **17**(1): 55-61.

Sazanov, L. A. (2015) A giant molecular proton pump: structure and mechanism of respiratory complex I. *Nat Rev Mol Cell Biol* **16**(6): 375-88.

Scarpulla, R. C. (2011) Metabolic control of mitochondrial biogenesis through the PGC-1 family regulatory network. *Biochimica et biophysica acta* **1813**(7): 1269-78.

Scarpulla, R. C., Vega, R. B. and Kelly, D. P. (2012) Transcriptional integration of mitochondrial biogenesis. *Trends Endocrinol Metabol* **23**(9): 459-66.

Schell, J. C. and Rutter, J. (2013) The long and winding road to the mitochondrial pyruvate carrier. *Cancer Metab* **1**: 6.

Scheller, K., Sekeris, C. E., Krohne, G., Hock, R., Hansen, I. A. and Scheer, U. (2000) Localization of glucocorticoid hormone receptors in mitochondria of human cells. *Eur J Cell Biol* **79**(5): 299-307.

Schermer, S. J., Bird, J. A., Lomax, M. A., Shepherd, D. A. and Symonds, M. E. (1996) Effect of fetal thyroidectomy on brown adipose tissue and thermoregulation in newborn lambs. *Reprod Fertil Dev* **8**(6): 995-1002.

Schmittgen, T. D. and Livak, K. J. (2008) Analyzing real-time PCR data by the comparative C-T method. *Nat Protoc* **3**(6): 1101-8.

Schrauwen, P. and Hesselink, M. (2002) UCP2 and UCP3 in muscle controlling body metabolism. *J Exp Biol* **205**(15): 2275-85.

Schrauwen, P., Hoppeler, H., Billeter, R., Bakker, A. H. and Pendergast, D. R. (2001) Fiber type dependent upregulation of human skeletal muscle UCP2 and UCP3 mRNA expression by high-fat diet. *Int J Obes Relat Metab Disord* **25**(4): 449-56.

Schrepfer, E. and Scorrano, L. (2016) Mitofusins, from mitochondria to metabolism. *Mol Cell* **61**(5): 683-94.

Schönfeld, P., Fritz, S., Halangk, W. and Bohnensack, R. (1993) Increase in the adenine nucleotide translocase protein contributes to the perinatal maturation of respiration in rat liver mitochondria. *Biochim Biophys Acta Bioenerg* **1144**(3): 353-8.

Seckl, J. R. (2004) Prenatal glucocorticoids and long-term programming. *Eur J Endocrinol* **151**(Suppl 3): U49-62.

Selak, M. A., Storey, B. T., Peterside, I. and Simmons, R. A. (2003) Impaired oxidative phosphorylation in skeletal muscle of intrauterine growth-retarded rats. *Am J Physiol Endocrinol Metab* **285**(1): e130-7.

Sharma, S. and Black, S. M. (2009) Carnitine homeostasis, mitochondrial function and cardiovascular disease. *Drug Discov Today Dis Mech* **6**(1-4): e31-9.

Shields, B. M., Knight, B. A., Hill, A., Hattersley, A. T. and Vaidya, B. (2011) Fetal Thyroid Hormone Level at Birth Is Associated with Fetal Growth. *J Clin Endocrinol Metab* **96**(6): e934-8.

Short, K. R., Nygren, J., Barazzoni, R., Levine, J. and Nair, K. S. (2001) T(3) increases mitochondrial ATP production in oxidative muscle despite increased expression of UCP2 and -3. *Am J Physiol Endocrinol Metab* **280**(5): e761-9.

Shukla, V. H., Dave, K. R. and Katyare, S. S. (2000) Effect of catecholamine depletion on oxidative energy metabolism in rat liver, brain and heart mitochondria; use of reserpine. *Comp Biochem Physiol C Toxicol Pharmacol* **127**(1): 79-90.

Silva, J. E. and Larsen, P. R. (1985) Potential of brown adipose tissue type II thyroxine 5'-deiodinase as a local and systemic source of triiodothyronine in rats. *J Clin Invest* **76**(6): 2296-305.

Silver, M. and Fowden, A. L. (1988) Induction of labour in domestic animals: Endocrine changes and neonatal viability. Künzel, W. & Jensen, A. The Endocrine Control of the Fetus: Physiologic and Pathophysiologic Aspects. Berlin, Heidelberg: Springer Berlin Heidelberg, pp. 401-411.

Simard, J. R., Pillai, B. K. and Hamilton, J. A. (2008) Fatty acid flip-flop in a model membrane is faster than desorption into the aqueous phase. *Biochemistry* **47**(35): 9081-9.

Simoneau, J. A., Lortie, G., Boulay, M. R., Thibault, M. C., Theriault, G. and Bouchard, C. (1985) Skeletal muscle histochemical and biochemical characteristics in sedentary male and female subjects. *Can J Physiol Pharmacol* **63**(1): 30-5.

Simonsen, L., Stallknecht, B. and Bulow, J. (1993) Contribution of skeletal muscle and adipose tissue to adrenaline-induced thermogenesis in man. *Int J Obes Relat Metab Disord* **17**(Suppl 3): S47-51.

Simonyan, R. A., Jimenez, M., Ceddia, R. B., Giacobino, J. P., Muzzin, P. and Skulachev, V. P. (2001) Cold-induced changes in the energy coupling and the UCP3 level in rodent skeletal muscles. *Biochim Biophys Acta* **1505**(2-3): 271-9.

Smiles, W. J. and Camera, D. M. (2015) More than mitochondrial biogenesis: alternative roles of PGC-1alpha in exercise adaptation. *J Physiol* **593**(9): 2115-7.

Smith, H. E. and Page, E. (1977) Ultrastructural changes in rabbit heart mitochondria during the perinatal period. Neonatal transition to aerobic metabolism. *Dev Biol* **57**(1): 109-17.

Solaini, G., Baracca, A., Lenaz, G. and Sgarbi, G. (2010) Hypoxia and mitochondrial oxidative metabolism. *Biochim Biophys Acta Bioenerg* **1797**(6): 1171-7.

Song, Z., Chen, H., Fiket, M., Alexander, C. and Chan, D. C. (2007) OPA1 processing controls mitochondrial fusion and is regulated by mRNA splicing, membrane potential, and Yme1L. *J Cell Biol* **178**(5): 749-55.

Sperl, W., Sengers, R. C., Trijbels, J. M., Ruitenbeek, W., Doesburg, W. H., Smeitink, J. A., Kollee, L. A. and Boon, J. M. (1992) Enzyme activities of the mitochondrial energy generating system in skeletal muscle tissue of preterm and fullterm neonates. *Ann Clin Biochem* **29**(6): 638-45.

Spriet, L. L. (2014) New insights into the interaction of carbohydrate and fat metabolism during exercise. *Sports Med* **44**(Suppl 1): 87-96.

St-Pierre, J., Buckingham, J. A., Roebuck, S. J. and Brand, M. D. (2002) Topology of superoxide production from different sites in the mitochondrial electron transport chain. *J Biol Chem* **277**(47): 44784-90.

Stepien, G., Torroni, A., Chung, A. B., Hodge, J. A. and Wallace, D. C. (1992) Differential expression of adenine nucleotide translocator isoforms in mammalian tissues and during muscle cell differentiation. *J Biol Chem* **267**(21): 14592-7.

Stern, J. R. (1957) Crystalline beta-hydroxybutyryl dehydrogenase from pig heart. *Biochim Biophys Acta* **26**(2): 448-9.

Stewart, P. M., Whorwood, C. B. and Mason, J. I. (1995) Type 2 11 beta-hydroxysteroid dehydrogenase in foetal and adult life. *J Steroid Biochem Mol Biol* **55**(5-6): 465-71.

Stuart, C. A., McCurry, M. P., Marino, A., South, M. A., Howell, M. E., Layne, A. S., Ramsey, M. W. and Stone, M. H. (2013) Slow-twitch fiber proportion in skeletal muscle correlates with insulin responsiveness. *J Clin Endocrinol Metab* **98**(5): 2027-36.

Stump, C. S., Short, K. R., Bigelow, M. L., Schimke, J. M. and Nair, K. S. (2003) Effect of insulin on human skeletal muscle mitochondrial ATP production, protein synthesis, and mRNA transcripts. *Proc Natl Acad Sci U S A* **100**(13): 7996-8001.

Su, X. and Abumrad, N. A. (2009) Cellular fatty acid uptake: A pathway under construction *Trends Endocrinol Metabol* **20**(2): 72-7.

Sun, N., Youle, R. J. and Finkel, T. (2016) The mitochondrial basis of aging. *Mol Cell* **61**(5): 654-66.

Taanman, J. W. (1999) The mitochondrial genome: structure, transcription, translation and replication. *Biochim Biophys Acta* **1410**(2): 103-23.

Tarpenning, K. M., Wiswell, R. A., Hawkins, S. A. and Marcell, T. J. (2001) Influence of weight training exercise and modification of hormonal response on skeletal muscle growth. *J Sci Med Sport* **4**(4):431-46.

Tarry-Adkins, J. L., Blackmore, H. L., Martin-Gronert, M. S., Fernandez-Twinn, D. S., McConnell, J. M., Hargreaves, I. P., Giussani, D. A. and Ozanne, S. E. (2013) Coenzyme Q10 prevents accelerated cardiac aging in a rat model of poor maternal nutrition and accelerated postnatal growth. *Mol Metab* **2**(4): 480-90.

Tarry-Adkins, J. L., Fernandez-Twinn, D. S., Chen, J. H., Hargreaves, I. P., Neergheen, V., Aiken, C. E. and Ozanne, S. E. (2016) Poor maternal nutrition and accelerated postnatal growth induces an accelerated aging phenotype and oxidative stress in skeletal muscle of male rats. *Dis Model Mech* **9**(10): 1221-9.

Taylor, P. D., McConnell, J., Khan, I. Y., Holemans, K., Lawrence, K. M., Asare-Anane, H., Persaud, S. J., Jones, P. M., Petrie, L., Hanson, M. A. and Poston, L. (2005) Impaired glucose homeostasis and mitochondrial abnormalities in offspring of rats fed a fat-rich diet in pregnancy. *Am J Physiol Regul Integr Comp Physiol* **288**(1): R134-9.

Thomas, S. J., Wilson, D. W., Pierrepoint, C. G., Cameron, E. H. and Griffiths, K. (1976) Measurement of cortisol, cortisone, 11-deoxycortisol and corticosterone in foetal sheep plasma during the perinatal period. *J Endocrinol* **68**(2): 181-9.

Thorpe-Beeston, J. G., Nicolaides, K. H., Felton, C. V., Butler, J. and McGregor, A. M. (1991a) Maturation of the secretion of thyroid hormone and thyroid-stimulating hormone in the fetus. *N Engl J Med* **324**(8): 532-6.

Thorpe-Beeston, J. G., Nicolaides, K. H., Snijders, R. J., Felton, C. V. and McGregor, A. M. (1991b) Thyroid function in small for gestational age fetuses. *Obstet Gynecol* **77**(5): 701-6.

Vanduyne, C., Parker, H. R. and Holm, L. W. (1965) Metabolism of free fatty acids during perinatal life of lambs. *Am J Obstet Gynecol* **91**: 277-85.

Vaughan, O. R., Davies, K. L., Ward, J. W., de Blasio, M. J. and Fowden, A. L. (2016) A physiological increase in maternal cortisol alters uteroplacental metabolism in the pregnant ewe. *J Physiol* **594**(21): 6407-18.

Vidal-Puig, A., Solanes, G., Grujic, D., Flier, J. S. and Lowell, B. B. (1997) UCP3: an uncoupling protein homologue expressed preferentially and abundantly in skeletal muscle and brown adipose tissue. *Biochem Biophys Res Commun* **235**(1): 79-82.

Visser, T. J. (1994) Role of sulfation in thyroid hormone metabolism. *Chem Biol Interact* **92**(1-3): 293-303.

Visser, W. E., Friesema, E. C. and Visser, T. J. (2011) Thyroid hormone transporters: The knowns and the unknowns. *Mol Endocrinol* **25**(1): 1-14.

Wagenmakers, A. J. (1996) A malonyl-CoA fuel sensing mechanism in muscle: effects of insulin, glucose and denervation. *Clin Nutr* **15**(3): 144-5.

Walther, R. F., Lamprecht, C., Ridsdale, A., Groulx, I., Lee, S., Lefebvre, Y. A. and Haché, R. J. (2003) Nuclear export of the glucocorticoid receptor is accelerated by cell fusion-dependent release of calreticulin. *J Biol Chem* **278**(39):37858-64.

Wang, S. C., Myers, S., Dooms, C., Capon, R. and Muscat, G. E. (2010) An ERRbeta/gamma agonist modulates GRalpha expression, and glucocorticoid responsive gene expression in skeletal muscle cells. *Mol Cell Endocrinol* **315**(1-2):146-52.

Ward, J. W., Wooding, F. B. and Fowden, A. L. (2004) Ovine feto-placental metabolism. *J Physiol* **554**(2): 529-41.

Weber, K., Bruck, P., Mikes, Z., Kupper, J. H., Klingenspor, M. and Wiesner, R. J. (2002) Glucocorticoid hormone stimulates mitochondrial biogenesis specifically in skeletal muscle. *Endocrinology* **143**(1): 177-84.

Weisiger, R. A. and Fridovich, I. (1973) Superoxide dismutase. Organelle specificity. *J Biol Chem* **248**(10): 3582-92.

Weiss, R., Dziura, J., Burgert, T. S., Tamborlane, W. V., Taksali, S. E., Yeckel, C. W., Allen, K., Lopes, M., Savoye, M., Morrison, J., Sherwin, R. S. and Caprio, S. (2004) Obesity and the metabolic syndrome in children and adolescents. *N Engl J Med* **350**(23): 2362-74.

Weitzel, J. M., Radtke, C. and Seitz, H. J. (2001) Two thyroid-hormone mediated gene expression patterns in vivo identified by cDNA expression arrays in rat. *Nucleic Acids Res* **29**(24):5148-55.

Weitzel, J. M. and Iwen, K. A. (2011) Coordination of mitochondrial biogenesis by thyroid hormone. *Mol Cell Endocrinol* **342**(1-2):1-7.

Wende, A. R., Schaeffer, P. J., Parker, G. J., Zechner, C., Han, D. H., Chen, M. M., Hancock, C. R., Lehman, J. J., Huss, J. M., McClain, D. A., Holloszy, J. O. and Kelly, D. P. (2007) A role for the transcriptional coactivator PGC-1alpha in muscle refueling. *J Biol Chem* **282**(50): 36642-51.

White, P., Burton, K. A., Fowden, A. L. and Dauncey, M. J. (2001) Developmental expression analysis of thyroid hormone receptor isoforms reveals new insights into their essential functions in cardiac and skeletal muscles. *FASEB J* **15**(8): 1367-76.

White, R. B., Bierinx, A. S., Gnocchi, V. F. and Zammit, P. S. (2010) Dynamics of muscle fibre growth during postnatal mouse development. *BMC Dev Biol* **10**: 21.

Wilson, A. and Lichtwark, G. (2011) The anatomical arrangement of muscle and tendon enhances limb versatility and locomotor performance. *Philos Trans R Soc B Biological Sciences* **366**(1570): 1540-53.

Winder, W. W. (1979) Time course of the T3- and T4-induced increase in rat soleus muscle mitochondria. *Am J Physiol* **236**(3): C132-8.

Winder, W. W. and Hardie, D. G. (1996) Inactivation of acetyl-CoA carboxylase and activation of AMP-activated protein kinase in muscle during exercise. *Am J Physiol* **270**(2 Pt 1): e299-304.

Winder, W. W., Holmes, B. F., Rubink, D. S., Jensen, E. B., Chen, M. and Holloszy, J. O. (2000) Activation of AMP-activated protein kinase increases mitochondrial enzymes in skeletal muscle. *J Appl Physiol* **88**(6): 2219-26.

Wintour, E. M., Brown, E. H., Denton, D. A., Hardy, K. J., McDougall, J. G., Oddie, C. J. and Whipp, G. T. (1975) The ontogeny and regulation of corticosteroid secretion by the ovine foetal adrenal. *Acta Endocrinol* **79**(2): 301-16.

Wood, C. E. (1988) Insensitivity of near-term fetal sheep to cortisol: possible relation to the control of parturition. *Endocrinology* **122**(4): 1565-72.

Wood, C. E. and Keller-Wood, M. (2016) The critical importance of the fetal hypothalamus-pituitary-adrenal axis. *F1000 Research* **5**: F1000.

Wood, C. E. and Rudolph, A. M. (1983) Negative feedback regulation of adrenocorticotropin secretion by cortisol in ovine fetuses. *Endocrinology* **112**(6): 1930-6.

Wood, C. E. and Rudolph, A. M. (1984) Can maternal stress alter fetal adrenocorticotropin secretion? *Endocrinology* **115**(1): 298-301.

Woodley, S. J. and Mercer, S. R. (2005) Hamstring muscles: architecture and innervation. *Cells Tissues Organs* **179**(3): 125-41.

Wu, S. Y., Polk, D. H., Huang, W. S., Reviczky, A., Wang, K. and Fisher, D. A. (1993) Sulfate conjugates of iodothyronines in developing sheep: effect of fetal hypothyroidism. *Am J Physiol* **265**(1 Pt 1): e115-20.

Wu, Y. and Koenig, R. J. (2000) Gene regulation by thyroid hormone. *Trends Endocrinol Metab* **11**(6): 207-11.

Wulf, A., Harneit, A., Kröger, M., Kebenko, M., Wetzel, M. H., Weitzel, J. M. (2008) T3-mediated expression of PGC-1alpha via a far upstream located thyroid hormone response element. *Mol Cell Endocrinol* **287**(1-2):90-5.

Wyrwoll, C. S., Seckl, J. R. and Holmes, M. C. (2009) Altered placental function of 11beta-hydroxysteroid dehydrogenase 2 knockout mice. *Endocrinology* **150**(3): 1287-93.

Yamada, T., Yoneyama, Y., Sawa, R. and Araki, T. (2003) Effects of maternal oxygen supplementation on fetal oxygenation and lipid peroxidation following a single umbilical cord occlusion in fetal goats. *J Nippon Med Sch* **70**(2): 165-71.

Yang, D., Oyaizu, Y., Oyaizu, H., Olsen, G. J. and Woese, C. R. (1985) Mitochondrial origins. *Proc Natl Acad Sci U S A* **82**(13): 4443-7.

Yates, D. T., Cadaret, C. N., Beede, K. A., Riley, H. E., Macko, A. R., Anderson, M. J., Camacho, L. E. and Limesand, S. W. (2016) Intrauterine growth-restricted sheep fetuses exhibit smaller hindlimb muscle fibers and lower proportions of insulin-sensitive Type I fibers near term. *Am J Physiol Regul Integr Comp Physiol* **310**(11): R1020-9.

Ye, J., Coulouris, G., Zaretskaya, I., Cutcutache, I., Rozen, S. and Madden, T. L. (2012) Primer-BLAST: a tool to design target-specific primers for polymerase chain reaction. *BMC Bioinformatics* **13**: 134.

Yu, F., Gothe, S., Wikstrom, L., Forrest, D., Vennstrom, B. and Larsson, L. (2000) Effects of thyroid hormone receptor gene disruption on myosin isoform expression in mouse skeletal muscles. *Am J Physiol Regul Integr Comp Physiol* **278**(6): R1545-54.

Zhang, C. S. and Lin, S. C. (2016) AMPK promotes autophagy by facilitating mitochondrial fission. *Cell Metab* **23**(3): 399-401.

Zorzano, A. and Claret, M. (2015) Implications of mitochondrial dynamics on neurodegeneration and on hypothalamic dysfunction. *Front Aging Neurosci* **7**: 101.

Zorzano, A., Liesa, M., Sebastian, D., Segales, J. and Palacin, M. (2010) Mitochondrial fusion proteins: dual regulators of morphology and metabolism. *Semin Cell Dev Biol* **21**(6): 566-74.